The Dissertation Committee for Sang Taek Jung Certifies that this is the approved version of the following dissertation:

Engineering of Aglycosylated Antibody Fc for Effector Functions

Committee:

George Georgiou, Supervisor

Brent L. Iverson

Philip W. Tucker

Charles B. Mullins

Jennifer Maynard

Engineering of Aglycosylated Antibody Fc for Effector Functions

by

Sang Taek Jung, B.S.; M.S.

Dissertation

Presented to the Faculty of the Graduate School of

The University of Texas at Austin

in Partial Fulfillment

of the Requirements

for the Degree of

Doctor of Philosophy

The University of Texas at Austin

August, 2009

Dedication

To my family for their never ending love and support

Acknowledgements

I would like to begin my long list of people to be acknowledged with my advisor, Professor George Georgiou for his immense support, encouragement and patience throughout this work. I am really grateful to his invaluable guidance to my professional development and his considerate and caring personality which makes the long journey of Ph.D. study a more enjoyable experience. Also, I am particularly thankful to have been advised by Professor Brent L. Iverson. I greatly enjoyed working in the BIGG lab with him and benefited from his thoughtful comments and encouragements thoughout my graduate study. I also want to thank Professor Philip W. Tucker for a lot of helpful discussions, comments, and input on the ADCC experiments. Sincerely thanks are extended to another committee member, Professor Charles B. Mullins and Professor Jennifer Maynard for offering their advice, support, and analysis for my study. The opportunity to work with my committee has been a very rewarding professional and human experience.

Many people contributed to this work in different ways. Special thanks go to Dr. Sai T. Reddy for the ADCC experiments and many helpful discussions. I would like to also thank Chhaya Das for her technical assistance in the ADCC experiments. I am very grateful to Tae Hyun Kang for his works on the purification of full length IgGs and BIAcore experiments. I appreciate Dr. M. Jack Borrok for the expression of glycosylated trastzumab antibodies in HEK293 cells. Professor Inger Sandlie (University of Oslo, Norway) helped this study with providing us with valuable purified GST fused FcγRIIa, FcγRIIb, and FcRn proteins. I thank Dr. Ki Jun Jeong for many helpful discussions. Also

all the present and former members in the BIGG lab deserve my heartful thanks for their friendship and help. Finally, I appreciate the financial support from Clayton foundation for research.

Engineering of Aglycosylated Antibody Fc for Effector Functions

Publication No._____

Sang Taek Jung, Ph.D.

The University of Texas at Austin, 2009

Supervisor: George Georgiou

The antibody Fc region is critical for the therapeutic potency by virtue of its role in recruiting and activating the cytotoxic pathways of immune cells, complement activation and its role in antibody homeostasis (a process mediated by the pH dependent binding to the neonatal receptor FcRn). Bacterially produced antibodies lack of glycosylation at Asn297 and therefore do not bind to the surface FcγRs on effector innate immune cells, nor can they activate complement. This dissertation describes the engineering of aglycosylated bacterially expressed antibodies for binding to a specific FcγR and therefore eliciting therapeutically relevant effector functions. Aglycosylated Fc mutants that bind to desired Fc binding ligands were isolated by a new *E. coli* homodimeric Fc display system coupled with high throughput flow cytometry. Two amino acids mutation in the CH3 domain (Fc5) conferred selectively high binding affinity of aglycosylated Fc domains to the FcγRI receptor. Flow cytometry screening from a randomized Fc5 library resulted in the isolation of Fc mutants exhibiting higher

affinity binding to FcγRI receptor than the Fc5. Aglycosylated FcγRI specific IgG containing the variable regions of the clinically important anti-Her2 antibody trastuzumab elicited dendritic cell-mediated ADCC in sharp contrast to the clinical grade trastuzumab (Herceptin) or the glycosylated coutreparts of the engineered antibodies, neither of which could potentiate target cell lysis with dendritic cells as effectors. In separate studies, a system was developed for the screening of periplasmically anchored *E. coli* libraries and the isolation of clones expressing antibodies that are specific to insoluble antigens or to cell surface markers. Following three rounds of flow cytometric screening, spheroplasts expressing specific scFvs were enriched 950-fold from a large excess (1,000x) of spheroplasts expressing nonspecific antibodies.

Table of Contents

List of Tables ..... **xiv**

List of Figures ..... **xv**

Chapter 1: Introduction and Background **1**

1. 1 Introduction 1

1. 2 Background 3

1.2.1 Structure and function of immunoglobulin and Fc 3

1.2.2 Human Fc receptors 7

1.2.2.1 Human FcγR 7

1.2.2.2 Human FcRn 9

1.2.3 Engineering of monoclonal antibodies 10

1.2.3.1 Engineering the Fc domain for improved antibody dependent cellular cytotoxicity (ADCC) 10

1.2.3.2 Engineering of the Fc domain for improved pharmacokinetics 13

1.2.4 Antibody display systems for directed evolution 15

1.3 Research objectives 16

Chapter 2: Engineered, Bacterially Expressed, IgG Antibodies Displaying Selective Binding to Effector FcγRI Receptors **19**

2.1 Introduction 19

2.2 Materials and methods 22

2.2.1 Molecular biology techniques 22

2.2.2 FACS analysis and library screening 24

2.2.3 Expression and purification of Fc proteins 26
2.2.4 Preparative expression and purification of IgG 26
2.2.5 ELISA assays 28
2.2.6 BIAcore analysis for Fc mutants and Herceptin IgG1 Fc mutants 29
2.3 Results 33
2.3.1 Bacterial display of aglycosylated functional homodimeric Fc domains 36
2.3.2 Isolation of mutants aglycosylated Fc fragments exhibiting FcγRI binding 43
2.3.3 Expression of homodimeric Fc domains in *E. coli* and characterization of affinity to FcγRI 46
2.3.4 Expression of aglycosylated trastuzumab in *E. coli* 52
2.4 Discussion 55
Chapter 3: Engineering of Aglycosylated Fc5 for Improved Effector Functions 55
3.1 Introduction 55
3.2 Materials and methods 57
3.2.1 Error prone PCR library for engineering aglycosylated IgG-Fc5 57
3.2.2 Construction of upper CH2 region randomization library 58
3.2.3 Spheroplasting and flow cytometry screening for affinity maturation of Fc5 60
3.2.4 Expression and purification of aglycosylated trastuzumab antibodies 60
3.2.5 BIAcore analysis for aglycosylated trastuzumab antibodies to FcγRI 62
3.2.6 ELISA analysis to measure the affinity of trastuzumab antibodies to Fc receptors 63

3.2.7 Preparation of human monocyte-derived dendritic cells (mDCs) 64
3.2.8 ADCC assays 65
3.3 Results 68
3.3.1 Isolation of aglycosylated Fc mutants exhibiting higher affinity to FcγRI binding compared to Fc5 68
3.3.2 Characterization of aglycosylated trastuzumab-Fc601 in *E. coli* 76
3.3.3 mDC mediated tumor cells killing by aglycosylated trastuzumab-Fc5 and trasutuzumab-Fc601 81
3.3.4 Isolation of aglycosylated Fc mutants exhibiting higher affinity to FcγRI binding than Fc5 with retaining pH dependent FcRn binding 84
3.3.5 Characterization of aglycosylated trastuzumab-Fc701 88
3.4 Discussion 92
Chapter 4: Development of high-throughput antibody screening system for immobilized antigen 95
4.1 Introduction 95
4.2 Materials and methods 99
4.2.1 Reagents 99
4.2.2 Construction of plasmids for anchored antibody and GFP 99
4.2.3 Digoxigenin immobilization onto beads 100
4.2.4 Culture conditions 101
4.2.5 Preparation of spheroplasts and FC analysis 101
4.2.6 Spheroplast enrichment onto beads with immobilized digoxigenin 102
4.3 Results 105

4.3.1 Display of scFv antibodies on *E. coli* inner membrane 105

4.3.2 Binding of spheroplasts on the antigen immobilized beads 108

4.3.3 Enrichment of 26-10 scFv anchoring spheroplasts 110

4.4 Discussion 112

Chapter5: Conclusion and Recommendations 116

5.1 Conclusion 116

5.2 Recommendations 118

Appendix 1: Bacterally Expressed Aglycosylated Fc Receptors 121

A1.1 Introduction 121

A1.2 Materials and methods 122

A1.2.1 Construction of plasmids for the expression of FcγRs 122

A1.2.2 Expression and purification of of FcγRs 123

A1.2.3 ELISA analysis 123

A1.3 Results 127

A1.3.1 Expression of aglycosylated FcγRs in *E. coli* 128

A1.3.2 Purification and of refolding FcγRs 131

A1.3.3 Affinity of aglycosylated FcγRs 132

A1.4 Discussion 134

Appendix 2: Development of covalently anchored full length IgG display system 134

A2.1 Introduction 134

A2.2 Materials and methods 136

A2.2.1 Solube expression and purification of homodimeric wild type Fc and Fc2a fragments 136

A2.2.2 Production and purification of full length aglycosylated trastuzumab IgG1 and aglycosylated trastuzumab-Fc2a 137
A2.2.3 ELISA analysis 139
A2.2.4. Construction of plasmids for covalently anchored full length IgG display system 140
A2.2.5 Preparation of spheroplasts and FACS analysis 141
A2.3 Reuslts 145
A2.3.1 Affinity of Fc2a (S298G/T299A) and trastuzumab-Fc2a to human FcγRIIa 145
A2.3.2 FACS analysis for the covalently anchored full length IgG display system to engineer IgG heavy chain 147
A2.4 Discussion 152
Appendix 3: *E. coli 2* Hybrid Systems for Engineering of Aglycosylated Antibody Fc 154
A3.1 Introduction 154
A3.2. Materials and methods 155
A3.2.1 Reagents 155
A3.2.2 Construction of plasmids for the display of homodimeric IgG-Fc 155
A3.2.3 Culture conditions for two plasmids system 158
A3.3 Results 162
A3.4 Discussion 167
Bibliography 168
Vita 181

List of Tables

Table 2-1. Plasmids used in this study……..**31**

Table 2-2. Primers used in this study ……...**32**

Table 2-3. Kinetic rates and equilibrium dissociation constants of isolated Fc mutants determined by BIACore analysis..…….....……...**46**

Table 2.4. Kinetic rates and equilibrium dissociation constants of trastuzumab antibodies determined by BIACore analysis..…….**49**

Table 3-1. Plasmids used in this study……..**66**

Table 3-2. Primers used in this study……**67**

Table 3.3. Kinetic rates and equilibrium dissociation constants obtained by BIACore analysis for binding to FcγRI…….**78**

Table 3.4. Kinetic rates and equilibrium dissociation constants for trastuzumab antibodies obtained by BIACore analysis for binding to FcγRI……**89**

Table 4-1. Plasmids used in this study……**104**

Table 4-2. Primers used in this study……..**105**

Table 4-3. Enrichment obtained by sorting of 26-10 and M18 scFv mixture (1:1,000).**111**

Table A1-1. Plasmids used in this study…….**124**

Table A1-2. Primers used in this study……...**125**

Table A2-1. Primers used in this study……...**143**

Table A2-2. Plasmids used in this study…….**144**

Table A3-1. Plasmids used in this study…….**160**

Table A3-2. Primers used in this study….....**161**

List of Figures

Figure 1-1. Comparison of protein expression systems……..**2**

Figure 1-2. Structure of IgG and Fc region of the IgG……...**5**

Figure 1-3. Carbohydrate sequence linked at the Asn297…….……**6**

Figure 1-4. Human Fc receptors…….**7**

Figure 2-1. Binding epitopes of FcγR proteins and C1q on IgG-Fc…….**21**

Figure 2-2. Schematic diagram showing the display system……**22**

Figure 2-3. Expression cassette for periplasmic display of Fc…….**35**

Figure 2-4. Effect of trehalose on periplasmic display of Fc…....……..**35**

Figure 2-5. Fluorescence histogram of spheroplasted cells from different rounds of sorting labeled with FcγRI-FITC..…….**37**

Figure 2-6. Fluorescence histogram of spheroplasted cells expressing either wt IgG Fc protein or high fluorescence mutants isolated from the fourth round……**38**

Figure 2-7. Protein sequences of isolated Fc mutant clones exhibiting high affinity to FcγRI..……**39**

Figure 2-8. Location of mutations for isolated aglycosylated Fc domains displayed FcγRI binding, in the 3D structure of glycosylated IgG (PBD Code: 1FC1)……...**40**

Figure 2-9. Saturation mutagenesis of a.a. 382 and 428 and adjacent residues in Fc…...**41**

Figure 2-10. Screening of the saturation library for high affinity Fcs to FcγRI..…….**41**

Figure 2-11. Protein sequences of isolated Fc mutants from the saturation library.....**42**

Figure 2-12. Expression cassette for DsbA leader peptide fused aglycosylated Fc…….**44**

Figure 2-13. Effect of signal peptide on the soluble expression of Fc proteins……**44**

Figure 2-14. Preparative expression of Fc proteins in shake flasks……..**44**

Figure 2-15. Purified wt Fc and high affinity Fc mutant proteins ....……...**45**

Figure 2-16. ELISA result of the purified aglycosylated wild type Fc, Fc5, Fc11, and Fc49……**45**

Figure 2-17. Map of plasmid pSTJ4-Herceptin IgG1……...**47**

Figure 2-18. Example of fed-batch fermentation for the production of aglycosylated trastuzumab or aglycosylated trastuzumab-Fc5 in a 3.3 L fermentor……**48**

Figure 2-19. Expression and purification of aglycosylated wild type or engineered trastuzumab antibodies……...**48**

Figure 2-20. Biacore sensorgrams for aglycosylated and glycosylated trastuzumab antibodies…….....**49**

Figure 2-21. ELISA assays for binding to FcγRIIa-GST……..**50**

Figure 2-22. ELISA assays for binding to FcγRIIb-GST……**50**

Figure 2-23. ELISA assays for pH dependent binding to FcRn. …….**51**

Figure 3-1. Mutation points of isolated aglycosylated Fc5 (382E and 428M) represented on the 3D structure of glycosylated IgG1 Fc (PBD Code: 1FC1)……**69**

Figure 3-2. The location of 382E in β-sheet C and 428M in β-sheet F of CH3 domain represented on the crystal structure of glycosylated IgG. (PBD Code: 1FC1)……..**70**

Figure 3-3. Error prone PCR library for engineering aglycosylated Fc5 domain…….**71**

Figure 3-4. Fluorescence histogram of spheroplasts labeled with FcγRI-FITC showing the enrichment by series rounds of FACS sorting…….**71**

Figure 3-5. Protein sequences of isolated Fc mutant clones exhibiting higher affinity to FcγRI than Fc5……...**72**

Figure 3-6. Amino acid substitutions in variants Fc601-619 represented on the 3D structure of glycosylated IgG1 Fc (PBD Code: 1FC1)……..**73**

Figure 3-7. Fluorescence histogram of spheroplasts expressing wild type Fc, Fc5, or Fc601 labeled with 30 nM of FcγRI-FITC……..……..**74**

Figure 3-8. Amino acid substitutions in Fc601 (K338R, G341V, E382V, M428I) represented on the 3D structure of glycosylated IgG1 Fc (PBD Code: 1FC1)……..**75**

Figure 3-9. Map of plasmid pSTJ4-Herceptin IgG1…….**77**

Figure 3-10. BIACore sensorgram for aglycosylated trastuzumab (A) and aglycosylated trastuzumab-Fc601 (B)……..**78**

Figure 3-11. ELISA assays for binding of trastuzumab antibodies to FcγRIIa-GST…...**79**

Figure 3-12. ELISA assays for binding of trastuzumab antibodies to FcγRIIb-GST…...**79**

Figure 3-13. ELISA assays for binding of trastuzumab antibodies to FcγRIIIa……...**80**

Figure 3-14. ELISA assays for pH dependent binding to FcRn at pH 7.4 and 6.0……...**80**

Figure 3-15. Flow cytometry histogram showing the expression of CD11c on activated DCs…… ….…….....**82**

Figure 3-16. Flow cytometry histogram showing the expression of FcγRI on activated DCs……**82**

Figure. 3-17. Antibody dependent cellular cytotoxicity (ADCC) induced by engineered aglycosylated Fc antibodies……...**83**

Figure 3-18. Library for the selection of higher affinity Fc fragments to FcγRI than Fc5 with pH dependent FcRn binding……..**85**

Figure 3-19. Protein sequences of isolated Fc mutant clones exhibiting higher affinity to FcγRI than Fc5….....**85**

Figure 3-20. Summary of mutations in Fc701 – 709……**86**

Figure 3-21. Fluorescence histogram of spheroplasted cells for wild type Fc, Fc5, Fc701, and Fc702 labeled with 1 nM of FcγRI-FITC…..…….…….....**86**

Figure 3-22. Fluorescence histogram of spheroplasted cells displaying wild type Fc, Fc5, Fc601, and Fc701 after labeling with 1 nM of FcγRI-FITC....……..**87**

Figure 3-23. Mutation points of isolated aglycosylated Fc701 represented on the 3D structure of glycosylated IgG1 Fc (PBD Code: 1FC1)……..**87**

Figure 3-24. BIAcore sensorgrams of aglycosylated trastuzumab-Fc701 antibody with binding to FcγRI……**89**

Figure 3-25. ELISA assays for pH dependent binding to FcRn at pH 6.0 and 7.4 .....**90**

Figure 3-26. ELISA assays for binding of trastuzumab antibodies to FcγRIIa-GST…...**90**

Figure 3-27. ELISA assays for binding of trastuzumab antibodies to FcγRIIb-GST…...**91**

Figure 3-28. ELISA assays for binding of trastuzumab antibodies to FcγRIIIa……...**91**

Figure 4-1. Selection of APEx spheroplasts via antibody-antigen interactions……**98**

Figure 4-2. Inner Membrane anchoring of scFvs display……...**107**

Figure 4-3. FC analysis of spheroplasts with beads containing immobilized antigen……..**109**

Figure 4-4. Enrichment of 26-10 scFv clones from a 1,000 excess of M18 scFv-gp3 by binding to beads with immobilized digoxigenin……..**111**

Figure A1-1. Gene casettes for the expression of FcγRIIa, FcγRIIb, and FcγRIIIa…...**128**

Figure A1-2. Expression of FcγRIIa, FcγRIIb, and FcγRIIIa…….**129**

Figure A1-3. Western blot showing the expression of FcγRI depending on the codon optimization, the terminal tag location, and the various DE3 lysogen containing *E. coli* strains……...**130**

Figure A1-4. SDS-PAGE showing the purified Fc receptors.……....**131**

Figure A1-5. ELISA assays for purified FcγRs (FcγRI, FcγRIIa, FcγRIIb, FcγRIIIa).**132**

Figure A2-1. Purified wild type Fc and Fc2a proteins. ……..**146**

Figure A2-2. ELISA assays showing the affinity of aglycosylated Fc fragment (Fc2a) and aglycosylated full length trastuzumab-Fc2a to FcγRIIa……**146**

Figure A2-3. Covalently anchored full length IgG display system …...……**147**

Figure A2-4. Fluorescence histograms showing the binding of FcγRI using either the 2-plasmid system or the dicistronic system…….**149**

Figure A2-5. Fluorescence histograms showing the binding of FcγRIIa using either the 2-plasmid system or the dicistronic system…….……**150**

Figure A2-6. FACS analysis of cells displaying covalently anchored full length IgG expressed by 2 plasmids and bound by FcγRI…….**151**

Figure A2-7. FACS analysis of cells displaying covalently anchored full length IgG expressed by 2 plasmids and bound by FcγRIIa …….……..……..**151**

Figure A3-1. Two plasmids system for the periplasmic display of Fc using cJun-cFos or cJun(Cys)-cFos(Cys) interaction…….**164**

Figure A3-2. FACS analysis results of periplasmic displayed Fc homodimer using cJun-cFos and cJun(Cys)-cFos(Cys) interaction pairs…….**165**

Figure A3-3. Two plasmids system for the periplasmic display of Fc using ColE2-Im2 interaction……**166**

Figure A3-4. Effect of ColE2 on the expression of target proteins, M18 scFv (Lane 1-3), 26-10 scFv (Lane 4-6), and Fc (Lane 7-9)……...**166**

Chapter 1

Introduction and Background

1. 1 INTRODUCTION

Currently, more than 20 monoclonal antibodies have been approved (Chames et al., 2009; Wang et al., 2007), and more than one hundred antibody drugs are in the clinical trial pipeline (Dimitrov and Marks, 2009; Reichert et al., 2005). Monoclonal antibodies currently constitute about a quarter of all biopharmaceutical products (Schrama et al., 2006). The market has expanded since the approval of the first monoclonal antibody product in 1986 and is forecasted to reach $26 billion in sales by 2010 (Chames et al., 2009).

Antibodies function by recognizing target cells through their so-called variable region which differs from antibody to antibody. In addition, the constant region of the antibody molecule binds to receptors present on a variety of immune cells. Antibodies bound on the surface of a target cell recruit leukocytes (white blood cells) which in turn destroy the target via a variety of mechanisms. The ability of antibodies to recruit cells is termed “the effector function” of the antibody and depends critically on the presence of a carbohydrate moiety attached to Asn297 in the constant region. In its absence, antibodies exhibit no binding to immune cells and thus do not display effector functions.

While antibody molecules can be expressed in different hosts (Fig. 1-1), expression in mammalian cells is necessary for proper glycosylation that gives desirable effector functions. From a production standpoint, antibodies produced in mammalian

cells are expensive and time consuming to produce. Also, heterogeneity of antibody carbohydrate structures causes loss of efficacy and problems in product quality control.

Alternatively, expression in bacteria allows production of antibodies in a host cell with tractable genetics, ease of genetic manipulation, rapid expression, low cost, and high yield, and facile scale-up. Two major drawbacks of bacterial systems for antibody production are the potential for improper folding and lack of glycosylation machinery. As a result, use of bacterial produced antibodies is mostly limited to research or diagnostic purposes rather than therapeutic purposes requiring effector functions. To satisfy both therapeutic and industrial demands, this dissertation is focused on the development of a screening system for bacterial produced aglycosylated Fc domains and on the isolation of engineered aglycosylated IgGs showing high effector functions.

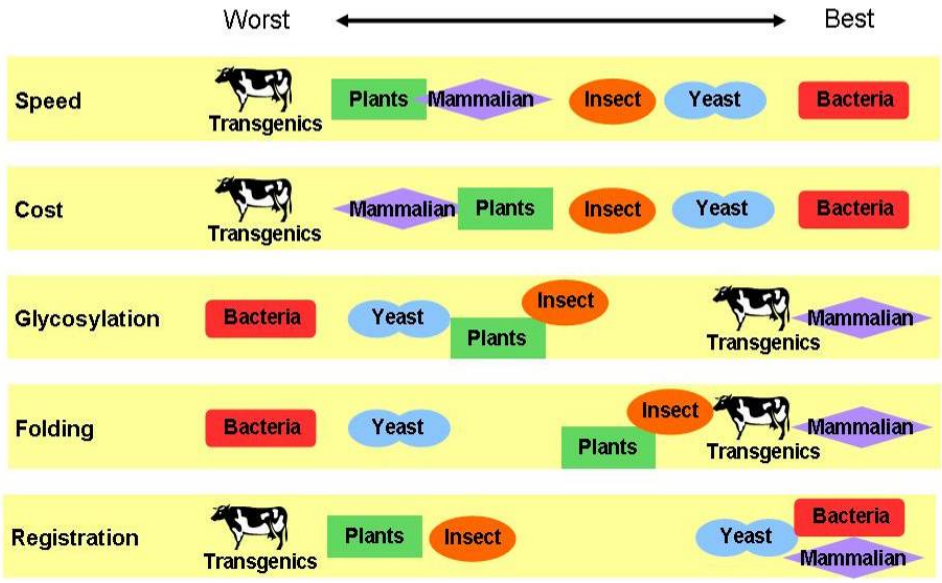

Figure 1-1. Comparison of protein expression systems. Hosts for protein expression including mammalian cells, insect cells, transgenics, plant cells, yeast, and bacteria were compared in the aspect of speed, cost, glycosylation, protein folding, and drug registration (Cox, 2004).

1. 2 BACKGROUND

1.2.1 Structure and function of immunoglobulin and Fc

Immunoglobulins, or antibodies, are globular glycoproteins involved in humoral immunity. The protein backbone of antibodies is composed of two identical heavy and two light polypeptide chains. The immunoglobulins found in human body fluids can be divided into five major classes (IgG, IgA, IgM, IgD, and IgE) based on the difference in amino acid sequences for the constant regions of the heavy polypeptide chains. IgG, the major immunoglobulin making up about 75 percent of the total serum immunoglobulin content (McKelvey and Fahey, 1965; Spiegelberg, 1974), recognizes, neutralizes, and eliminates foreign pathogens, defective human cells and soluble toxic molecules (Kaneko et al., 2006). Until now all of the monoclonal antibody drugs approved by US FDA have been of the IgG class. IgG antibodies are further categorized by four distinct subclasses (IgG1, IgG2, IgG3, and IgG4) that have distinguishable structural difference in the heavy chain polypeptides. Among the four subclasses, the most extensively studied is IgG1 due to its high concentration in serum and favorable immunological properties.

Human IgG molecules (~150 kDa) have a common structure of four polypeptide chains comprising two identical heavy (~ 2 × 50 kDa) and two identical light chains (~ 2 × 25 kDa) combined by inter-chain disulfide bonds (Fig. 1-2A) to form Y shaped structure. The heavy chains are constructed of four domains including an N-terminal variable domain (VH) and three constant domains CH1, CH2, and C-terminal CH3. The light chains are composed of two domains, a variable domain (VL) and a constant domain (CL). By proteolytic or functional fragmentation, IgG molecule can be also

divided into two identical Fabs (fragment antigen binding) and one Fc (fragment crystalizable) fragments.

The Fab domain is composed of a full light chain (VL and CL) and parts of heavy chain (VH and CH1) bridged by a disulfide bond at the carboxy terminal ends of the chains. The Fc region is formed by dimerization of CH2, and CH3 domains and has a highly conserved amino acid composition. The major function of the Fc is to regulate effector functions by binding to immune components proteins such as Fcγ receptors (FcγRI, FcγRII, FcγRIII), the serum complement C1q protein, and the neonatal Fc receptors (FcRn) (Duncan and Winter, 1988; Ghetie and Ward, 2000; Jefferis et al., 1998). The native human IgG has two N-linked biantennary oligosaccharide chains attached at Asn297 of each CH2 domain. The two carbohydrate chains are located between the CH2 domains and interact with hydrophobic parts of the Fc domains (Fig. 1-2B). The structure of the core carbohydrate residues containing *N*-acetylglucosamine (GlcNAc) and mannose (Man) is highly conserved. Highly variable carbohydrate residues including terminal *N*-acetylneuraminic acid (NeuAc: sialic acid), galactose (Gal), bisecting N-acetylglucosamine (GlcNAc) and fucose (Fuc) can be appended to these core carbohydrate (Fig. 1-3). Glycan heterogeneity is influenced by many factors such as cell line, culture condition, and downstream processing (Wang et al., 2007). Currently about 30 different glycan structures resulting in different orientations of CH2 domain pairing have been characterized (Burton and Dwek, 2006). Effector functions are largely dependent on the constituents of the oligosaccharide chains (Jefferis, 2005; Wright and Morrison, 1997).

A

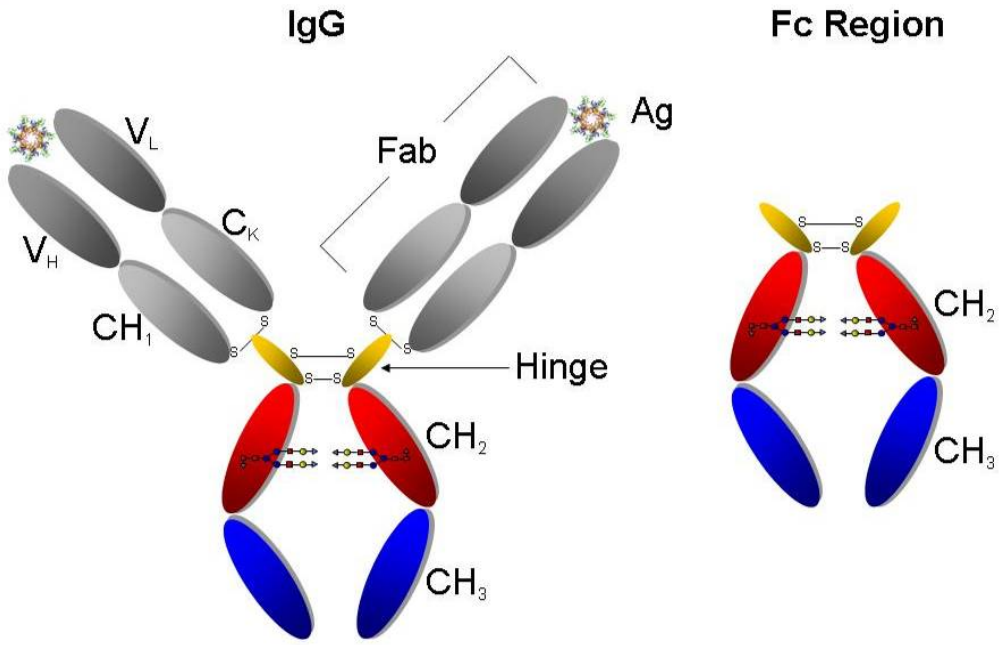

B

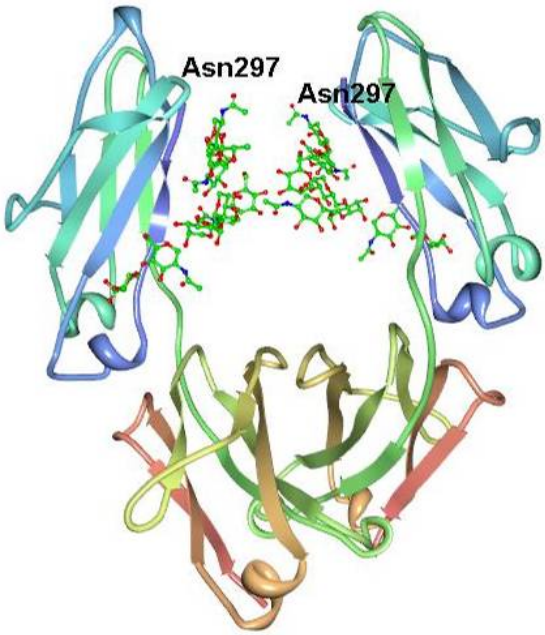

Figure 1-2. Structure of IgG and Fc region of the IgG. (a) Schematic structure IgG and Fc region of the IgG. (b) Crystral structure of homodimeric Fc (PDB: 1FC1).

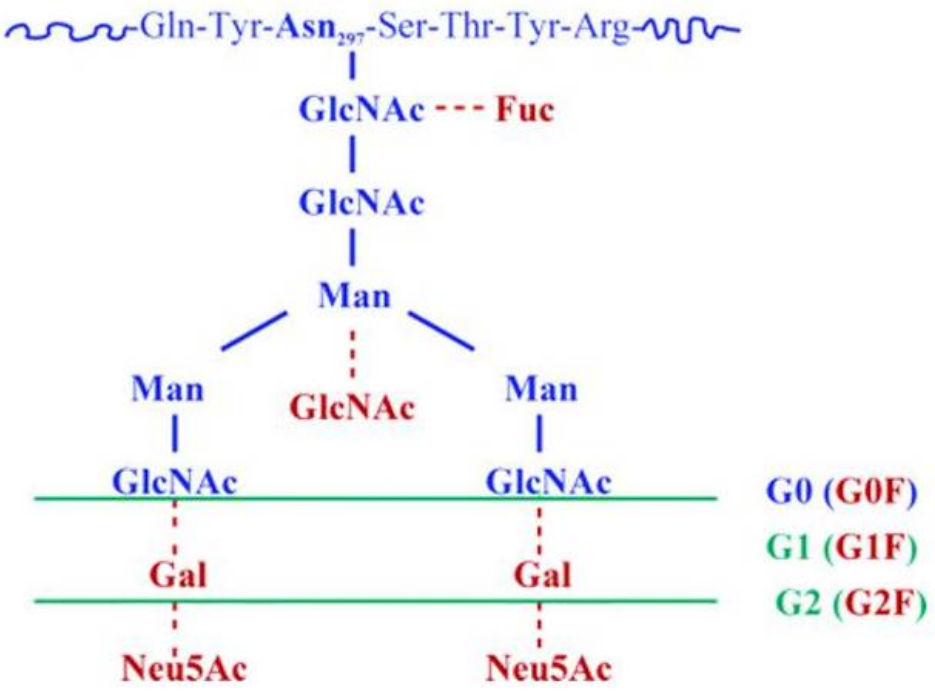

Figure 1-3. Carbohydrate sequence linked at the Asn297 (Jefferis, 2005).

In the absence of glycosylation, the Fc domain is not recognized by the various proteins it normally binds to and effector functions are abolished. Lack of glycosylation causes reduced binding to FcγRI by 2 orders of magnitude and completely eliminates the normally weak binding to FcγRII and FcγRIII (Jefferis, 2005). C1q binding to aglycosylated antibody is also reduced by 10-fold (Lund et al., 1996). The FcRn binding is not significantly affected by aglycosylation (Jefferis, 2005). It has been also reported that the pattern of glycosylation completely determine the ability of antibodies to induce or modulate inflammation (Anthony et al., 2008; Kaneko et al., 2006).

1.2.2 Human Fc receptors

1.2.2.1 Human FcγR

Human FcγRs (Fc gamma receptor) expressed in most immune cells (van de Winkel and Capel, 1993) bridge antibody associated humoral and cellular immune responses by binding to the Fc domain of IgG (Berken and Benacerraf, 1966; Ravetch and Bolland, 2001). The FcγRs initiate and regulate effector functions including phagocytosis, cytokine production, superoxide production, release of serotonin, and inhibition of B cell activation (Cohen-Solal et al., 2004). Currently three groups of human FcγRs (FcγRI, FcγRII, and FcγRIII) have been categorized based on differences in gene sequence, regulation, function, affinity to IgG, and expression in different cells (Ivan and Colovai, 2006). Human FcγRs except the FcγRIIIb are type I transmembrane glycoproteins (Fig. 1-4).

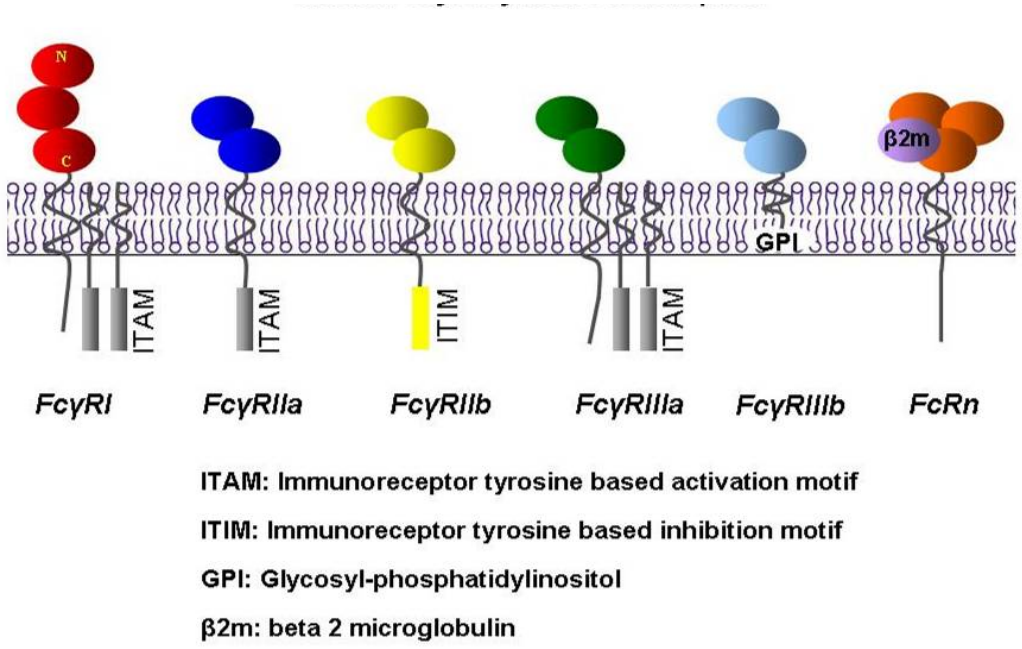

Figure 1-4. Human Fc receptors.

FcγRs can be divided into two groups, activating FcγRs and inhibitory FcγRs. Activating FcγRs such as FcγRI (CD64), FcγRIIa (CD32a), and FcγRIIIa (CD16a) have an Immunoreceptor Tyrosine-based Activation Motif (ITAM) in their cytoplasmic tail and trigger activation of immune responses. On the other hand, FcγRIIb (CD32b) has an Immunoreceptor Tyrosine-based Inhibitory Motif (ITIM) in its cytoplasmic tail and downregulates immune responses and therefore it acts as the inhibitory FcγR (Ravetch and Bolland, 2001). FcγRI exhibits high affinity to monomeric IgG ($K_d = 10^{-8}$~10^{-9} M) whereas the affinity of FcγRII and FcγRIII to monomeric IgG is low ($K_d = 10^{-6}$~10^{-7} M) (Krapp et al., 2003).

FcγRI is expressed mainly on monocytes, macrophages, and dendritic cells. Upon activation by cytokines such as IFN-γ, IL-10, and G-CSF, it is also expressed on neutrophils and eosinophils (Schmidt and Gessner, 2005). Kacskovics proposed that FcγRI is important in the early stage immune response when antibody concentration is low (Kacskovics, 2004). The binding affinity of the FcγRI to IgG is different depending on IgG subclasses. It has high affinity to IgG1 and IgG3 and low affinity to IgG2 and IgG4. FcγRIIa found on macrophages, monocytes, dendritic cells, neutrophils, and eosinophils activates immune cells (Siberil et al., 2006). Conversely, FcγRIIb expressed on B lymphocytes mast cells, macrophages and dendritic cells suppresses immune cells while preventing autoimmunity (Cohen-Solal et al., 2004; Ravetch and Lanier, 2000). The FcγRIII receptors show low affinity to IgG and are expressed on natural killer (NK) cells, T-cells, macrophages, monocytes, mast cells, and dendritic cells and activates ADCC (Cohen-Solal et al., 2004).

Among the human FcγRs, the structures for the extracellular domains of FcγRs including FcγRIIa [PDB code 1H9V (Sondermann et al., 2001) and 1FCG (Maxwell et al., 1999)], FcγRIIb [PDB code 2FCB (Sondermann et al., 1999)], and FcγRIIIb [PDB code 1E4J (Sondermann et al., 2000)] have been solved. The structures of FcγRIIIb extracellular domain bound to human Fc CH2 region [PDB code 1E4K (Sondermann et al., 2000), 1IIS, 1IIX, 1T83, and 1T89 (Radaev et al., 2001)] is also available. However, structural information for FcγRI is not available.

1.2.2.2 Human FcRn

The neonatal Fc receptor (FcRn) was identified during studies of neonatal rat absorbing maternal immunoglobulins from ingested milk (Brambell et al., 1958; Jones and Waldmann, 1972). It is a heterodimer composed of a transmembrane heavy FcRn α chain and a β2-microglobulin. The human FcRn α chain has one potential glycosylation site (West and Bjorkman, 2000) and is highly homologous to MHC class I α chain in sequence and domain structure. The light chain of FcRn, β2-microglobulin does not only provide structural support but also contacts the Fc domain of IgG as shown via the crystal structure of rat FcRn bound IgG Fc fragments [PDB code 1FRT (Burmeister et al., 1994b) and 1I1A (Martin et al., 2001)].

Two FcRn molecules bind to one Fc homodimer with making 2:1 FcRn-Fc complex (Raghavan and Bjorkman, 1996). The binding of FcRn to the Fc domain of IgG is strongly pH dependent. It exhibits high affinity under slightly acidic pH condition and low affinity at neutral or basic pH (Ober et al., 2004a; Ober et al., 2004b; Raghavan and Bjorkman, 1996; Rodewald, 1976). The pH-dependent binding is critically important for

the regulation of serum IgG concentration by allowing pinocytosed IgGs to make strong IgG-FcRn complexes in acidified endosomes for recycling to blood across vascular endothelial cell membrane instead of degradation in lysosomes (Ghetie and Ward, 2000).

1.2.3 Engineering Fc domain of monoclonal antibodies

Antibodies are highly specific and can bind to target molecules (antigens) with high affinities. Apart from antigen binding, the therapeutic efficacy and pharmacokinetics of the monoclonal antibodies are determined by the effector functions triggered by (i) binding of the Fc domain to FcγRs for ADCC (Antibody dependent cell mediated cytotoxicity) resulting in the elimination of antibody bound target cells by effector immune cells, (ii) binding of complement factors for CDC (Complement dependent cytotoxicity) which involves the killing of target cells by the immune complement system, and (iii) binding of FcRn for the regulation of serum clearance rate. Therefore, the effector functions of antibodies can be modulated by regulating affinity of Fc to the FcγRs, the complement protein C1q, and to the neonatal Fc receptor.

1.2.3.1 Engineering the Fc domain for improved antibody dependent cellular cytotoxicity (ADCC)

Various methods have been used to enhance binding of antibodies to FcγRs and thus improve ADCC. One approach, termed glycoengineering seeks to optimize the composition of the carbohydrate attached to Asn297. Alternatively, protein engineering seeks to optimize the sequence of the Fc polypeptide for improved binding (Presta, 2006). IgG Fc regions produced in animal cells contain an N-linked glycan at Asn297.

The carbohydrate sequence can be heterogeneous depending on the type of cells that express the antibodies (for *in vitro* production), culture conditions and the state of the B lymphocytes (in animals) (Fig. 1-3). Most of the heterogeneity is derived from terminal sialic acid and galactose residues. The carbohydrate structure has an essential function in stabilizing the IgG molecule by contributing to structural stability of CH2 and CH3 regions (Sondermann et al., 2001). It has been reported that truncated or deglycosylated antibodies prevent FcγR or C1q binding (Mimura et al., 2001; Radaev and Sun, 2001; Simmons et al., 2002).

Protein engineering that has been employed for the optimization of IgG Fc amino acid residues has been performed to improve binding to FcγR. A variety of site directed mutation studies showed that the lower hinge region (230-236) is critical for FcγR binding (Armour et al., 2003; Duncan et al., 1988; Lund et al., 1991; Shields et al., 2001). By making a single mutation (E235L) in mouse IgG2b, Duncan *et al*. showed 100-fold increased binding to FcγRI. Using alanine scanning mutagenesis, Shields *et al*. identified critical amino acids that interact with FcγRI, FcγRIIa, FcγRIIb, FcγRIIIa, and FcRn. Subsequent mutations to non-alanine of some of these critical residues showed improved or reduced binding to specific FcγRs individually or simultaneously. Mutants with improved binding to activating FcγRs also exhibited enhanced ADCC (Shields et al., 2001).

Lazar *et al.* selected mutated glycosylated Fc variants using a computational design algorithm followed by semi-automated high throughput screening. They isolated mutants (S239D/I332E/A330L) and (S239D/I332E) showing enhanced affinity to FcγRIIIa and reduced affinity to FcγRIIb. They also showed more than 2 orders of

magnitude enhanced *in vitro* ADCC for the selected mutants (S239D/I332E/A330L and S239D/I332E) and *in vivo* cytotoxicity for the mutant (S239D/I332E) compared to wild type IgG (Lazar et al., 2006). Using structure based high throughput mutagenesis, Richards *et al.* isolated a G236A Fc variant displaying selectively high affinity binding to FcγRIIa relative to FcγRIIb. The glycosylated Fc variants with the single mutation (G236A) showed significantly enhanced antibody dependent cell-mediated phagocytosis (ADCP) mediated by macrophages. The combination of this mutation with the previously isolated mutations (S239D/I332E) could further improve ADCP and NK cells mediated ADCC (Richards et al., 2008).

In addition to the structure based approach, a combinatorial screening approach using yeast surface displayed Fc library and FACS screening was also employed to isolate high affinity glycosylated Fc variants. Stavenhagen *et al.* used an initial round of negative selection of Fc libraries to FcγRIIb immobilized on magnetic beads to recover Fc clones not showing high binding affinity to inhibitory FcγRIIb reeptors. Following sequential rounds of FACS screening using tetravalent biotinylated FcγRIIIa-streptavidin-PE (Phycoerythrin) complex, they isolated glycosylated Fc variants exhibiting high affinity to FcγRIIIa and low affinity to FcγRIIb. Two Fc variants containing either five mutations (F243L/R292P/Y300L/V305I/P396L) or three mutations (F243L/R292P/Y300L) showed more than about 100-fold enhanced NK cells mediated ADCC (Stavenhagen et al., 2007).

Recently, structure-based mutagenesis and, in a separate study, the screening of mixture of saturation libraries (amino acid residues at 296-299, 297-299, and 297-300) of the FcγRIIa binding epitope within the CH2 C'/E loop by yeast display were used to

isolate aglycosyated IgG1 variants lacking N297 or carrying mutations in residues S298 and T299 that conferred binding to FcγRIIIa or FcγRIIa, respectively (Lazar et al., 2009; Sazinsky et al., 2008). However, the antibody variants, expressed in HEK293 or 293T cells were also found to also exhibit significant binding to the inhibitory FcγRIIb receptor, a result that is not unexpected given the overlap of the binding epitopes and the high degree of homology of FcγRIIa and FcγRIIb (Sazinsky et al., 2008).

1.2.3.2 Engineering of the Fc domain for improved pharmacokinetics

Site directed mutagenesis, and sequence homology comparison using rodent IgG Fc and FcRn led to the identification of critical amino acid residues for the interaction between IgG and FcRn (Kim et al., 1994; Medesan et al., 1998; Medesan et al., 1997; Medesan et al., 1996). The critical residues (Ile253, His310, and His435) are located at the interface of CH2 and CH3 domains, similar to the binding site for staphylococcal Protein A (SpA) (Kim et al., 1994; Shields et al., 2001). X-ray crystallographic experiments of the rat FcRn bound rat Fc provided important amino acid residues of Fc for FcRn binding (Burmeister et al., 1994a; Burmeister et al., 1994b; Martin et al., 2001; West and Bjorkman, 2000).

It has been suggested that engineering of Fc region of the IgG binding to FcRn could provide engineered monoclonal antibodies with enhanced pharmacokinetic properties (Medesan et al., 1998; Vaughn et al., 1997). Based on the intracellular trafficking and recycling mechanisms, engineered IgGs with enhanced affinity to FcRn at pH 6.0 while preserving pH dependent binding have been developed and shown to

exhibit improved serum persistence (Dall'Acqua et al., 2002; Dall'Acqua et al., 2006; Ghetie et al., 1997; Hinton et al., 2006).

Guided by the crystal structures of rat (Burmeister et al., 1994a) and human FcRn (West and Bjorkman, 2000) and by computational modeling of the rat FcRn–rat Fc complex (Weng et al., 1998), Hinton *et al.* substituted three amino acid residues (Thr250, Leu314, and Met428) of IgG2 to all the other 19 amino acids and then determined the binding to FcRn expressed on the cell surface through competitive binding assays. Two mutations (T250Q) and (M428L) increased affinity to FcRn. In a rhesus monkey serum stability model, a single mutant (M428L) showed 2-fold longer half-life and a 2.6-fold improvement was observed for the double mutant (T250Q/M428L) (Hinton et al., 2004). These two mutations were introduced into different IgG subtypes, IgG1 and IgG4. The IgG1 mutant (T250Q/M428L) showed ~2.5 fold improved serum half-life in the same rhesus monkey model (Hinton et al., 2006).

Screening of libraries by phage display was employed for the isolation of high affinity Fc variants to human FcRn under slightly acidic condition (pH 6.0). A triple mutation (M252Y/S254T/T256E) in IgG-Fc at the CH2-CH3 interface enabled about 10-fold increase in pH dependent FcRn affinity at pH 6.0 and about 4-fold improvement of serum half-life in the cynomolgus monkey model (Dall'Acqua et al., 2006; Dall'Acqua et al., 2002; Oganesyan et al., 2009). The N434A mutant Fc domain exhibiting increased affinity to human FcRn selectively at pH 6.0 could improve about 2 fold in serum half-life. In contrast, the N434W mutant Fc domain showing improved affinity both at pH 6.0 and pH 7.4 and did not improve the IgG pharmacokinetics highlighting the critical

relationship between pH dependent FcRn binding and serum half life of therapeutic antibodies (Yeung et al., 2009).

1.2.4 Antibody display systems for directed evolution

The isolation of antibodies exhibiting high affinity and specificity for target antigens is of great importance for numerous aspects of biotechnology ranging from proteomics to the development of therapeutics. Starting in the 1980s, the isolation of useful recombinant antibody fragments has been greatly facilitated by the introduction of display technologies for the screening of large libraries of antibody genes (Hoogenboom, 2005). Antibody display systems rely on the establishment of a physical linkage between an antibody gene and the antibody itself. In phage display, the first technique used for antibody fragment isolation from repertoire libraries, polypeptides are presented on the surface of filamentous bacteriophage via fusion to a phage coat protein (Smith, 1985). Numerous antibodies to widely diverse antigens have been isolated from either immune repertoires or synthetic libraries by employing sequential rounds of filamentous phage panning against immobilized antigen (Bradbury and Marks, 2004). Alternatively, very high affinity antibodies have been isolated using display on bacteria (Daugherty et al., 2000a; Daugherty et al., 2000b; Georgiou et al., 1997; Lofblom et al., 2005) or yeast (Boder et al., 2000; Boder and Wittrup, 1997; Feldhaus et al., 2003) in conjuction with flow cytometric screening for antigen-binding clones (Mattanovich and Borth, 2006).

Harvey *et al*. developed a new *E. coli* protein display system, called Anchored Periplasmic Expression (APEx) (Harvey et al., 2004). This technology relies on fusing the protein of interest to an inner membrane anchor such as a transmembrane segment of

a native inner membrane protein (Jeong et al., 2004), an anchoring motif derived from a lipoprotein (Pugsley, 1993; Sankaran and Wu, 1994), or an exogenous protein such as the M13 phage coat protein gp3 (Barbas Cf et al., 1991). Spheroplasting using EDTA and lysozyme is then used to remove the outer membrane allowing the inner membrane-anchored polypeptide to interact and bind to desired ligands. The removal of the outer membrane eliminates the steric barrier presented by lipopolysaccharide and surface carbohydrates and facilitates interactions with much larger soluble ligands, compared to bacterial surface display (Harvey et al., 2004). Recently, our lab developed the *E-clonal* system for the display of full length aglycosylated IgG and the isolation of high affinity IgGs. In this system, periplasmic expressed full length assembled IgG is captured by an APEx displayed Protein A fragment ZZ domain that binds to the Fc region (Mazor et al., 2007).

1.3 RESEARCH OBJECTIVES

As described in the background, natural monoclonal antibodies exhibit three effector functions, antibody dependent cell-mediated cytotoxicity (ADCC), complement dependent cytotoxicity (CDC), and regulation of serum half-life. These effector functions are keys in determining therapeutic efficacy and pharmacokinetics of antibody drugs. I sought to engineer *E.coli* expressed, aglycosylated antibodies exhibiting high affinity and specificity to particular Fc receptors on effector cells. Such engineered aglycosylated antibodies are expected to have improved pharmacological efficacy for cancer therapy and other purposes and, also can be produced efficiently in bacteria at significantly lower costs

In chapter 2, a platform tool for library screening and isolation of engineered aglycosylated antibodies showing high affinity to Fc binding ligands was developed. The system allowed the display of properly folded homodimeric Fc for flow cytometry library screening purposes. Engineered aglycosylated Fc domains showing high affinity and exquisite selectivity to the extracellular domain of FcγRI were isolated using the developed bacterial display system and flow cytometry screening.

In chapter 3, from a variety of combinatorial Fc mutant libraries, affinity maturation was performed to isolate engineered aglycosylated antibodies showing higher affinity to FcγRI and improved effector functions compared to the isolated clone (Fc5) discussed in chapter 2. The effector function of the isolated Fc engineered antibodies was evaluated by monocyte-derived dendritic cells mediated ADCC assays. Also, aglycosylated antibodies were isolated both for improved FcγRI binding and for pH dependent FcRn binding.

In chapter 4, for the isolation of antibodies that bind specifically to insoluble antigens or receptors expressed on the surface of mammalian cells, a new cell (spheroplast)-based method to recognize antigens immobilized on beads was developed. Using the system, it was shown that cells displaying antibody specific to immobilized antigen can be successfully isolated from a mixture with a large excess of non-specific antibody displaying cells.

To deeply investigate the interaction of FcγRs and antibody IgG, aglycosylated FcγRs were expressed in *E. coli*, purified and refolded. This additional study is described in appendix 1. In appendix 2, to engineer aglycosylated Fc domains as full length IgGs, a new full length IgG display system was developed. Optimization of expression system

and culture conditions enabled robust anchoring of full length IgG on *E. coli* inner membrane as well as good tetrameric assembly of antibody heavy chains and light chains. To develop a bacterial display system that is suitable for the isolation of effector functional aglycosylated antibody Fc, a variety of 2 hybrid systems were attemped. This additional study was described in appendix 3.

Chapter 2

Engineered, Bacterially Expressed, IgG Antibodies Displaying Selective Binding to Effector FcγRI Receptors

2.1 INTRODUCTION

Fc receptors (FcRs) play an extremely important role in linking the adaptive immune system to the effector functions of innate cells in antigen presentation and in antibody homeostasis. Humans express six effector FcRs (FcγRI, FcγRIIa, FcγRIIb, FcγRIIc, FcγRIIIa, FcγRIIIb) whose activation by binding to immune complexes results in phagocytosis, cytokine production, superoxide production, release of serotonin, or inhibition of B cell activation (Cohen-Solal et al., 2004; Nimmerjahn and Ravetch, 2008). In addition, binding to the FcRn neonatal receptor mediates intracellular trafficking of IgG for recycling to blood across vascular endothelial cell membrane instead of degradation in lysosomes (Ghetie and Ward, 2000). Human FcγRs, except from FcγRIIIb, are type I transmembrane glycoproteins. Activating FcγRs such as FcγRI (CD64), FcγRIIa (CD32a), and FcγRIIIa (CD16a) have an Immunoreceptor Tyrosine-based Activation Motif (ITAM) in their cytoplasmic tail that triggers activation of immune responses. On the other hand, FcγRIIb (CD32b) has an Immunoreceptor Tyrosine-based Inhibitory Motif (ITIM) in its cytoplasmic tail and downregulates immune responses and therefore it acts as an inhibitory FcγR (Ravetch and Bolland, 2001). The affinity of FcγRII and FcγRIII to monomeric IgG is very low ($K_d = 10^{-6}$~10^{-7}

M) and requires immune compelxed IgG for activation. On the other hand, FcγRI exhibits high affinity to monomeric IgG ($K_d = 10^{-8}$~10^{-9} M) (Krapp et al., 2003).

Unlike FcRn, which binds at CH2-CH3 interface regions of the IgG Fc domain (Roopenian and Akilesh, 2007) and is not significantly affected by the glycosylation status of the antibody, the effector FcγRs interact with the upper CH2 and hinge region (Fig. 2-1) in a manner that is critically dependent on the presence and composition of the single N-linked glycan attached to Asn297. The glycosylation state of IgG determines its affinity for effector FcγRs and thus, modulates the activation of cytotoxic innate immune cells (Desjarlais et al., 2007; Jefferis, 2005). In turn, the destruction of target cells, or antibody dependent cell-mediated cytotoxicity (ADCC), is important for the clinical efficacy and outcomes of widely-used antibody therapeutics (Liu et al., 2008). The glycan composition and glycoform heterogeneity, which is intrinsic to the expression of antibodies in mammalian cells, has a well-documented effect on the response to widely used therapeutics such as Rituxan (rituximab, anti-CD20) and Herceptin (trastuzumab, anti-Her2) (Jefferis, 2005; Liu et al., 2008). This has led to intense efforts to generate improved antibodies via glycoengineering (Desjarlais et al., 2007; Jefferis, 2005; Liu et al., 2008). Wild type aglycosylated antibodies can be expressed at a high yield in bacterial cells and exhibit normal serum persistence and binding to FcRn, but completely lack the ability to bind to effector FcγRs (Simmons et al., 2002).

In this chapter, we report the isolation of bacterially expressed aglycosylated IgG antibodies engineered to enable specific binding to FcγRI. For the engineering of *E. coli* expressed aglycosylated IgG Fc region, we developed a new display system for homodimeric Fcs. Optimized culture and spheroplasting allowed robust display of

homodimeric Fc protein, as required for high throughput flow cytometry screening, without either fusion of inner membrane anchoring domain or coexpression of displaying protein binding ligands (Fig. 2-2). Two amino acids change of CH3 region that is distal from the FcγR binding region (Sondermann et al., 2001) make aglycosylated IgG1 highly selective to FcγRI without increasing affinity significantly to other effector FcγRs including inhibitory FcγRIIb.

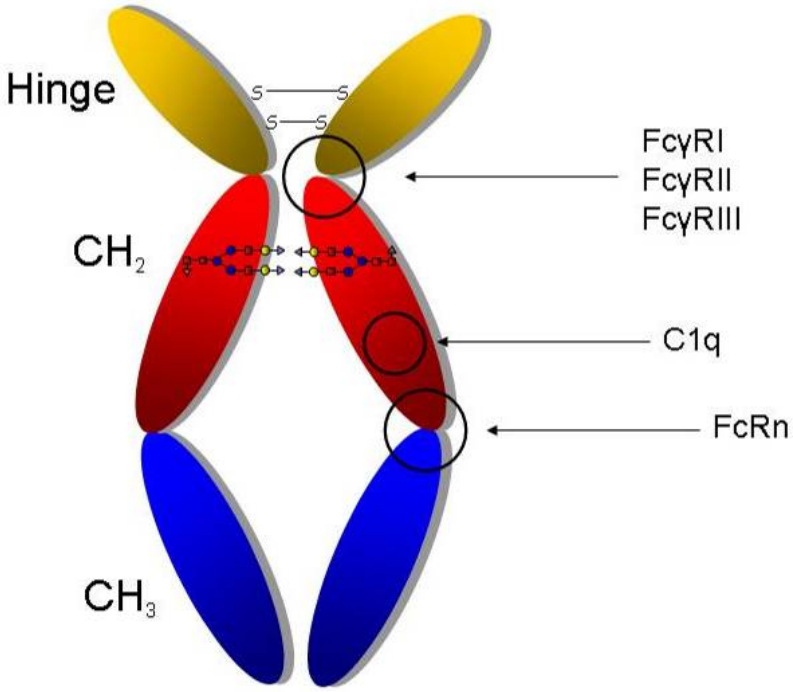

Figure 2-1. Binding epitopes of FcγR proteins and C1q on IgG-Fc (Duncan and Winter, 1988; Jefferis et al., 1998; Kacskovics, 2004).

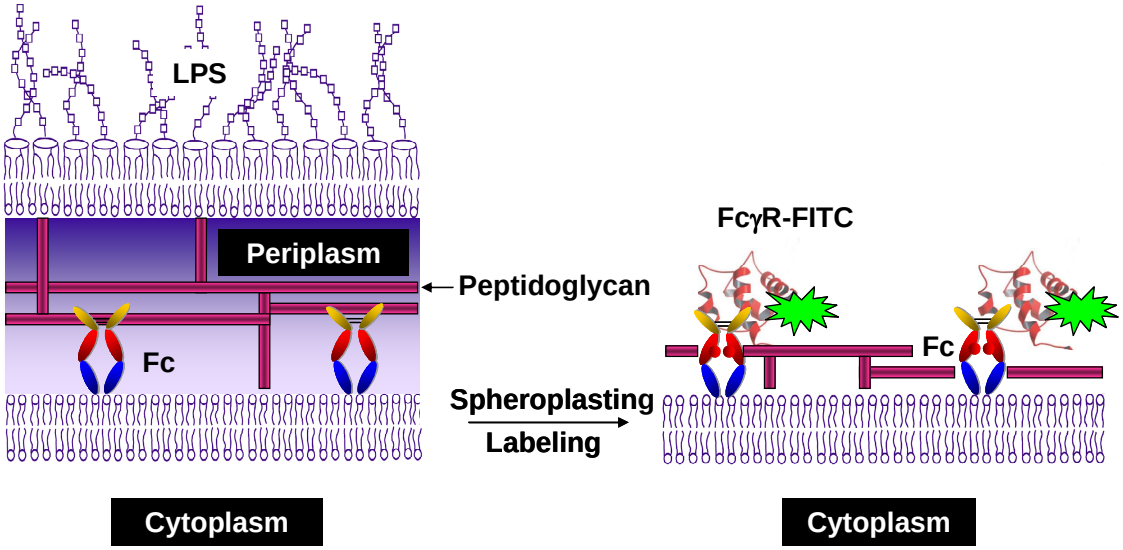

Figure 2-2. Schematic diagram showing the display system. We hypothesize that the Fc protein is entrapped within the cell wall.

2.2 MATERIALS AND METHODS

2.2.1 Molecular biology techniques

All plasmids and primers used in this chapter are described in Table 2-1 and 2-2. Plasmid pPelBFLAG was generated by ligating *Bam*HI-*Hin*dIII digested skp gene from pMopac12 into pMopac1 (Hayhurst et al., 2003) digested with the same restriction endonucleases and by replacing polyhistidine tag and c-myc tag with a sequence encoding the FLAG tag (DYKDDDDK). Subcloning of PCR amplified and *Sfi*I digested Fc gene encoding human IgG1-Fc fragment, hinge, CH2 and CH3 region of human IgG1 heavy chain (McLean et al., 2000) (GeneBank Accession No. AF237583) into *Sfi*I digested pPelBFLAG generated pPelBFLAG-Fc. *Sfi*I digested genes from pMoPac1-

FLAG-M18 for M18 scFv (Harvey et al., 2004) specific for the PA antigen of *Bacillus anthracis* were introduced to pPelBFLAG to generate pPelBFLAG-M18 scFv.

To construct pTrc99A-DsbA-Fc-FLAG, firstly, 53bp of DsbA signal sequence (ATGAAAAAGATTTGGCTGGCGCTGGCTGGTTTAGTTTTAGCGTTTAGCGCAT CGGCG) was introduced using the *Fat*I restriction enzyme that is compatible with *Nco*I of pTrc99A (Amersham Biosciences, Piscataway, NJ) and with *Sal*I restriction enzyme. The PCR products of Fc fragments amplified using primers STJ#144 and STJ#145 were ligated into the *Sal*I and *Hin*dIII restriction enzyme sites of pTrc99A-DsbA plasmid (Table 2-1).

For the construction of pSTJ4-Herceptin IgG1, *E. coli* codon optimized (Hoover and Lubkowski, 2002) VL and VH domains of humanized 4D5 (anti-p185HER2) were synthesized by total gene synthesis with overlap extension PCR using 12 oligonucleotides that included 2 external primers (STJ#302 and STJ#313) and 10 internal primers (STJ#303-312) for VL and 14 primers total 2 external primers (STJ#314 and STJ#327) and 12 internal primers (STJ#315-326) for VH, respectively. The ligation of the amplified VL and VH into pMAZ360-M18.1-Hum-IgG1 using *Nco*I / *Not*I for VL and *Nhe*I / *Hin*dIII restriction endonuclease sites generated pSTJ4-Herceptin IgG1.

For error prone PCR library construction, the standard error prone PCR method (Fromant et al., 1995) was employed using the wt Fc as the template with primers STJ#196 and STJ#197. A random 10 a.a. insertion library was constructed by PCR amplification using forward primer (STJ#194) encoding 10 degenerate codons and reverse primer (STJ#195) with the same template. The amplified PCR fragments were ligated into pPelBFLAG with *Sfi*I restriction sites for error prone PCR library and *Sac*II /

*Eco*RI restriction sites for random 10 a.a. insertion library, respectively. For the three sublibraries randomized around E382V and M428I, PCR products amplified using forward primers (both STJ#283 and STJ#284) and reverse primers (STJ#285, STJ#286, or STJ#287) for each three sublibrary were subcloned into *Sex*AI / *Sap*I digested pPelBFLAG-Fc. The resulting plasmids were transformed into *E. coli* Jude-1(F' [Tn*10(*Tet^r*)* $proAB^+$ $lacI^q$ Δ(*lacZ*)M15] *mcrA* Δ(*mrr-hsdRMS-mcrBC*) ϕ80d*lac*ZΔM15 Δ*lacX74 deoR recA1 araD139* Δ(*ara leu*)7697 *galU galK rpsL endA1 nupG*) (Kawarasaki et al., 2003).

2.2.2 FACS analysis and library screening

E. coli Jude-1 were cultured overnight at 37 °C with 250 rpm shaking in Terrific Broth (TB) with 2% (w/v) glucose. Antibiotics, chloramphenicol (40 μg/ml) or ampicillin (50 μg/ml) were added as needed. Following overnight growth cells were diluted 1:50 in fresh TB medium with 0.5 M trehalose (Fisher Scientific, Fair Lawn, NJ) and antibiotics as needed. After incubation at 37 °C for 3 h cultures were transferred to 25 °C for 20 min with shaking at 250 rpm and protein expression was induced with 1 mM of isopropyl-1-thio-β-D-galactopyranoside (IPTG). Protein expression in cells grown in media without trehalose was performed as above except that the cells were incubated for 2 h instead of 3 h at 37 ºC before IPTG induction.

For library screening, the extracellular domain of glycosylated FcγRI (R&D Systems, Minneapolis, MN) was labeled with FITC according to the manufacturer's instruction (Invitrogen, Carlsbad, CA). Binding of FITC-labeled soluble FcγRI to human

IgG Fc was confirmed by fluorescent ELISA on plates coated with glycosylated human IgG-Fc (Bethyl Laboratories, Montgomery, TX).

Cells were grown and induced with IPTG as above. 5 h after induction, an aliquot of the culture broth equivalent to 8 ml/OD_{600} was harvested by centrifugation and washed two times in 1 ml of cold 10 mM Tris-HCl (pH 8.0). After resuspension in 1 ml of cold STE solution (0.5 M Sucrose, 10 mM Tris-HCl, 10 mM EDTA, pH 8.0) the cells were incubated with rotating mixing at 37°C for 30 min, pelleted by centrifugation at 12,000 × g for 1 min and washed in 1 ml of cold Solution A (0.5 M Sucrose, 20 mM $MgCl_2$, 10 mM MOPS, pH 6.8). The washed cells were incubated in 1 ml of Solution A with 1 mg/ml of hen egg lysozyme (Sigma-Aldrich, St. Louis, MO) at 37 °C for 15 min. After centrifugation at 12,000 × g for 1 min pelleted spheroplasts were resuspended in 1 ml of cold PBS. 200 μl of the spheroplast suspension was further diluted in 800 μl of PBS and mixed with either 0.5 μl of Protein A-FITC (5 mg/ml), 2 μl of PA-FITC (1 mg/ml) (List Biological Laboratories, Campbell, CA) or 2.5 μl of FcγRI-FITC (0.6 mg/ml). After incubation for 1 h with vigorous shaking at 25°C in the dark the spheroplasts were pelleted by centrifugation at 12,000 × g for 1 min and resuspended in 1 ml of PBS. A 100 μl of this suspension was diluted in 1 ml of PBS and analyzed on a BD FACSort instrument (BD Bioscience, San Jose, CA). Spheroplasts prepared as above were sorted on a MoFlo droplet deflection flow cytometry (Dako Cytomation, Fort Collins, Colorado) using a 488 nm Argon laser for excitation and detection through a 530/40 band pass filter. Sorted cells were resorted immediately after initial sorting. The Fc mutant genes in the resorted spheroplasts rescued by PCR using two specific primers STJ#16 and STJ#220

were cloned into *Sfi*I digested pPelBFLAG vector, and transformed in electrocompetent *E. coli* Jude-1 cells. The resulting transformants were subjected to the next round sorting and resorting.

2.2.3 Expression and purification of Fc proteins

E. coli Jude-1 cells harboring pTrc99A-DsbA-Fc-FLAG encoding either wild type or mutant Fc domains were cultured in 2 L flasks with 500 ml working volume of TB media at 37 °C. The shake flasks were transferred to 30 °C and 15 minutes later 1 mM IPTG (OD_{600} approximately 0.6) was added. 8 h after induction the cells were harvested and the expressions of soluble Fc proteins was detected by Western blot using Rabbit anti-ECS antibody peroxidase conjugate (Bethyl Laboratories, Montgomery, TX). Culture supernatant from the induced cells was separated by centrifugation at 7,000 rpm for 30 min filtered through a 0.22 µm filter and 400 ml were loaded onto a column packed with 1 ml of Immobilized Protein A agarose (Pierce Biotechnology, Rockford, IL) by gravity flow. The column was washed with 75 ml of 20 mM sodium phosphate buffer (pH 7.0) and with 50 ml of 40 mM sodium citrate (pH 5.0). Wild type Fc and Fc mutants were eluted using 0.1 M glycine (pH 2.5) and neutralized immediately with 1M Tris (pH 8.0). Fc containing fractions were concentrated by ultrafiltration (10 kDa Mw cutoff) and purified by gel filtration on a Superdex 200 column (Amersham Pharmacia, Piscataway, NJ).

2.2.4 Preparative expression and purification of IgG

Preparative expression was performed by fed-batch fermentation using a 3.3 L jar fermentor (New Brunswick Scientific, Edison, NJ) with 1.2 L working volume. Cells were grown at 30 ^{o}C in R/2 medium (Jeong and Lee, 2003) consisting of: 2 g of $(NH_4)_2HPO_4$, 6.75 g of KH_2PO_4, 0.93 g of citric acid-H_2O, 0.34 g of $MgSO_4$, 20 g of glucose, 0.05 g of ampicillin and 5 ml of trace metal solution dissolved in 2 N HCl (10 g of $FeSO_4$-$7H_2O$, 2.25 g $ZnSO_4$-$7H_2O$, 1 g of $CuSO_4$-$5H_2O$, 0.35 g of $MnSO_4$-H_2O, 0.23 g of $Na_2B_4O_7$-$10H_2O$, 1.5 g of $CaCl_2$, and 0.1 g of $(NH_4)_6Mo_7O_{24}$ per L). *E. coli* BL21(DE3) (EMD Chemicals, Gibbstown, NJ) harboring pSTJ4-Herceptin IgG1 or pSTJ4-Herceptin IgG1-Fc5 were cultured in 500 mL baffled-flask with 120 ml R/2 media at 30 ^{o}C at 250 rpm for 8 h and used to inoculate the fermentor. The dissolved oxygen (DO) concentration was maintained at 40% of air saturation using automatic cascaded control by increasing the agitation speed from 100 rpm to 1000 rpm and the air flow rate from 1 to 3 SLPM (Standard liquid per minute) and with pure oxygen flow rate from 0 to 1.5 SLPM when required. Initial pH was adjusted to 6.8 and controlled by the addition of 30% (v/v) ammonium hydroxide when the pH decreased to less than 6.75, and by the supply of either growth feeding solution (700 g/L of glucose and 10 g/L of $MgSO_4$-$7H_2O$) before induction or production feeding solution (500 g/L glucose, 10 g/L of $MgSO_4$-$7H_2O$, and 100 g/L of yeast extract) after induction when the pH increased above 6.9. When OD_{600} reached 100, the culture temperature was reduced to 25 ^{o}C and 30 min later, protein expression was induced with 1 mM of IPTG. The culture broth was harvested 7 h after induction.

Cells were pelleted by centrifugation at 11,000 × g for 30 min, suspended in 1.2 L 100 mM Tris, 10 mM EDTA (pH 7.4), 4 mg of lysozyme (per g of dry cell weight), 1/5

working concentration of protease inhibitor cocktail (complete, EDTA-free, Roche Diagnostics, Indianapolis, IN), and 1 mM PMSF and were incubated with shaking at 250 rpm at 30 ^{o}C for 16 h to release periplasmic proteins. After centrifugation at 14,000 × g for 30 min, the supernatant was mixed with polyethyleneimine (MP Biomedical, Solon, OH) to a final concentration of 0.2% (w/v) recentrifuged at 14,000 × g for 30 min, and filtered through 0.2 μm filter. Immobilized Protein A agarose resin pre-equilibrated in 20 mM sodium phosphate buffer (pH 7.0) was added to the supernatant and incubated at 4 ^{o}C for 16 h. After washing with 200 ml of 20 mM sodium phosphate buffer (pH 7.0) and 200 ml of 40 mM sodium citrate (pH 5.0), IgG1 was eluted from the resin using 15 ml of 0.1 M glycine (pH 3.0) and neutralized immediately with 1 M Tris (pH 9.0) solution. The eluted samples were concentrated by ultrafiltration through a 10 kDa Mw cutoff membrane and the retentate was applied to a Superdex 200 gel filtration column developed with PBS (pH 7.4).

2.2.5 ELISA assays

50 μl of 4 μg/ml of wild type Fc, Fc mutants, glycosylated IgG1 (Sigma-Aldrich, St. Louis, MO) aglycosylated trastuzumab, aglycosylated trastuzumab Fc5 purified from *E. coli*, or glycosylated trastuzumab (Clinical grade, Fox Chase Cancer Center or MD Anderson Pharmacy) were diluted in 0.05 M Na_2CO_3 (pH 9.6) buffer and used to coat 96 well polystyrene ELISA plate (Corning, Corning, NY) overnight at 4 °C. After blocking with 1x PBS (pH 7.4), 0.5% BSA for 2 h at room temperature, the plate was washed 4 times with PBS containing 0.05% Tween20, and incubated with serially diluted FcγRIIa (Berntzen et al., 2005), FcγRIIb (Berntzen et al., 2005), FcγRI (R&D Systems,

Minneapolis, MN), FcγRIIIa (R&D Systems, Minneapolis, MN) or FcγRIIIb (R&D Systems, Minneapolis, MN) at room temperature for 1 h. Purified GST fused FcγRIIa and FcγRIIb were provided by Dr. Inger Sandlie (University of Oslo, Norway). After washing 4 times with the same buffer, 1:10000 diluted anti-polyhistidine antibody HRP conjugate (Sigma-Aldrich, St. Louis, MO) for FcγRIIIa and FcγRIIIb or 1:5000 diluted anti-GST antibody HRP conjugate (Amersham Pharmacia, Piscataway, NJ) for FcγRIIa and FcγRIIb was added and plates were washed and developed as described previously (Mazor et al., 2007). To determine the binding of IgG to FcRn at pH 7.4, 2 μg/ml of GST fused FcRn (Berntzen et al., 2005) (Providied by Dr. Inger Sandlie, University of Oslo, Norway) preincubated with 1:5000 diluted Anti-GST-HRP for 1 h as previously described (Andersen et al., 2006) was added to plates coated with IgG. To evaluate binding at pH 6.0 or 5.5 ELISAs were carried out as above except that the washing buffer and sample dilution buffers were adjusted to pH 6.0 or 5.5.

2.2.6 BIAcore analysis for Fc mutants and Herceptin IgG1 Fc mutants

Binding of IgG1-Fc domains to the human FcγRI was analyzed by surface plasmon resonance using a BIAcore 3000 biosensor (Biacore, Piscataway, NJ). The soluble monomeric FcγRI was immobilized on the CM-5 sensor chip by amine coupling kit as recommended by the manufacturer. Binding experiments were done in HBS-EP buffer (10 mM HEPES pH 7.4, 150 mM NaCl, 3.4 mM EDTA, and 0.005% P20 surfactant). The soluble human IgG1, wild type aglycosylated IgG1-Fc fragments, and isolated aglycosylated Fc mutants (Fc5, Fc49) were injected at a flow rate of 100 ul/min for 30 s with dissociation time 300 s. Regeneration of the ligand, FcγRI, was performed

by single injection of 100 mM citric acid, pH 3.0. Binding of the soluble monomeric FcγRI to IgG1 was determined by injection of IgG1 in duplicate at concentrations of 0, 40, 60, 80, 100, and 200 nM for 30 s at a flow rate of 100 μl/min over immobilized FcγRI. Affinities of FcγRI toward Fc5 and Fc49 were obtained by IgG1 injections of IgG1 Fcs in duplicates at concentrations 0, 80, 100, 200, 400, 600 nM and 0, 200, 400, 600, 800, and 1,000 nM for 30 s at a flow rate of 100 μl/min over immobilized FcγRI, respectively.

Similarly, binding of FcγRI to the full assembled IgG trastuzumab was analyzed by immobilizing glycosylated trastuzumab, aglycosylated trastuzumab, and aglycosylated trastuzumab-Fc5 individually on the CM5 sensor chip. Binding experiments were done in the same HBS-EP buffer. The soluble monomeric FcγRI was injected at a flow rate of 30 μl/min for 60 s with dissociation time 300 s. Regeneration of the ligand, FcγRI, was performed by single injection of 100 mM citric acid, pH 3.0. Binding kinetics of the soluble monomeric FcγRI with glycosylated trastuzumab, aglycosylated and trastuzumab, trastuzumab Fc5 were measured by injection of soluble FcγRI in duplicate at concentrations of 0, 25, 50, 100, 200 nM for 60 s at a flow rate of 30 μl/min over immobilized glycosylated trastuzumab, and aglycosylated trastuzumab-Fc5. The binding of FcγRI toward wild type aglycosylated trastuzumab was obtained by FcγRI injections in duplicates at concentrations 0, 200, 300, 400, 500, and 600 nM for 60 s at a flow rate 30 μl/min over immobilized aglycosylated trastuzumab. Binding curve at zero concentration was subtracted as a blank. Equilibrium dissociation constants (K_D) were determined by fitting of equilibrium responses to steady-state affinity model provided by BIAevaluation 3.0 software.

Table 2-1. Plasmids used in this study.

Plasmids	Relevant characteristics	Reference or source
pMoPac1	Cm^r, *lac* promoter, *tetA* gene, C-terminal polyhistidine tag and c-myc tag	(Hayhurst et al., 2003)
pMoPac12	Ap^r, *lac* promoter, *tetA* gene, *skp* gene, C-terminal polyhistidine tag and c-myc tag	(Hayhurst et al., 2003)
pMoPac1-FLAG-M18	NlpA fused *M18 scFv gene*, C-terminal FLAG tag in pMoPac1	(Jung et al., 2007)
pPelBFLAG	Cm^r, *lac* promoter, *tetA* gene, *skp* gene, C-terminal FLAG tag	This study
pPelBFLAG-Fc	*IgG1-Fc* gene in pPelBFLAG	This study
pPelBFLAG-M18 scFv	*M18 scFv* gene in pPelBFLAG	This study
pMAZ360-M18.1-Hum-IgG1	*M18.1 humanized IgG1* gene in pMAZ360	(Mazor et al., 2007)
pTrc99A	Ap^r, *trc* promoter, $lacI^q$	Amersham Biosci., (Piscataway, NJ)
pTrc99A-DsbA	*dsbA* signal sequence gene in pTrc99A	This study
pTrc99A-DsbA-Fc-FLAG	dsbA fused *IgG1-Fc* gene, C-terminal FLAG tag in pTrc99A	This study
pSTJ4-Herceptin IgG1	*Herceptin IgG1* gene in pMAZ360-M18.1-Hum-IgG1	This study

Table 2-2. Primers used in this study (Underlining indicates the restriction enzyme sites).

Primer Name	Primer nucleotide sequence (5' → 3')
STJ#16	TTGTGAGCGGATAACAATTTC
STJ#144	TTTTAGGGGTCGACGACAAAACTCACACATGCCCACCGTG
STJ#145	TTTAAGGGAAGCTTCTATTAGGCGCGCCCTTTGTCATCG
STJ#194	CTAGGGAGCCGCGGGAGGAGCAGTACAACNNSNNSNNSNNSNNSNNSNNSNNSNNS AGCACGTACCGTGTGGTCAGCG
STJ#195	CTAGAGGAATTCGGCCCCCGAGGCCCCTTTAC
STJ#196	CGCAGCGAGGCCCAGCCGGCCATGGCG
STJ#197	CGCAATTCGAATTCGGCCCCCCGAGGCCCC
STJ#220	CAATTTTGTCAGCCGCCTGAGCAGAAG
STJ#283	CTTCTATCCCAGCGACATCGCCGTGNNSTGGNNSAGCNNSGGGCAGCCGGAGAACAACT ACAAG
STJ#284	GACCAAGAACCAGGTCAGCCTGACCTGCCTGGTCAAAGGCTTCTATCCCAGCGACATCG CCGTG
STJ#285	AGGGAGAGGCTCTTCTGCGTGTAGTGGTTGTGCAGAGCWNNATGWNNCACWNNGCATG AGAAGACGTTCCCCTGCTG
STJ#286	AGGGAGAGGCTCTTCTGCGTGTAGTGGTTGTGCAGAGCCTCATGWNNWNNCACGGAGC ATGAGAAGACGTTCCCCTGCTG
STJ#287	AGGGAGAGGCTCTTCTGCGTGTAGTGGTTGTGCAGAGCCTCATGWNNWNNWNNCACGG AGCATGAGAAGACGTTCCCCTGCTG
STJ#302	GCGGAATTCCCATGGCGGATATTCAAATGACCC
STJ#303	CAGACGCGCTTAAAGAAGACGGGCTTTGGGTCATTTGAATATCCGCCATG
STJ#304	CGTCTTCTTTAAGCGCGTCTGTCGGTGATCGCGTGACCATCACGTGTCGT
STJ#305	AGGCCACCGCCGTATTAACATCTTGGCTCGCACGACACGTGATGGTCACG
STJ#306	GTTAATACGGCGGTGGCCTGGTATCAACAAAAACCGGGTAAAGCCCCGAA
STJ#307	GAGTACAGAAAGCTGGCGCTGTAGATTAACAGCTTCGGGGCTTTACCCGG
STJ#308	CAGCGCCAGCTTTCTGTACTCTGGCGTCCCGAGCCGCTTTTCTGGCAGCC
STJ#309	TGCTAATGGTCAGCGTGAAGTCCGTACCGCTGCGGCTGCCAGAAAAGCGG
STJ#310	ACTTCACGCTGACCATTAGCAGCCTGCAGCCGGAGGATTTCGCCACCTAT
STJ#311	TGGCGGGGTGGTGTAGTGCTGCTGACAATAATAGGTGGCGAAATCCTCCG
STJ#312	ACTACACCACCCCGCCAACCTTTGGCCAGGGTACGAAAGTGGAGATTAAA
STJ#313	GACAGATGGTGCGGCCGCCGTGCGTTTAATCTCCACTTTCGTACCCTGG
STJ#314	ATTGTTATTGCTAGCGGCTCAGCCGGCAATGGCG
STJ#315	ACCAGACCACCGCCAGATTCCACTAATTGAACCTCCGCCATTGCCGGCTG
STJ#316	TCTGGCGGTGGTCTGGTGCAGCCAGGCGGTAGCTTACGTCTGAGCTGTGC
STJ#317	AGGTATCTTTGATGTTGAAGCCAGACGCTGCACAGCTCAGACGTAAGCTA
STJ#318	TCTGGCTTCAACATCAAAGATACCTACATTCATTGGGTTCGCCAAGCCCC
STJ#319	ATAGATACGGGCCACCCACTCCAGGCCTTTACCTGGGGCTTGGCGAACCC
STJ#320	GAGTGGGTGGCCCGTATCTATCCAACCAATGGCTACACGCGTTATGCAGA
STJ#321	GCGCTAATGGTGAAGCGGCCTTTCACAGAGTCTGCATAACGCGTGTAGCC
STJ#322	CCGCTTCACCATTAGCGCCGACACCTCTAAGAACACCGCATATTTACAGA
STJ#323	GTCCTCTGCGCGTAAAGAGTTCATCTGTAAATATGCGGTGTTCTTAGAGG
STJ#324	AACTCTTTACGCGCAGAGGACACGGCGGTGTACTACTGCTCTCGTTGGGG
STJ#325	AGTAGTCCATCGCGTAGAAACCGTCACCGCCCCAACGAGAGCAGTAGTAC
STJ#326	GGTTTCTACGCGATGGACTACTGGGGTCAGGGTACGCTGGTCACGGTCAG
STJ#327	GCCCTTGAAGCTTGCAGAGCTGACCGTGACCAGCGT

2.3 RESULTS

2.3.1 Bacterial display of aglycosylated functional homodimeric Fc domains

A gene encoding the hinge region and Fc domain followed by a FLAG tag and preceeded by a PelB signal peptide for secretion into the periplasm was constructed (Fig. 2-3). *E. coli* does not have glycosylation machinery, thus the Fc protein secreted into the periplasmic space does not have a glycan attached at Asn297. To identify mutations that enable aglycosylated Fc to bind to the extracellular domain of FcγRs, it was first necessary to develop an *E. coli* display system suitable for the screening of aglycosylated Fc mutant libraries. The *E-clonal* system developed earlier is well suited for the isolation of IgGs with desired antigen specificities. However, it cannot be used to detect binding of Fc receptors to the Fc domain because the latter is occupied by the membrane-anchored Fc-binding protein which is used to display the IgG on spheroplasts. To overcome this problem, we initially attempted to use the fatty acyl chain anchored binding motifs (cJun (Kouzarides and Ziff, 1988; Landschulz et al., 1988) or ColE2 mutants (Garinot-Schneider et al., 1996; Li et al., 2004), respectively) provided by N terminal fusion of NlpA(1-6) (Harvey et al., 2004) and the expression of PelB leader peptide fused Fc with c-terminal fusion partners (cFos or Im2) for the tethering of Fc domains on spheroplasts via interaction of cJun-cFos (Kouzarides and Ziff, 1988; Landschulz et al., 1988) or ColE2-Im2 (Garinot-Schneider et al., 1996; Li et al., 2004), Preliminary experiments revealed no significantly distinguishable FACS signal compared with negative controls that did not express protein fused to the NlpA anchoring motif (data not shown). However, in the course of these studies we noticed that spheroplasts generated from cells expressing secreted Fc protein that lacked any tethering sequence (Fig 2-2) exhibited

slight (2-fold) higher fluorescence upon labeling with Protein A-FITC relative to spheroplasts expressing an unrelated protein, namely the M18 scFv that binds to the PA subunit of the *Bacillus anthracis* toxin (Fig 2-4). Similarly, secreted and solubly-expressed antibody fragments (M.W.>30 kDa), but not smaller proteins (e.g., C-terminal polyhistidine-cMyc tagged β2-microglobulin; M.W. 15.24 kDa), were substantially retained by spheroplasts, resulting in selective staining of *E. coli* by fluorescent antigens (Fig. 2-2). Spheroplasted cells expressing full length IgG or antibody fragments, M18.1 humanized (Harvey et al., 2004) scFv, scAb, Fab and IgG and labeled with PA-FITC fluorescent antigen displayed fluorescence significantly higher than negative controls 26-10 (Francisco et al., 1993) scFv, scAb, Fab, and IgG above background (data now shown). On the other hand, smaller protein such as C-terminal polyhistidine-cMyc tagged β2-microglobulin (M.W. 15.24 kDa) are more thoroughly released upon conversion of cells into spheroplasts and thus the respective cells exhibited low fluorescence following labeling with FITC-conjugated ligand. The retention of secreted Fc domain proteins by spheroplasted cells was highly dependent on growth conditions. Optimal labeling with Protein A-FITC was obtained with cells grown at 25 °C in the presence of 0.5 M trehalose but not with other non-metabolizable sugars such as sucrose or sorbitol. Under these conditions spheroplasts expressing the Fc and labeled with Protein A-FITC exhibited 10-fold higher signal than controls (Fig. 2-4). Western blot analysis revealed that a significant fraction of the Fc was retained in cells grown with 0.5 M trehalose (data not shown). Secretion of Fc by the signal recognition particle (SRP)-dependent DsbA signal sequence (Schierle et al., 2003) did not result in significant protein retention following spheroplasting, even in the presence of 0.5 M trehalose. While the precise mechanism for

the retention of soluble proteins by spheroplasted cells remains to be determined, the fluorescent signal obtained is well suited for library screening purposes.

Figure 2-3. Expression cassette for periplasmic display of Fc.

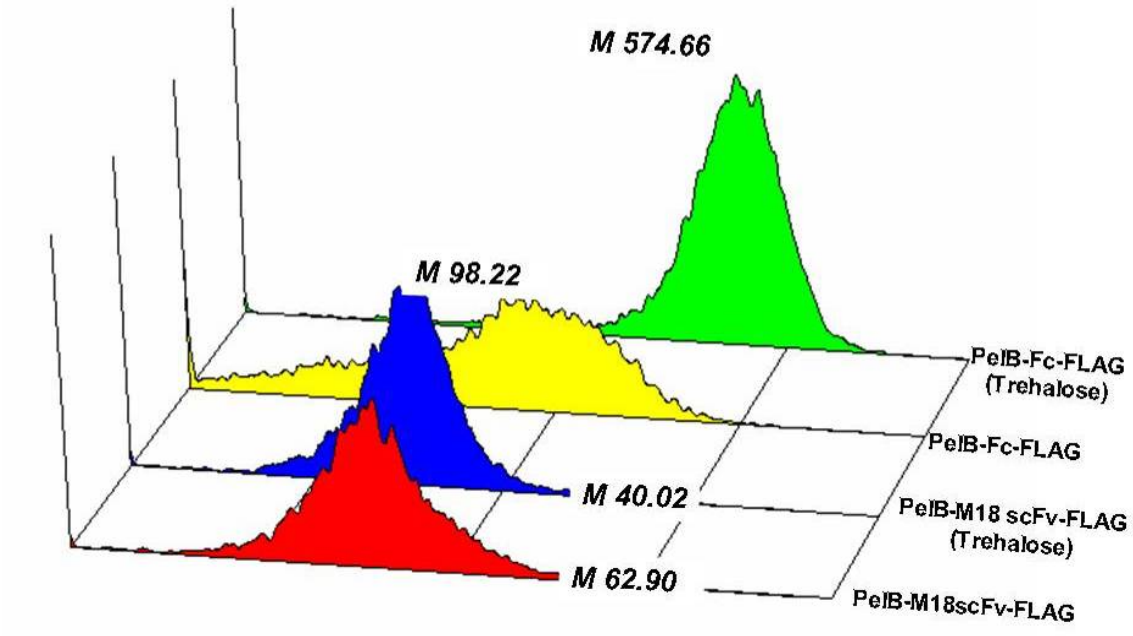

Figure 2-4. Effect of trehalose on periplasmic display of Fc. Cells expressing either the IgG Fc domain or the M18 scFv as a control were grown with or without 0.5 M trehalose, spheroplasted and labeled with Protein A-FITC probe for detection.

2.3.2 Isolation of mutants aglycosylated Fc fragments exhibiting FcγRI binding

Simmons *et al*. reported that aglycosylated antibodies exhibit negligible binding to the FcγRI receptor (Simmons et al., 2002). To isolate mutants of the Fc domain capable of binding to the extracellular domain of Fcγ receptors we initially constructed libraries composed of: (i) random mutants by error prone PCR (~9.2×10^8 transformants) containing 0.49% nt substitutions per gene (as determined by the sequencing of 20 random clones) and (ii) 10 a.a. random insertions encoded by NNS randomization scheme (N any nucleotide, S=C and G) (~2.8×10^7 transformants representing a miniscule fraction of the theoretical diversity) into residues 297 or 298 with the intent of replacing the glycan that is normally attached to Asn297 with a peptide epitope. Transformants from the two libraries were pooled and, following induction of protein synthesis, spheroplasts were prepared and labeled with the appropriate FcγR conjugated to FITC (Fig. 2-2), and highly fluorescent clones were isolated by flow cytometry. The respective genes were rescued by PCR, subcloned, and transformants were subjected to additional rounds of FACS sorting. As shown in Figure 2-5, a positive population was enriched following screening with fluorescently labeled extracellular domain of FcγRI, the high affinity receptor expressed by monocytes, dendritic and to a lesser extent by polymorphonuclear cells (Desjarlais et al., 2007). After the 4^{th} round, 50 clones were randomly selected and their fluorescence was determined individually. Six clones displaying the highest fluorescence (>5x above background) upon labeling with FcγRI-FITC were isolated (Fig. 2-6) and sequenced (Fig. 2-7). All six clones were derived from the error prone PCR Fc library. The isolated clones contained two consensus mutations,

E382V and M428I located within the C and F β-strands of CH3 region (Lefranc et al., 2005) (Fig. 2-8 A and B), respectively. This finding was surprising since these mutations are far from the FcγRI binding epitope which is proposed to comprise of the lower hinge and the upper part of the CH2 domain (Jefferis et al., 1998). The clone exhibiting the highest fluorescence, Fc5, contained only these two substitutions.

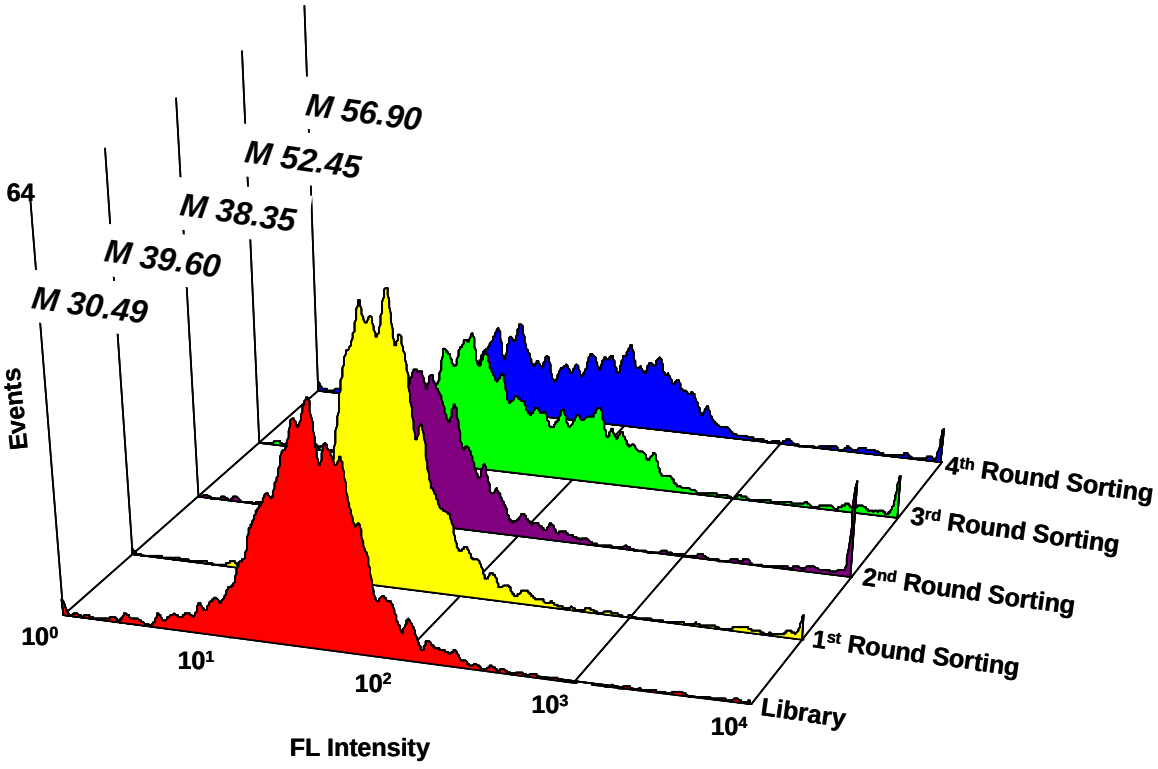

Figure 2-5. Fluorescence histogram of spheroplasted cells from different rounds of sorting labeled with FcγRI-FITC. M: Mean fluorescence intensity.

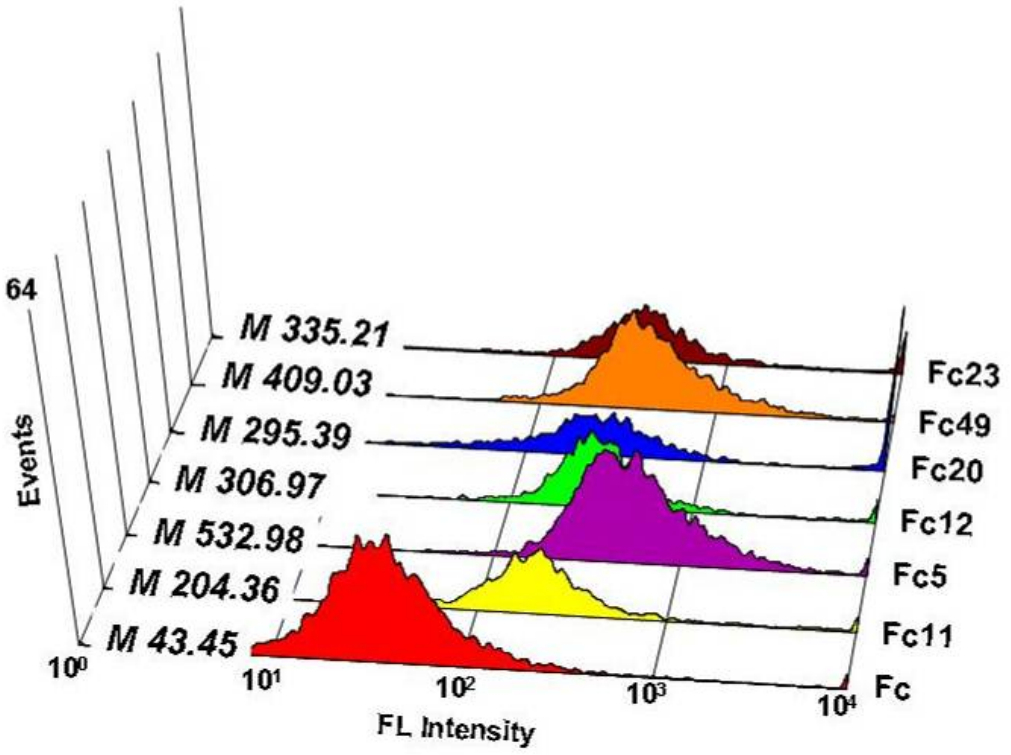

Figure 2-6. Fluorescence histogram of spheroplasted cells expressing either wt IgG Fc protein or high fluorescence mutants isolated from the fourth round (statistically significant high fluorescence; $P < 0.001$ using unpaired students *t* test relative to wt IgG Fc). M: Mean fluorescence intensity.

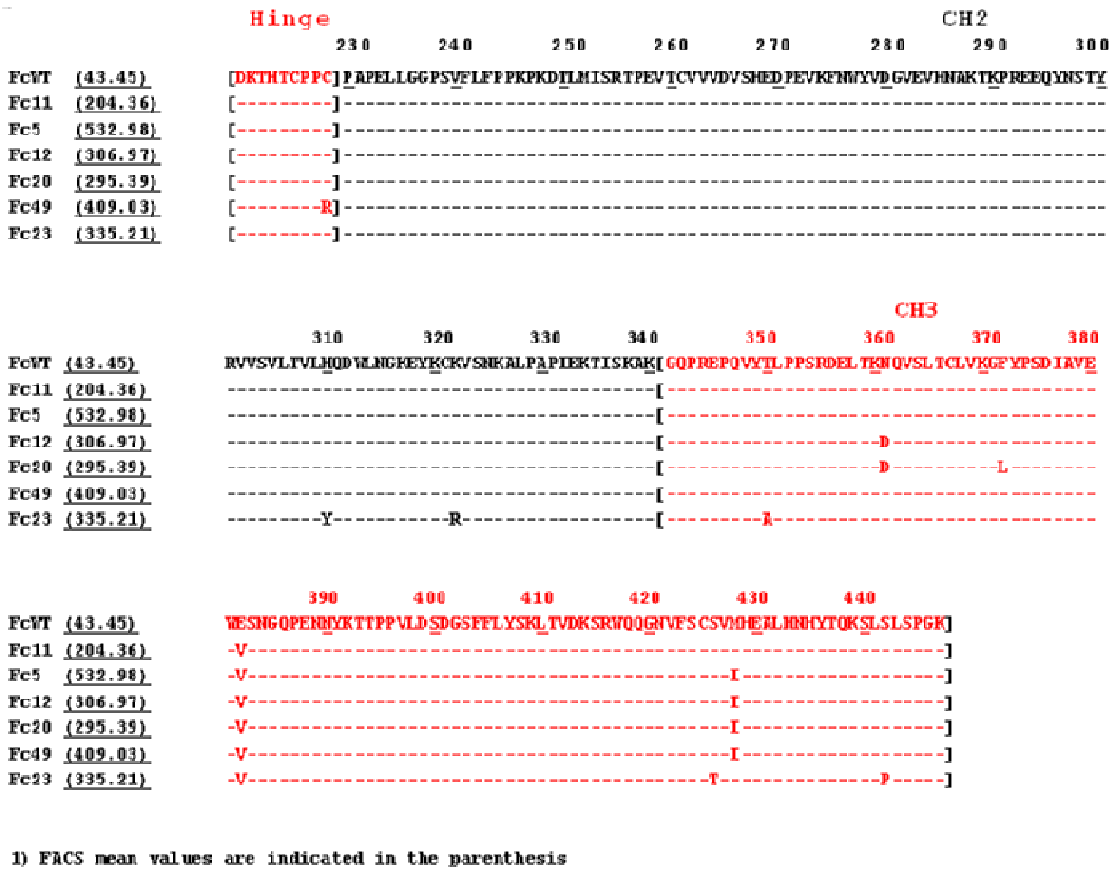

Figure 2-7. Protein sequences of isolated Fc mutant clones exhibiting high affinity to FcγRI. Mean fluorescence values for the respective clones labeled with FcγRI are shown in parenthesis.

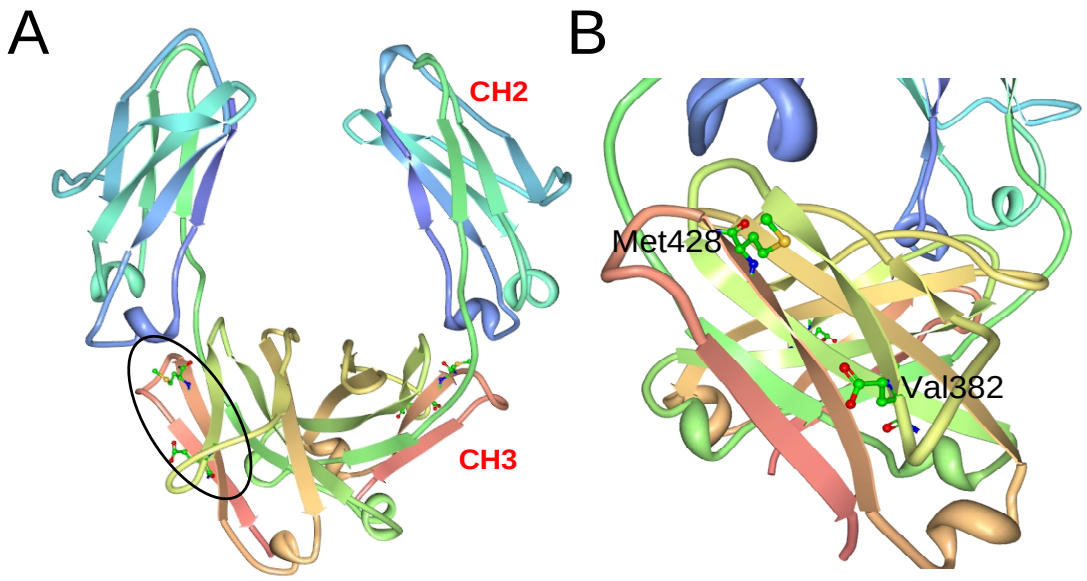

Figure 2-8. Location of mutations in isolated aglycosylated Fc domains displayed FcγRI binding, in the 3D structure of glycosylated IgG (PBD Code: 1FC1). (A) Isolated aglycosylated Fc5 (382E and 428M) represented on the 3D structure of glycosylated IgG1 Fc (PBD Code: 1FC1). (B) Two beta sheets including 382E in β-sheet C and 428M in β-sheet C of CH3 region represented on the crystal structure of full glycosylated IgG.

Next, additional saturation mutagenesis of: (i) a.a. 380, 382 and 384 in β-sheet C of CH3 that makes contact with β-sheet F; (ii) residues 426, 428 and 430 in the F β-sheet, (iii) insertional mutagenesis between a.a. 428-429 was performed (Fig. 2-9) and screened for binding to FcγRI-FITC. Over 1×10^8 spheroplasts were sorted and in every round the top 3% of the population showing the highest fluorescence was isolated (Fig. 2-10). 14 individual clones isolated from the 4^{th} round of sorting were sequenced. Once again, the consensus mutations were E382V and M428I indicating that these amino acid substitutions, and especially the introduction of Val at position 382, are critical for conferring binding to FcγRI (Fig. 2-11).

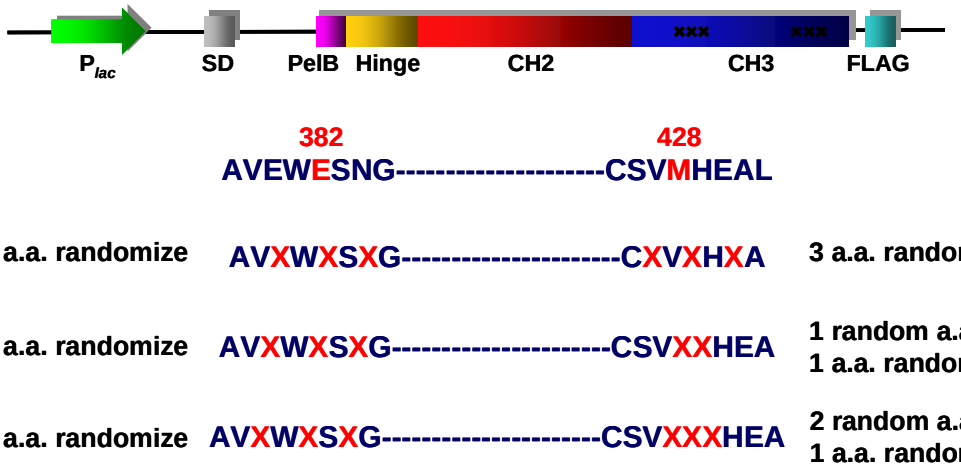

Figure 2-9. Saturation mutagenesis of a.a. 382 and 428 and adjacent residues in Fc. Three sub-libraries in which residues 380, 382, 384 and either (1) 426,428,430; (2) 428 and following one additional amino acids; or (3) 428 and following two additional amino acids were constructed by total gene synthesis and pooled to give a master library of over 1×10^7 clones.

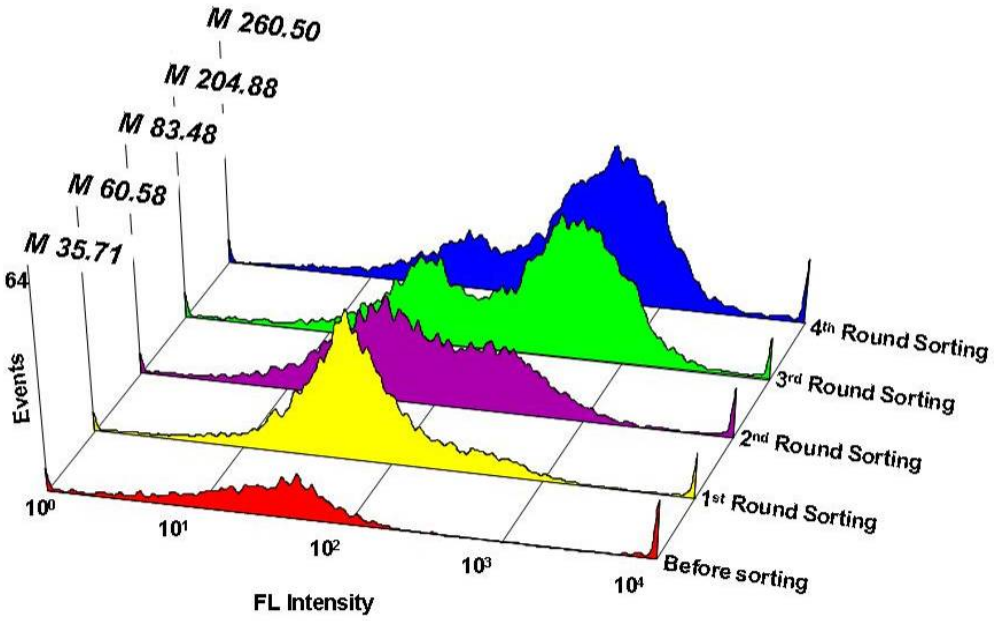

Figure 2-10. Screening of the saturation library for high affinity Fcs to FcγRI. Fluorescence histogram of spheroplasted cells isolated after different rounds and labeled with 30 nM of FcγRI-FITC. M: Mean fluorescence intensity.

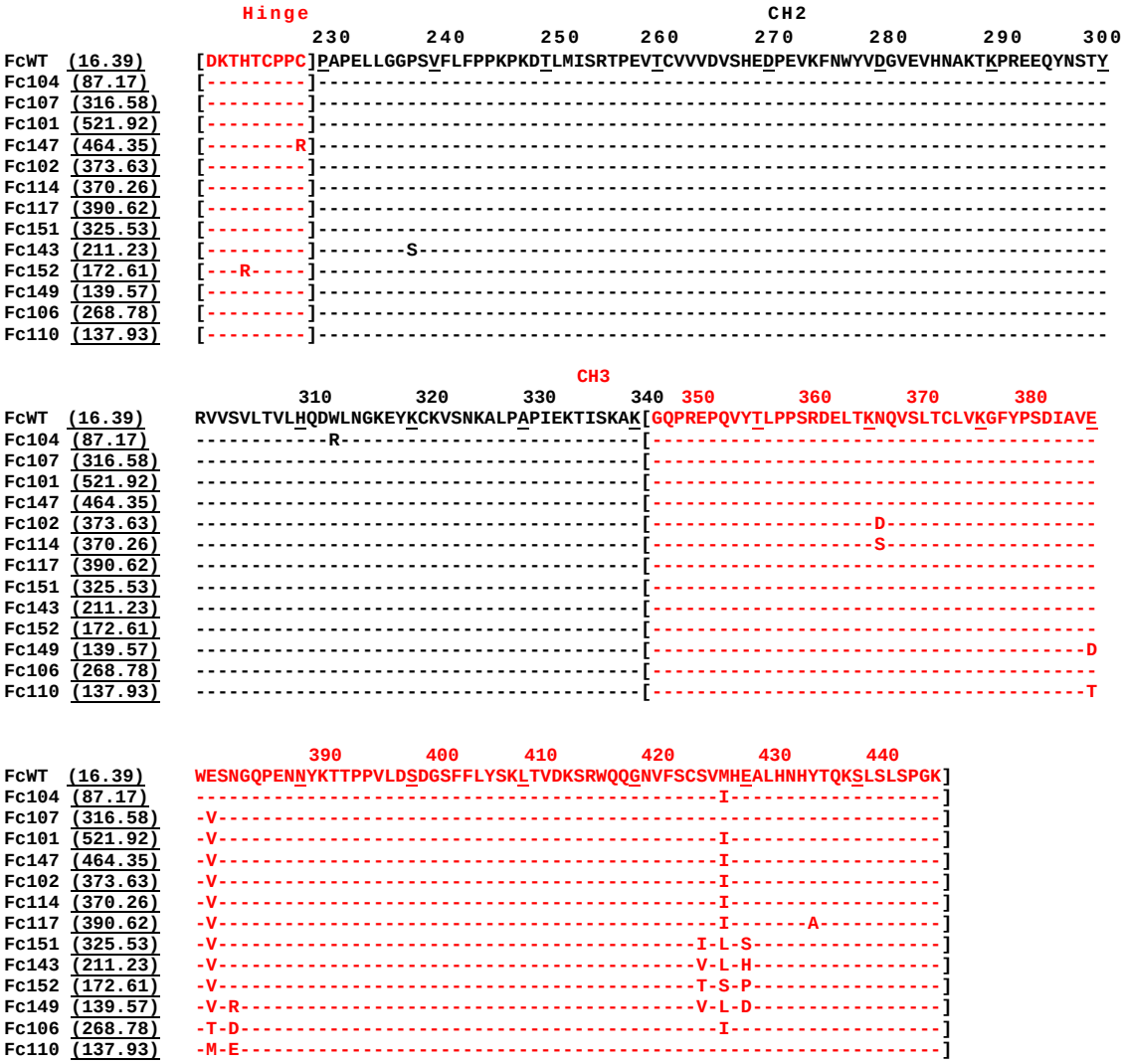

Figure 2-11. Protein sequences of isolated Fc mutants from the saturation library. Mean fluorescence values for the respective clones labeled with FcγRI are shown in parenthesis.

2.3.3 Expression of homodimeric Fc domains in *E. coli* and characterization of affinity to FcγRI

Aglycosylated (wt) Fc and the mutants Fc5 (E382V, M428I), Fc 11 (E382V) and Fc49 (C289R, E382V, M428I) that exhibited the highest fluorescence were expressed and purified to near homogeneity. Optimal soluble expression of homodimeric Fc fragments was obtained at 30 ºC in *E. coli* Jude-1 cells in which secretion into the periplasm was mediated by the co-translational ssDsbA signal peptide (Schierle et al., 2003) (Fig. 2-12) that led to a substantially higher amount of correctly assembled Fc both in the periplasmic fraction and in the growth medium compared to secretion via the PelB signal peptide (Fig. 2-13).

Following Protein A and gel filtration chromatography, ~ 0.8 mg/L of dimeric Fc protein was routinely obtained in shake flask cultures (Fig. 2-14 and 2-15). The affinity of the purified homodimeric Fc fragments for FcγRI measured by ELISA (Fig. 2-16) are in good correlation with the flow cytometry analysis result for Fc-displaying spheroplasts (Fig. 2-6). BIAcore analysis revealed that wt Fc does not bind to FcγRI (K_D>30 µM). In contrast, Fc5 and Fc49 exhibited K_D values of 31 and 92 nM respectively. For comparison the equilibrium dissociation constant of commercially available, glycosylated IgG was 18 nM. Notably, the aglycosylated Fc5 mutant and the glycosylated human IgG exhibited experimentally indistinguishable dissociation rate constants, k_{off} and a 2-fold lower association rate constant, k_{on} (Table 2-3).

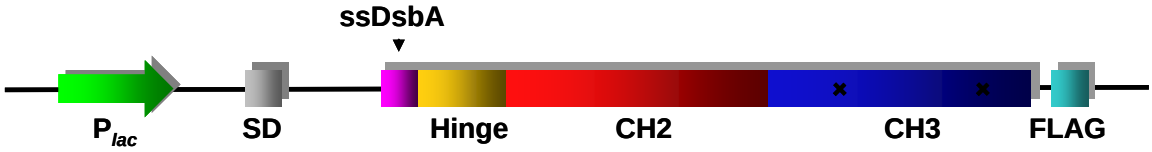

Figure 2-12. Expression cassette for DsbA leader peptide fused aglycosylated Fc.

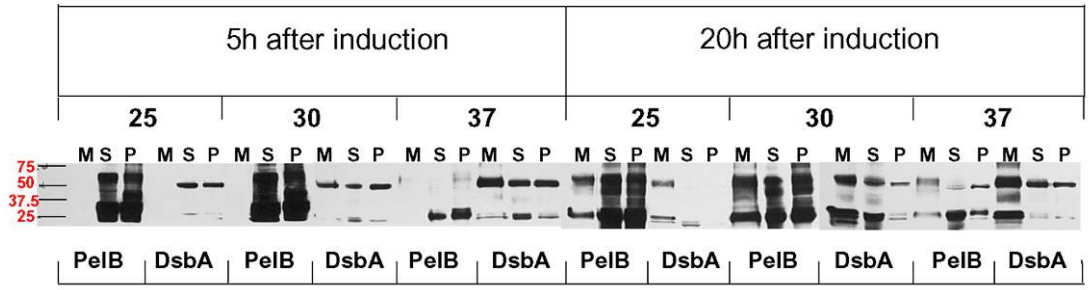

Figure 2-13. Effect of signal peptide on the soluble expression of Fc proteins. Cells expressing Fc secreted via the PelB or DsbA signal peptide were induced at either 25, 30 or 37 ^{o}C, harvested after either 5 or 20 hrs and fractionated into media (M), total soluble (S) and periplasmic (P) fractions. Proteins resolved by gel electrophoresis under nonreducing conditions and detected by Western blotting using anti-ECS-HRP conjugate.

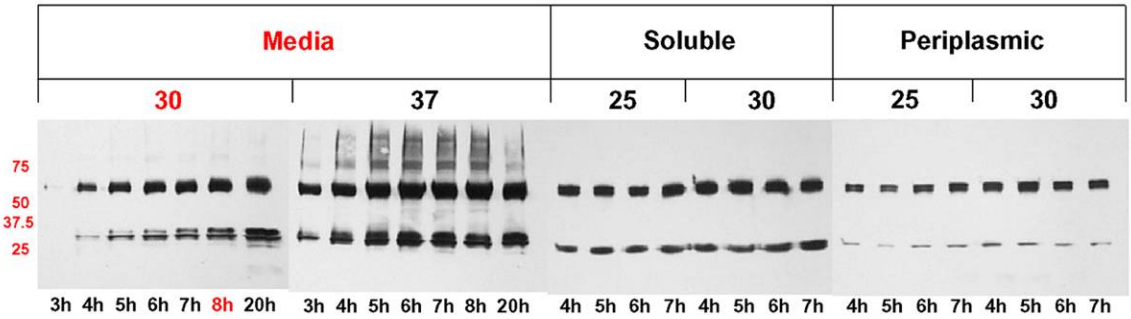

Figure 2-14. Preparative expression of Fc proteins in shake flasks. Cells expressing Fc secreted via the DsbA signal peptide were grown in 500 ml media in shake flasks, induced at either 25, 30 or 37 ^{o}C, harvested after either 5 hrs or 20 hrs, fractionated into media (M), total soluble (S) and periplasmic (P) fractions. Fc proteins were detected as in Figure 2-13 above.

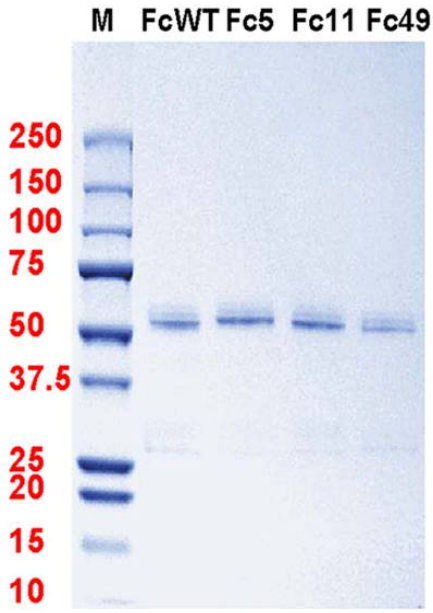

Figure 2-15. Purified wt Fc and high affinity Fc mutant proteins. Lane 1: M.W. standards; Lane 2: Wild type Fc; Lane 3: Fc5; Lane 4: Fc11; Lane 5: Fc49.

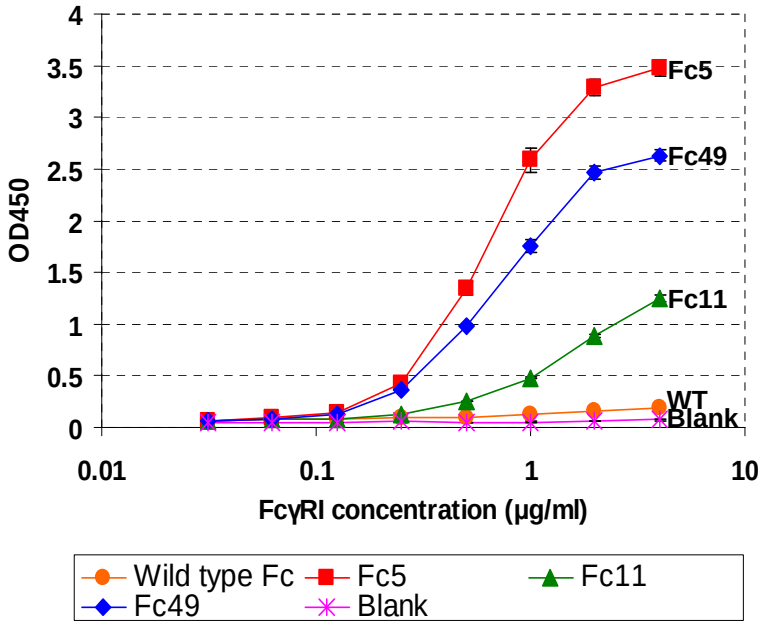

Figure 2-16. ELISA result of the purified aglycosylated wild type Fc, Fc5, Fc11, and Fc49.

Table 2-3. Kinetic rates and equilibrium dissociation constants of isolated Fc mutants determined by BIACore analysis.

	k_{on} (M^{-1} sec^{-1})	k_{off} (sec^{-1})	K_D (nM)
Glycosylated-hIgG1	8.0×10^4	1.4×10^{-3}	18
Aglycosylated-Fc	Undetectable	Undetectable	(a)
Aglycosylated-Fc49	2.5×10^4	2.3×10^{-3}	92
Aglycosylated-Fc5	4.5×10^4	1.4×10^{-3}	31

[(a)] K_D> 30 μM

2.3.4 Expression of aglycosylated trastuzumab in *E. coli*

Trastuzumab is a highly effective chemotherapeutic antibody specific for Her2/neu (Erb2) which is overexpressed in ~30% of breast carcinomas (Liu et al., 2008). Extensive evidence indicates that recruitment of innate immune cells via interactions with Fcγ receptors plays an important role in the therapeutic action of trastuzumab (Liu et al., 2008). For preparative production of aglycosylated trastuzumab and trastuzumab-Fc5 in *E. coli* the heavy and light chains were fused to the PelB signal peptide and placed downstream from the *lac* promoter in a dicistronic operon (Fig. 2-17). Briefly, *E. coli* BL21(DE3) cells were grown at 30 ºC to an OD_{600} of ~100 by fed-batch fermentation in pH-stat control mode, protein synthesis was induced, the fermentor was cooled to 25 ºC, and cells were harvested 7 hr later at an OD_{600} of ~130-140 (Fig. 2-18). Under these conditions, the yield of aglycosylated tetrameric IgG1 was 40-50 mg/L with >70% retained in the periplasmic space. The IgG1 was released from the cell pellet by incubation with lysozyme and EDTA for 16 hr at 30 ºC and purified to >80% homogeneity by Protein A affinity and size exclusion chromatography (Fig. 2-19).

Biacore analysis (Table 2-4 and Fig. 2-20 A-D) revealed that the *E. coli* expressed trastuzumab-Fc5 showed greatly improved binding affinity. Trastuzumab-Fc5 bound to FcγRI with similar affinity to commercial-grade glycosylated trastuzumab from CHO cells and over 67-fold higher affinity compared with wild type aglycosylated trastuzumab. Both glycosylated trastuzumab and aglycosylated trastuzumab-Fc5 displayed higher affinity for FcγRI compared to isolated Fc domains alone.

Notably, unlike glycosylated trastuzumab, which binds to all effector human Fcγ receptors with physiologically relevant affinities, the aglycosylated trastuzumab-Fc5 exhibited poor binding for FcγRIIa, FcγRIIb ($EC_{50}\geq$ 1000-fold and 100-fold higher for GST fused FcγRIIa and FcγRIIb, respectively, Fig. 2-21 and Fig. 2-22) and FcγRIIIa (data not shown). The a.a. substitutions in trastuzumab Fc5 did not affect pH-dependent binding (high affinity binding at pH 5.5 and pH 6.0 and low binding at pH 7.4) to the neonatal FcRn, which is essential for the prolonged half life of IgG and also for transfer of maternal IgG to offspring (Ghetie and Ward, 2000) (Fig. 2-23 A and B).

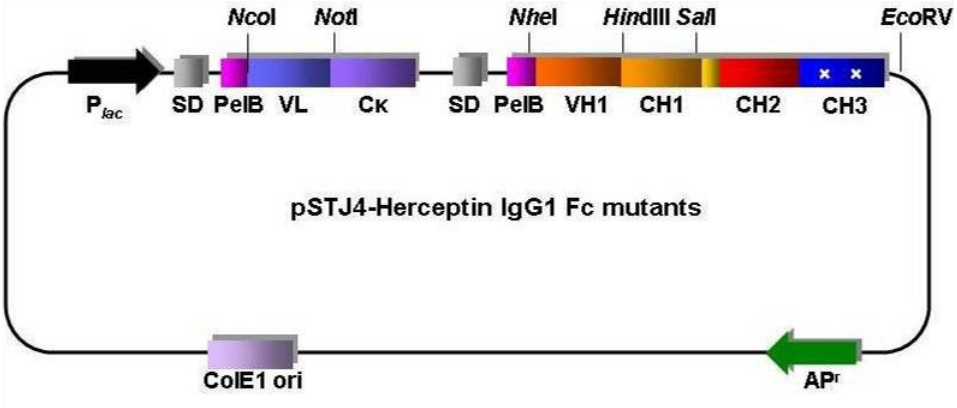

Figure 2-17. Map of plasmid pSTJ4-Herceptin IgG1.

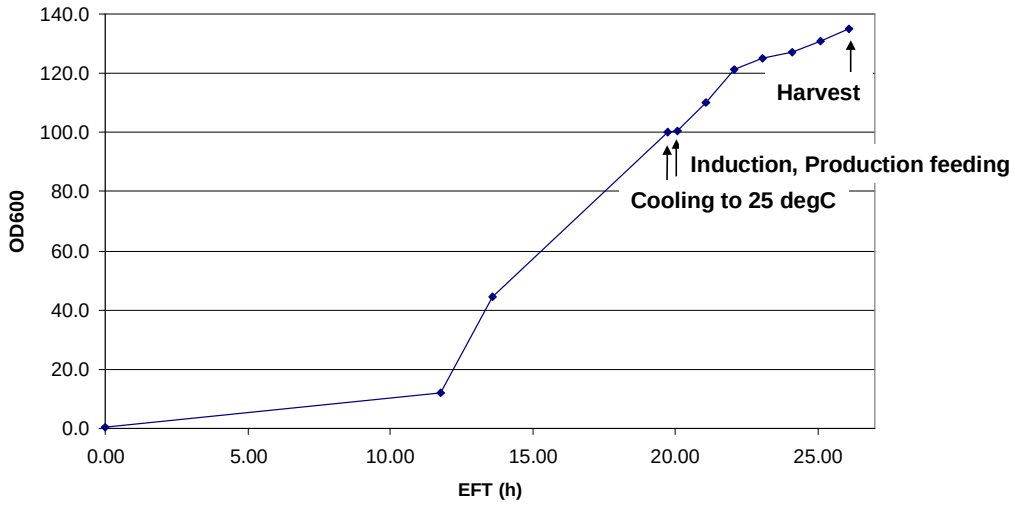

Figure. 2-18. Example of fed-batch fermentation for the production of aglycosylated trastuzumab or aglycosylated trastuzumab-Fc5 in a 3.3 L fermentor. OD_{600} as a function of time after inoculation during the expression of trastuzumab in *E. coli*.

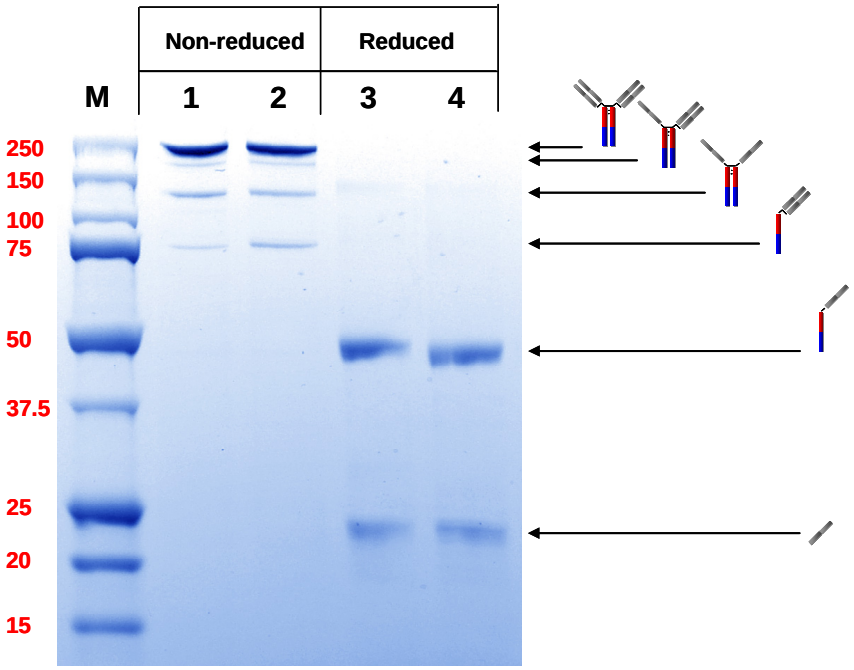

Figure 2-19. Expression and purification of aglycosylated wild type or engineered trastuzumab antibodies. SDS-PAGE showing the purified aglycosylated trastuzumab and aglycosylated trastuzumab Fc5, Lane 1, 3: Wild type Fc aglycosylated trastuzumab; Lane 2, 4: aglycosylated trastuzumab Fc5.

Table 2.4. Kinetic rates and equilibrium dissociation constants of trastuzumab antibodies determined by BIACore analysis.

	K_{on} (M^{-1} sec^{-1})	K_{off} (sec^{-1})	K_D (nM)
Aglycosylated wild type trastuzumab	**1.31×10^5**	**5.02×10^{-2}**	**382**
Aglycosylated trastuzumab-Fc5	**2.17×10^5**	**1.23×10^{-3}**	**5.69**
Glycosylated Herceptin	**1.77×10^5**	**2.66×10^{-4}**	**1.5**

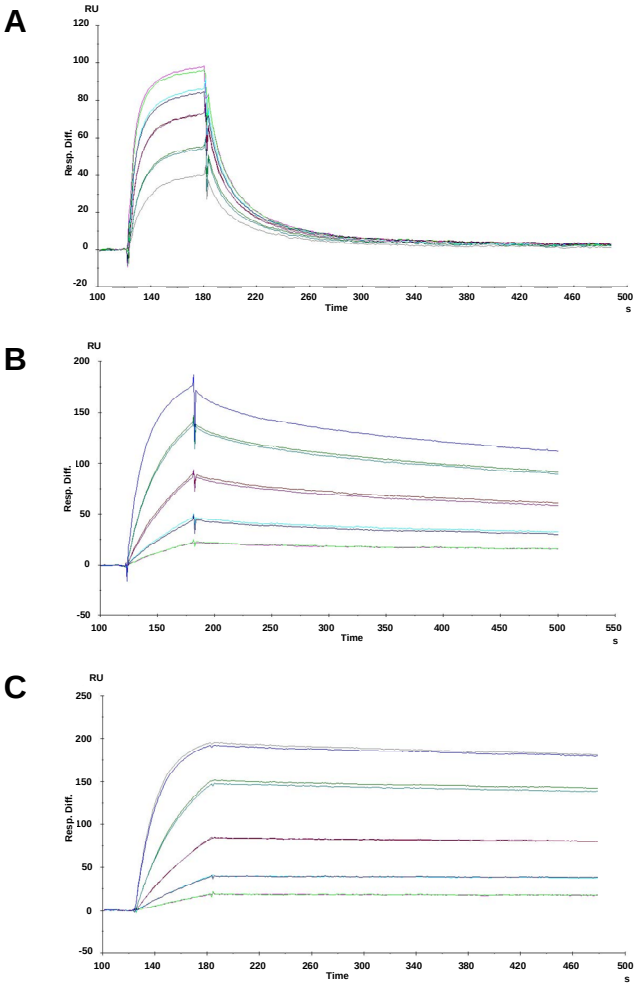

Figure 2-20. Biacore sensorgrams for aglycosylated and glycosylated trastuzumab antibodies. (A-C) Biacore sensorgrams of (A) wild type aglycosylated trastuzumab, (B) aglycosylated trastuzumab-Fc5, and (C) glycosylated trastuzumab for binding to FcγRI.

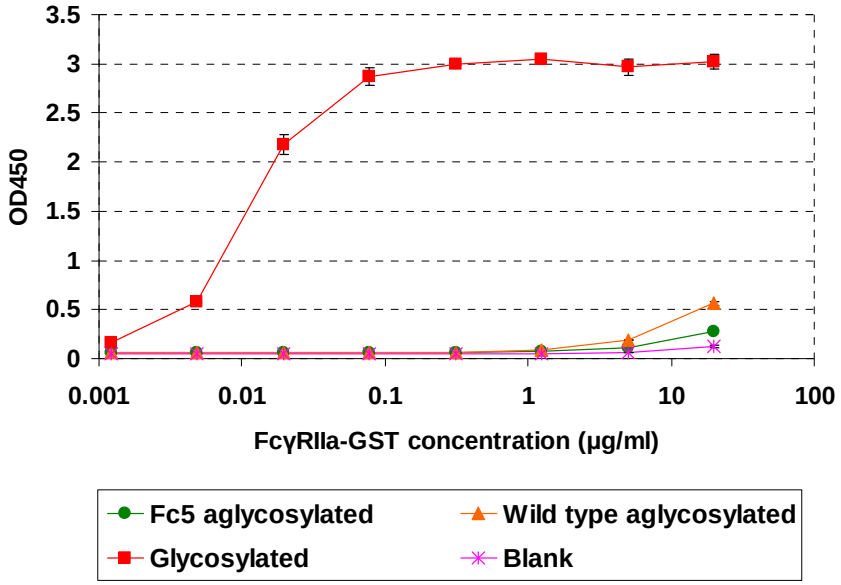

Figure 2-21. ELISA assays for binding to FcγRIIa-GST

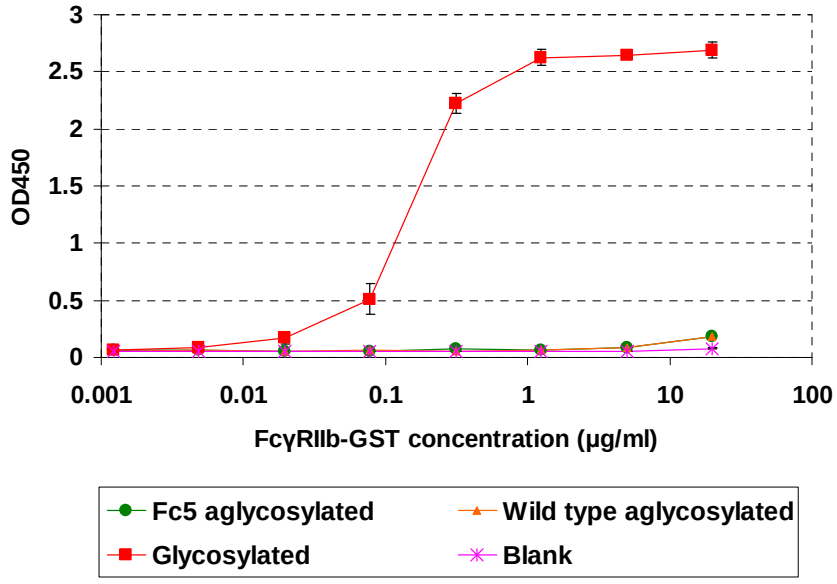

Figure 2-22. ELISA assays for binding to FcγRIIb-GST.

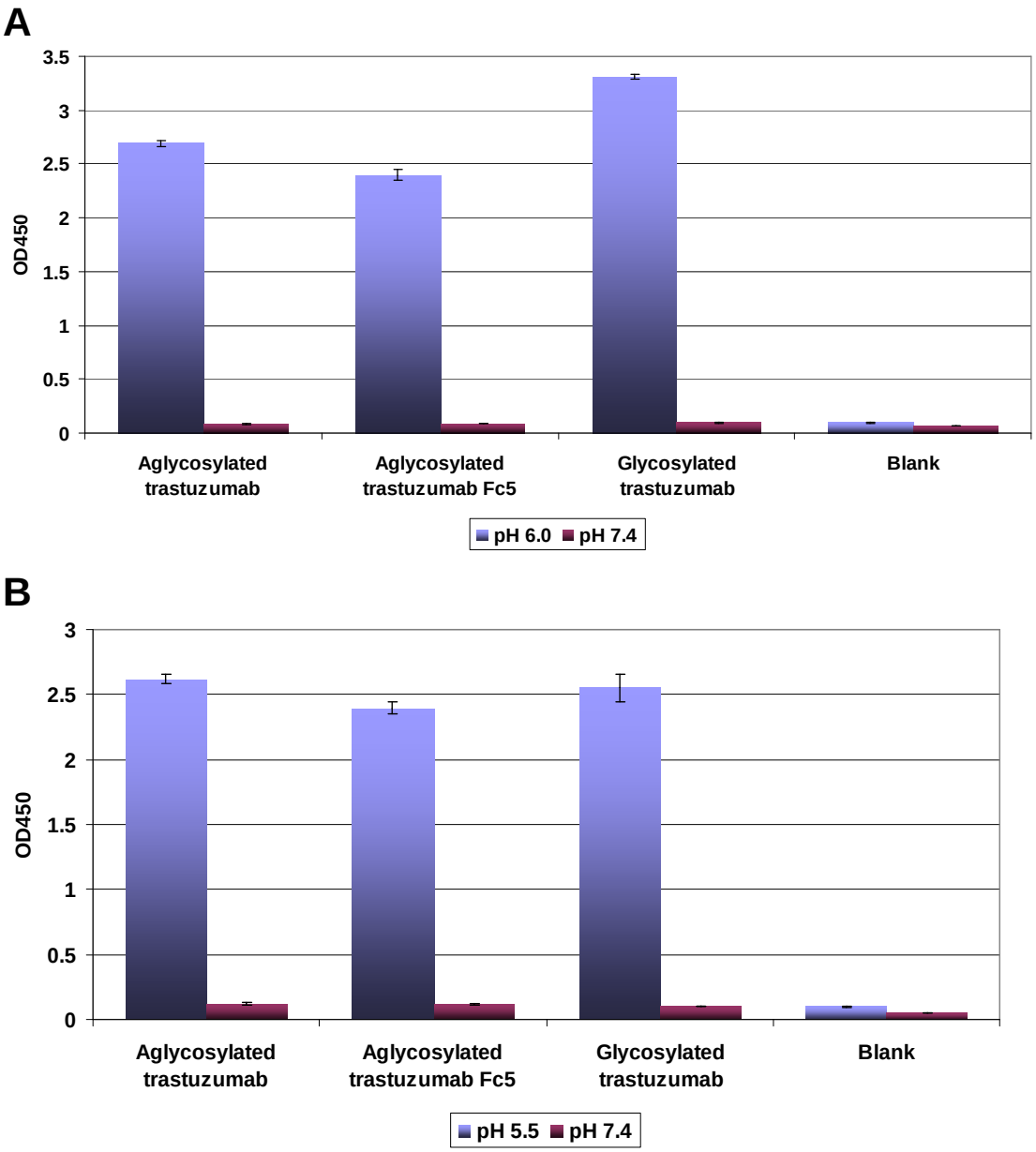

Figure 2-23. ELISA assays for pH dependent binding to FcRn. (A and B) ELISAs at pH 7.4 and at acidic pH 6.0 (A) or 5.5 (B). Plates were coated with purified aglycosylated trastuzumab antibodies, or with commercial glycosylated trastuzumab and the binding of FcRn was detected using anti-GST-HRP.

2.4 DISCUSSION

One important mechanism underlying the potency of antibody therapeutics is their ability to recruit immune cells for the clearance of target antigens or cells. Thus, the Fc region of an antibody is critical for the recruitment of immunological cells and for the regulation of antibody dependent cell-mediated cytotoxicity (ADCC). In particular, the nature of the ADCC response elicited by antibodies depends on the interaction of the Fc region with receptors (FcγRs) located on the surface of a variety of immune cell types.

The carbohydrate chain attached to the Fc region of glycosylated antibodies affects its conformation by packing the space between the two heavy chains in the CH2 domain and enables the antibody to bind to FcγRs (Krapp et al., 2003). In contrast to glycosylated antibodies produced in mammalian cells, aglycosylated antibodies produced in bacteria cannot bind to FcγRs and therefore are unable to elicit ADCC. In this chapter aglycosylated antibodies were engineered to display high affinity binding to specific effector FcγRs, a prerequisite for binding to effector cells and for ADCC. Specifically, in this study, we initially developed a new homodimeric Fc display system for the engineering aglycosylated Fc domains. Periplasmic expression of PelB leader peptide-fused Fc fragments cells grown in the presence of high concentrations of trehalose allowed the display of the protein onto spheroplasts. The disaccharide trehalose has been known to stabilize protein structure and prevent protein aggregation (Nishant Kumar Jain et al. 2008 Protein Sci.). Although the mechanism for the effect of trehalose on improving the FACS signal intensity and the signal to noise ratio upon display onto spheroplasts is not clear, it is possible that its effect is related to the ability of this dissacharide to affect the folding stability of proteins.

While aglycosylated human antibodies lack the ability to bind effector FcγRs, by screening large mutant libraries we isolated aglycosylated Fc domains that can bind to FcγRI with high affinity and specificity using the homodimeric Fc display system and high throughput flow cytometry. In this work we have focused on aglycosylated IgG1 that bind to FcγRI with an affinity essentially similar with CHO-derived, glycosylated antibodies. However, amino acid substitutions that afford binding to other effector FcγRs, or enhanced pH dependent binding to FcRn can also be isolated by this methodology from judiciously constructed mutant libraries (S.T.J., S.R., T.H.K., Jan Terje Andersen, I.S., P.W. T., G.G., unpublished data). Only two amino acid substitutions in CH3 were sufficient to confer full FcγRI binding. All human FcγRs for which crystal structures are available, bind to an epitope comprising residues in the hinge and CH2. Biochemical data indicate that FcγRI also binds to the same region (Shields et al., 2001). Therefore, it is possible that amino acid substitutions in CH3 induce a conformational change in the aglycosylated Fc that make the CH2 domains bulge out mimicking the “open” structure found in glycosylated IgG (Krapp et al., 2003). Unfortunately, a detailed structural interpretation is not possible at the moment, as neither the structure of aglycosylated IgGs nor that of FcγRI is available.

Glycosylated antibodies produced in mammalian cells display binding affinity to all effector FcγRs including inhibitory FcγRIIb. In contrast, aglycosylated trastuzumab-Fc5 was highly specific only to FcγRI. The binding of an antibody to specific Fc receptors determines its ability to recruit other immunological cells and the type of cell recruited. Hence, the ability to engineer antibodies that can recruit only certain kinds of cells can be critically important for therapy. The aglycosylated antibodies engineered to

selectively bind and activate a specific FcγR mediates theareputically relevant and altered effector functions as discussed in the following chapter.

Chapter 3

Engineering of Aglycosylated Fc5 for Improved Effector Functions

3.1 INTRODUCTION

FcγRI, an integral membrane glycoprotein, is expressed mainly on monocytes derived cells including macrophages and dendritic cells. It can be expressed on neutrophils and eosinophis by the induction of cytokines such as IFNγ, IL-10, and G-CSF (Schmidt and Gessner, 2005). The FcγRI protein is composed of three extracellular domains (D1, D2, and D3) and mediates activation signals for ADCC, phagocytosis, and cytokine production upon binding to IgG immune complexes (Cohen-Solal et al., 2004). The three FcγRI isoforms (FcγRIA, FcγRIB, and FcγRIC) are highly homologous sharing over 98% sequence identity at the nucleotide level (van de Winkel and Capel, 1993). In contrast to low affinity FcγRs, FcγRII and FcγRIII ($K_d = 10^{-6} \sim 10^{-7}$ M), the FcγRI has an additional extracellular domain (D3) (Hulett et al., 1991) and exhibits high affinity to monomeric IgG ($K_d = 10^{-8}$ M) (Krapp et al., 2003). FcγRI is important in the early stage immune response for low antibody concentration (Kacskovics, 2004).

For high affinity and specific binding to FcγRI, we isolated Fc engineered aglycosylated IgG Fc5 containing 2 mutations in the CH3 region (E382V and M428I). The Fc engineered aglycosylated trastuzumab-Fc5 showed similar binding affinity to FcγRI with glycosylated trastuzumab and specificity only to FcγRI without increasing binding affinities significantly to the other activating or inhibitory FcγRs includling FcγRIIa, FcγRIIb, and FcγRIIIa.

Here we focused on the isolation of aglycosylated IgG that binds exclusively to FcγRI. The role of FcγRI in ADCC is much less well understood relative to the other activating receptors. It has been suggested that because of its high affinity, FcγRI on effector cells is occupied by circulating IgG and therefore it may be involved in ADCC only during the early stage immune response when antibody concentration is low (Krapp et al., 2003). However, there is increasing evidence that the activation of FcγRI plays an important role in the resolution of certain infections and cancer (Bevaart et al., 2006; Pfefferkorn and Fanger, 1989; Tillinger et al., 2009). Here we showed that engineered, bacterially expressed trastuzumab IgGs potentiate the lysis of Her2 overexpressing SkBr3 breast cancer cells by monocyte-derived dendritic (mDC) cells. Strikingly, glycosylated, clinical grade trastuzumab failed to activate the cytotoxic ability of mDCs. Aglycosylated IgGs engineered to display unique FcR binding characteristics may thus be useful for elucidating the function of FcγRI and for the selective recruitment of mDCs in cancer therapy.

The high binding affinity of antibodies to human FcRn at slightly acidic pH (5.5 – 6.0) and the low affinity at neutral pH are critically important for recycling the serum antibodies through acidified endosomes leading to longer serum half life of serum antibody (Ober et al., 2004a; Ober et al., 2004b; Raghavan and Bjorkman, 1996; Rodewald, 1976). In this study, high throughput flow cytometry library screening was employed to isolate antibodies exhibiting higher binding affinity to FcγRI than Fc5 and similar pH dependent FcRn binding with clinical grade glycosylated trastuzumab.

3.2 MATERIALS AND METHODS

3.2.1 Error prone PCR library for engineering aglycosylated IgG-Fc5

All plasmids and primers used in this study are described in Table 3-1 and Table 3-2. Standard error prone PCR method (Fromant et al., 1995) was employed with the template of the pPelBFLAG-Fc5 and two primers (STJ# 196 and STJ#197) synthesized from Integrated DNA Technologies (Coralville, IA). The amplified PCR fragments were ligated into *Sfi*I digested pPelBFLAG. The resulting plasmids were transformed into *E. coli* Jude-1(F' [Tn*10(*Tet^{r}*)* proAB^{+} *lacI*^{q} Δ(*lacZ*)M15] *mcrA* Δ(*mrr-hsdRMS-mcrBC*) ϕ80d*lac*ZΔM15 Δ*lacX74 deoR recA1 araD139* Δ(*ara leu*)7697 *galU galK rpsL endA1 nupG*) (Kawarasaki et al., 2003).

3.2.2 Construction of upper CH2 region randomization library

4 sub-libraries were constructed as follows: Four parts of upper CH2 region (234L-239S, 264V-268H, 297N-299T, 328L-332I) (Kabat et al., 1991) were substituted by random amino acids using NNS degenerate codons. For the first sub-library, DNA fragments were amplified using the primers (STJ#465 and STJ#220) and the template, pPelBFLAG-Fc5. The N-terminal sequence extension of the PCR amplified fragments using the primer STJ#473 generated the sub-library replacing 5 amino acids in the region 234L-239S with random amino acids. Gene assembly PCR products using DNA fragments amplified by the primers (STJ#467 and STJ#220) and DNA fragments amplified by the primers (STJ#473 and STJ#468) generated the second sub-library that randomized 5 amino acid residues for 264V-268H. The third sub-library randomized 297N-299T was generated using the primer pairs (STJ#473/STJ#470 and

STJ#469/STJ#220) and the fourth sub-library (328L-332I) was generated using the primer pairs (STJ#473/STJ#470 and STJ#469/STJ#220) using the same PCR template plasmid, pPelBFLAG-Fc5. Based on the number of possible mutations, the same amount of DNA from three sub-libraries (234L-239S; 264V-268H; 328L-332I) that randomized 5 amino acid residues were mixed with and $20^3/20^5$ fold lower amount of DNA from the third sub-library (297N-299T) that randomized 3 amino acid residues. Each of the three sub-libraries was subcloned into *Sfi*I digested pPelBFLAG. The resulting plasmids were transformed into *E. coli* Jude-1.

.

3.2.3 Spheroplasting and flow cytometry screening for affinity maturation of Fc5

The library cells grown overnight at 37 °C with 250 rpm shaking in Terrific Broth media (Becton Dickinson Diagnostic Systems Difco™, Sparks, MD) with 2% (wt/vol) glucose and chloramphenicol (50 μg/ml) were diluted 1:50 in fresh TB media containing 0.5 M trehalose (Fisher Scientific, Fair Lawn, NJ) and chloramphenicol (50 μg/ml). After 3 h incubation at 37 °C with 250 rpm shaking and then 20 min cooling at 25°C, the expression of Fc fragments was induced with 1 mM isopropyl-1-thio-β-D-galactopyranoside (IPTG) and the cells were incubated for 5 hours at 25 °C with 250 rpm shaking. 4.5 ml of the culture broth was harvested by centrifugation and washed two times in 1 ml of cold 10 mM Tris-HCl (pH 8.0). After centrifugation at 12,000 x g for 1 min, 1 ml of, the cells resuspened in 1 ml of cold STE solution (0.5 M Sucrose, 10 mM Tris-HCl, 10 mM EDTA, pH 8.0) were incubated with rotating mixing at 37°C for 30 min, pelleted by centrifugation at 12,000 x g for 1 min and washed in 1 ml of cold

Solution A (0.5 M Sucrose, 20 mM $MgCl_2$, 10 mM MOPS, pH 6.8). The washed cells suspended in 1 ml of Solution A with 1 mg/ml of hen egg lysozyme were incubated at 37°C for 15 min. After centrifugation at 12,000 × g for 1 min, the resulting spheroplasts pellets were resuspended in 1 ml of cold PBS. For library screening, extracellular domain of recombinant glycosylated FcγRI/CD64 (R&D Systems, Minneapolis, MN) was labeled with FITC using a FITC protein conjugation kit according to the manufacturer's instructions (Invitrogen, Carlsbad, CA). After the conjugation reaction, the affinity of FITC-conjugated FcγRI (FcγRI-FITC) for human IgG Fc was confirmed by fluorescent ELISA displaying high fluorescence in the Fc glycosylated human IgG-Fc coated wells comparing in the BSA coated wells. Spheroplasts were labeled with 30 nM of FcγRI-FITC. In the subsequent round of sorting, reduced concentration of FcγRI-FITC (10, 3, and 1 nM for the 2^{nd}, 3^{rd}, and 4^{th} round sorting, respectively) was used for the labeling of spheroplasts for the screening from the error prone PCR library. For the screening aglycosylated Fc5 variants from 4 sub-libraries, 10 nM (3 nM for the 2^{nd} round, 1 nM for the 3^{rd} round, 0.3 nM for the 4^{th} round) of FcγRI-FITC was used for the labeling. More than 4×10^8 spheroplasts per round were sorted by MoFlo (Dako Cytomation, Fort Collins, CO) equipped with a 488 nm argon laser for excitation. In each round the top 3% of the population showing the highest fluorescence due to FcγRI-FITC labeling was isolated by sorting and resorting immediately after the initial sorting. The Fc genes in the spheroplasts were rescued by PCR amplification using two specific primers (STJ#16 and STJ#220), ligated into pPelBFLAG-Fc using *Sfi*I restriction endonuclease site, and transformed in electrocompetent *E. coli* Jude-1 cells. The resulting transformants were

grown on chloramphenicol containing media, and then spheroplasted as above in preparation for the next round of sorting.

3.2.4 Expression and purification of aglycosylated trastuzumab antibodies

For pSTJ4-Herceptin-Fc5-IgG1, pSTJ4-Herceptin-Fc601-IgG1, and pSTJ4-Herceptin-Fc701-IgG1, Fc5, Fc601, and Fc701 mutant genes were amplified using the primers (STJ#290 and STJ#291) and the templates, pPelBFLAG-Fc5, pPelBFLAG-Fc601, or pPelBFLAG-Fc701 ligated into pSTJ4-Herceptin IgG1 digested using *Sal*I / *Eco*RV. For preparative production of wild type or Fc engineered aglycosylated trastuzumab antibodies in *E. coli,* dicistronic plasmids, pSTJ4-Herceptin-IgG1, pSTJ4-Herceptin-Fc5-IgG1, pSTJ4-Herceptin-Fc601-IgG1, and pSTJ4-Herceptin-Fc701-IgG1 were constructed. In these plasmids protein expression is under the control of the *lac* promoter. Heavy and light chains are expressed a dicistronic operon and fused to the PelB leader peptide for secretion across the cytoplasmic membrane. After transformation of the plasmids into *E. coli* BL21(DE3) (EMD Chemicals, Gibbstown, NJ), cells grown in LB complex medium for overnight were cultured overnight twice for adaptation in R/2 medium used for high cell density fermentation (Jeong and Lee, 2003). The R/2 medium is composed of: 2 g of $(NH_4)_2HPO_4$, 6.75 g of KH_2PO_4, 0.93 g of citric acid H_2O, 0.34 g of $MgSO_4$, 20 g of glucose, 0.05 g of ampicillin and 5 ml of trace metal solution dissolved in 2 N HCl (10 g of $FeSO_4$-$7H_2O$, 2.25 g $ZnSO_4$-$7H_2O$, 1 g of $CuSO_4$-$5H_2O$, 0.35 g of $MnSO_4$-H_2O, 0.23 g of $Na_2B_4O_7$-$10H_2O$, 1.5 g of $CaCl_2$, and 0.1 g of $(NH_4)_6Mo_7O_{24}$ per L). *E. coli* BL21(DE3) harboring pSTJ4-Herceptin-IgG1, pSTJ4-Herceptin-IgG1-Fc5, pSTJ4-Herceptin-IgG1-Fc601, or pSTJ4-Herceptin-IgG1-Fc701

were cultured in 500 ml baffled-flask with 120 ml R/2 media at 30 °C at 250 rpm for 8 h and then inoculated to 3.3L fermentor (BioFlo 310, New Brunswick Scientific Co., Edison, NJ) with 1.2 L R/2 medium. Cells were grown at 30 °C by fed-batch fermentation with pH-stat glucose feeding strategy. To maintain the dissolved oxygen (DO) concentration at 40% of air saturation, the automatic cascade controller increased agitation speed from 100 rpm to 1000 rpm, air flow rate from 1 to 3 SLPM (Standard liquid per minute) and pure oxygen flow rate from 0 to 1.5 SLPM when needed. The initial pH was adjusted to 6.8 and controlled by the addition of 30% (v/v) ammonium hydroxide when it decreased to less than 6.75 and by the supply of feeding solutions, (700 g/L of glucose and 10 g/L of $MgSO_4$-$7H_2O$; before induction) and (500 g/L glucose, 10 g/L of $MgSO_4$-$7H_2O$, and 100 g/L of yeast extract; after induction), when it increased to more than 6.9. When the OD_{600} reached about 100, the cells were cooled at 25 °C for 30 min, and then induced for protein synthesis with 1 mM of isopropyl-1-thio-β-D-galactopyranoside (IPTG). 7 h later at an OD_{600} of ~130-140, the culture broth was harvested by centrifugation at 11,000 x g for 30 min.

For the release of periplasmic proteins, cells were suspended in 1.2 L of 100 mM Tris, 10 mM EDTA (pH 7.4) solution supplemented with 4 mg of lysozyme (per g of dry cell weight) and 1 mM PMSF, and then incubated with shaking at 250 rpm at 30 °C for 16 h. After centrifugation at 14,000 × g for 30 min, the supernatant was mixed with polyethyleneimine (MP Biomedical, Solon, OH) to a final concentration of 0.2% (w/v) recentrifuged at 14,000 × g for 30 min, and filtered through 0.2 μm filter. Clear filtrate was mixed with Immobilized Protein A agarose resin (Pierce Biotechnology, Rockford, IL) pre-equilibrated in 20 mM sodium phosphate buffer (pH 7.0) and incubated at 4 °C

for 16 h. After washing with 200 ml of 20 mM sodium phosphate buffer (pH 7.0) and 200 ml of 40 mM sodium citrate (pH 5.0), wild type aglycosylated trastuzumab, aglycosylated trastuzumab-Fc5, aglycosylated trastuzumab-Fc601, and aglycosylated trastuzumab-Fc701 were eluted from the resin using 15 ml of 0.1 M glycine (pH 3.0) and neutralized immediately with 1M Tris (pH 8.0) solution. The eluted samples were concentrated by ultrafiltration through a 10 kDa Mw cutoff membrane and the retentate was applied to a Superdex 200 gel filtration column developed with PBS (pH 7.4).

3.2.5 BIAcore analysis for aglycosylated trastuzumab antibodies to FcγRI

Glycosylated trastuzumab, trastuzumab, trastuzumab-Fc5, trastuzumab-Fc601, and trastuzumab-Fc701 were immobilized on CM5 sensor chip using amine coupling method recommened by the manufacturer (Biacore, Piscataway, NJ). The soluble monomeric FcγRI in HBS-EP buffer (10 mM HEPES pH 7.4, 150 mM NaCl, 3.4 mM EDTA, and 0.005% P20 surfactant) was injected at a flow rate of 30 μl/min for 60 s with dissociation time 300 s. The FcγRI ligands were regenerated by single injection of 100 mM citric acid, pH 3.0. Binding kinetics the soluble monomeric FcγRI with glycosylated trastuzumab, aglycosylated trastuzumab, trastuzumab-Fc5, and trastuzumab-Fc601 were obtained by injection of soluble FcγRI in duplicate at concentrations of 0, 25, 50, 100, 200 nM for 60 s at a flow rate of 30 μl/min over immobilized trastuzumab antibodies. Binding kinetics for wild type aglycosylated trastuzumab to FcγRI was measured by injecting FcγRI in duplicate at concentrations 0, 200, 300, 400, 500, and 600 nM for 60 s at a flow rate 30 μl/min over immobilized aglycosylated trastuzumab. Binding curves at zero concentration was subtracted as a blank. Fitting of equilibrium responsess to steady-

state affinity model provided by BIAevaluation 3.0 software generated equilibrium dissociation constants (K_D).

3.2.6 ELISA analysis to measure the affinity of trastuzumab antibodies to Fc receptors

50 µl of 4 µg/ml of aglycosylated trastuzumab, trastuzumab-Fc5, trasuzumab-Fc601, or trasuzumab-Fc701 purified from *E. coli*, glycosylated IgG trastuzumab were diluted in 0.05 M Na_2CO_3 (pH 9.6) buffer and coated on 96 well polystyrene ELISA wells (Corning, Corning, NY) by incubation at 4 °C for 16 hr. The coated wells were blocked with 1 × PBS (pH 7.4), 0.5% BSA for 2 hr at room temperature, washed 4 times with PBS containing 0.05% Tween20, and incubated with serially diluted FcγRIIa, FcγRIIb C-terminally fused to GST (Berntzen et al., 2005), FcγRIIIa (R&D Systems, Minneapolis, MN) at room temperature for 1 h. After washing 4 times with the same buffer, 1:5,000 diluted anti-GST antibody HRP conjugate (Amersham Pharmacia, Piscataway, NJ) for FcγRIIa and FcγRIIb or 1:10,000 diluted anti-polyhistidine antibody HRP conjugate (Sigma-Aldrich, St. Louis, MO) for FcγRIIIa was added and plates were washed and developed using Ultra-TMB substrate (Pierce Biotechnology, Rockford, IL). To determine the binding of IgG to FcRn at pH 7.4, 2 µg/ml of FcRn preincubated in PBS (pH 7.4) containing 1:5,000 diluted anti-GST-HRP at room temperature for 1 h as previously described (Andersen et al., 2006) was added to plates coated with trastuzumab antibodies. To evaluate binding at pH 6.0, ELISAs were carried out as above except 20 mM MES was added to washing buffer and sample dilution buffers and pH was adjusted to 6.0.

3.2.7 Preparation of human monocyte-derived dendritic cells (mDCs)

Human blood buffy coats collected from healthy donors (Gulf Coast Blood Center, Galveston, TX) and added to histopaque solution (Sigma-Aldrich, St. Louis, MO) at 1:1 volume, avoiding mixing of the contents. The blood-histopaque solution was centrifuged at 1600 rpm for 30 minutes at 23°C without centrifugation braking. The PBMC layer was isolated following gradient centrifugation, and washed twice through centrifugation with wash buffer (PBS, 2.5% FBS, 1mM EDTA). Cells were then resuspended in IMDM (Cambrex, Walkersville, MD) and added to a 24 well plate and incubated at 37°C for 2h to allow monocytes to adhere to the plate. Media and non-adherent cells were then removed by asipration and adherent cells were washed 5 times with wash buffer. Cells were then resuspended with 1ml/well of growth media consisting of IMDM (Cambrex, Walkersville, MD), 10% FBS (Invitrogen, Carlsbad, CA), and cytokines IL-4 (R&D systems, Minneapolis, MN) at 200 ng/ml and granulocyte macrophage colony stimulating factor (GM-CSF, R&D systems, Minneapolis, MN) at 200 ng/ml. IL-4 and GM-CSF were added on day 2 and 5 without changing media. The presence of DCs was evaluated by flow cytometry by staining with a fluorescent antibody (Anti-CD11c-FITC, eBioscience, San Diego, CA) against the DC-specific surface marker CD11c.

3.2.8 ADCC assays

Target SkBr3 tumor cells were labeled with the isotope $Na^{51}CrO_4$ (Perkin Elmer Life Sciences) at 100 uCi/10^6 cells for 1h at 37°C. Cells were then washed twice with PBS, resuspended in RPMI and added to a 96 well plate at 10^4 cells/well. Engineered Fc antibodies and relevant controls were added to the target cells in triplicate wells and incubated at 37°C for 1h. The plate was then centrifuged at 2000 rpm for 1 minute and washed twice with PBS. Effector cells, either fully differentiated mDCs (day 7) or freshly isolated PBMCs, were resuspended in RPMI, 2% low IgG FBS (Invitrogen, Carlsbad, CA), LPS (250 ng/10^6 cells) and added to the wells at various ratios. In blocking experiments, the FcγRI blocking antibody 10.1 was added to mDCs at 12 μg/250,000 cells for 1h at 37°C (eBioscience, San Diego, CA) and then added to target cells. Target cells and mDCs were incubated at 37°C for 24h. The isotope levels present in cell media were then measured in a liquid scintillation counter. Incubation of target cells with 2% SDS was used as a positive control for maximum lysis and incubation with no effector cells was used as background lysis.

Table 3-1. Plasmids used in this study.

Plasmids	Relevant characteristics	Reference or source
pMoPac1	Cm^r, *lac* promoter, *tetA* gene, C-terminal polyhistidine tag and c-myc tag	(Hayhurst et al., 2003)
pMoPac12	Ap^r, *lac* promoter, *tetA* gene, *skp* gene, C-terminal polyhistidine tag and c-myc tag	(Hayhurst et al., 2003)
pMoPac1-FLAG-M18	NlpA fused *M18 scFv gene*, C-terminal FLAG tag in pMoPac1	(Jung et al., 2007)
pPelBFLAG	Cm^r, *lac* promoter, *tetA* gene, *skp* gene, C-terminal FLAG tag	This study
pPelBFLAG-Fc	*IgG1-Fc* gene in pPelBFLAG	This study
pPelBFLAG-Fc5	*IgG1-Fc5* gene in pPelBFLAG	This study
pPelBFLAG-Fc601	*IgG1-Fc601* gene in pPelBFLAG	This study
pPelBFLAG-Fc701	*IgG1-Fc601* gene in pPelBFLAG	This study
pMAZ360-M18.1-Hum-IgG	*M18.1 humanized IgG1* gene in pMAZ360	(Mazor et al., 2007)
pSTJ4-Herceptin IgG1	*Herceptin IgG1* gene in pMAZ360-M18.1-Hum-IgG1	This study
pSTJ4-Herceptin-Fc5-IgG1	*Herceptin IgG1-Fc5* gene in pMAZ360-M18.1-Hum-IgG1	This study
pSTJ4-Herceptin-Fc601-IgG1	*Herceptin IgG1-601* gene in pMAZ360-M18.1-Hum-IgG1	This study
pSTJ4-Herceptin-Fc701-IgG1	*Herceptin IgG1-701* gene in pMAZ360-M18.1-Hum-IgG1	This study

Table 3-2. Primers used in this study.

Primer Name	Primer nucleotide sequence (5' → 3')
STJ#16	TTGTGAGCGGATAACAATTTC
STJ#196	CGCAGCGAGGCCCAGCCGGCCATGGCG
STJ#197	CGCAATTCGAATTCGGCCCCCGAGGCCCC
STJ#220	CAATTTTGTCAGCCGCCTGAGCAGAAG
STJ#327	GCCCTTGAAGCTTGCAGAGCTGACCGTGACCAGCGT
STJ#465	CCCACCGTGCCCAGCACCTGAANNSNNSNNSGGANNSNNSGTCTTCCTCTTCCCCCCAAAACCC
STJ#466	GGGTTTTGGGGGGAAGAGGAAGACSNNSNNTCCSNNSNNSNNTTCAGGTGCTGGGCACGGTGGG
STJ#467	CCTGAGGTCACATGCGTGGTNNSNNSNNSNNSNNSGAAGACCCTGAGGTCAAGTTCAACTGG
STJ#468	CCAGTTGAACTTGACCTCAGGGTCTTCSNNSNNSNNSNNSNNACCACGCATGTGACCTCAGG
STJ#469	GCCGCGGGAGGAGCAGTACNNSNNSNNSTACCGTGTGGTCAGCGTCCTC
STJ#470	GAGGACGCTGACCACACGGTASNNSNNSNNGTACTGCTCCTCCCGCGGC
STJ#471	CAAGTGCAAGGTCTCCAACAAAGCCNNSNNSNNSNNSNNSGAGAAAACCATCTCCAAAGCCAAAGGG
STJ#472	CCCTTTGGCTTTGGAGATGGTTTTCTCSNNSNNSNNSNNSNNGGCTTTGTTGGAGACCTTGCACTTG
STJ#473	CGCAGCGAGGCCCAGCCGGCCATGGCGGACAAAACTCACACATGCCCACCGTGCCCAGCACCTG
STJ#471	CAAGTGCAAGGTCTCCAACAAAGCCNNSNNSNNSNNSNNSGAGAAAACCATCTCCAAAGCCAAAGGG
STJ#472	CCCTTTGGCTTTGGAGATGGTTTTCTCSNNSNNSNNSNNSNNGGCTTTGTTGGAGACCTTGCACTTG
STJ#473	CGCAGCGAGGCCCAGCCGGCCATGGCGGACAAAACTCACACATGCCCACCGTGCCCAGCACCTG
STJ#474	CGCAGCGAGGCCCAGCCGGCCATGGCGGAGGTTCAATTAGTGGAATCTG
STJ#475	CGCAGCGAGGCCCAGCCGGCCATGGCGGATATTCAAATGACCCAAAGCCCG
STJ#476	CGCAATTCGGCCCCCGAGGCCCCGCACTCTCCCCTGTTGAAGCTCTTTG
STJ#479	GACAAAACTCACACATGCCCACCGTGCC
STJ#480	GGCACGGTGGGCATGTGTGAGTTTTGTC

3.3 RESULTS

3.3.1 Isolation of aglycosylated Fc mutants exhibiting higher affinity to FcγRI binding compared to Fc5

For the isolation of IgG1 Fc fragments displaying higher binding affinity to FcγRI than the Fc fragment (Fc5; E328V/M428I) (Fig. 3-1 and 3-2) described in chapter 2, the Fc5 gene was subjected to random mutagenesis by error prone PCR. The library was 7×10^8 individual transformats with 0.264% error rate per gene based on the sequence of 20 library clones randomly selected (Fig. 3-3).

After the 5^{th} round flow cytometry sorting of over 4×10^8 spheroloplasts labeled with FcγRI-FITC, high fluorescent clones were enriched following successive rounds of sorting (Fig. 3-4). After the 5^{th} round, 19 individual clones exhibiting higher fluorescence than Fc5 were isolated (Fig. 3-5). Sequence analysis showed that all amino acid substitutions that contributed to the higher fluorescence signal of the isolated clones were located in one of three distinct regions; the upper CH2 region that is likely to directly contact FcγRI, the interdomain region connecting the CH2 region F β-sheets and CH3 B β-sheets, and the CH3 region that may contribute conformational changes for FcγRI binding (Fig. 3-6). Fc601 showed the highest affinity and contained two additional mutations K338R, G341V on the G strand of CH2 and A strand of CH3, respectively (Fig. 3-7 and 3-8).

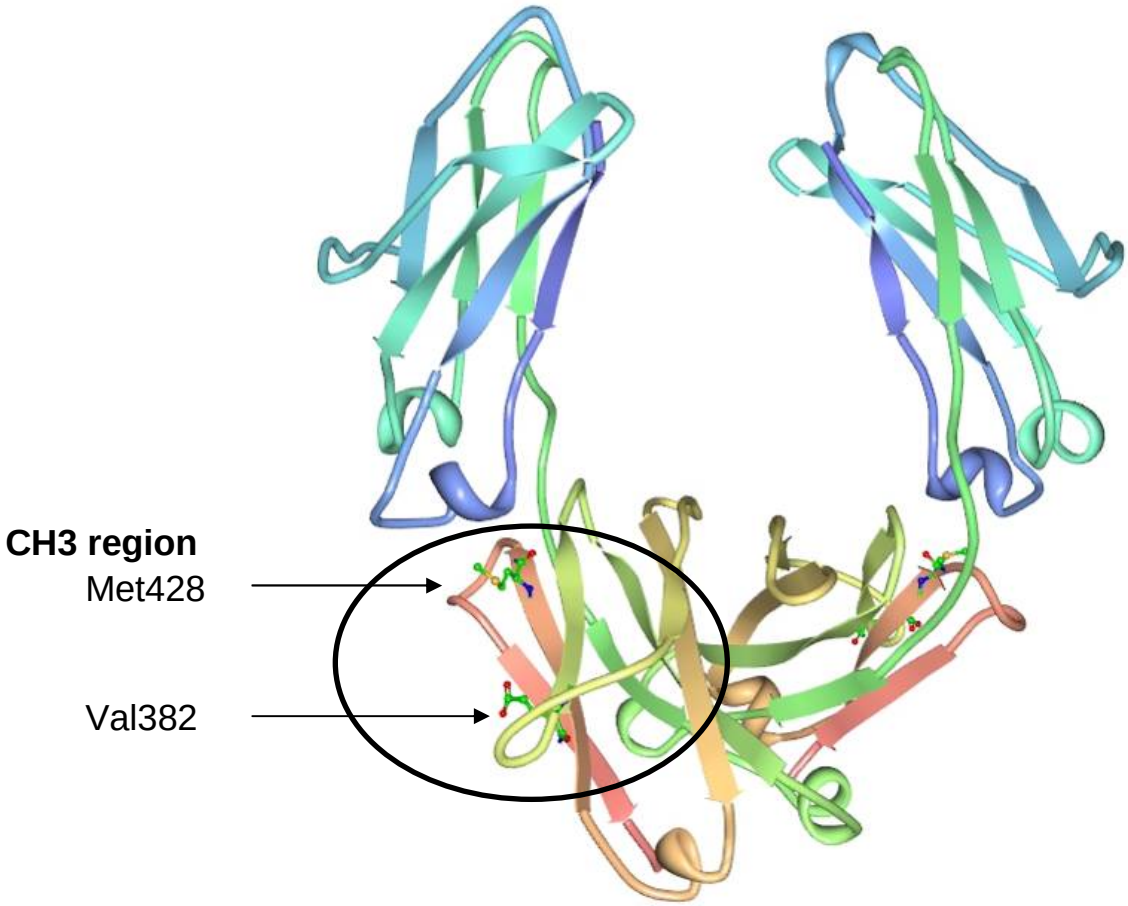

Figure 3-1. Mutation points of isolated aglycosylated Fc5 (382E and 428M) represented on the 3D structure of glycosylated IgG1 Fc (PBD Code: 1FC1).

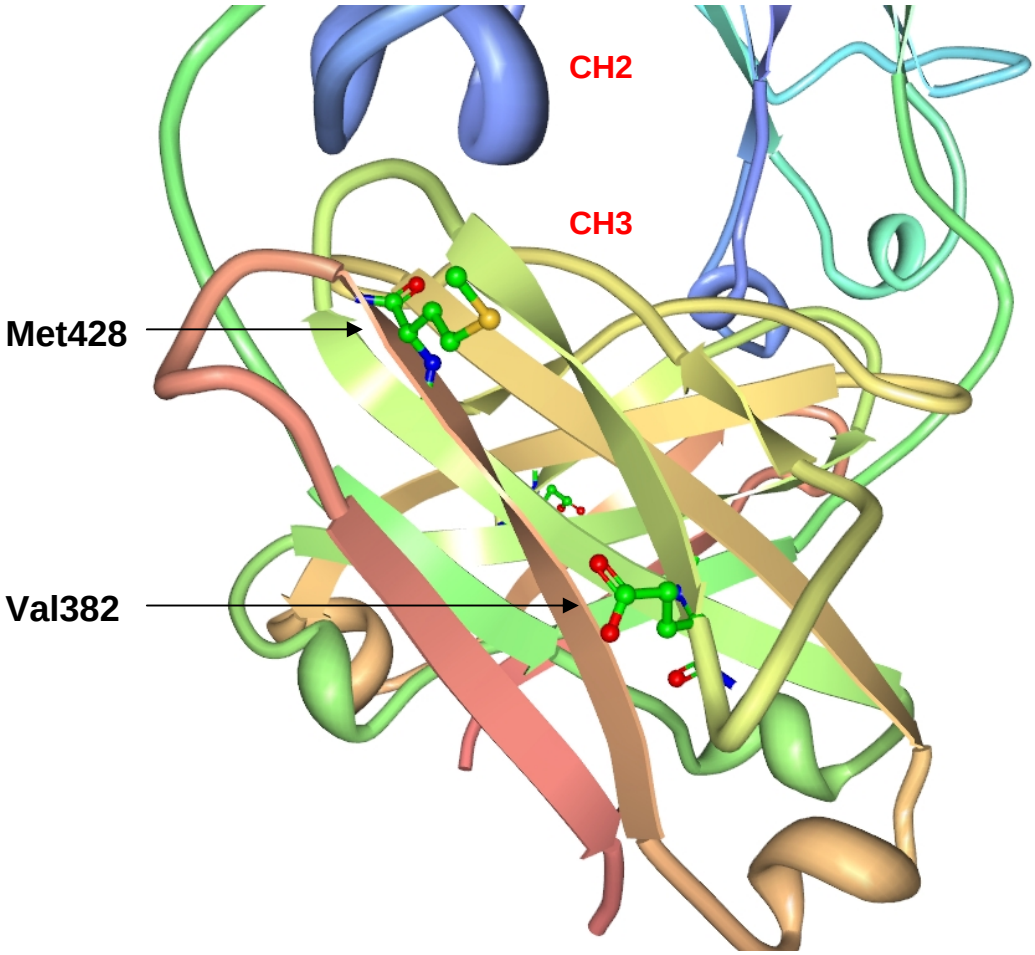

Figure 3-2. The location of 382E in β-sheet C and 428M in β-sheet F of CH3 domain represented on the crystal structure of glycosylated IgG. (PBD Code: 1FC1).

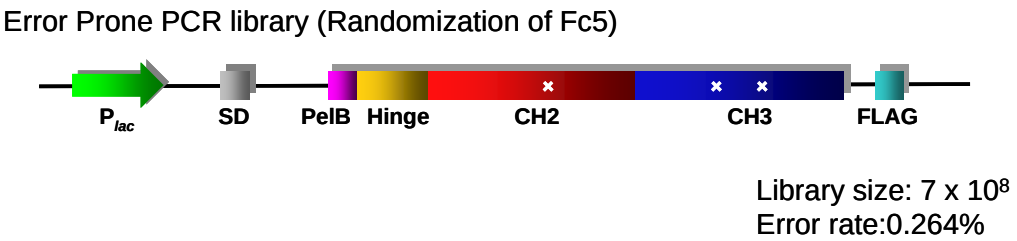

Figure 3-3. Error prone PCR library for engineering aglycosylated Fc5 domain.

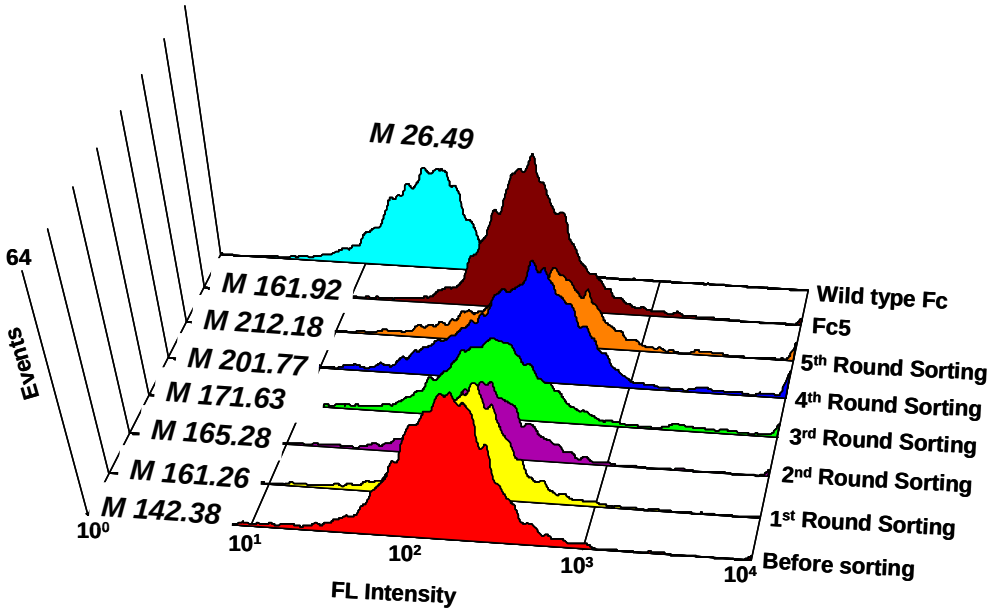

Figure 3-4. Fluorescence histogram of spheroplasts labeled with FcγRI-FITC showing the enrichment by series rounds of FACS sorting.

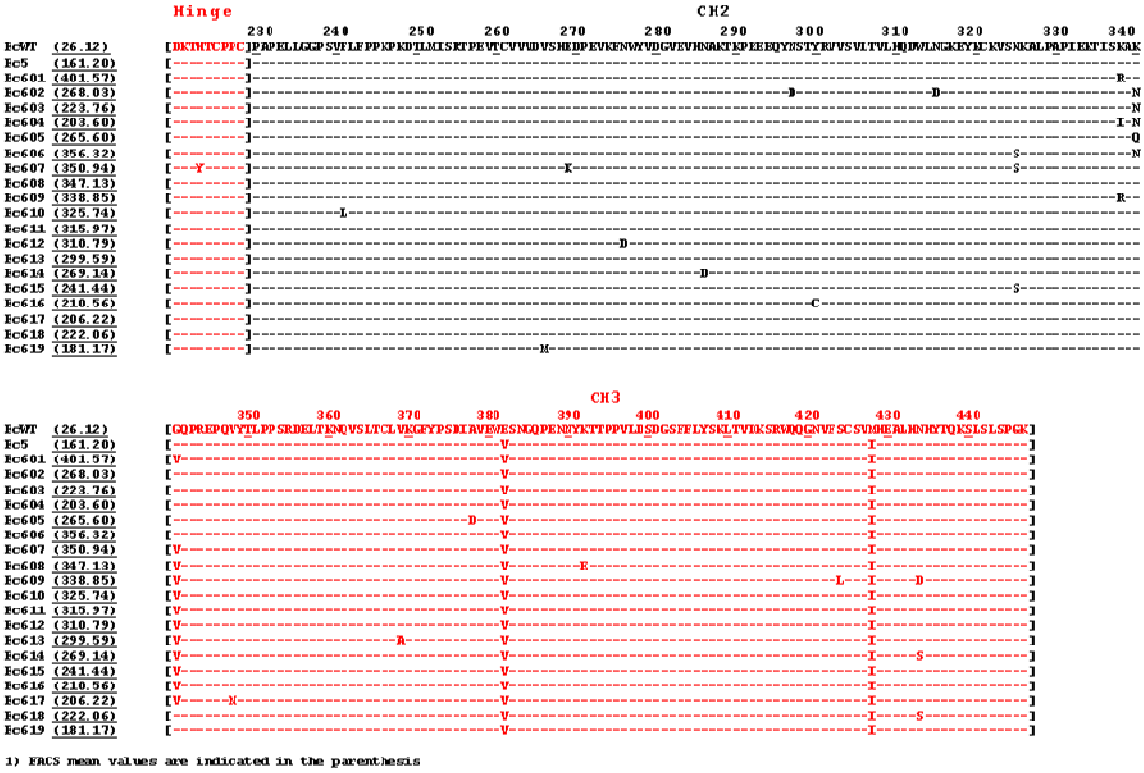

Figure 3-5. Protein sequences of isolated Fc mutant clones exhibiting higher affinity to FcγRI than Fc5. Mean fluorescence values for the respective clones labeled with FcγRI-FITC are shown in parenthesis.

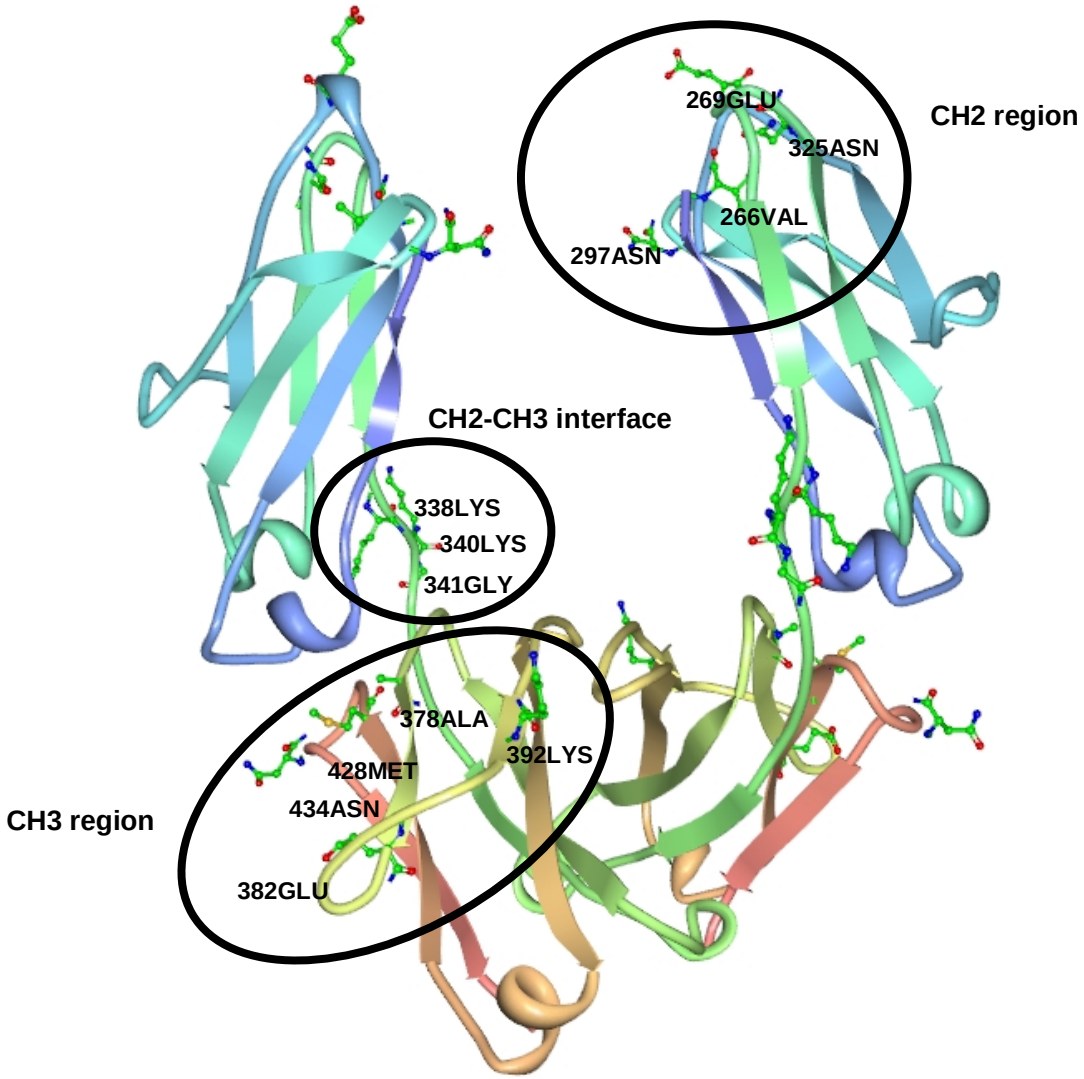

Figure 3-6. Amino acid substitutions in variants Fc601-619 represented on the 3D structure of glycosylated IgG1 Fc (PBD Code: 1FC1).

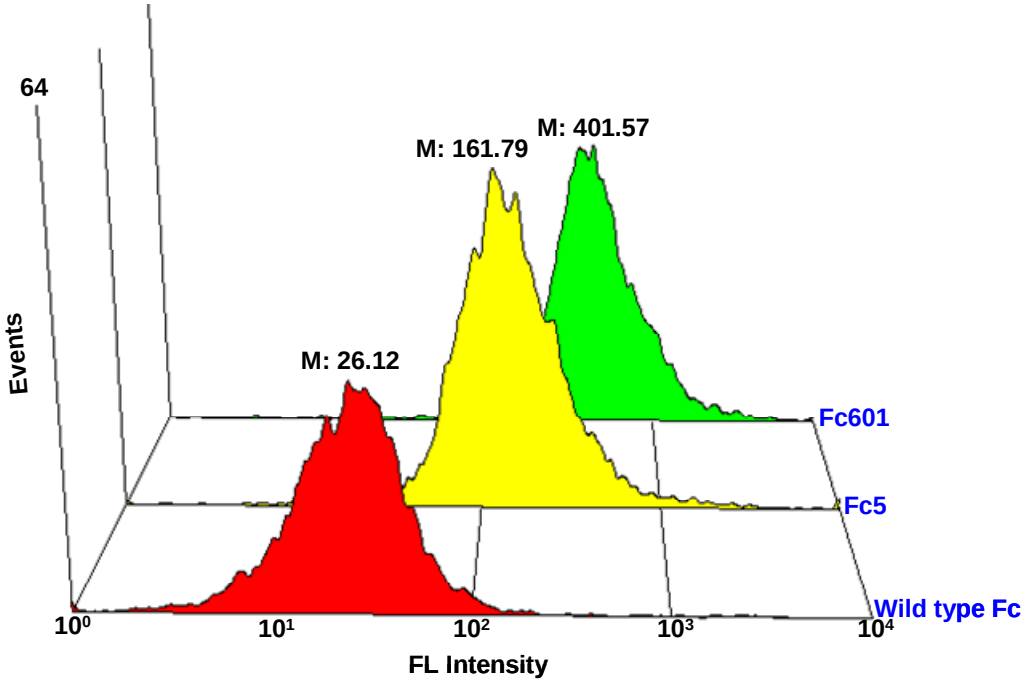

Figure 3-7. Fluorescence histogram of spheroplasts expressing wild type Fc, Fc5, or Fc601 labeled with 30 nM of FcγRI-FITC. M: Mean fluorescence intensity.

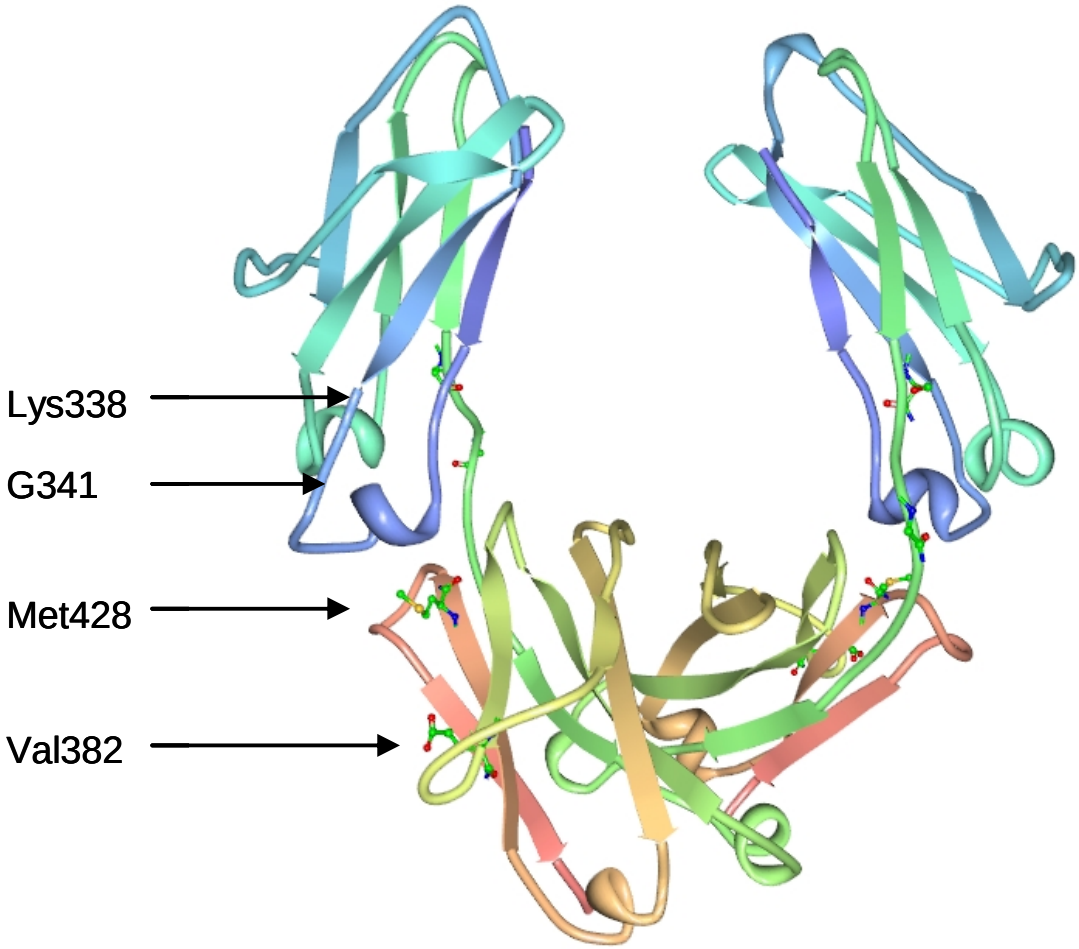

Figure 3-8. Amino acid substitutions in Fc601 (K338R, G341V, E382V, M428I) represented on the 3D structure of glycosylated IgG1 Fc (PBD Code: 1FC1).

3.3.2 Characterization of aglycosylated trastuzumab-Fc601 in *E. coli*

Trastuzumab (Herceptin™) has been clinically utilized for the treatment of breast metastatic carcinomas that overexpress HER2/neu (Erb2) (Sergina and Moasser, 2007). Trastuzumab recognizes HER2/neu (Erb2) and interacts with surface FcγRs of immune cells leading to antibody dependent cell mediated cytotoxicity (ADCC), an important mechanism for therapeutic action (Lazar et al., 2006; Sergina and Moasser, 2007). Fc fragment genes engineered for high FcγRI affinity were incorporated into full length trastuzumab antibodies. For preparative production aglycosylated trastuzumab, trastuzumab-Fc5, and trastuzumab-Fc601 in *E. coli* the heavy and light chains were fused to the PelB signal peptide and placed downstream from the *lac* promoter in a dicistronic operon (Figure 3-9). Aglycosylated antibodies were produced by fed-batch fermentation of *E. coli* BL21(DE3) cells with a pH-stat glucose feeding strategy. Subsequently the aglycosylated antibodies were purifed from the periplasmic proteins using Protein A affinity chromatography followed by gel filtration chromatography as described in chapter 2.

The binding kinetic constants of of full assembled aglycosylated trastuzumab-Fc601 to FcγRI were measured by BIACore using immobilized trastuzumab-Fc601 on the CM5 sensor chip. As shown in Table 3-3 and Figure 3-10, trastuzumab-Fc601 bound to FcγRI with similar affinity to that of commercial-grade glycosylated trastuzumab from CHO cells and over 130-fold higher affinity compared with wild type aglycosylated trastuzumab (Table 3-3 and Fig. 3-10). The affinity of the trastuzumab-Fc601 for the extracellular domain of FcγRIIa, FcγRIIb, and FcγRIIIa was analyzed by ELISA. Similar to aglycosylated trastuzumab or aglycosylated trastuzumab-Fc5, the aglycosylated

tratuzumab exhibited low affinity to FcγRIIa or FcγRIIb (EC_{50}≥ 1000-fold and 100-fold higher equilibrium dissociation constant for GST fused to FcγRIIa or FcγRIIb (Fig. 3-11 and Fig. 3-12), FcγRIIIa (Fig. 3-13). The trastuzumab-Fc601 antibody exhibited only slightly higher affinity for FcγRIIb. We examined whether the amino acid substitutions in Fc5 and Fc601 affect pH dependent binding to the neonatal FcRn receptor which recognizes an epitope located in the CH2-CH3 interface (Martin et al., 2001). Aglycosylated trastuzumab-Fc5 showed pH-dependent binding to human FcRn at pH 5.5 and pH 6.0 and significantly reduced binding at pH 7.4 similar to clinical grade, trastuzumab purified from CHO cells. On the other hand, aglycosylated trastuzumab-Fc601 showed reduced affinity to FcRn binding at pH 6.0 indicating that the additional two amino acids substitutions in the CH2-CH3 of Fc601 interfered with binding to the neonatal Fc receptor (Fig. 3-14).

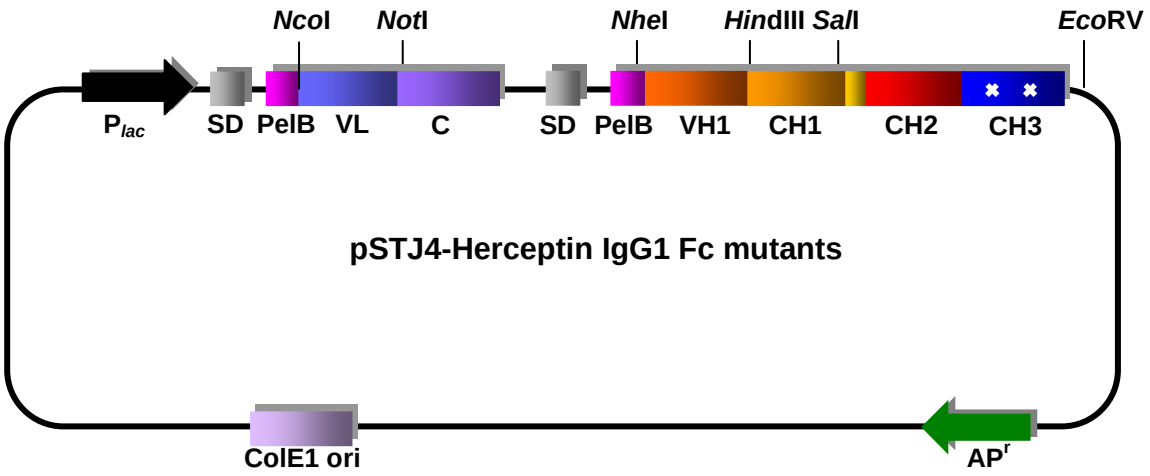

Figure 3-9. Map of plasmid pSTJ4-Herceptin IgG1.

Table 3.3. Kinetic rates and equilibrium dissociation constants obtained by BIACore analysis for binding to FcγRI.

	K_{on} (M^{-1} sec^{-1})	K_{off} (sec^{-1})	K_D (nM)
Aglycosylated wild type trastuzumab	1.31×10^5	5.02×10^{-2}	382
Aglycosylated trastuzumab-Fc5	2.17×10^5	1.23×10^{-3}	5.69
Aglycosylated trastuzumab-Fc601	1.34×10^5	3.92×10^{-4}	2.92
Glycosylated Herceptin	1.77×10^5	2.66×10^{-4}	1.5

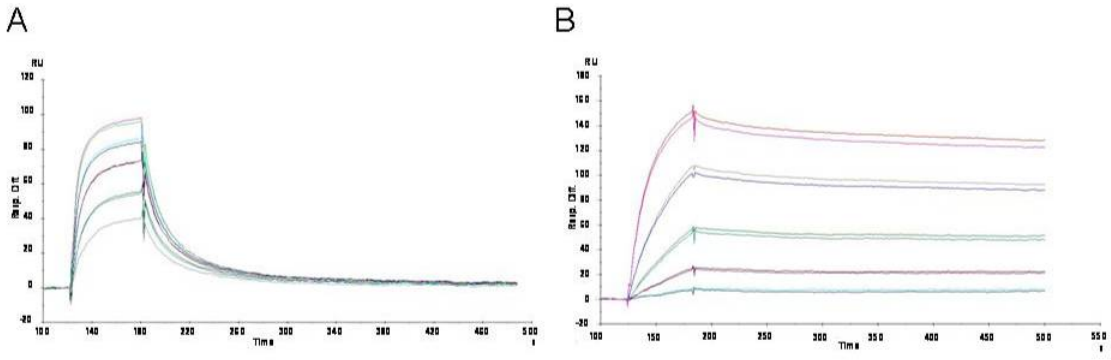

Figure 3-10. BIACore sensorgram for aglycosylated trastuzumab (A) and aglycosylated trastuzumab-Fc601 (B).

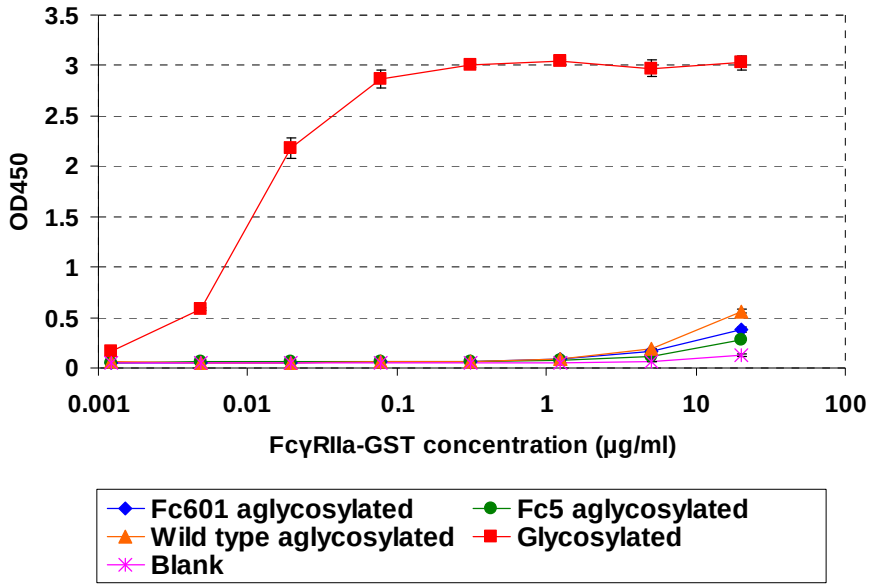

Figure 3-11. ELISA assays for binding of trastuzumab antibodies to FcγRIIa-GST.

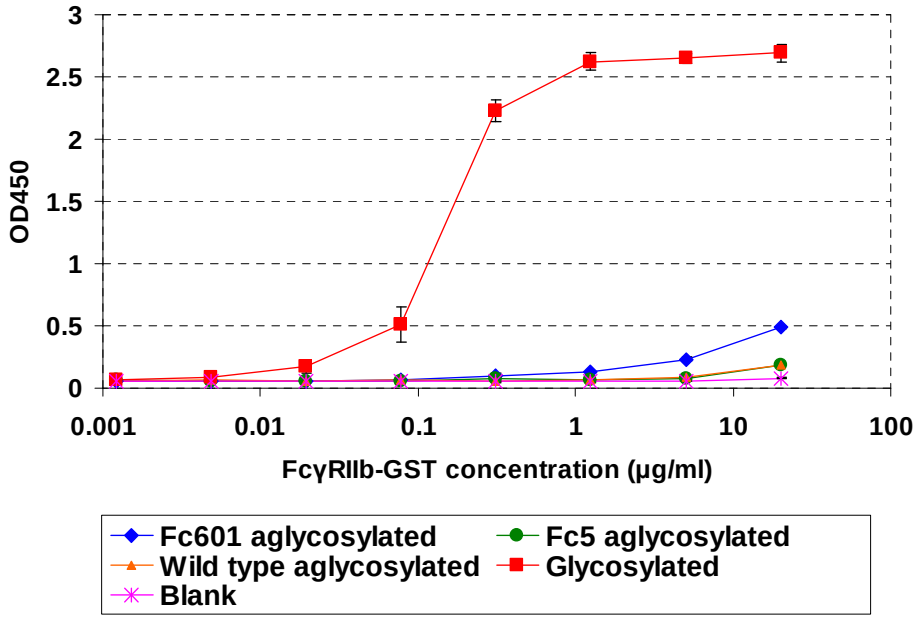

Figure 3-12. ELISA assays for binding of trastuzumab antibodies to FcγRIIb-GST.

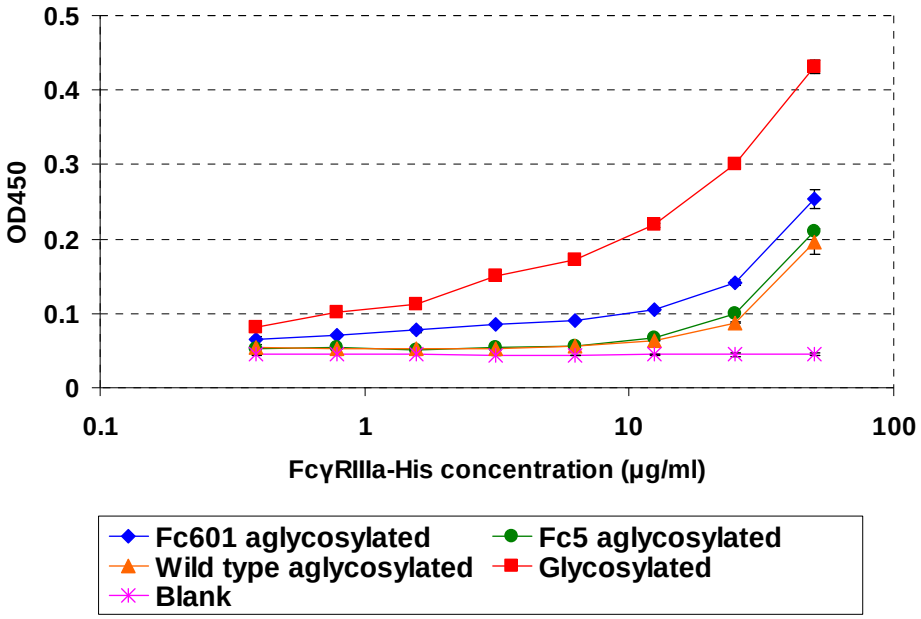

Figure 3-13. ELISA assays for binding of trastuzumab antibodies to FcγRIIIa.

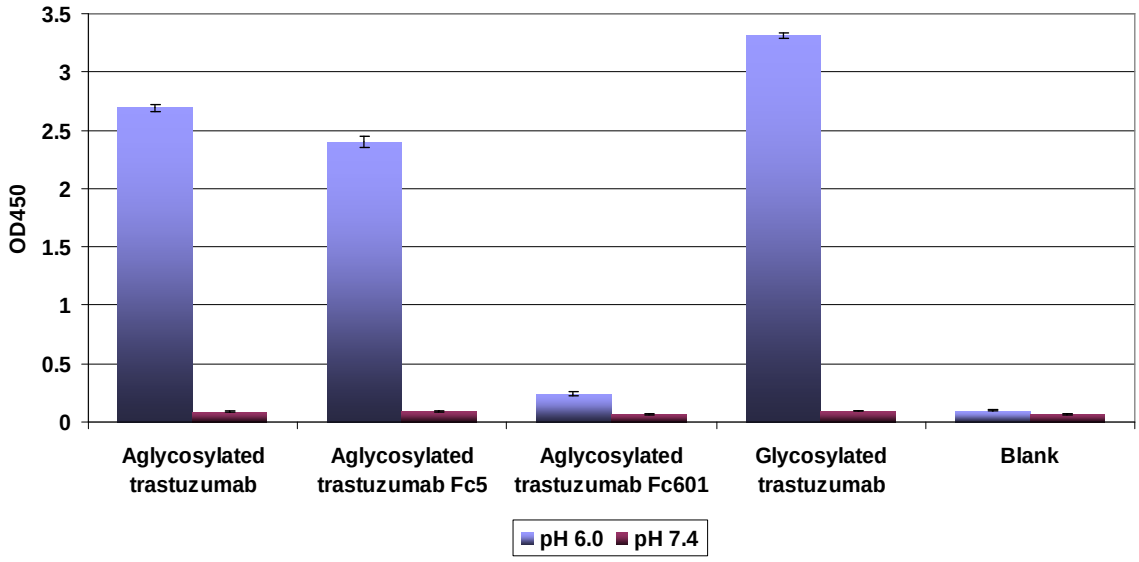

Figure 3-14. ELISA assays for pH dependent binding to FcRn at pH 7.4 and 6.0. Plates were coated with aglycosylated trastuzumab, trastuzumab-Fc5, trastuzumab-Fc601 or commercial glycosylated trastuzumab (Herceptin) and the binding of FcRn was detected using anti-GST-HRP.

3.3.3 mDC mediated tumor cells killing by aglycosylated trastuzumab-Fc5 and trasutuzumab-Fc601

Macrophages and immature dendritic cells greatly outnumber the classical killer cells (NK and T cells) in tumors (Bonmort et al., 2008). In recent years, the cytotoxic properties of various subpopulations of DCs towards cancer cells have attracted significant interest (Wesa and Storkus, 2007). Human circulating DCs express FcγRI, FcγRIIa, and FcγRIIb, but not FcγRIIIa (Fanger et al., 1996). The expression of FcγRI on DCs is largely dependent on the cytokine environment. We found that human mDCs isolated from PBMCs following differentiation for 7 days in the presence of IL-4 and GM-CSF and activated by exposure to LPS expressed high levels of CD11c (Fig. 3-15) and FcγRI (Fig. 3-16). SkBr3 breast carcinoma epithelial cells overexpressing Her-2 were incubated either with either clinical grade trastuzumab, aglycosylated trastuzumab-Fc5 or aglycosylated trastuzumab-Fc601 at 10 μg/ml. Wild type aglycosylated trastuzumab or media without effector cells were used as controls. Activated mDCs were then added at either 25:1 or 100:1 ratios and the lysis of the SkBr3 target cells was determined by monitoring ^{51}Cr release 24 hours later. No cell lysis above background was detected with glycosylated trastuzumab. In contrast, aglycosylated trastuzumab-Fc5 conferred ~40% (25:1; E:T ratio) and ~70% (100:1; E:T ratio) tumor cell killing, A comparable degree of cell lysis was observed with aglycosylated trastuzumab-Fc601 (Fig. 3-17A). Consistent with earlier studies (Lazar et al., 2006; Suzuki et al., 2007), when PBMCs which express all FcγRs were used as effector cells, glycosylated trastuzumab showed excellent ADCC (Fig. 3-17B). Thus, the highly specific and selective affinity binding of Fc5 or Fc601 to FcγRI is able to mediate DC-mediated killing of target tumor cells.

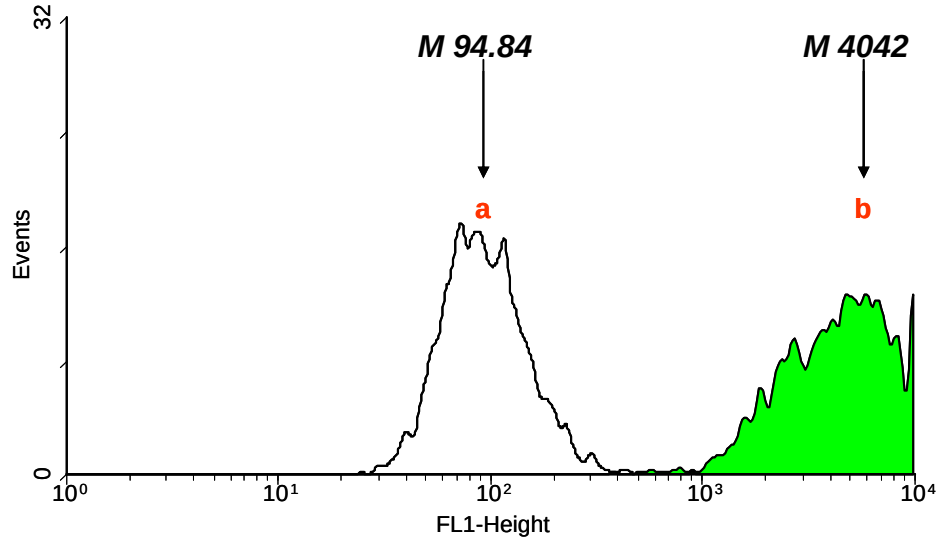

Figure 3-15. Flow cytometry histogram showing the expression of CD11c on activated DCs. Unlabeled DCs (unshaded); labeled DCs (shaded).

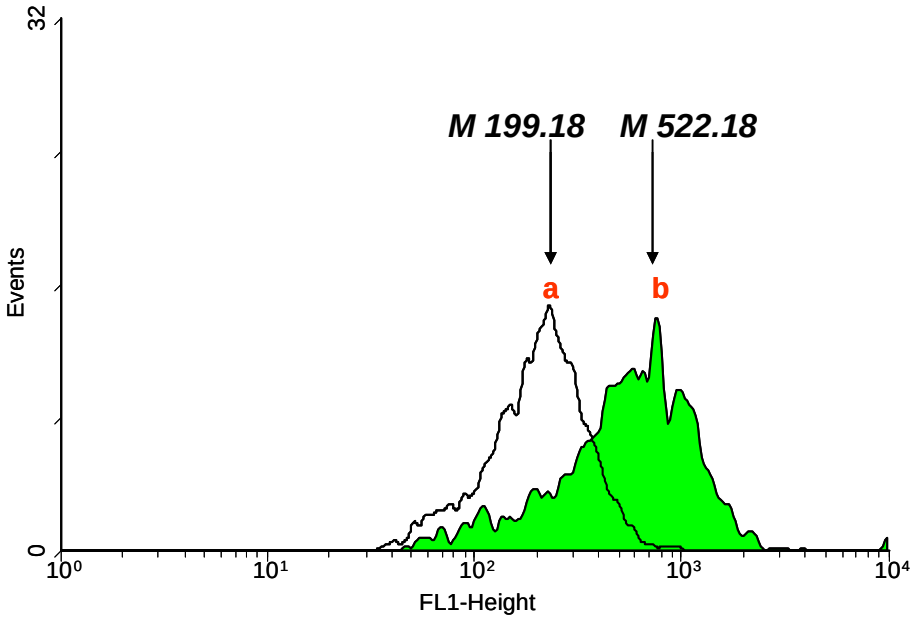

Figure 3-16. Flow cytometry histogram showing the expression of FcγRI on activated DCs. Unlabeled DCs (unshaded); labeled DCs (shaded).

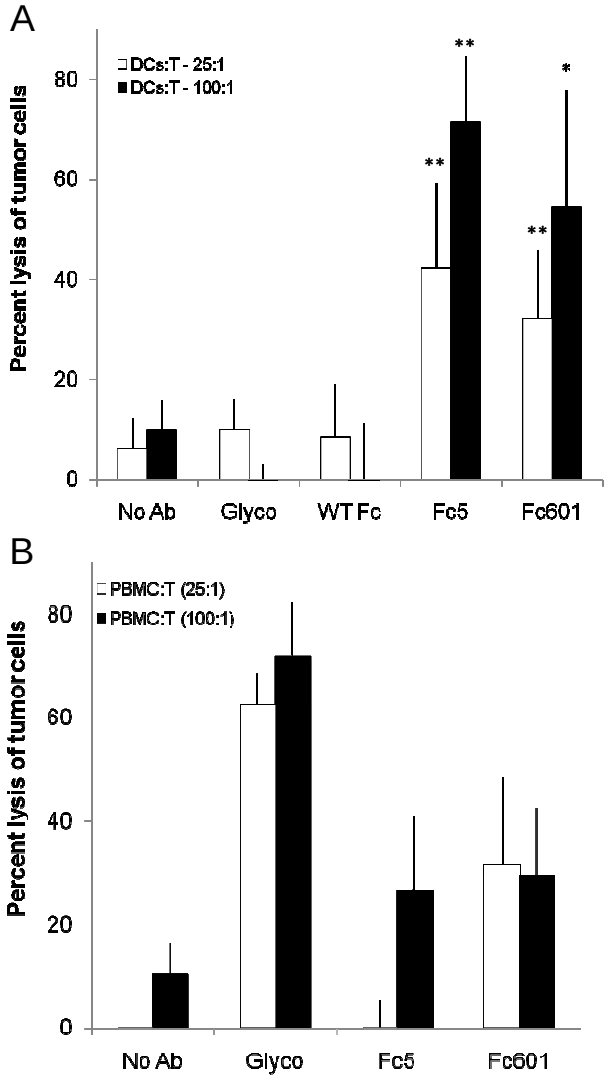

Figure. 3-17. Antibody dependent cellular cytotoxicity (ADCC) induced by engineered aglycosylated Fc antibodies. (A) Target Her2 expressing tumor cells (SkBr3) were exposed to Her2/neu binding purified aglycosylated or clinical grade glycosylated trastuzumab IgG1 antibodies. Effector cells (monocyte derived dendritic cells, mDCs) were then introduced and cell lysis was measured by ^{51}Cr release. Trastuzumab-Fc5 and Fc601 with high affinity binding to FcγRI induce high levels of ADCC, while glycosylated IgGs show very little ADCC activity. (B) SkBr3 cells were exposed to engineered IgGs as in A) and exposed to peripheral blood mononuclear cells (PBMCs) as effector cells. Glycosylated IgGs show very high ADCC activity while trastuzumab-Fc5 and Fc601 display reduced levels. (statistical significance using unpaired Student's *t*-test relative to wt Fc and No Ab controls in (A) and (B), respectively *, $P < 0.05$; **, $P < 0.01$).

3.3.4 Isolation of aglycosylated Fc mutants exhibiting higher affinity to FcγRI binding than Fc5 with retaining pH dependent FcRn binding

Human FcRn has high affinity to human IgG under slightly acidic pH condition and low affinity at neutral or basic pH (Ober et al., 2004a; Ober et al., 2004b; Raghavan and Bjorkman, 1996; Rodewald, 1976). The FcRn binding sites are located at the interface of CH2 and CH3 domains, similar binding sites for staphylococcal Protein A (SpA) (Kim et al., 1994; Shields et al., 2001). Fc601 showed improved FcγRI binding affinity than Fc5. However, two additional mutations (K338R, G341V) of Fc601 in lower CH2 region of IgG1 impaired the pH depended FcRn binding that is critical for the regulation of serum IgG concentration by allowing pinocyosed IgGs to make strong IgG-FcRn complex in acidified endosomes for recycling to blood across vascular endothelial cell membrane instead of degradation in lysosomes (Ghetie and Ward, 2000).

To isolate engineered Fc domains showing higher affinity to FcγRI than Fc5 with retaining the pH dependent FcRn binding, new combinatorial libraries consisting of random amino acids in upper CH2 region were constructed. The library cells were composed of 4 sub-libraries (Figure 3-18) that randomized lower hinge, B/C loop, C'/E loop, and F/G loop parts of upper CH2 regions. Spheroplasts were sorted with selectively gating the top 3% of the population showing the highest fluorescence due to FcγRI-FITC binding. After the 4^{th} round of sorting, 8 individual clones exhibiting higher fluorescence than Fc5 were isolated (Fig. 3-19). All of the clones were isolated from the library randomized F/G loop of CH2 region and have consensus mutations in L328W and I332Y mutations. Also, the amino acid residue 329P was well conserved suggesting the critical role of the specific amino acid residue in the binding of FcγRI (Fig. 3-20). The highest

fluorescent clone was Fc701 that have L328W, A330V, P331A, I332Y mutations in 328L-332I region and one additional Q295R mutation (Fig. 3-21 ~ 3-23).

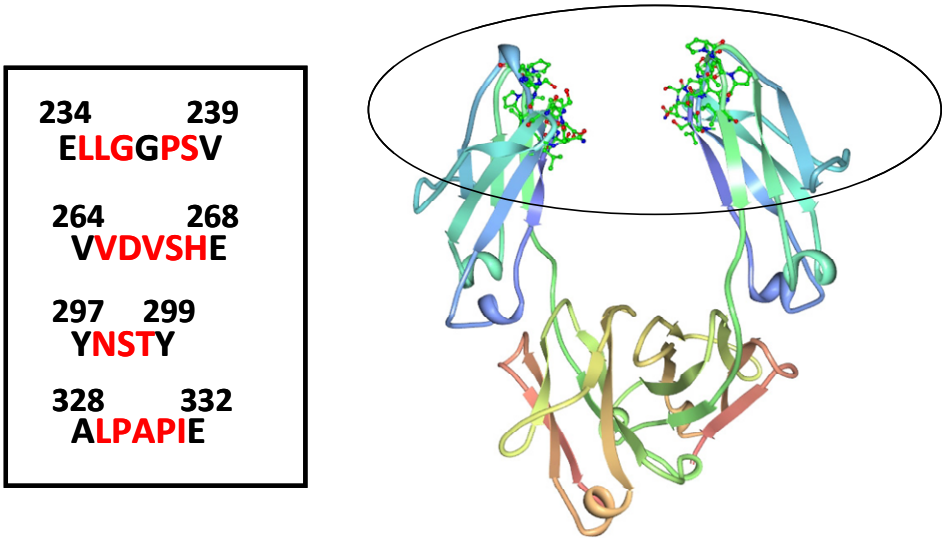

Figure 3-18. Library for the selection of higher affinity Fc fragments to FcγRI than Fc5 with pH dependent FcRn binding.

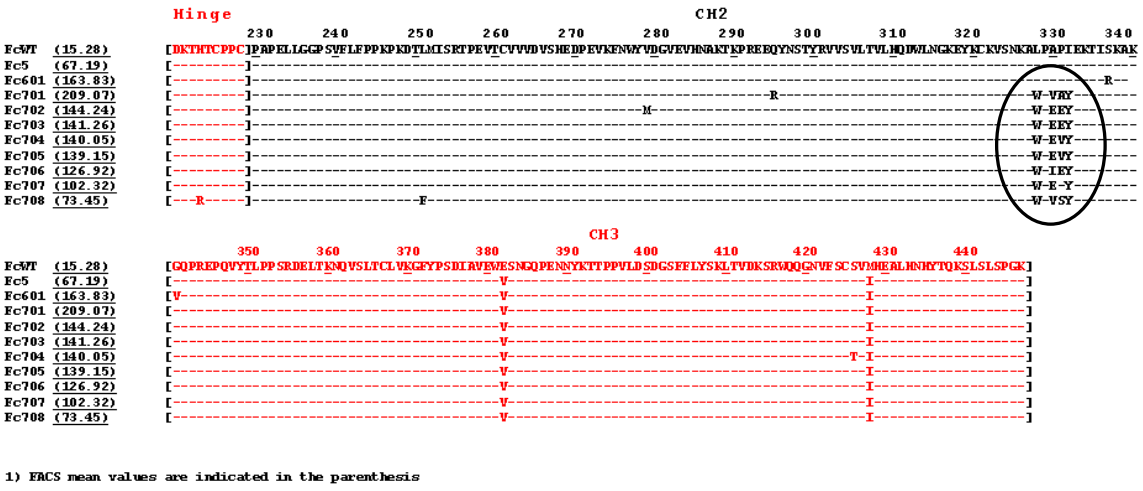

Figure 3-19. DNA sequences of isolated Fc mutant clones exhibiting higher affinity to FcγRI than Fc5. Mean fluorescence values for the respective clones labeled with FcγRI are shown in parenthesis.

FcWT	32	LPAPI 33	
Fc701		W-VAY	Q295R
Fc702		W-EEY	V279M
Fc703		W-EEY	
Fc704		W-EVY	S426T
Fc705		W-EVY	
Fc706		W-IEY	
Fc707		W-EPY	
Fc708		W-VSY	H224R, L251F

Figure 3-20. Summary of mutations in Fc701 – 709.

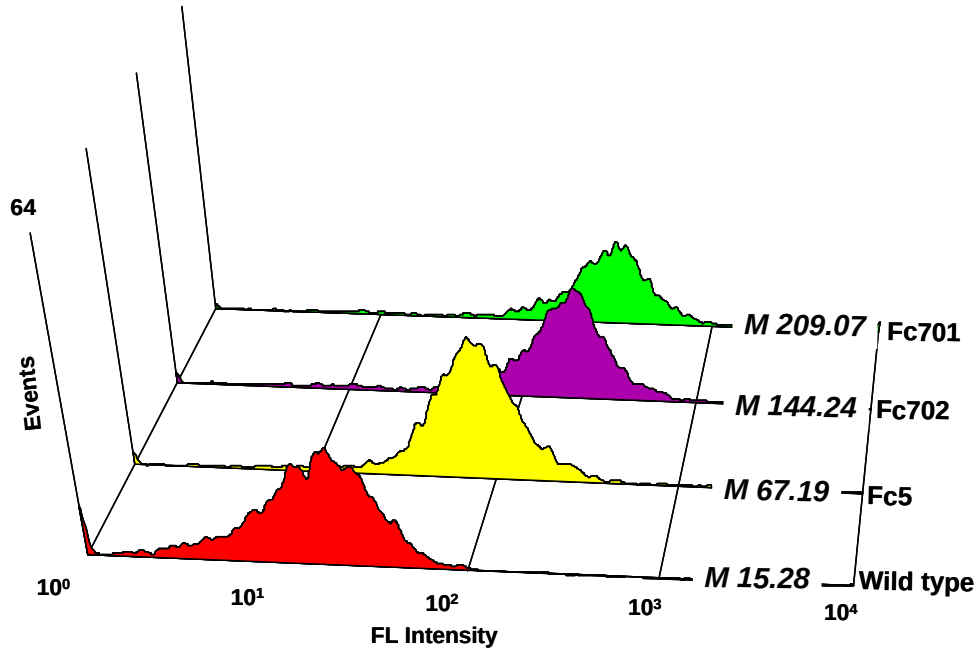

Figure 3-21. Fluorescence histogram of spheroplasted cells for wild type Fc, Fc5, Fc701, and Fc702 labeled with 1 nM of FcγRI-FITC. M: Mean fluorescence intensity.

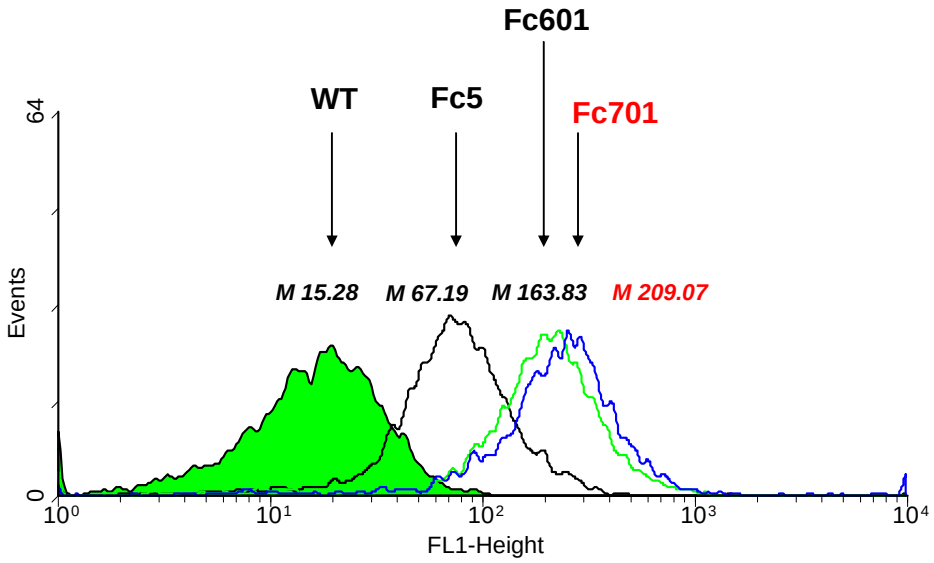

Figure 3-22. Fluorescence histogram of spheroplasted cells displaying wild type Fc, Fc5, Fc601, and Fc701 after labeling with 1 nM of FcγRI-FITC. M: Mean fluorescence intensity.

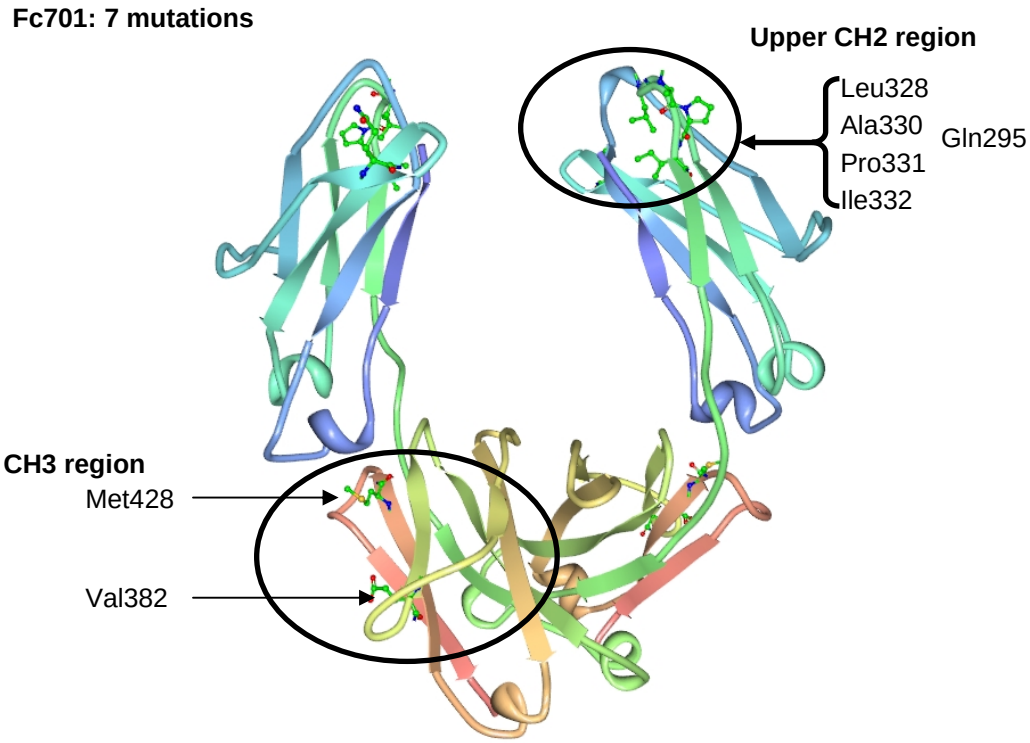

Figure 3-23. Mutation points of isolated aglycosylated Fc701 represented on the 3D structure of glycosylated IgG1 Fc (PBD Code: 1FC1).

3.3.5 Characterization of aglycosylated trastuzumab-Fc701

Full length trastuzumab-Fc701 IgG1 was produced by fed batch fermentation and purified using Protein A affinity chromatography followed by gel filtration chromatography as described in chapter 2. The kinetic rate constants for the binding of full length trastuzumab-Fc701 to FcγRI were measured by BIAcore sensor using trastuzumab-Fc701 antibodies immobilized on CM5 sensor chip and soluble FcγRI. Trastuzumab-Fc701 bound to FcγRI with similar affinity with trastuzumab Fc601 with slightly higher on and off rates than trastuzumab Fc601 (Table 3-4 and Fig. 3-24).

The pH dependent FcRn binding was analyzed by ELISA at pH 6.0 and at pH 7.4. Trastuzumab-Fc601 containing 2 mutations at CH2-CH3 interface did not showed significant FcRn binding at pH 6.0. In contrast, trastuzumab Fc701 containing 4 mutations in F/G loop and one mutation in B/C loop of CH2 region showed strong pH dependent binding property with higher affinity binding to FcRn at pH 6.0 than wild type aglycosylated or glycosylated trasutuzumab antibodies and no significant binding afftinity at pH 7.4 (Fig. 3-25).

Similary with previsously isolated engineered aglycosylated trastuzumab-Fc5 or –Fc601, aglycosylated trastuzumab-Fc701 was very specific to FcγRI without showing significant binding affinity to effector FcγRIIa (Fig. 3-26), FcγRIIb (Fig. 3-27) and FcγRIIIa (Fig. 3-28).

Table 3.4. Kinetic rates and equilibrium dissociation constants for trastuzumab antibodies obtained by BIACore analysis for binding to FcγRI.

	K_{on} (M^{-1} sec^{-1})	K_{off} (sec^{-1})	K_D (nM)
Aglycosylated wild type trastuzumab	1.31×10^5	5.02×10^{-2}	382
Aglycosylated trastuzumab-Fc5	2.17×10^5	1.23×10^{-3}	5.69
Aglycosylated trastuzumab-Fc601	1.34×10^5	3.92×10^{-4}	2.92
Aglycosylated trastuzumab-Fc701	2.96×10^5	9.25×10^{-4}	3.12
Glycosylated Herceptin	1.77×10^5	2.66×10^{-4}	1.5

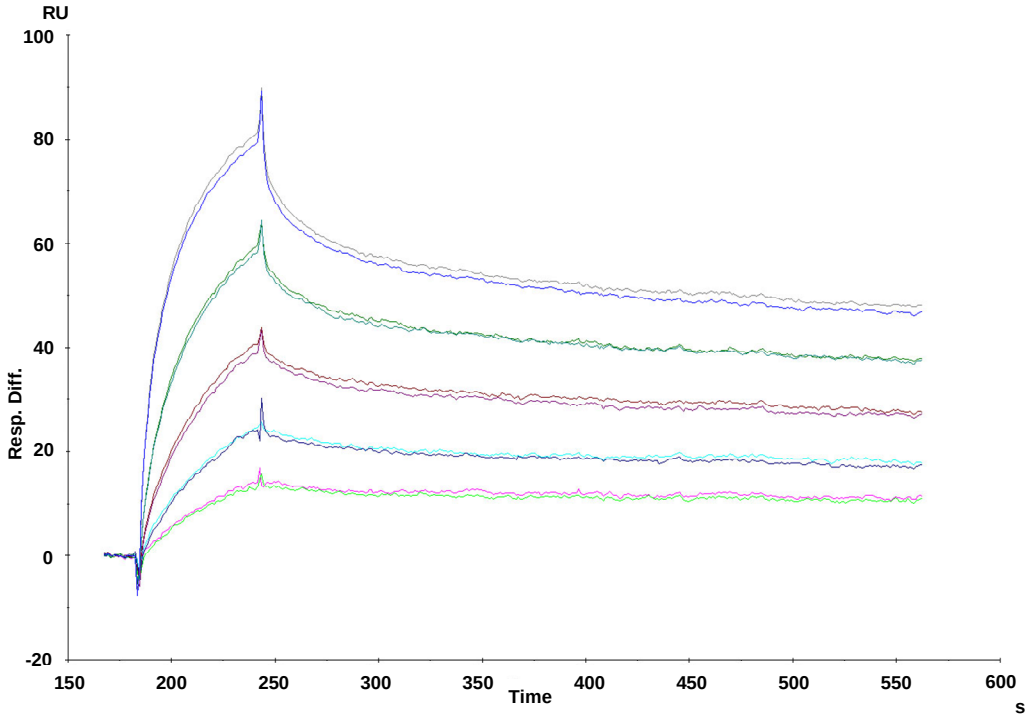

Figure 3-24. BIAcore sensorgrams of aglycosylated trastuzumab-Fc701 antibody with binding to FcγRI.

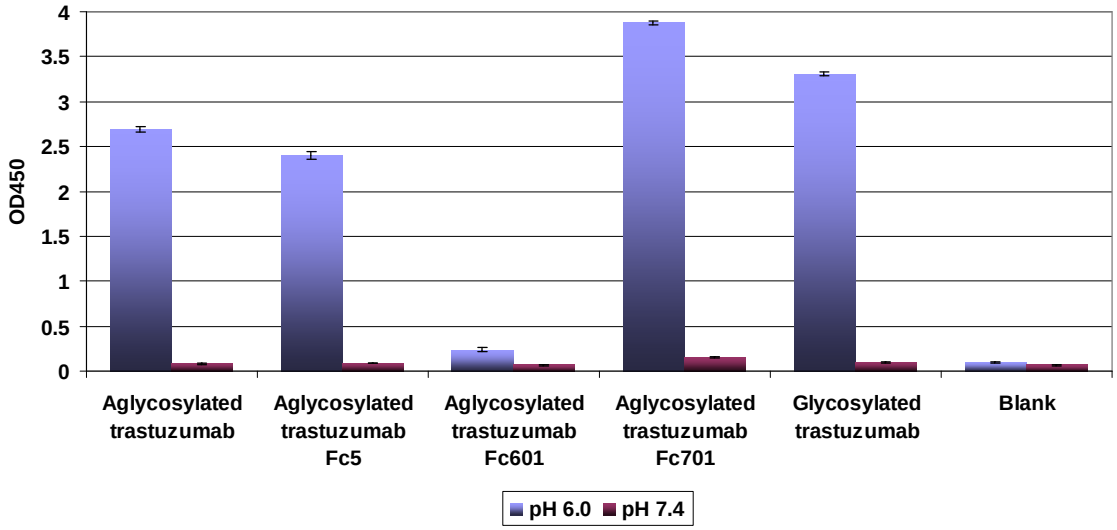

Figure 3-25. ELISA assays for pH dependent binding to FcRn at pH 6.0 and 7.4. Plates were coated with aglycosylated trastuzumab, trastuzumab-Fc5, trastuzumab-Fc601, trasutuzumab-Fc701 or commercial glycosylated trastuzumab and the binding of FcRn was detected using anti-GST-HRP.

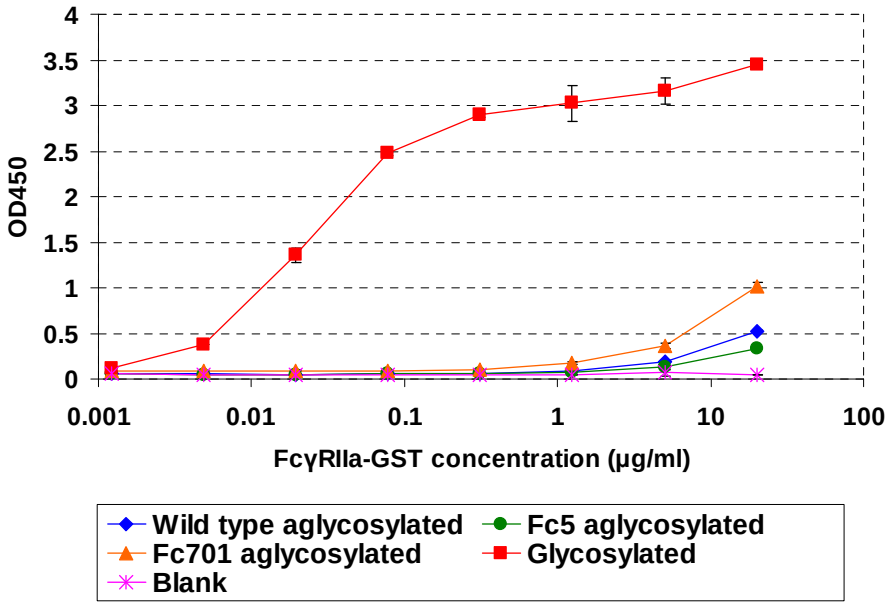

Figure 3-26. ELISA assays for binding of trastuzumab antibodies to FcγRIIa-GST.

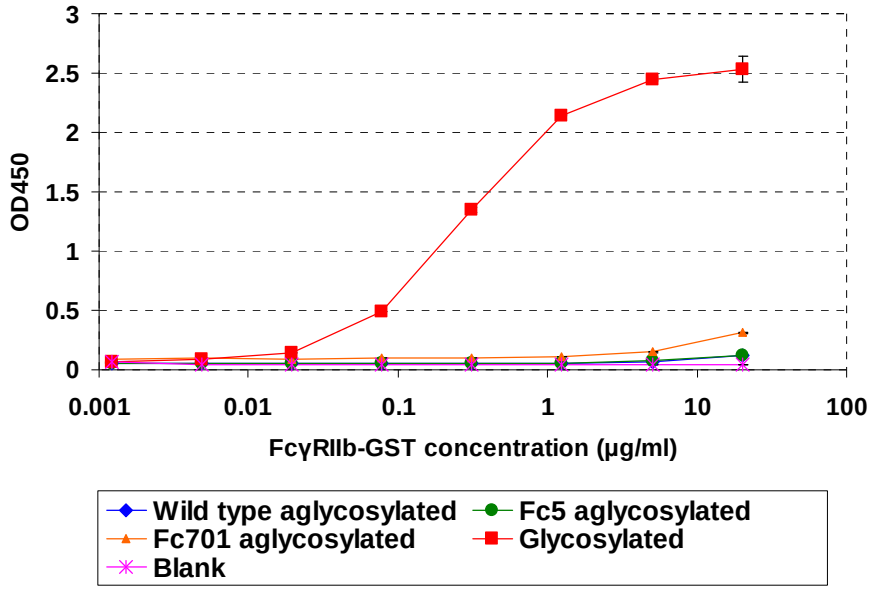

Figure 3-27. ELISA assays for binding of trastuzumab antibodies to FcγRIIb-GST.

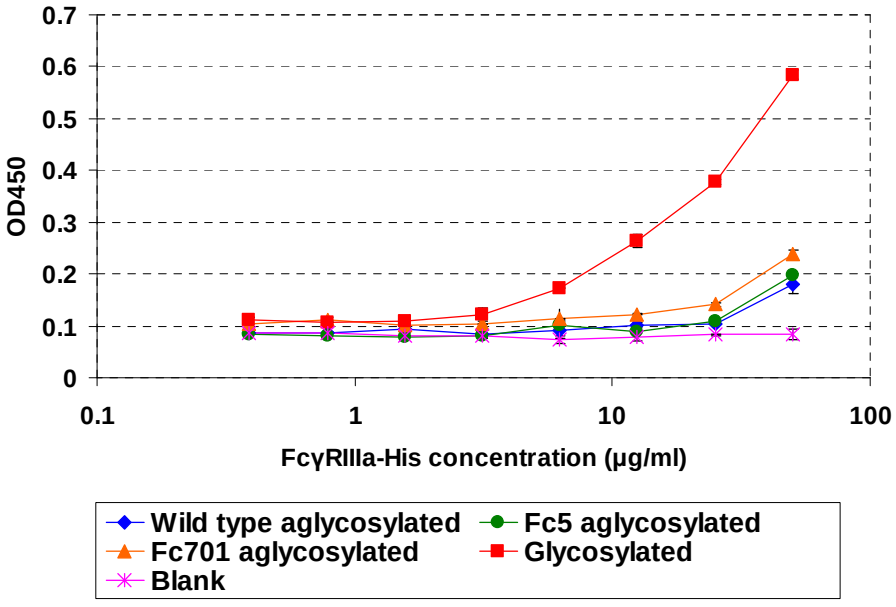

Figure 3-28. ELISA assays for binding of trastuzumab antibodies to FcγRIIIa.

3.4 DISCUSSION

In this study, a variety of Fc libraries were used in order to isolate aglycosylated antibody Fc mutants exhibiting higher affinity to FcγRI. High throughput screening from the error prone PCR library that introduced random amino acid substitutions into the Fc5 antibody described in chapter 2, generated aglycosylated trastuzumab-Fc601 exhibiting 130-fold increased affinity to FcγRI compared with the wild type aglycosylated trastuzumab. But 2 mutations (K338R, G341V) additionally introduced at the interface of CH2 and CH3 regions for Fc5 fragments abolished the binding affinity to human FcRn at slightly acidic condition (pH 6.0) that is critically required for maintaining longer serum half-life (Ghetie and Ward, 2000). Screening of a saturation library that randomized select amino acid residues in upper CH2 of Fc5 resulted in the isolation of trastuzumab-Fc701 that displayed similar affinity with trastuzumab-Fc601 but also exhibited strong pH-dependent FcRn binding, with a slightly higher affinity at pH 6.0 compared to clinical grade glycosylated trastuzumab and no significant binding at neutral pH.

Dendritic cells are professional antigen presentation cells but can mediate tumor cells killing directly by a variety of apoptosis and necrosis pathways (Wesa and Storkus, 2007) or indirectly by stimulating tumor killing cytotoxic by T cells (Rongcun Yang, 2001) or NK cells (Moretta, 2002; Schmitz et al., 2005). From a subpopulation of pheripheral blood DCs ($CD64^-$ M-$DC8^+$), Schmitz *et al.* reported that the trastuzumab antibody mediated ADCC of target cells via its interaction with FcγRII and FcγRIII (Schmitz et al., 2002). The myeloid-derived DCs used in our study are $CD11c^+$ $CD64^+$ and therefore can be categorized as the mature DCs. Schäkel *et al.* have reported that

mature DCs express a high level of CD33, HLA-DR, CD45RO, and CD83 but not CD16 (Schäkel, et al., 1998). Therefore there seems to be an inconsistency between the activation of mature DCs via FcγRIIIa (CD16) reported by Schmitz *et al.* (Schmitz et al., 2002) and the lack of expression of the receptor reported by Schäkel *et al*. (Schäkel, et al., 1998). Also, in our studies clinical grade tarstuzumab which binds well to the FcRIIa receptor on DCs did not mediate ADCC. It appears that the DC subpopulation that mediated cytotoxicty in our studies is different from the $CD64^{-}$ M-$DC8^{+}$ employed by Schmitz *et al.* (Schmitz et al., 2002). Importantly, we showed that trastuzumab-Fc5 and trastuzumab-Fc601 exhibited potent DC-mediated lysis of Her2 overexpressing tumor cells whereas clinical grade glycosylated tratsuzumab did not. It is likely that the inability of glycosylated trastuzumab to induce high levels of DC-mediated ADCC is due to its non-discriminate binding to other Fc receptors including the inhibitory FcγRIIb. In contrast, aglycosylated trastuzumab-Fc5 and trasutuzmab-Fc601 have selective and high affinity binding to FcγRI only. This result is consistent with the previous results for the enhanced tumor protection in mice by abrogation of inhibitory FcγRIIb signaling on DCs (Kalergis and Ravetch, 2002). The activation of PBMCs by glycosylated trastuzumab most likely due to a high concentration of NK cells that express FcγRIIIa; and since the levels of circulating immune cells expressing FcγRI is low, it is not surprising that trastzumab-Fc5 and trastuzumab-Fc601 showed low PBMC-mediated ADCC. The full therapeutic potential of selective activation of FcγRI and DC-mediated ADCC in tumor immunotherapy is still unclear. Future studies will need to explore this by determining if other relevant DC-mediated functions (i.e., antigen presentation and activation of tumor specific T cells) are enhanced by aglycosylated FcγRI binding antibodies.

Aglycosylated antibodies engineered for ADCC bypass the need for glycoengineering, mammalian expression and problems related to glycan heterogeneity. Together with technologies for IgG isolation (Mazor et al., 2007) and commercial level expression (Simmons et al., 2002), it is now feasible to carry out the complete development of therapeutic antibodies in bacteria. The therapeutic utility of aglycosylated antibodies will be further determined by pharmacological parameters, including stability, biodistribution and immunogenicity in humans.

Chapter 4

Development of high-throughput antibody screening system for immobilized antigen[1]

4.1 INTRODUCTION

The isolation of antibodies exhibiting high affinity and specificity for target antigens is of great importance for numerous aspects of biotechnology, ranging from proteomics to the development of therapeutics. Starting in the 1980s, the isolation of useful recombinant antibody fragments has been greatly facilitated by the introduction of display technologies for the screening of large libraries of antibody genes (Hoogenboom, 2005). Antibody display systems rely on the establishment of a physical linkage between an antibody gene and the antibody itself. In phage display, the first technique used for antibody fragment isolation from repertoire libraries, polypeptides are presented on the surface of filamentous bacteriophage via fusion to a phage coat protein (Smith, 1985). Numerous antibodies to widely diverse antigens have been isolated from either immune repertoires or synthetic libraries by employing sequential rounds of filamentous phage panning against immobilized antigen (Bradbury and Marks, 2004). Alternatively, very high affinity antibodies can be isolated using display on bacteria (Daugherty et al., 2000a; Daugherty et al., 2000b; Georgiou et al., 1997; Lofblom et al., 2005) or yeast (Boder et al.,

---

This chapter appeared as a paper in Jung, S. T., Jeong, K. J., Iverson, B. L. & Georgiou, G. (2007) *Biotechnol Bioeng* **98**, 39-47.

2000; Boder and Wittrup, 1997; Feldhaus et al., 2003) followed by flow cytometric screening for antigen-binding clones (Mattanovich and Borth, 2006).

For many applications it is desirable to isolate antibodies to antigens that are bound on either synthetic surfaces or on cellular membranes (Binyamin et al., 2006; Linenberger et al., 2002). With phage display, antibody libraries can be readily screened for binding to either purified membranes in lipid vesicles or to antigens presented on whole cells (Barry et al., 1996; Brown, 2000; Du et al., 2006; McGuire et al., 2004). In principle, bacterial and yeast display systems can also be employed for the discovery of polypeptides that bind to surface immobilized ligands (Dane et al., 2006; Richman et al., 2006; Wang and Shusta, 2005). However, the larger size and more complex surfaces presented by microbial cells relative to filamentous phage could introduce additional complications such as non-specific association between other components of the cellular surface. An additional problem with libraries displayed on the surface of *E. coli* is that the lipopolysaccharide layer on the external surface of intact outer membrane introduces a negatively charged steric barrier to prevent the interaction of displayed proteins and immobilized ligands (Vaara and Nurminen, 1999).

Recently, we have developed a new *E. coli* protein display system, called Anchored Periplasmic Expression (APEx) (Harvey et al., 2004). In this technology, proteins are not displayed on the cell surface but instead they are tethered to the periplasmic side of the inner membrane. This is accomplished by fusing the protein of interest to an inner membrane anchor such as a transmembrane segment of a native inner membrane protein (Jeong et al., 2004), an anchoring motif derived from a lipoprotein which becomes fatty acylated during protein translocation and is thus embedded into the lipid bilayer (Pugsley,

1993; Sankaran and Wu, 1994), or an exogenous protein such as the M13 phage coat protein gp3 known to association with the periplasmic side of the inner membrane (Barbas Cf et al., 1991). Spheroplasting using EDTA and lysozyme is then used to remove the outer membrane allowing the inner membrane-anchored polypeptide to interact and bind to desired ligands. The removal of the outer membrane eliminates the steric barrier presented by lipopolysaccharide and surface carbohydrates and facilitates interactions with much larger soluble ligands, compared to bacterial surface display (Harvey et al., 2004). However, the binding of displayed receptor proteins on spheroplasted *E. coli* to ligand presenting surfaces via specific receptor-ligand interactions has not been investigated previously.

In this chapter, we show that APEx can be employed to allow the specific binding of spheroplasts expressing inner membrane anchored antibodies onto immobilized antigens on beads. As model antibodies for this study we used the 26-10 scFv which binds to digoxin and related cardiac glycosides such as digoxigenin with low nanomolar affinity (Francisco et al., 1993), and the M18 scFv, which binds to the protective antigen (PA) of *B. anthracis* with an affinity of in the low picomolar range (Harvey et al., 2004). Expression of GFP in the cytoplasm was employed to render the spheroplasts fluorescent and facilitate their detection upon binding onto beads (Fig. 4-1A). Spheroplast binding was shown to be mediated by the recognition of the immobilized antigen by the displayed scFv. Protocols for the enrichment of spheroplasts binding to immobilized antigen from a large excess of spheroplasts expressing unrelated scFvs were developed. These results suggest that APEx can be employed for the screening of antibody libraries to immobilized antigens and potentially to antigens expressed on cell surfaces.

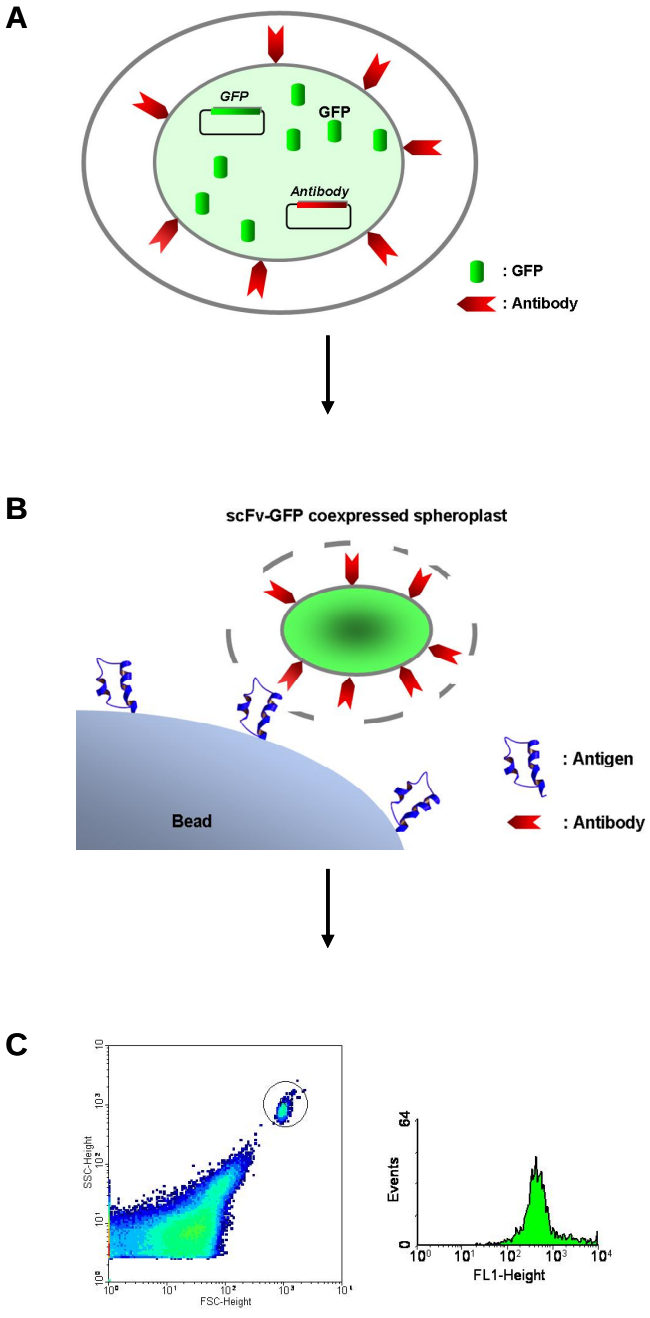

Figure 4-1. Selection of APEx spheroplasts via antibody-antigen interactions. (a) GFP expression and display of antibody (scFv) via APEx. (b) Binding of fluorescent spheroplasts on antigen-immobilized beads. (c) Selection of highly fluorescent spheroplast-bound beads using FC by gating the region defined by the high FL1 signal and the distinct scatter of the beads (FSC and SSC).

4.2 MATERIALS AND METHODS

4.2.1 Reagents

O Oligonucleotides primers and restriction endonucleases were purchased from Integrated DNA Technologies (Coralville, IA) and New England Biolabs (Ipswich, MA), respectively. Expanded High Fidelity Polymerase, Digoxigenin-3-O-methyl-carbonyl-e-aminocaproic acid N-hydroxysuccinimide ester (DIG-NHS-ester), and monoclonal Anti-Digoxigenin-Fluorescein Fab fragments from sheep were from Roche Diagnostics Corporation Biolab (Indianapolis, IN). Digoxigenin-BODIPY (Digoxigenin-4,4-difluoro-5,7-dimethyl-4-bora-3a,4a-diaza-s-indacene-3-propionyl ethtylenediamine) was synthesized as described previously (Harvey et al., 2004). PA-FITC was purchased from List Biological Laboratories, Inc (Campbell, CA). Amine functionally activated beads (D: 10 μm, TentaGel M NH_2) were purchased from Rapp Polymere GmbH (Tübingen, Germany). *N*,*N*,-Dimethylformamide (absolute, over molecular sieves) were from Fluka (Buchs, Switzerland). Analytical grades of all other chemical reagents were purchased from Sigma-Aldrich (St. Louis, MO) unless stated otherwise.

4.2.2 Construction of plasmids for anchored antibody and GFP

All plasmids and primers used in this study are summarized in Table 4-1 and Table 4-2. For the expression of the 26-10 scFv and M18 scFv fused to the signal peptide and first six *N*-terminal amino acid residues of NlpA(1-6: CDQSSS), pAPEx1-2610 and pAPEx-M18 were digested with *Sfi*I, and the gene fragments containing 26-10 scFv and M18 scFv gene were subcloned into *Sfi*I-digested pMoPac1-FLAG in which polyhistidine tag and c-myc tag was replaced by FLAG tag (DYKDDDDK) from the pMoPac1 to yield

pMoPac1-FLAG-2610 and pMoPac1-FLAG-M18, respectively. For the expression of 26-10 scFv as MalF(1-175) fusion pTOPO-2610 (Jeong et al., 2004) was modified by the addition of a sequence encoding a *C*-terminal FLAG tag epitope. Similarly, the M18 scFv gene was fused to MalF(1-175) by first amplifying the M18 scFv gene with specific primers STJ#50 and STJ#51 and subcloning into *Bgl*II – *Hin*dIII digested pTOPO-FLAG-2610 to yield pTOPO-FLAG-M18. pAK200-2610 and pAK200-M18 were used to express the 26-10 and M18 scFv respectively, fused at the *C*-terminus to the M13 gp3 protein. Finally, pBAD30-KmR-GFPmut2 was constructed by amplifying the *gfpmut2* gene (Cormack et al., 1996) with primers STJ#38 and STJ#39 and subcloning it into *Sac*I - *Hin*dIII digested pBAD30-KmR, a derivative of pBAD30 (Guzman et al., 1995) but the Ap^r gene had been replaced with Km^r gene. All plasmids for antibody expression were co-transformed with pBAD30-Km^r-GFPmut2 into *E. coli* Jude-1(F' [Tn*10(*Tet^r*)* $proAB^+$ *lacI*^{q} Δ(*lacZ*)M15] *mcrA* Δ(*mrr-hsdRMS-mcrBC*) ϕ80d*lacZ*ΔM15 Δ*lacX74 deoR recA1 araD139* Δ(*ara leu*)7697 *galU galK rpsL endA1 nupG*) (Kawarasaki et al., 2003).

4.2.3 Digoxigenin immobilization onto beads

30 mg of amine functionally activated beads (TentaGel M NH_2) were resuspended in 3 ml of *N*,*N*,-Dimethylformamide for 1 h then mixed with 5 mg of Digoxigenin-3-O-methyl-carbonyl-ε-aminocaproic acid *N*-hydroxysuccinimide ester (DIG-NHS-ester) and incubated overnight. The digoxigenin immobilized beads were washed by centrifugation 3000 x g for 1 min and resuspended in 10 ml of PBS (Phosphate buffered saline) three times and finally were resuspended in 3 ml PBS. The immobilization of digoxigenin on beads was confirmed by FC analysis using a

monoclonal Anti-Digoxigenin-Fluorescein Fab conjugate. Specifically, 50 μl of a 1% (wt/vol) digoxigenin immobilized beads solution was added to 150 μl of PBS containing 4 μl of Anti-Digoxigenin-Fluorescein Fab fragments (200 μg/ml). After a 1 hr incubation at room temperature with shaking, the immobilized bead solution was diluted 5x in PBS and the bead-associated fluorescence was monitored on a BD FACSort through a 530/30 band pass filter (BD Biosciences, San Jose, CA).

4.2.4 Culture conditions

E. coli transformed with pBAD30-KmR-GFPmut2 and plasmids expressing inner membrane tethered 26-10 scFv or M18 scFv as appropriate, were grown overnight at 37°C in Terrific Broth (TB) (Becton Dickinson Diagnostic Systems Difco™, Sparks, MD) supplemented with 2% (wt/vol) glucose, chloramphenicol (40 μg/ml) and kanamycin (50 μg/ml). After overnight culture, the cells were diluted 1:100 in fresh TB medium without glucose, incubated at 37°C for 2 h and then at 25°C. For induction of antibody fragments and GFP, 1 mM of isopropyl-1-thio-β-D-galactopyranoside (IPTG) and 0.2% (wt/vol) arabinose, respectively, were added when the culture OD_{600} reached approximately 0.6.

4.2.5 Preparation of spheroplasts and FC analysis

5 h after induction, an aliquot of the culture equivalent to 4.5 ml/OD_{600} was collected, the cells harvested by centrifugation, washed two times in 1 ml of 10 mM Tris-HCl (pH 8.0), and resuspended in 1 ml of STE solution (0.5 M Sucrose, 10 mM Tris-

HCl, 10 mM EDTA, pH 8.0). After incubation with rotating mixing at 37°C for 30 min, the cells were pelleted by centrifugation at 12,000 x g for 1 min and washed in 1 ml of Solution A (0.5 M Sucrose, 20 mM $MgCl_2$, 10 mM MOPS, pH 6.8). The washed pellet was resuspended in 1 ml of Solution A containing 1 mg/ml of hen egg lysozyme and incubated at 37°C for 15 min. The resulting suspension was centrifuged at 12,000 x g for 1 min and the spheroplasts were resuspended in 1 ml of PBS. 300 μl of the spheroplasts and 50 μl of the 1% (wt/vol) digoxigenin immobilized beads were mixed in a glass test tube and incubated at room temperature for 2 h with shaking and washed in 1 ml of PBS to remove unbound spheroplasts by centrifugation at 3,000 rpm for 3 min. FC analysis was performed using a BD FACSort.

4.2.6 Spheroplast enrichment onto beads with immobilized digoxigenin

Spheroplasts displaying the 26-10 scFv and the M18 scFv were prepared and mixed at 1:100 and 1:1000 ratios. Beads rendered fluorescent by the binding of GFP-expressing spheroplasts were sorted on a MoFlo droplet deflection FC (Dako Cytomation, Fort Collins, Colorado) equipped with a 488 nm Argon laser for excitation. Spheroplasts bound on beads were detected through a 530/40 band pass filter (FL1). By gating on the populations displaying the distinctive high forward scattering (FSC) and side scattering (SSC) of spheroplasted cells as well as the highest ~2.5% FL1 signal, the bead-bound spheroplasts were sorted. The scFv genes in the spheroplasts were amplified by PCR using two specific primers STJ#16 and STJ#130, cloned into pAK200 vector using *Sfi*I cloning sites, and transformed in electrocompetent *E. coli* Jude-1 cells

harboring the plasmid pBAD30-KmR-GFP. The resulting transformants were subjected to the second round sorting. To determine sorting efficiency, 40 clones after every round sorting were randomly selected and the number of 26-10 scFv clones was confirmed by colony PCR using 26-10 scFv specific primers STJ#128 and STJ#129.

Table 4-1. Plasmids used in this study.

Plasmids	Relevant characteristics	Reference or source
pMoPac1	Cm^r, *lac* promoter, *tetA* gene, C-terminal polyhistidine tag and c-myc tag	(Hayhurst et al., 2003)
pAPEx1-2610	NlpA fused *26-10 scFv* gene in pMoPac1	(Chen et al., 1999)
pAPEx1-M18	NlpA fused *M18 scFv* gene in pMoPac1	(Harvey et al., 2004)
pMoPac1-FLAG-2610	NlpA fused *26-10 scFv* gene, C-terminal FLAG in pMoPac1	This study
pMoPac1-FLAG-M18	NlpA fused *M18 scFv gene*, C-terminal FLAG tag in pMoPac1	This study
pTOPO-2610	MalF fragment fused *26-10 scFv* gene, C-terminal polyhistidine tag in pMoPac1	(Jeong et al., 2004)
pTOPO-FLAG-2610	C-terminal FLAG tag in pTOPO-2610	This study
pTOPO-FLAG-M18	MalF fragment fused *M18 scFv* gene, C-terminal FLAG tag in pTOPO-2610	This study
pAK200	Cm^r, *lac* promoter, *tetA* gene, C-terminal Gene III fusion	(Krebber et al., 1997)
pAK200-2610	*26-10 scFv* gene in pAK200	(Harvey et al., 2004)
pAK200-M18	*M18 scFv* gene in pAK200	(Harvey et al., 2004)
pBAD30	Ap^r, BAD promoter	(Guzman et al., 1995)
pBAD30-KmR	Km^r, BAD promoter	This study
pGFPmut2	Ap^r, *tac* promoter	(Cormack et al., 1996)
pBAD30-KmR-GFPmut2	Km^r, BAD promoter, *gfpmut2* gene	This study

Table 4-2. Primers used in this study[a].

Primer Name	Primer nucleotide sequence (5' → 3')
STJ#16	TTGTGAGCGGATAACAATTTC
STJ#38	ACCGGAGCTCTTAAAGAGGAGAAAGGTCATGAGTAAAGGAGAAGAACTTTTCAC
STJ#39	TTAGGGAAGCTTTTATCATTTGTATAGTTCATCCATGCCATG
STJ#43	TTTTAGGGCTGCAGCTCAGAATGACTTGGTTGAGTG
STJ#44	GCGGAATTCGCCGGAAGGGCCCAGTGCTGCAATGATACCG
STJ#50	GGCTAGATCTGGAGGTGGCAGCGAGGCCCAGCCGGC
STJ#51	TTAGGGAAGCTTCTATTAGGCGCGCCCTTTGTC
STJ#128	GGGTACATTTTCACCGACTTCTACATG
STJ#129	GAACATGCGTAGTTTGGCTACAGTAATATATTG
STJ#130	GCGTTTGCCATCTTTTCATAATCAAAATCACC

[a]Underlining indicates the restriction enzyme sites

4.3 RESULTS

4.3.1 Display of scFv antibodies on *E. coli* inner membrane

Three different anchoring domains were employed for the display of the scFv antibodies (26-10 scFv and M18 scFv) onto the periplasmic side of the inner membrane (Fig. 5-2A). First, the signal peptide and the 6 *N*-terminal amino acid residues of the mature *E. coli* lipoprotein NlpA were fused to the scFv antibodies. The resulting proteins, NlpA(1-6)-scFvs, become fatty acylated at the *N*-terminal Cys residue. Upon translocation into the periplasmic space, the lipid tail anchors the constructs on the periplasmic side of the inner membrane. Second, we constructed fusions containing aa 1-

175 of MalF encoding the three *N*-terminal transmembrane α-helices followed by 93 amino acid residues presumed to be located within a long periplasmic loop (Tapia et al., 1999). In these fusions, it is anticipated that the transmembrane α-helices serve as the membrane anchor whereas aa 82-175 serve as a linker to remove spatially the antibody binding site from the surface of the inner membrane and potentially facilitate binding to immobilized antigens. Also, we reasoned that integral membrane proteins such as MalF might be localized at different sites than lipoproteins on the inner membrane, and such differences in localization of the fusion might affect antigen binding. Finally, *C*-terminal anchoring was achieved by fusing the 3' of the scFv genes to the gp3 protein of M13, which is localized on the inner surface of the inner membrane until the later stages of filamentous phage assembly (Barbas Cf et al., 1991). All scFv fusions were expressed from the *lac* promoter.

The display of the anchored scFvs on spheroplasts via NlpA(1-6), MalF(1-175) or gp3 fusions was evaluated by flow cytometry (FC), following labeling with digoxigenin-BODIPY (for 26-10 scFv fusions) and PA-FITC (for M18 scFv fusions) respectively (Fig. 4-2B). To aid the visualization of spheroplasts by FC, the cells were also transformed with pBAD30-KmR-GFPmut2, a plasmid encoding the mut2 version of GFP (Cormack et al., 1996), which fluoresces approximately 100 times more intensely than wild-type GFP and also has highly red shifted maximum excitation wavelength suitable for FACS applications using standard FITC emission filters. As expected, upon induction of GFPmut2 expression with arabinose the cells became brightly fluorescent.

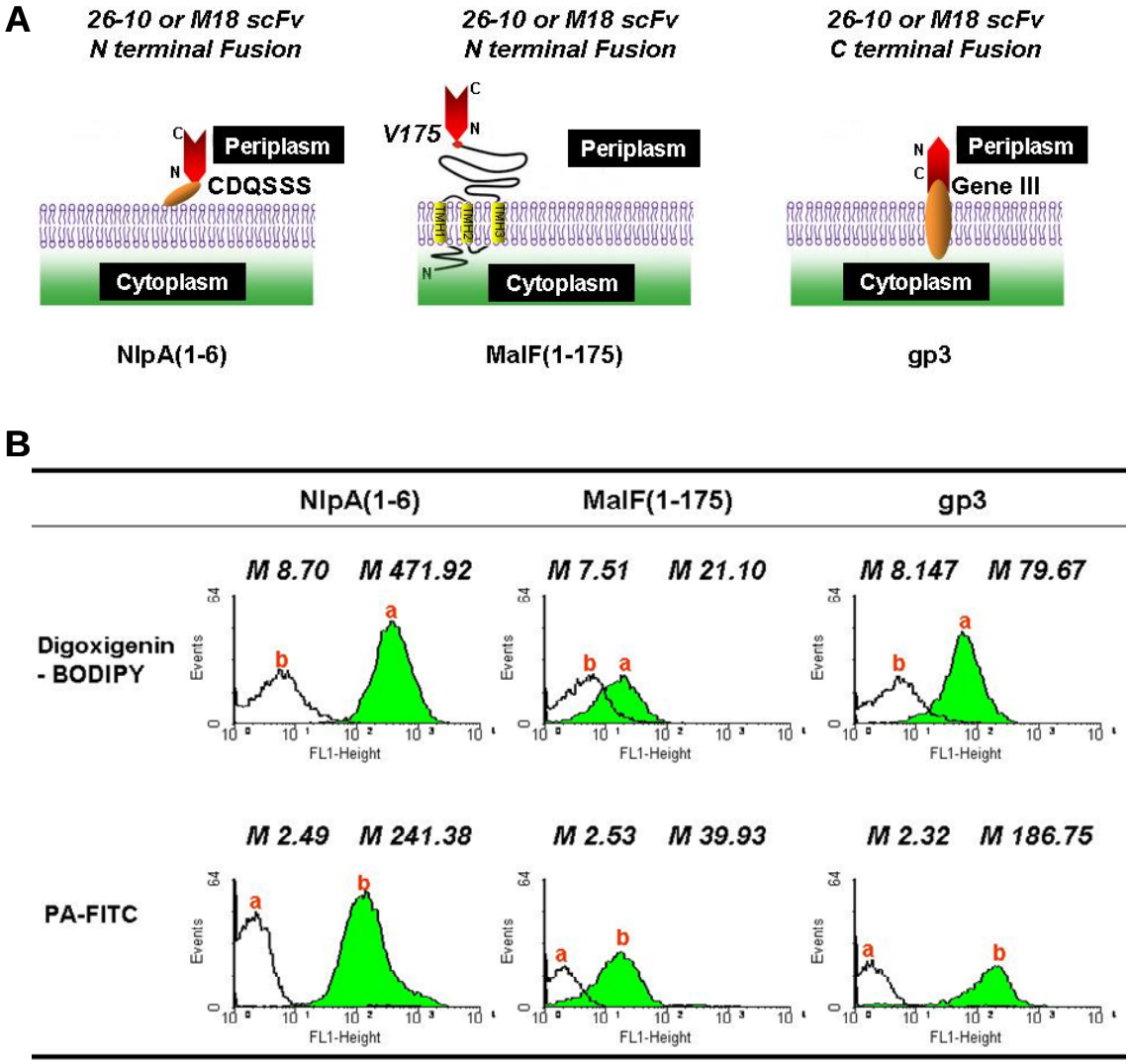

Figure 4-2. Inner Membrane anchoring of scFvs display. (A) scFv antibodies were fused to the NlpA signal peptide followed by six amino acid residues (CDQSSS) from the mature protein, the *E. coli* MalF 1-175, or the filamentous phage gp3 protein. The first two result in N-terminal display whereas with the latter the scFv is displayed from its C-terminus. (B) Fluorescence histograms showing spheroplasts displaying 26-10 scFv (peak a) and M18 scFv (peak b) fused to NlpA(1-6), MalF (1-175), or gp3 and incubated with either soluble PA-FITC or soluble Digoxigenin-BODIPY. M: Mean fluorescence intensity.

4.3.2 Binding of spheroplasts on the antigen immobilized beads

Digoxigenin was immobilized via an amide linkage onto amine functionally activated beads as described in Materials and Methods. FC analysis confirmed the efficient immobilization of digoxigenin on beads (Fig. 4-3A). The binding between digoxigenin-derivatized beads and spheroplasts expressing the 26-10 or the M18 anti-PA scFv fused to either NlpA(1-6), MalF(1-175) or gp3 was evaluated by FC analysis. An FC gate was set up based on the side and forward scatter (SSC and FSC, respectively) of the beads, which is clearly distinct from that of the cells (Fig. 4-3C). Fluorescence with both the 26-10 and M18 antibodies would be indicative of non-specific binding of the spheroplasts onto the beads, whereas fluorescence with only one or more of the 26-10 scFv expressing constructs would indicate a specific interaction.

As can be seen in Figure 4-3B, the highest fluorescence was observed in spheroplasts expressing the 26-10 scFv-gp3 fusion where the antibody fragment is tethered to the inner membrane via its *C*-terminus. The FACS data presented in Figure 5-3 indicate that spheroplasts can bind specifically onto a solid surface by virtue of the interaction between an inner membrane tethered antibody and the immobilized antigen. Binding of the 26-10 scFv-gp3 onto digoxigenin-derivatized beads was also confirmed by fluorescence microscopy (data not shown). By comparison, the fluorescence of beads incubated with spheroplasts expressing either NlpA(1-6)-26-10 scFv or MalF(1-175)-26-10 sc Fv was about 3-fold lower than that of spheroplasts expressing 26-10 scFv-gp3 and did not show specific binding.

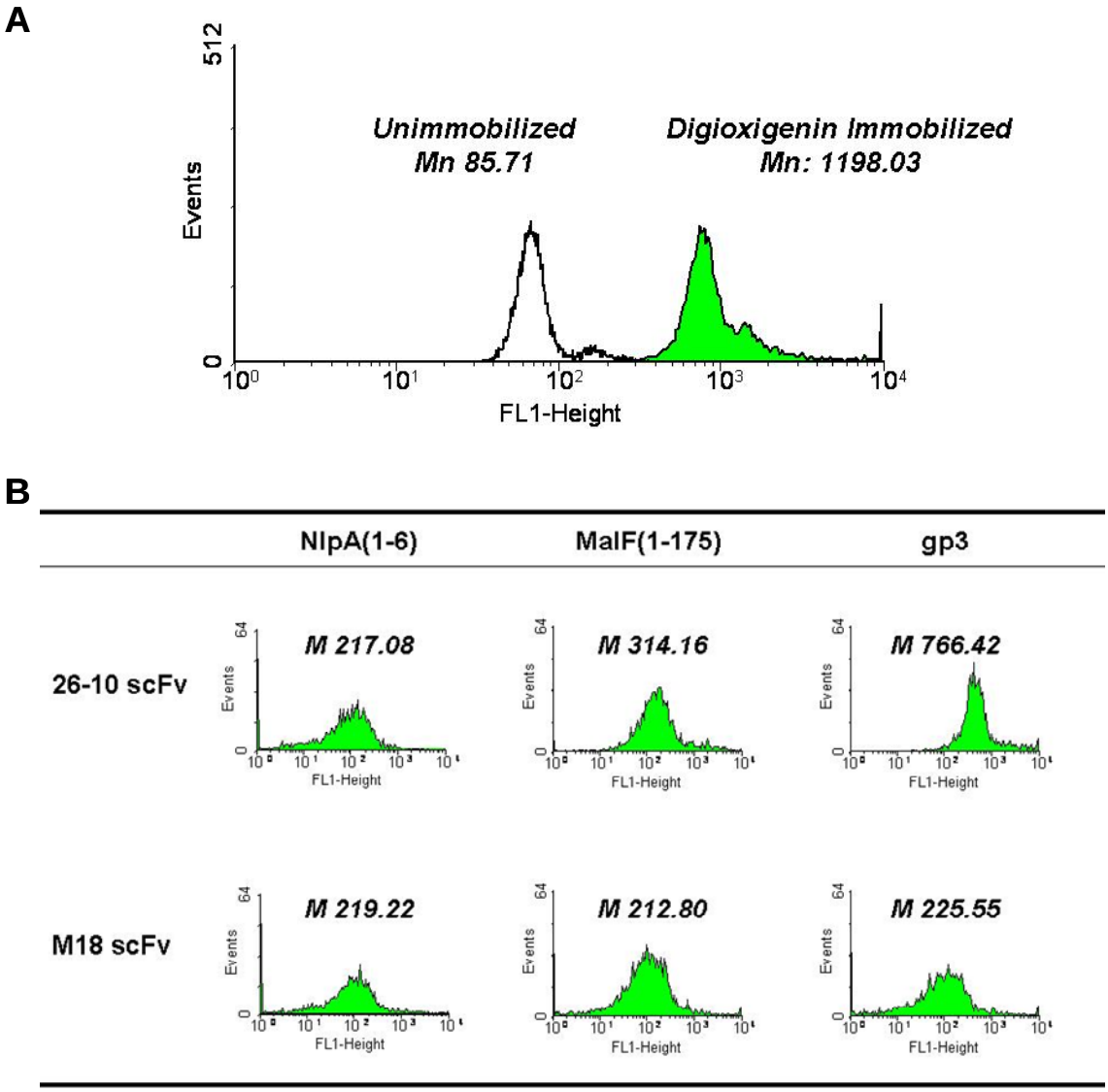

Figure 4-3. FC analysis of spheroplasts with beads containing immobilized antigen. (A) Detection of immobilized digoxigenin using Anti-Digoxigenin-Fluorescein Fab fragments. The fluorescent histogram of beads in the absence of immobilization is also shown. (B) Histograms for digoxigenin immobilized beads incubated with spheroplasts displaying 26-10 scFv and M18 scFv as fusions to NlpA(1-6), MalF (1-175) or gp3. M: Mean fluorescence intensity.

4.3.3 Enrichment of 26-10 scFv anchoring spheroplasts

As a prerequisite for the screening of libraries of spheroplast-anchored scFvs onto antigen-immobilized beads, we optimized conditions for the enrichment of spheroplasts on the basis of antibody-immobilized antigen binding. Spheroplasts expressing the 26-10 scFv were mixed with either 100-fold or 1,000-fold excess of M18 scFv clones. The resulting mixture was incubated with digoxigenin-immobilized beads and spheroplast-bound beads were sorted by FC selectively gating for high GFP fluorescence in the scattering region of the beads. When the M18 scFv was present in a 100-fold excess, sorting resulted in the collection of 1,772 beads out of an input of 5.6 x 10^6. The DNA encoding the scFv genes associated with the collected beads was rescued by PCR and subcloned into pAK200. Following transformation and plating onto selective media, colony PCR revealed that 9/40 clones picked at random contained the 26-10 scFv indicating a 22.5-fold enrichment per round. Next, we examined the degree of enrichment obtained in the presence of 1,000-fold excess of spheroplasts expressing the M18 scFv. Fluorescent beads were sorted as above, the rescued scFv genes were subcloned into pAK200 and the ligation mixture was transformed into cells that were used as the input for the next round of sorting. Following three rounds of enrichment, which took approximately two weeks, FC analysis revealed a clear increase in the fluorescence signal of the sorted population (Fig. 4-4). 38/40 third round colonies picked at random contained the 26-10 scFv gene indicating that a 950-overall enrichment had been achieved over three rounds.

Table 4-3. Enrichment obtained by sorting of 26-10 and M18 scFv mixture (1:1,000).

Round of Sorting	Number of 26-10 scFv clones[a]	Number of M18 scFv clones[a]	% positives	Enrichment from Presort
Presort	1	1,000	0.1	-
First round	0	40	-	-
Second round	2	38	5.0	50
Third round	38	2	95.0	950

[a]Determined by colony PCR of randomly selected colonies after each round of sorting.

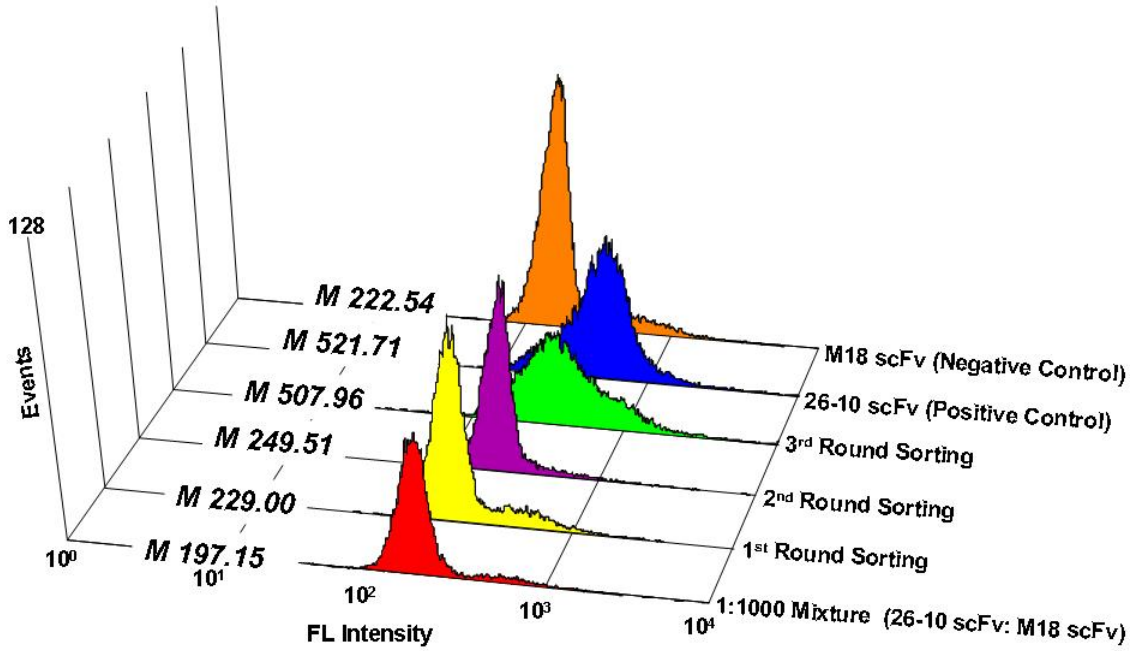

Figure 4-4. Enrichment of 26-10 scFv clones from a 1,000 excess of M18 scFv-gp3 by binding to beads with immobilized digoxigenin. FC histograms represent the mean fluorescence intensity (M) of the spheroplast population after each round of sorting.

4.4 DISCUSSION

In this chapter, we demonstrated that spheroplasts expressing scFv antibodies displayed on the periplasmic side of the inner membrane could bind to immobilized antigens. To facilitate the detection of spheroplasts bound onto beads, we co-expressed GFP in the cytoplasm. FACS and fluorescent microscopy analyses clearly showed the selective binding of spheroplasts expressing scFv onto beads decorated with antigen (Fig. 5-3 and data not shown). Interestingly, the recognition of immobilized antigen by spheroplasts was critically dependent on how the scFv is anchored onto the inner membrane. In earlier studies we had employed the leader peptide and the 6 amino acid residues that comprise the fatty acylation motif in the *E. coli* protein NlpA to anchor successfully various scFvs and other proteins onto the inner membrane. NlpA(1-6)-scFv fusions were shown to recognize fluorescent soluble antigens up to at least 250 kDa M.W. However, spheroplasts displaying the anti-digoxin 26-10 scFv as an NlpA(1-6) fusion failed to bind to beads decorated with immobilized hapten. We reasoned that lack of binding to the immobilized antigen might be due to the close proximity of the scFv *N*-terminus to the lipid bilayer. To circumvent this problem, antibody fragments were anchored onto the membrane by fusion to the first three transmembrane domains and the large periplasmic loop of MalF. In this construct the scFv is fused to amino acids 1-175 of MalF that is thought to be periplasmically exposed and should be able to serve as a spacer to distance the antibody fragment from the inner membrane. Nonetheless, MalF(1-175)-scFv fusions also failed to mediate the binding of spheroplasts onto antigen immobilized on beads.

The gp3 protein of the filamentous bacteriophages becomes associated with the inner membrane prior to its incorporation into the growing virion. The ability of gp3 to tolerate polypeptides fused to its *N*-terminus has been widely exploited for phage display. Similarly, scFv-gp3 fusions are suitable for APEx and antigen binding can be detected by FACS following spheroplasting. In scFv-gp3 fusions, the *C*-terminus of the antibody fragment is covalently linked to the gp3 protein. Although the fusion junction is in close proximity to the VH CDR3 region that plays an important role in antigen recognition, it does not affect the binding of soluble antigens. Moreover, we show here that scFv-gp3 display allows the binding of spheroplasts to antigens immobilized on beads. The precise molecular mechanism responsible for the higher accessibility of scFv anchored on spheroplasts as *C*-terminal fusions compared to *N*-terminal fusions are not clear at the moment. It is well established that the orientation of proteins immobilized on solid surfaces is critical to function and to their interaction with other molecules (Cha et al., 2005; Seong and Choi, 2003). Analogous orientation effects may be important in this instance as well. Alternatively, it is possible that the different anchoring domains localize to distinct sites in the inner membrane which are more or less accessible following spheroplasting. Recent studies in Gram-positive bacteria have revealed that the leader peptide can direct secreted polypeptides either to the septum or the poles (Carlsson et al., 2006). By analogy, it is possible that a gp3 fusion is directed to an inner membrane site distinct from the location where NlpA or MalF reside, meaning that the different fusions are in distinct local environments that may influence surface binding. Whatever the explanation, the data presented in this chapter clearly show that gp3 fusions are suitable

for mediating the binding of spheroplasts onto immobilized antigens via antibody-antigen interactions.

We have demonstrated that spheroplasted cells expressing scFv-gp3 fusions can be enriched by binding to beads with immobilized antigen (Table 4-1, Fig. 4-4). Experiments using 100-fold and 1,000-fold excess of spheroplasts expressing a scFv-gp3 fusion of unrelated specificity revealed that the degree of enrichment per round is relatively low, of the order of 20-25-fold per round. As a result, 3 rounds of sorting were required to enrich 26-10 scFv-gp3 expressing spheroplasts present in a 1:1,000 mixture.

As can be seen in Figure 4-4, the enhancement of the fluorescent signal is low in the initial rounds but increases significantly in round 3. There may be a relatively straightforward and general explanation for this finding: In the flow cytometric enrichment of cells via binding to soluble fluorescent molecules, the ligand is present in a large stoichiometric excess relative to the number of receptors per cell. As a result, cells that bind to the ligand become highly fluorescent by binding many fluorescent antigen molecules, so that binders can be enriched from the overall population with high efficiency. In contrast, when the ligand is immobilized on particles such as beads or, by analogy, the surface of mammalian cells, the number of spheroplasts expressing ligand-binding proteins is much lower than the number of antigen containing particles. The positive, ligand-binding spheroplasts will, on average, end up distributed onto different beads. With only one spheroplast per bead, the fluorescence due to the expression of GFP is low resulting in a low initial enrichment. The degree of enrichment increases in subsequent rounds as the ratio of positive spheroplasts to the number of beads becomes higher.

In summary, the experiments described here indicate that APEx can be employed for the binding of *E. coli* to immobilized antigens and is suitable for the library screening of antibodies recognizing insoluble ligands including receptors or antigens on whole mammalian cells and is further extended to the proteomic research to find interacting proteins that activate specific cells. Recently, we have succeeded in displaying full length IgG antibodies on spheroplasts and have demonstrated the isolation of specific antibodies from very complex libraries (Mazor et al., 2007). The APEx display of bivalent IgGs could be exploited for the isolation of weak binders that are better represented in repertoire libraries and may thus facilitate the selection of IgGs specific to insoluble antigens from large repertoire libraries.

Chapter 5

Conclusion and Recommendations

5.1 CONCLUSION

The work presented in this dissertation describes the development of screening systems for the engineering of aglycosylated antibody Fc region, the isolation of aglycosylated antibodies displaying highly selective binding to Fc receptors and conferring unique effector functions in ADCC, and finally, a new high-throughput screening method for the isolation of antibodies specific to insoluble antigens.

For the engineering of aglycosylated antibody Fc domains with altered binding affinity to Fc binding ligands, we have developed a new bacterial display system. In this system, the Fc polypeptide was secreted with the PelB leader peptide and properly folded and dimerized in the *E. coli* periplasmic space. Spheroplasted cells after cultivation at optimized condition retained a significant fraction of Fc protein that was accessible to Fc binding ligands. Using this display system and flow cytometry screening upon labeling with fluorescently labeled FcγRI, aglycosylated Fc variants showing high affinity to FcγRI were isolated from a large error prone PCR library. Among the isolated Fc mutant domains, the Fc5 mutant exhibiting high affinity to FcγRI was found to contain only two mutations (E382V and M428I) located within the CH3 C and F β-sheets that are distal from the reported FcγRs binding site. Notably, *E. coli*-expressed engineered anti-Her2 IgG1 antibody (trastuzumab) containing these 2 mutations was highly specific to FcγRI with negligible binding affinity to other effector FcγRs including the inhibitory FcγRIIb.

The pH dependent human FcRn binding that is critical for the homeostasis of serum IgG molecules with intracellular trafficking and recycling was not significantly affected by the two mutations in CH3 region.

High-throughput FACS screening from a new library randomized from Fc5 generated Fc mutants displaying higher affinities relative to the parental Fc5 protein towards FcγRI. Among them, Fc601 containing the mutations, K338R and G341V in addition to Fc5 (E382V and M428I), showed the highest affinity for FcγRI. Following expression in *E. coli* and purification for the Fc engineered aglycosylated trastuzumab antibodies possessing the isolated mutant domains, either Fc5 or Fc601, effector function and ADCC were evaluated by measuring the cytotoxicity of Her2 overexpressing tumor cells using monocyte-derived dendritic cells. Remarkably, *E. coli*-expressed aglycosylated IgG variants (Fc5 and Fc601) that are highly specific to FcγRI, but not clinical grade glycosylated trastuzumab (Herceptin) that is non-specific to all FcγRs, was able to potentiate the killing of the cells. These results show that aglycosylated antibodies showing complete loss of ADCC can be engineered for highly selective binding affinity to an FcγR and for unique ADCC that nonselective FcγR binding glycosylated antibodies cannot elicit. To isolate Fc domains displaying higher affinity to FcγRI than Fc5 without abrogating pH-dependent human FcRn binding, FACS screening was employed using libraries that randomized the lower hinge and upper CH2 region. The isolated trastuzumab-Fc701 that has mutations in CH2 region F/G loop (L328W, A330V, P331A, I332Y) and one additional mutation (Q295R) showed higher affinity to FcγRI than trastuzumab-Fc5 and also higher binding affinity to FcRn at pH 6.0 than the clinical grade trastuzumab.

Finally, we showed that the APEx system previously developed for the screening of high affinity proteins to soluble binding ligands is suitable for the discovery of proteins that bind to cell surface molecules or antigens immobilized on synthetic surface. In this study, scFv antibodies specific for the cardiac digoxin or for the PA antigens of *Bacillus anthracis* were expressed in *E. coli* as fusions to either *N*-terminal or *C*-terminal membrane anchoring domains. Upon spheroplasting at optimized condition, only the *C*-terminally anchored scFv-gp3 fusions enabled specific binding to the antigens immobilized on beads. From spheroplasts expressing anti-digoxin (26-10) scFvs in a large excess (1000-fold) of spheroplasts expressing unrelated anti-PA (M18) scFv, three rounds FACS screening allowed 950 fold enrichment of the insoluble antigen specific spheroplasts. These results demonstrate the utility of the APEx display system for the isolation of antibodies specific to insoluble biomarkers on cell surfaces or solid surfaces.

5.2 RECOMMENDATIONS

Currently, we have no structural information for the wild type aglycosylated Fc domain, the Fc5 mutant domain, or the extracellular domain of FcγRI. Structural analysis of the aglycosylated Fc domains and FcγRI by X-ray crystallography could provide information how the two mutations (E382V and M428I) in CH3 domain allow highly selective binding of the aglycosylated antibody to FcγRI. In using monocyte-derived dendritic cells as effector cells, aglycosylated antibodies (Fc5 or Fc601), could potentiate the killing of tumor cells. On the other hand, clinical grade glycosylated trastuzumab showed only background level cytotoxicity. We hypothesize that the selective

engagement of the engineered aglycosylated antibodies to FcγRI enables the high cytotoxicity of tumor cells in contrast to the glycosylated antibodies that bind nonspecifically to all effector FcγRs. To elucidate this mechanism, blocking the binding of engineered aglycosylated antibodies to FcγRI on the effector monocyte-derived dendritic cells can be used. Preliminary blocking experiment using commercially available FcγRI blocking antibodies was not successful due to the much lower affinity of these blocking antibodies relative to the binding affinity of the engineered aglycosylated antibodies containing either Fc5 or Fc601 domains to FcγRI. However, we can try to block the FcγRI mediated signaling by antisense FcγRI siRNA. If we can isolate a new FcγRI blocking antibody clone with higher affinity than the interaction between FcγRI and engineered aglycosylated antibodies containing either Fc5 or Fc601, it can be useful for investigating the mechanism about our proposed FcγRI mediated effector function.

In this work, we focused on the binding to FcγRI among effector FcγRs and isolated aglycosylated antibodies showing highly selective binding affinity to FcγRI and a unique effector function that their glycosylated counterpart antibodies could not exhibit. However, aglycosylated Fc engineered antibodies that bind to other activating FcγRs including FcγRIIa or FcγRIIIa can be also isolated using either homodimeric Fc display system described in chapter 2 or covalently inner membrane anchored full length IgG display system described in appendix 2. Since IgG binding to FcγRIIb down-regulates the recruitment of immune cells and immunological functions, screening of aglycosylated antibodies exhibiting high affinity to FcγRIIa and FcγRIIIa relative to FcγRIIb can be utilized for the isolation of aglycosylated antibodies with improved ADCC in immunotherapy. Additionally, the screening of IgG variants for better pH dependent

hFcRn binding can be employed to isolate antibodies with enhanced serum stability. To determine the therapeutic utility of the aglycosylated antibodies, pharmacokinetic study in mice or primate animals and immunogenicity in humans should be followed.

Finally, we demonstrated the successful binding and enrichment of spheroplasts displaying insoluble antigen specific scFv using C-terminally fused APEx format and antigen immobilized Tenta-Gel beads. The methodology developed in chapter 4 can be applied for the isolation of antibodies binding to membrane bound or cell surface antigens from large library screening.

Appendix 1

Bacterally Expressed Aglycosylated Fc Receptors

A1.1 INTRODUCTION

Fc receptors are surface glycoproteins expressed on leukocytes that play a critical role in the human immune system by mediating humoral and cellular immunity. To deeply investigate the interaction of IgG Fc and Fc receptors as well as to use them in library screening for high affinity Fc, an efficient production and purification system for large amount of Fc receptors is required. In addition, the effect of glycosylation of Fc receptors on function and the binding of IgG has not been extensively studied. So far FcγRIIa, FcγRIIb, and FcγRIIIb have been successfully expressed in *E. coli* and used for structural analysis by crystallography (Galon et al., 1997; Sondermann et al., 1999; Sondermann et al., 2000; Sondermann and Jacob, 1999). However, efficient processes for the expression of large amounts of these proteins are not available. Additionally FcγRI has not yet been expressed in any significant amount. In an earlier study, Paetz *et al*. reported the production of only 40ng/ g pellet or 17 μg/L culture (Paetz et al., 2005) in bacteria.

In this study, we have optimized the expression of extracellular domain of FcγRs (FcγRI, FcγRIIa, FcγRIIb, FcγRIIIa) in *E. coli*. The proteins have been purified and refolded from *E. coli* inclusion bodies. In ELISA assays using the purified FcγRs on the plate coated glycosylated IgG1, all the refolded proteins showed affinity to the glycosylated IgG1.

A1.2 MATERIAS AND METHOD

A1.2.1 Construction of plasmids for the expression of FcγRs

Human FcγRs cDNAs were purchased from ATCC (Manassas, VA). DNA fragments encoding FcγRI were PCR amplified using the primers (STJ#266 and STJ#267) using the template plasmid, pCMV-SPORT6 (ATCC: MGC-45021), digested with *Nde*I / *Hin*dIII endonucleases, ligated into pET21a (EMD Chemicals, Gibbstown, NJ) digested using the same restriction enzymes to generate pET21a-FcγRI. PCR amplification using the primers (STJ#199 and STJ#200) from the template plasmid, pDNR-LIB (ATCC: MGC-23887), ligation into *Nde*I / *Hin*dIII digested pET21a generated pET21a-FcγRIIa. pET21a-FcγRIIb was constructed by PCR amplification using the primers (STJ#294 and STJ#295) and the template plasmid, pCMV-SPORT6.ccdb (ATCC: MGC-21364), and ligation into pET21a digested with *Nde*I / *Hin*dIII. For pET21a-FcγRIIIa, DNA fragments were amplified using the primers (STJ#296 and STJ#297) and the template pCMV-SPORT6 (ATCC: MGC-45020) and ligated into *Nde*I / *Hin*dIII digested pET21a.

DNA fragments encoding *E. coli* codon optimized FcγRI was synthesized using gene assembly PCR using the primers (STJ#148 ~ STJ#173, STJ#241 and STJ#242) for FcγRI, the primers (STJ#201 ~ STJ#218) for FcγRIIa, the primers (STJ#247 ~ STJ#264) for FcγRIIb, the primers (STJ#174 ~ STJ#193, STJ#243 and STJ#244) for FcγRIIIa were ligated into *Nde*I / *Hin*dIII digested pET21a to generate *E. coli* codon optimized FcγR expression plasmids, pET21a-FcγRI-opt, pET21a-FcγRIIa-opt, pET21a-FcγRIIb-opt, pET21a-FcγRIIIa-opt. The resulting plasmids were transformed into *E. coli* BL21(DE3) (EMD Chemicals, Gibbstown, NJ).

A1.2.2 Expression and purification of of FcγRs

E. coli BL21(DE3) cells harboring FcγR expression plasmids were cultured in 500 ml of LB medium supplemented with 50 μg/ml of ampicillin at 37 °C with 250 rpm shaking. Protein expression was induced by adding 1 mM of isopropyl-1-thio-β-D-galactopyranoside (IPTG) when OD_{600} of culture reached 0.6. Cells were harvested by centrifuging at 7,000g for 20 min after 5 h of induction. FcγRs expressed as inclusion bodies were solubilized in 8M urea solution, purfied using Ni-NTA agarose resin (Qiagen, Valencia, CA), and refolded as described in the previous study (Jung et al., 2003).

A1.2.3 ELISA analysis

50 μl of 4 μg/ml of glycosylated serum human IgG1 (Sigma-Aldrich, St. Louis, MO) were diluted in 0.05 M Na_2CO_3 (pH 9.6) buffer and used to coat 96 well polystyrene ELISA wells (Corning, Corning, NY) for 16 h at 4 °C. After blocking with 1 × PBS (pH 7.4), 0.5% BSA for 2 h at room temperature, the plate was washed 4 times with PBS containing 0.05% Tween20, and incubated with serially diluted FcγRs at room temperature for 1 h. After washing 4 times with the same buffer, 1:10,000 diluted anti-polyhistidine HRP conjugate (Sigma-Aldrich, St. Louis, MO) was added and plates were washed and developed using Ultra-TMB substrate (Pierce Biotechnology, Rockford, IL).

Table A1-1. Plasmids used in this study.

Plasmids	Relevant characteristics	Reference or source
pCMV-SPORT6-FcrRI	ATCC: MGC-45021	ATCC (Manassas, VA)
pDNR-LIB-FcrRIIa	ATCC: MGC-23887	ATCC (Manassas, VA)
pCMV-SPORT6.ccdb-FcrRIIb	ATCC: MGC-21364	ATCC (Manassas, VA)
pCMV-SPORT6-FcrRIIIa	ATCC: MGC-45020	ATCC (Manassas, VA)
pET21a	Ap^r, *T7* promoter, $lacI^q$	EMD Chemicals (Gibbstown, NJ)
pET21a-FcγRI	*FcγRI* gene in pET21a	This study
pET21a-FcγRIIa	*FcγRIIa* gene in pET21a	This study
pET21a-FcγRIIb	*FcγRIIb* gene in pET21a	This study
pET21a-FcγRIIIa	*FcγRIIIa* gene in pET21a	This study
pET21a-FcγRI-opt	*E. coli codon optimized FcγRI* gene in pET21a	This study
pET21a-FcγRIIa-opt	*E. coli codon optimized FcγRIIa* gene in pET21a	This study
pET21a-FcγRIIb-opt	*E. coli codon optimized FcγRIIb* gene in pET21a	This study
pET21a-FcγRIIIa-opt	*E. coli codon optimized FcγRIIIa* gene in pET21a	This study

Table A1-2. Primers used in this study.

Primer Name	Primer nucleotide sequence (5' → 3')
STJ#148	CGCAGCGAGGCCCAGCCGGCCATGGCGCAGGTGGATACC
STJ#149	CACCCACGGCGGCTGAAGGGTAATCACCGCTTTGGTGGTATCCACCTGCGCCAT
STJ#150	CAGCCGCCGTGGGTGAGCGTGTTTCAGGAAGAAACCGTAACGCTTCATTGCGAG
STJ#151	ACTGGGTGCTAGAGGACCCCGGCAGATGCAGCACCTCGCAATGAAGCGTTACGG
STJ#152	GGGTCCTCTAGCACCCAGTGGTTTCTGAACGGCACCGCGACCCAGACCTCAACC
STJ#153	ATCATTCACGCTCGCGCTAGTAATACGATAGCTCGGGGTTGAGGTCTGGGTCGC
STJ#154	TAGCGCGAGCGTGAATGATTCAGGGGAATACCGTTGTCAGCGTGGTCTGAGCGG
STJ#155	GCCACGATGAATTTCCAGCTGAATTGGATCGCTACGGCCGCTCAGACCACGCTG
STJ#156	CAGCTGGAAATTCATCGTGGCTGGCTGCTTCTGCAGGTGTCTAGCCGGGTGTTT
STJ#157	GCATGGCAACGCAACGCTAACGGTTCGCCTTCGGTAAACACCCGGCTAGACACC
STJ#158	GCGTTGCGTTGCCATGCGTGGAAAGATAAACTTGTGTATAATGTGCTGTATTAT
STJ#159	AACTTAAACGCTTTGCCATTACGATAATACAGCACATTATACACAAGTTTATCT
STJ#160	CGTAATGGCAAAGCGTTTAAGTTTTTCCATTGGAATTCGAACCTGACCATTCTG
STJ#161	GATACGTTCCATTATGGCTAATATTGGTTTTCAGAATGGTCAGGTTCGAATTCC
STJ#162	CCAATATTAGCCATAATGGAACGTATCATTGTAGCGGAATGGGCAAACATCGTT
STJ#163	TCTTTCACTGTCACGCTAATGCCTGCGCTGGTGTAACGATGTTTGCCCATTCCG
STJ#164	GCATTAGCGTGACAGTGAAAGAACTTTTTCCGGCTCCGGTGTTGAATGCCAGTG
STJ#165	GGTCACCAGATTGCCTTCCAACAGCGGGCTAGTCACACTGGCATTCAACACCGG
STJ#166	TGGAAGGCAATCTGGTGACCCTGAGCTGCGAAACCAAACTGTTACTGCAGCGCC
STJ#167	CCCATATAGAAGCTAAAATACAGTTGCAGCCCTGGGCGCTGCAGTAACAGTTTG
STJ#168	GCAACTGTATTTTAGCTTCTATATGGGCAGCAAAACCCTGCGTGGCCGGAACAC
STJ#169	TTCACGACGCGCGGTCAGAATCTGATATTCACTAGAGGTGTTCCGGCCACGCAG
STJ#170	GACCGCGCGTCGTGAAGATAGCGGCCTGTATTGGTGCGAAGCGGCGACCGAAGA
STJ#171	CAGTTCCAGTTCCGGGCTACGTTTCAATACATTACCATCTTCGGTCGCCGCTTC
STJ#172	GTAGCCCGGAACTGGAACTGCAAGTGTTAGGCCTGCAGCTTCCGACACCAGGGG
STJ#173	CGCAATTCGGCCCCCGAGGCCCCTGGTGTCGGAAGC
STJ#174	CGCAGCGAGGCCCAG
STJ#175	TTTGGGCAGATCTTCGGTACGCATGCCCGCCATGGCCGGCTGGGCCTCGCTGCG
STJ#176	CGTACCGAAGATCTGCCCAAAGCGGTGGTGTTTCTGGAACCGCAGTGGTATCGT
STJ#177	TGGCATTTCAGTGTGACGCTATCTTTCTCCAGCACACGATACCACTGCGGTTCC
STJ#178	TAGCGTCACACTGAAATGCCAGGGCGCGTATAGCCCTGAGGATAATTCTACCCA
STJ#179	GGCTGCTAATCAGGCTTTCATTATGAAACCACTGGGTAGAATTATCCTCAGGGC
STJ#180	ATGAAAGCCTGATTAGCAGCCAGGCGAGCTCTTACTTTATCGATGCGGCGACCG
STJ#181	AGATTGGTCTGACAACGATATTCGCCGCTGTCATCCACGGTCGCCGCATCGATA
STJ#182	CGAATATCGTTGTCAGACCAATCTGAGCACCTTGAGCGATCCGGTGCAGTTAGA
STJ#183	GAGGCGCTTGCAGCAGTAACCAGCCAATATGCACTTCTAACTGCACCGGATCGC
STJ#184	ACTGCTGCAAGCGCCTCGTTGGGTGTTTAAAGAAGAAGATCCGATTCATCTGCG
STJ#185	ATGCAGCGCGGTATTTTTCCAGCTATGGCAACGCAGATGAATCGGATCTTCTTC
STJ#186	GGAAAAATACCGCGCTGCATAAAGTGACCTATTTACAGAATGGCAAAGGCCGTA
STJ#187	GAATATAGAAATCGCTATTATGATGAAAATACTTACGGCCTTTGCCATTCTGTA
STJ#188	AGTATTTTCATCATAATAGCGATTTCTATATTCCGAAAGCGACCTTGAAGGATT
STJ#189	TTCCGACAAGCCCACGACAGAAATAGCTGCCAGAATCCTTCAAGGTCGCTTTCG
STJ#190	GTCGTGGGCTTGTCGGAAGCAAAAATGTGAGCAGCGAAACCGTGAATATTACCA
STJ#191	CTTATGGTGCTAACGCTCAGGCCCTGGGTAATGGTAATATTCACGGTTTCGCTG
STJ#192	CCTGAGCGTTAGCACCATAAGCAGCTTTTTTCCTCCGGGGTATCAGGGGGCCTC
STJ#193	CGCAATTCGGCCCCCGAGGCCCCCTGATACCCC

STJ#199	GCGGAATTCCATATGCAAGCTGCTCCCCCAAAGGCTGTG
STJ#200	TTAGGGAAGCTTAATGACCCCCATTGGTGAAGAGCTGC
STJ#201	GCGGAATTCCATATGCAGGCTGC
STJ#202	GGCGGTTCCAGTTTCAGCACGGCTTTCGGTGGGGCAGCCTGCATATGGAATTCC
STJ#203	TGCTGAAACTGGAACCGCCGTGGATTAATGTGTTGCAGGAAGATAGCGTGACCC
STJ#204	TCGCTTTCAGGGCTACGCGCTCCCTGACAGGTCAGGGTCACGCTATCTTCCTGC
STJ#205	GCGTAGCCCTGAAAGCGATTCTATTCAGTGGTTTCACAATGGAAATCTGATTCC
STJ#206	TAAAACGATAGCTCGGCTGGGTATGGGTCGGAATCAGATTTCCATTGTGAAACC
STJ#207	CCCAGCCGAGCTATCGTTTTAAAGCGAACAATAATGATAGCGGCGAATACACCT
STJ#208	CCGGATCGCTCAGGCTGGTCTGGCCCGTCTGGCAGGTGTATTCGCCGCTATCAT
STJ#209	CAGCCTGAGCGATCCGGTGCATCTGACCGTGCTTAGCGAATGGCTGGTGCTGCA
STJ#210	ATGGTTTCGCCTTCCTGAAATTCCAGATGCGGGGTTTGCAGCACCAGCCATTCG
STJ#211	AATTTCAGGAAGGCGAAACCATTATGCTGCGTTGCCATAGCTGGAAAGATAAAC
STJ#212	CATTCTGAAAAAAGGTCACTTTCACCAGCGGTTTATCTTTCCAGCTATGGCAAC
STJ#213	GGTGAAAGTGACCTTTTTTCAGAATGGCAAAAGCCAGAAATTTTCTCACCTGGA
STJ#214	AATGATTCGCCTGCGGAATGCTAAAGGTCGGATCCAGGTGAGAAAATTTCTGGC
STJ#215	CATTCCGCAGGCGAATCATTCTCACTCCGGCGATTACCATTGTACCGGCAATAT
STJ#216	ACCGGTTTGCTGCTAAACAGGGTATAGCCTATATTGCCGGTACAATGGTAATCG
STJ#217	CTGTTTAGCAGCAAACCGGTGACAATTACCGTGCAGGTGCCGAGCATGGGCAGC
STJ#218	TAAGGGAAGCTTAATCACGCCCATCGGTGAGCTGCTGCCCATGCTCGGC
STJ#241	GCGGAATTCCATATGCAGGTGGATACCACCAAAGCGGTG
STJ#242	TTAGGGAAGCTTTGGTGTCGGAAGCTGCAGGCC
STJ#243	GCGGAATTCCATATGGGCATGCGTACCGAAGATCTGCC
STJ#244	TTAGGGAAGCTTCTGATACCCCGGAGGAAAAAAGCTGC
STJ#247	GCGGAATTCCATATGGGCACACCTGCGGCACCTC
STJ#248	TTAATCCACTGCGGTTCCAGTTTCAGCACCGCTTTTGGAGGTGCCGCAGGTGTG
STJ#249	ACTGGAACCGCAGTGGATTAATGTGTTACAGGAAGATAGCGTTACCCTGACCTG
STJ#250	ATACTATCGCTTTCCGGGCTATGGGTGCCACGGCAGGTCAGGGTAACGCTATCT
STJ#251	TAGCCCGGAAAGCGATAGTATTCAGTGGTTTCATAACGGCAATCTGATTCCGAC
STJ#252	TCGCTTTAAAACGATAGCTCGGCTGGGTATGGGTCGGAATCAGATTGCCGTTAT
STJ#253	CCGAGCTATCGTTTTAAAGCGAATAACAACGACTCTGGCGAATACACGTGCCAG
STJ#254	AGATGCACCGGGTCGCTCAGGCTCGTCTGGCCGGTCTGGCACGTGTATTCGCCA
STJ#255	AGCGACCCGGTGCATCTGACCGTGCTGAGTGAATGGCTGGTGCTGCAGACCCCG
STJ#256	CGCAGCACAATGGTTTCGCCTTCCTGAAATTCCAGATGCGGGGTCTGCAGCACC
STJ#257	GCGAAACCATTGTGCTGCGTTGCCATAGCTGGAAAGATAAACCGCTGGTGAAAG
STJ#258	TTTTTGCTTTTGCCATTCTGAAAAAAGGTCACTTTCACCAGCGGTTTATCTTTC
STJ#259	TTTTTCAGAATGGCAAAAGCAAAAAGTTTAGCCGTTCCGATCCGAATTTTAGCA
STJ#260	ATCGCCGCTGTGGCTATGATTCGCCTGCGGAATGCTAAAATTCGGATCGGAACG
STJ#261	CATAGCCACAGCGGCGATTATCATTGTACCGGCAACATCGGCTATACTCTGTAT
STJ#262	CCTGCACGGTGATGGTCACCGGTTTGCTGCTATACAGAGTATAGCCGATGTTGC
STJ#263	TGACCATCACCGTGCAGGCGCCGAGCAGCAGCCCGATGGGCATTATCAAGCTTC
STJ#264	TTAGGGAAGCTTGATAATGCCCATCGG
STJ#266	GCGGAATTCCATATGCAAGTGGACACCACAAAGGCAGTGATC
STJ#267	TTAGGGAAGCTTAGGAGTTGGTAACTGGAGGCCAAGCAC
STJ#294	GCGGAATTCCATATGGGGACACCTGCAGCTCCCCCAAAGGCTGTGCTG
STJ#295	TTAGGGAAGCTTAATGATCCCCATCGGTGAAGAGCTGGGAGCTTGGACAGTGATGGTCAC
STJ#296	GCGGAATTCCATATGGGCATGCGGACTGAAGATCTCCC
STJ#297	TTAGGGAAGCTTTTGGTACCCAGGTGGAAAGAATG

A1.3 RESULTS

A1.3.1 Expression of aglycosylated FcγRs in *E. coli*

For the expression of aglycosylated human FcγRs, human FcγR cDNAs were subcloned into pET21a plasmids under the control of T7 promoter (Fig. A1-1). Synthetic genes encoding FcγRs optimized for *E. coli* codon usage and overlapping oligonucleotides for the amplification of the synthetic genes were designed by the online program DNAWorks (http://helixweb.nih.gov/dnaworks) (Hoover and Lubkowski, 2002). The expression levels of FcγRIIa and FcγRIIb were improved by using the synthetic genes through codon optimization for full coding sequences (Fig. A1-2). As expected, the overexpressed proteins (FcγRIIa, FcγRIIb, and FcγRIIIa) were localized entirely in the inclusion body fraction. The expression level of FcγRI was extremely low and could not be detected on the Western blot even after the codon optimization. One possible explanation for the lack of protein expression was that stable RNA structures at the 5' could have prevented ribosome binding and/or translation initiation (De Smit et al., 1990). Indeed the RNAStructure software (Ver. 3.71) indicated a strong propensity for the formation of stable structures in the mRNA. To increase translation efficiency, a C-terminal polyhistidine tag was fused to the N-terminal of both the codon optimized synthetic FcγRI gene and the wild type FcγRI gene. The expression level could be significantly increased by adding the polyhistidine tag at the N-terminus. However, significant degradation was observed by Western blotting. To further increase expression level and reduce degradation products, expression in a variety of DE3 lysogen *E. coli* strains such as BL21(DE3), BLR(DE3), HMS174(DE3), Tuner(DE3), (DE3),

Rosetta2(DE3), Rosetta-gami(DE3), Rosetta-gami B(DE3), Orgami (DE3), and Orgami B(DE3) were attempted. Also, to reduce C-terminal degradation, a C-terminal FLAG was introduced in addition to the N-terminal polyhistidine tag. By using dual tags, namely N-terminal polyhistidine tag and C-terminal FLAG tag, the FcγRI protein could be successfully overexpressed in Rosetta-gami (DE3) cells (Fig. A1-3).

A1.3.2 Purification and refolding of FcγRs

For the purification of FcγRs, inclusion bodies were collected, washed, solubilized in 8 M urea buffer, and further purified using immobilized metal affinity chromatography (IMAC) column. The purified FcγRs were refolded by the previously published stepwise dialysis method (Jung et al., 2003). The yields were over 20 mg / L culture for FcγRIIa, FcγRIIb, and FcγRIIIa. The yield of FcγRI was 1.74 mg / L (Fig. A1-4).

Figure A1-1. Gene casettes for the expression of FcγRIIa, FcγRIIb, and FcγRIIIa.

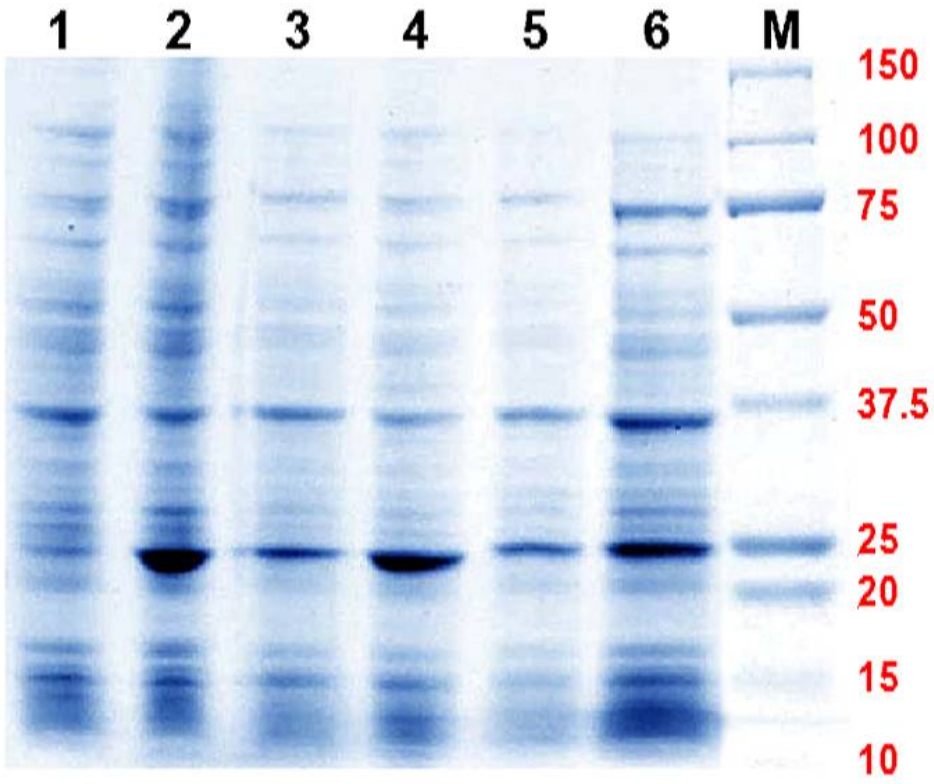

Figure A1-2. Expression of FcγRIIa, FcγRIIb, and FcγRIIIa. Lane1: wild type FcγRIIa-His; Lane 2: codon optimized FcγRIIa-His; Lane 3: wild type FcγRIIb-His; Lane 4: codon optimized FcγRIIb-His; Lane 5: wild type FcγRIIIa-His; Lane 6: codon optimized FcγRIIIa-His.

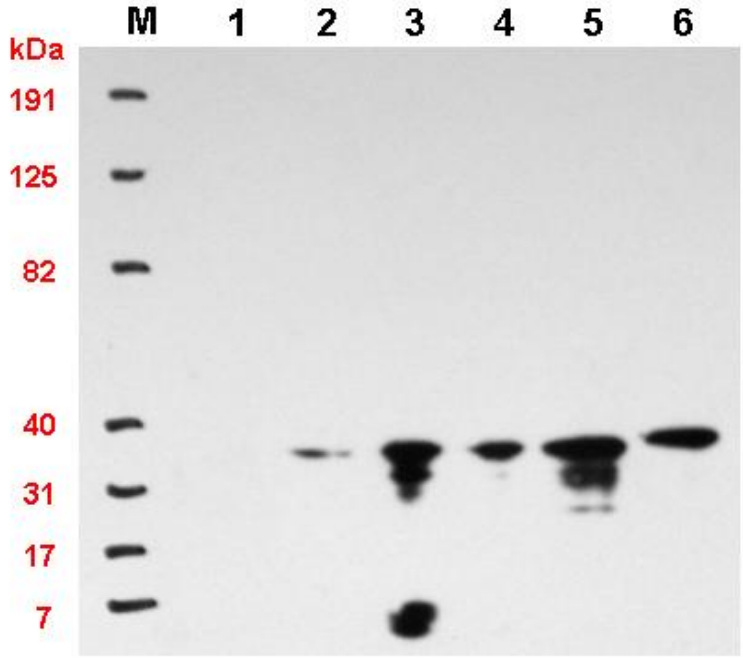

Figure A1-3. Western blot showing the expression of FcγRI depending on the codon optimization, the terminal tag location, and the various DE3 lysogen containing *E. coli* strains. Lane 1: BL21(DE3) harboring human FcγRI cDNA with C-terminal 6xHis tag; Lane 2: BL21(DE3) harboring FcγRI gene optimized for *E. coli* codon usage with C-terminal 6xHis tag; Lane 3: BL21(DE3) harboring human FcγRI cDNA with N-terminal 6xHis tag; Lane 4: BL21(DE3) harboring FcγRI gene optimized for *E. coli* codon usage with N-terminal 6xHis tag; Lane 5: Rosetta gami(DE3) harboring FcγRI gene optimized for *E. coli* codon usage with N-terminal 6xHis tag; Lane 6: Rosetta gami(DE3) harboring FcγRI gene optimized for *E. coli* codon usage with both N-terminal 6xHis and C-terminal FLAG tags.

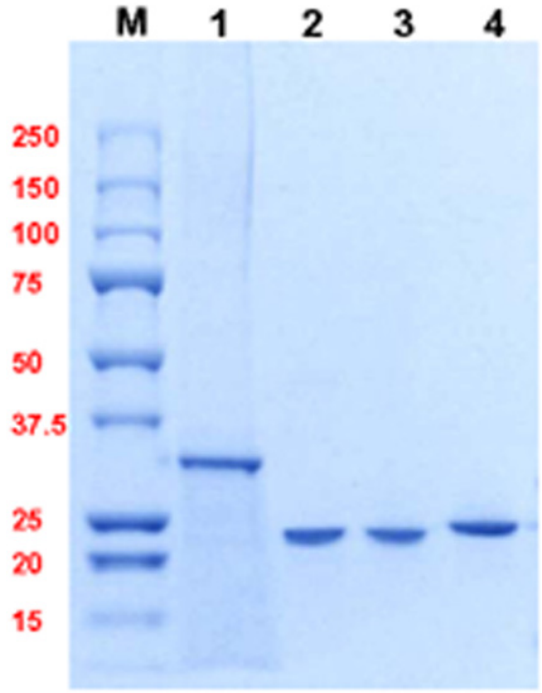

Figure A1-4. SDS-PAGE showing the purified Fc receptors. Lane1: FcγRI-His; Lane 2: FcγRIIa-His; Lane 3: FcγRIIb-His; Lane 4: FcγRIIIa-His.

A1.3.3 Affinity of aglycosylated FcγRs

The activity of the purified FcγRs was analyzed by ELISA. Plates were coated with glycosylated serum human IgG1 and binding of the purified FcγRs was detected using anti-His antibody HRP conjugate. FcγRI FcγRIIa, FcγRIIb, and FcγRIIIa all showed affinity to human IgG1 relative to the negative control (BSA) (Fig. A1-5).

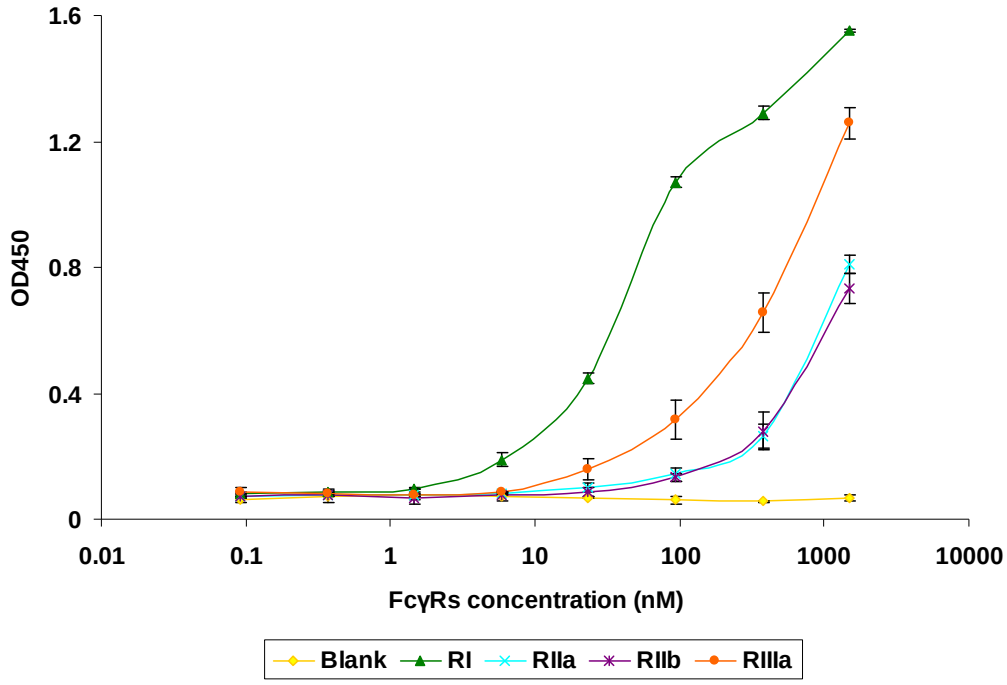

Figure A1-5. ELISA assays for purified FcγRs (FcγRI, FcγRIIa, FcγRIIb, and FcγRIIIa). ELISA plate was coated with 4 µg/ml of glycosylated human IgG1 (Sigma-Aldrich, St. Louis, MO) and binding of purified FcγRs was detected by anti-polyhistidine-HRP conjugate (Sigma-Aldrich, St. Louis, MO).

A1.4 DISCUSSION

Human effector FcγRs are expressed in most immune cells (van de Winkel and Capel, 1993) and play essential roles in linking antibody associated humoral and cellular immune responses by binding to the Fc domain of IgG (Berken and Benacerraf, 1966; Ravetch and Bolland, 2001). In this chapter, we expressed the aglycosylated extracellular domains of FcγRs in *E. coli*. Use of *E. coli* codon optimized synthetic genes and, in the case of FcγRI, minimization of 5' mRNA secondary structure by fusion to a gene

encoding an N-terminal 6xHis sequence could increase expression level. The FcγRs were expressed as inclusion bodies and soluble active protein was obtained by refolding.

The kinetic constants for the binding of IgG to aglycosylated FcγRIIa, FcγRIIb, and FcγRIIIb have been reported (Maenaka et al., 2001). However, the binding kinetics of aglycosylated FcγRI and FcγRIIIa are not available. To elucidate questions about the effect of glycosylation on the binding affinity of Fc receptors to IgG, the quantitative kinetic analysis of the purified aglycosylated FcγRI and FcγRIIIa needs to be performed and the results will be compared with the published values for glycosylated recombinant FcγRs. Also, it will be interesting to investigate the specificity of FcγRs for the various IgG subclasses (IgG1, IgG2, IgG3, and IgG4). Finally the purified functional FcγRs may be used for the screening of antibodies for improved effector functions or the study on the interaction between IgG and FcγRs.

Appendix 2

Development of a covalently anchored full length IgG display system

A2.1 INTRODUCTION

Phage display, the oldest and the most widely used technique for library screening, relies on the presentation of diverse polypeptides on the surface of filamentous bacteriophage via fusion to a phage coat protein (Smith, 1985). It has been successfully used for the discovery of antigen specific antibody fragments from immune or nonimmune library (Bradbury and Marks, 2004). Compared with phage display, cell surface display systems using bacteria (Daugherty et al., 2000a; Daugherty et al., 2000b; Georgiou et al., 1997; Lofblom et al., 2005) or yeast (Boder et al., 2000; Boder and Wittrup, 1997; Feldhaus et al., 2003) are attractive since their relatively large size of cells allows high-throughput screening by flow cytometry (FC) with real-time optimization of quantitative multi-parameter and sorting (Mattanovich and Borth, 2006). Cell surface display approaches in *Escherichia coli* are attractive because of the rapid cell growth, high transformation efficiency, simple gene manipulation, and efficient production of target proteins of the bacteria (Daugherty et al., 2000a; Daugherty et al., 2000b; Georgiou et al., 1997). However, *E coli* cell surface display can be limited by the reduction of library diversity resulting from protein export to outer membrane and complications in screening caused by interfering biomolecules on the surface of outer membrane (Chen et al., 2001). In addition to cell surface display in *E. coli*, display in the periplasmic space has been developed for the screening of antigen specific proteins (Chen et al., 2001).

The anchored periplasmic expression (APEx) system was developed in our group (Harvey et al., 2004). In this system, fusion to lipoprotein (NlpA) or the Gene III protein (gp3) of bacteriophage M13, are employed to target and anchor proteins to the periplasmic face of the inner membrane (Harvey et al., 2004). Osmotic shock and chemical/enzyme treatment of *E. coli* is used to remove the outer membrane and most of the peptidoglycan layer to generate spheroplasts. For the screening of high affinity antibody/proteins, the spheroplasts expressing antibody/protein tethered onto the inner membrane are mixed with a fluorescently labeled antigen/ligand and fluorescent cells are collected by FACS.

While APEx system has been successfully used for the screening of high affinity antibody fragments for soluble antigens (Harvey et al., 2004; Harvey et al., 2006), it cannot be directly used for the display of multimeric proteins such as dimeric Fc protein or full length IgG. Also, the *E-clonal* system developed earlier for the isolation of IgGs with desired antigen specificities (Mazor et al., 2007) cannot be used to detect binding of Fc binding ligands to the Fc domain because the latter is occupied by the membrane-anchored Fc-binding protein which is used to display the IgG on spheroplasts. Here we report a new covalent full length IgG display and screening system. In this system, IgG light chains (VL-Ck) are designed for soluble periplasmic expression and covalent anchoring onto inner membrane. Tetrameric assembly of homodimeric IgG heavy chains (VH-CH1-Hinge-CH2-CH3) with both soluble and inner membrane anchored IgG light chains (VL-Ck) generates covalent anchored full length IgG for the engineering of Fc domains in full length IgG.

A2.2 MATERIALS AND METHODS

A2.2.1 Solube expression and purification of homodimeric wild type Fc and Fc2a fragments

All primers and plasmids used in this study are described in Table A2-1 and Table A2-2. Fc2a is an aglycosylated antibody variant optimized for FcγRIIa binding by two mutations (S298G/T299A) in the upper CH2 region; it has been reported that IgG containing Fc2a displays FcγRIIa binding (Sazinsky et al., 2008). For the expression of correctly assembled, homodimeric wild type Fc and FcγRIIa binding Fc (Fc2a, S298G/T299A) in the periplasmic space of *E. coli*, the plasmids pDsbA-Fc-FLAG and pDsbA-Fc2a-FLAG were constructed for the export of Fc via the DsbA signal peptide. Cleavage of pTrc99A (Amersham Pharmacia) with *Fat*I restriction endonuclease which is compatible with the *Nco*I and also with *Sal*I followed by ligating synthetic DNA fragment encoding the 53 bp DsbA signal peptide gene generated pDsbA. The parental Fc genes were amplified using he primers STJ#144 and STJ#145, ligated into pDsbA plasmid using *Sal*I and *Hin*dIII restriction enzyme sites giving rise to pDsbA-Fc-FLAG. The Fc2a mutant gene was amplified using the primers (STJ#422 and STJ#147) and the template (pDsbA-Fc-FLAG), ligated into *Sac*II / *Hin*dIII digested pDsbA-Fc-FLAG to generate pDsbA-Fc2a-FLAG. pDsbA-Fc5-FLAG was constructed by ligating Fc5 (E382V / M428I) fragments using the primers (STJ#290 and STJ#220) digested with *Sal*I / *Eco*RI into pDsbA-Fc-FLAG using the same restriction sites.

For the expression of wild type and Fc2a Fc fragments, *E. coli* Jude-1 cells harboring pDsbA-Fc-FLAG or pDsbA-Fc2a-FLAG were cultured in 2L flasks with 500 ml working volume. The culture supernatant from the induced cells was separated by

centrifugation at 7,000 rpm for 30 min. The supernatant was filtered through 0.22 μm bottle top filters (Corning, Corning NY) and loaded onto a column packed with 1 ml of Immobilized Protein A agarose (Pierce, Rockford, IL). After loading of 400 ml of supernatants by gravity flow, the columns were washed with 75 ml of 20 mM sodium phosphate buffer (pH 7.0) and with 50 ml of 40 mM sodium citrate (pH 5.0). Wild type Fc and mutant Fc2a fragments were eluted using 0.1M glycine (pH 2.5) and immediately neutralized with 1M Tris (pH 8.0) solution.

A2.2.2 Production and purification of full length aglycosylated trastuzumab and aglycosylated trastuzumab-Fc2a

For pSTJ4-Herceptin-Fc2a-IgG1 or pSTJ4-Herceptin-Fc5-IgG1, Fc5 or Fc2a mutant genes were amplified using the primers (STJ#290 and STJ#291) and the templates, pDsbA-Fc5-FLAG for Fc5 fragments or pDsbA-Fc2a-FLAG for Fc2a fragments, respectively. The amplified PCR fragments were ligated into *Sal*I / *Eco*RV digested pSTJ4-Hercepin IgG1 to make pSTJ4-Herceptin-Fc5-IgG1 or pSTJ4-Herceptin-Fc2a-IgG1. The plasmids for full length wild type trastuzumab and mutant trastuzumab-Fc2a are under the control of *lac* promter in a dicistronic operon with PelB leader peptide fusions to both heavy and light chains.

After transformation of the plasmids into *E. coli* BL21(DE3) (EMD Chemicals, Gibbstown, NJ), cells were grown in LB complex medium overnight and then subcultured overnight twice for adaptation in R/2 medium (Jeong and Lee, 2003). *E. coli* BL21(DE3) harboring pSTJ4-Herceptin-IgG1 or pSTJ4-Herceptin-IgG1-Fc2a were cultured in 500 ml baffled-flask with 120 ml R/2 media at 30 °C for 8 h with 250 rpm

shaking and then inoculated to 3.3L BioFlo 310 fermentor (New Brunswick Scientific Co., Edison, NJ) with 1.2L R/2 medium. Fed-batch fermentations were performed at 30 °C using a pH-stat glucose feeding strategy. The dissolved oxygen (DO) concentration was monitored and maintained at 40% of air saturation using automatic cascade control that increases agitation speed from 100 rpm to 1,000 rpm, air flow rate from 1 to 3 SLPM (Standard liquid per minute) and pure oxygen flow rate from 0 to 1.5 SLPM when needed. The initial pH was adjusted to 6.8 and controlled by the addition of 30% (v/v) ammonium hydroxide when it decreased to less than 6.75 and by the supply of feeding solutions, (700 g/L of glucose and 10 g/L of $MgSO_4$-$7H_2O$; before induction) and (500 g/L glucose, 10 g/L of $MgSO_4$-$7H_2O$, and 100 g/L of yeast extract; after induction), when it increased to more than 6.9. When the OD600 reached 100, the culture temperature was set to 25 °C and 30 min later, protein synthesis was induced with 1 mM of isopropyl-1-thio-β-D-galactopyranoside (IPTG). 7 h after induction at OD600 of ~130-140, the culture broth was harvested.

Cells were harvested by centrifugation at 11,000 × g for 30 min and resuspended in 1.2 L solution containing 100 mM Tris, 10 mM EDTA (pH 7.4) supplemented with 4 mg of lysozyme (per g of dry cell weight) and 1 mM PMSF. Periplasmic proteins were released by the incubation of the suspended solution with shaking at 250 rpm at 30 °C for 16 h. After centrifugation at 14,000 × g for 30 min, polyethyleneimine (MP Biomedical, Solon, OH) was added dropwise to the supernatant until its concentration reaches 0.2 % (w/v). Large amount of nucleic acids complexed with cationic polyethyleneimine polymers were removed by centrifugation at 14,000 × g for 30 min followd by filtration through 0.2 μm filter. The clear filtrate was mixed with Immobilized Protein A agarose

resin pre-equilibrated in 20 mM sodium phosphate buffer (pH 7.0) and incubated at 4 °C for 16 h. After washing with 200 ml of 20 mM sodium phosphate buffer (pH 7.0) and 200 ml of 40 mM sodium citrate (pH 5.0), wild type aglycosylated trastuzumab or trastuzumab-Fc2a were eluted from the Protein A resin using 15 ml of 0.1 M glycine (pH 3.0) and neutralized immediately with 1M Tris (pH 8.0) solution. The eluted samples were concentrated by ultrafiltration through a 10 kDa Mw cutoff membrane and the retentate was further purified using a Superdex 200 gel filtration column developed with PBS (pH 7.4).

A2.2.3 ELISA analysis

96 well polystyrene ELISA plates (Corning, Corning, NY) were coated with 50 µl of 4 µg/ml of aglycosylated trastuzumab, aglycosylated trastuzumab-Fc2a, or clinical grade glycosylated IgG trastuzumab diluted in 0.05 M Na_2CO_3 (pH 9.6) buffer for 16 hr at 4 °C. The plate was blocked with 1 × PBS (pH 7.4), 0.5% BSA for 2 hr at room temperature, washed 4 times with PBS containing 0.05% Tween20, and incubated with serially diluted FcγRIIa-GST fusion proteins (Berntzen et al., 2005) at room temperature for 1 h. After washing 4 times with the same buffer, addition of 1:5,000 diluted anti-GST antibody HRP conjugate (Amersham Pharmacia, Piscataway, NJ), washing 4 times again, the plates were developed using Ultra-TMB substrate (Pierce, Rockford, IL).

A2.2.4. Construction of plasmids for covalently anchored full length IgG display system

Ligation of PCR-amplified and *Sfi*I-digested Fc gene encoding human IgG1-Fc fragment, hinge, CH2 and CH3 region of human IgG1 heavy chain (GeneBank Accession No. AF237583) into pPelBFLAG digested with *Sfi*I generated pPelBFLAG-Fc. pBADNlpAHis-M18 was constructed by ligating *Xba*I / *Hin*dIII digested NlpA-fused M18 scFv gene from pMoPac1-FLAG-M18 into pBAD30-KmR digested with same restriction endonucleases. Subcloning of *Sfi*I digested trastuzumab VL-Ck amplified using the primers (STJ#475 and STJ#476) and the template, pSTJ4-Herceptin IgG1 into *Sfi*I digested pBADNlpAHis-M18 generated pBADNlpA-VL-Ck-His. PelB leader peptide fused trastuzumab VL-Ck was amplified using the primers (STJ#16 and STJ#340) and the template (pSTJ4-Herceptin IgG1), digesteted by *Xba*I / *Hin*dIII endonucleases and ligated into pBAD-NlpA-VL-Ck-His using the same restriction enzyme sites to generate pBADPelB-VL-Ck. pBADPelB-VL-Ck-NlpA-VL-Ck-His was constructed by ligating *Xba*I digested PCR fragments amplified using the primers (STJ#70 and STJ#332) and the template (pBADPelB-VL-Ck) into pBADNlpA-VL-Ck-His digested using the same endonuclease. Trastuzumab heavy chains were amplified using the primers (STJ#474 and STJ#67) and the template pSTJ4-Herceptin IgG1 for pPelB-Herceptin(H)-FLAG, pPelB-Hercepin(H)-Fc5-FLAG, and pPelB-Herceptin(H)-Fc2a-FLAG, respectively. For the expression of correctly assembled, homodimeric wild type Fc and Fc2a in the periplasmic space of *E. coli*, the plasmids pDsbA-Fc-FLAG and pDsbA-Fc2a-FLAG were constructed for the export of Fc via the DsbA signal peptide. The PCR amplified fragments were digested with *Sfi*I, ligated into pPelBFLAG digested

with the same endonuclease to generate pPelB-Herceptin(H)-FLAG, pPelB-Herceptin(H)-Fc5-FLAG and pPelB-Herceptin(H)-Fc2a-FLAG.

A2.2.5 Preparation of spheroplasts and FACS analysis

Two plasmids, pBADPelB-VL-Ck-NlpA-VL-Ck-His and pPelB-Herceptin(H)-FLAG, were co-transformed into *E. coli* Jude-1 (F' [Tn*10(*Tet^r*)* $proAB^+$ $lacI^q$ Δ(*lacZ*)M15] *mcrA* Δ(*mrr-hsdRMS-mcrBC*) ϕ80d*lac*ZΔM15 Δ*lacX74 deoR recA1 araD139* Δ(*ara leu*)7697 *galU galK rpsL endA1 nupG*) (Kawarasaki et al., 2003) for the display of aglycosylated trastuzumab full length IgG1. Co-trasnformation of *E. coli* Jude-1 with pBADPelB-VL-Ck-NlpA-VL-Ck-His and pPelB-Herceptin(H)-Fc5-FLAG were performed for the display aglycosylated trastuzumab-Fc5 full length IgG1. To display display aglycosylated trastuzumab-Fc2a full length IgG1, Jude-1 cells were co-transformed with the plasmids, pBADPelB-VL-Ck-NlpA-VL-Ck-His and pPelB-Herceptin(H)-Fc2a-FLAG. The transformed *E. coli* cells were cultured overnight at 250 rpm at 37 °C in Terrific Broth (Becton Dickinson Diagnostic Systems Difco™, Sparks, MD) with 2% (wt/vol) glucose supplemented with chloramphenicol (50 μg/ml) and kanamycin (50 μg/ml). The overnight cultured cells were diluted 1:100 in fresh 7 ml of TB medium with chloramphenicol (50 μg/ml) and kanamycin (50 μg/ml) in 125 ml Erlenmeyer flasks. After incubation at 37°C for 2 h and cooling at 25°C for 20 min with 250 rpm shaking, protein expression was induced with 1 mM of isopropyl-1-thio-D-galactopyranoside (IPTG) and 0,2 % arabinose.

20 h after IPTG induction, 6 ml of the culture broth was harvested by centrifugation and washed two times in 1 ml of cold 10 mM Tris-HCl (pH 8.0). Cells were resuspended in 1 ml of cold STE solution (0.5 M Sucrose, 10 mM Tris-HCl, 10 mM EDTA, pH 8.0), incubated with rotating mixing at 37°C for 30 min, pelleted by centrifugation at 12,000 x g for 1 min and washed in 1 ml of cold Solution A (0.5 M Sucrose, 20 mM MgCl2, 10 mM MOPS, pH 6.8). The washed cells were incubated in 1 ml Solution A with 1 mg/ml of hen egg lysozyme at 37°C for 15 min. After centrifugation at 12,000 x g for 1 min the resulting spheroplast pellets were resuspended in 1 ml of cold PBS. 300 µl of the spheroplasts were further diluted in 700 µl of PBS was labeled with 30 nM FcγRI-FITC to analyze the binding of FcγRI. For the FACS analysis of FcγRIIa binding, spheroplasts were incubated with 90 nM FcγRIIa C-terminal fused to GST (Berntzen et al., 2005), washed in 1 ml of PBS, and labeled with polyclonal goat anti-GST-FITC (Abcam, Cambridge, MA) diluted 1:200 in 1 ml of PBS. After incubation for 1 h with vigorous shaking at 25°C in dark condition, the mixture was pelleted by centrifugation at centrifuged at 12,000 x g for 1 min and resuspended in 1 ml of PBS. The fluorescently labeled spheroplasts were diluted in 2.5 ml of PBS and analyzed on BD FACSCalibur (BD Bioscience, San Jose, CA).

Table A2-1. Primers used in this study.

Primer Name	Primer nucleotide sequence (5' → 3')
STJ#16	TTGTGAGCGGATAACAATTTC
STJ#67	AATTCGGCCCCCGAGGCCCCTTTACCCGGGGACAGGGAGAGGCTCTTCTGCGTG
STJ#70	CTACCTGACGCTTTTTATCGC
STJ#144	TTTTAGGGGTCGACGACAAAACTCACACATGCCCACCGTG
STJ#145	TTTAAGGGAAGCTTCTATTAGGCGCGCCCTTTGTCATCG
STJ#147	GGCAAATTCTGTTTTATCAGACCGCTTCTG
STJ#220	CAATTTTGTCAGCCGCCTGAGCAGAAG
STJ#290	TTTTAGGGGTCGACAAGAAAGTTGAGCCCAAATCTTGTGACAAAACTCACACATGCCCACCG
STJ#291	GGCCACCGGATATCTTATTATTTACCCGGGGACAGGGAGAGG
STJ#332	GGGAATTCTAGACTATTAGCACTCTCCCCTGTTGAAGCTCTTTG
STJ#340	TTTAAGGGAAGCTTCTATTAGCACTCTCCCCTGTTGAAGCTCTTTG
STJ#422	CTAGGGAGCCGCGGGAGGAGCAGTACAACGGCGCGTACCGTGTGGTCAGCGTCCTC
STJ#474	CGCAGCGAGGCCCAGCCGGCCATGGCGGAGGTTCAATTAGTGGAATCTG
STJ#475	CGCAGCGAGGCCCAGCCGGCCATGGCGGATATTCAAATGACCCAAAGCCCG
STJ#476	CGCAATTCGGCCCCCGAGGCCCCGCACTCTCCCCTGTTGAAGCTCTTTG

Table A2-2. Plasmids used in this study.

Plasmids	Relevant characteristics	Reference or source
pMoPac1	Cm^r, *lac* promoter, *tetA* gene, C-terminal polyhistidine tag and c-myc tag	(Hayhurst et al., 2003)
pMoPac12	Ap^r, *lac* promoter, *tetA* gene, *skp* gene, C-terminal polyhistidine tag and c-myc tag	(Hayhurst et al., 2003)
pMoPac1-FLAG-M18	NlpA fused *M18 scFv gene*, C-terminal FLAG tag in pMoPac1	(Jung et al., 2007)
pPelBFLAG-M18	Cm^r, *lac* promoter, *tetA* gene, *skp* gene, C-terminal FLAG tag	This study
pPelBFLAG-Fc	*IgG1-Fc* gene in pPelBFLAG	This study
pPelBFLAG-Fc5	*IgG1-Fc5* gene in pPelBFLAG	This study
pPelBFLAG-Fc2a	*IgG1-Fc2a* gene in pPelBFLAG	This study
pMAZ360-M18.1-Hum-IgG	*M18.1 humanized IgG1* gene in pMAZ360	(Mazor et al., 2007)
pSTJ4-Herceptin IgG1	*Trastuzumab IgG1* gene in pMAZ360-M18.1-Hum-IgG1	This study
pSTJ4-Herceptin IgG1-Fc5	*Trastuzumab IgG1-Fc5* gene in pMAZ360-M18.1-Hum-IgG1	This study
pSTJ4-Herceptin IgG1-Fc2a	*Trastuzumab IgG1-Fc2a* gene in pMAZ360-M18.1-Hum-IgG1	This study
pPelB-Herceptin(H)- FLAG	*IgG1* heavy chain gene in pPelBFLAG	This study
pPelB-Herceptin(H)-Fc5-FLAG	*IgG1-Fc5* heavy chain gene in pPelBFLAG	This study
pPelB-Herceptin(H)-Fc2a-FLAG	*IgG1-Fc2a* heavy chain gene in pPelBFLAG	This study
pDsbA	*DsbA* signal sequence gene in pTrc99A	This study
pDsbA-Fc-FLAG	*DsbA fused IgG1-Fc* gene, C-terminal FLAG tag in pTrc99A	This study
pDsbA-Fc5-FLAG	*DsbA fused IgG1-Fc5* gene, C-terminal FLAG tag in pTrc99A	This study
pDsbA-Fc2a-FLAG	*DsbA fused IgG1-Fc2a* gene, C-terminal FLAG tag in pTrc99A	This study
pBAD30	Apr, BAD promoter	(Guzman et al., 1995)
pBAD30-KmR	Km^r, BAD promoter	(Jung et al., 2007)
pBADNlpAHis-M18	NlpA fused *M18 scFv*, C-terminal polyhistidine tag in pBAD30	This study
pBAD-PelB-VL-Ck-His	PelB fused trastuzumab VL-Ck domain, C-terminal polyhistidine tag and c-myc tag in pBAD30-KmR	This study
pBAD-PelB-VL-Ck-NlpA-VL-Ck-His	PelB fused trastuzumab VL-Ck domain and NlpA fused trastuzumab VL-Ck-His in pBAD30-KmR	This study

A2.3 RESULTS

A2.3.1 Binding of Fc2a (S298G/T299A) and trastuzumab-Fc2a to human FcγRIIa

DsbA leader peptide fused wild type Fc and Fc2a fragments were purified using Protein A affinity chromatography. Most of the purified wild type Fc and Fc2a were dimeric forms. (Fig. A2-1). For preparative production of aglycosylated trastuzumab and trastuzumab-Fc2a in *E. coli*, dicistronic plasmids, pSTJ4-Herceptin-IgG1 and pSTJ4-Herceptin-Fc2a-IgG1, were constructed. Using the Fed-batch fermentation with pH-stat glucose feeding strategy, full length aglycsoylated wild type trastuzumab or trastuzumab-Fc2a antibodies were produced. The trastumab antibodies produced in *E. coli* periplasmic space were released with incubation in the solution containing lysozyme and EDTA, and purified using Protein A affinity chromatography followed by size exclusion chromatography. The binding affinity of purified homodimeric mutant Fc fragments (Fc2a) or aglycosylated trastuzumab-Fc2a to extracellular domain of FcγRIIa was analyzed by ELISA. As expected, the aglycosylated Fc mutant full length tratuzumab (S298G/T299A) exhibited similar high binding affinity to FcγRIIa with glycosylated full length trastuzumab. In contrast, purified homodimeric Fc fragments engineered for FcγRIIa (S298G/T299A) did not show binding affinity to extracellular domain of FcγRIIa (Fig. A2-2) suggesting the structural and functional roles of Fab arms for the binding of the FcγRIIa receptor proteins.

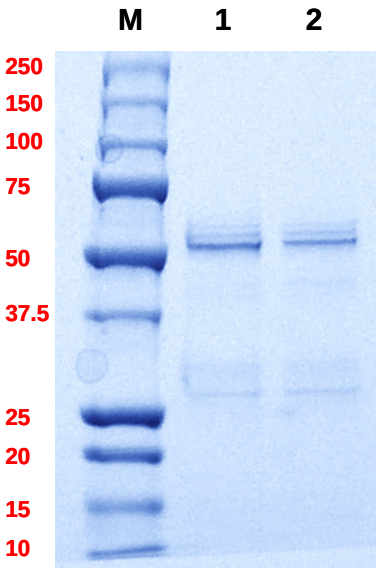

Figure A2-1. Purified wild type Fc and Fc2a proteins. Lane M: M.W. standards; Lane 1: Wild type Fc; Lane 2; Fc2a (S298G/T299A).

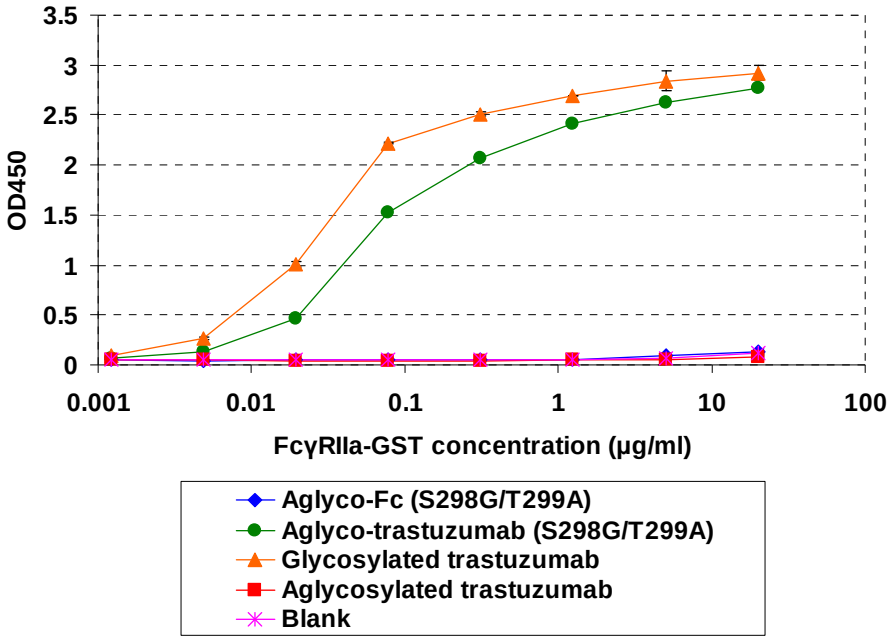

Figure A2-2. ELISA assays showing the affinity of aglycosylated Fc fragment (Fc2a) and aglycosylated full length trastuzumab-Fc2a to FcγRIIa.

A2.3.2 FACS analysis for the covalently anchored full length IgG display system to engineer IgG heavy chain

To use bacterial full length IgG display system for library screening, four factors should be considered. Firstly, IgG heavy chains and light chains must be well expressed. Secondly, the heavy and light chains should be assembled well in *E. coli*. Thirdly, binding ligands should be accessible to the full length IgG in bacterial cells. Finally, the anchoring of the displayed full length IgG should be robust during library screening. Two plasmids co-expression system was used for stable and covalent anchoring of full length IgG (Fig. A2-3).

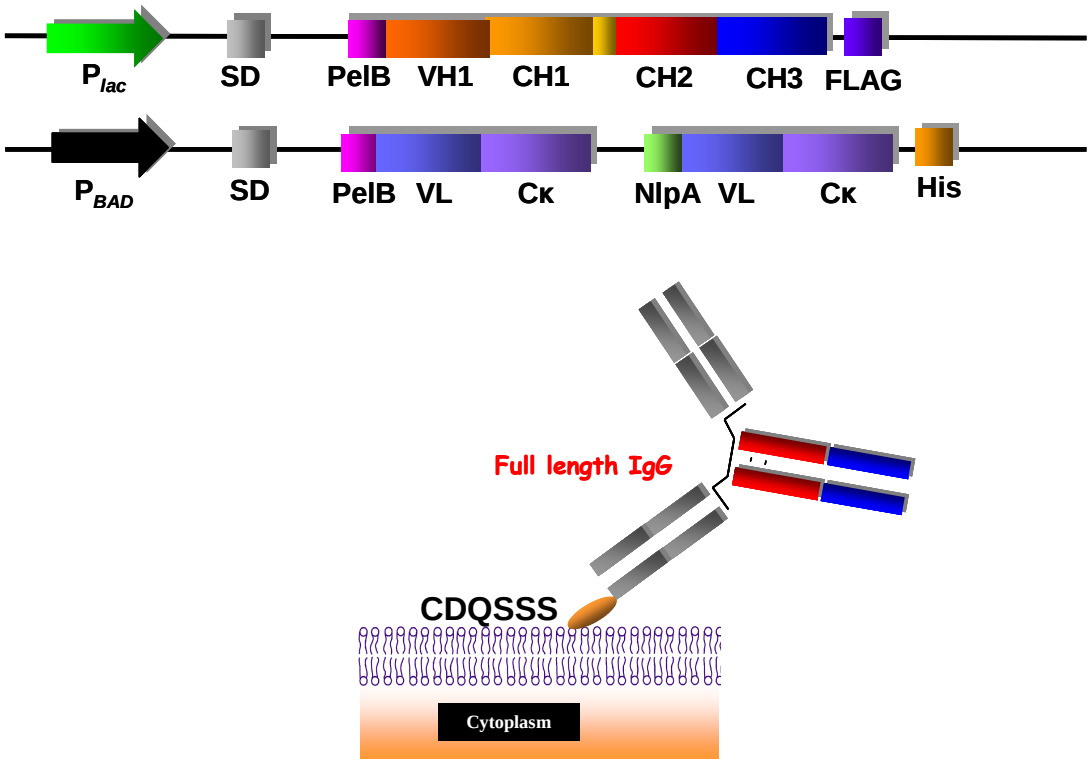

Figure A2-3. Covalently anchored full length IgG display system.

The pBADPelB-VL-Ck-NlpA-VL-Ck-His plasmid enables the expression of the NlpA leader peptide fused IgG light chain (VL-Ck) and the PelB leader peptide fused IgG light chain (VL-Ck). Thus a portion of the light chain becomes anchored on the periplasmic side of the inner membrane where it associates with heavy chain to produce tetrameric full length, IgG. pPelB-Herceptin(H)-FLAG is a high copy number plasmid encoding the IgG heavy chain under the control of the *lac* promoter.

For affinity maturation using FACS sorting method based on gating selective fluorescence and scattering regions, it is required to get distinguishable high or low fluorescence signal comparing a negative control with low coefficient of variation (CV = [Standard Deviation/Mean Value] × 100). For full length trastuzumab antibodies, the fluorescense profile of spheroplasts expressing inner membrane anchored IgG (via the NlpA-VL-Ck polypeptide) and spheroplasts expressing soluble IgG from a dicistronic vector system (Mazor et al., 2007) were compared. The 2 plasmids anchored full length IgG display system clearly exhibited dramatically improved signal intensity and CV value upon labeling with FcγRI-FITC. The fluorescence signal for the anchored full length IgG display system was tested with cells cultured at 12 °C or 25 °C in TB. Spheroplasts generated from trastuzumab-Fc5 displaying cells using the 2 plasmids covalently anchored full length IgG display system cultured at 25 °C exhibited much higher fluorescence and improved CV upon labeling with FcγRI-FITC relative to spheroplasts expressing a wild type trastuzumab (Fig A2-4). Also, in the FACS analysis to measure the affinity of spheroplasts for FcγRIIa-GST (Fig. A2-5), 2 plasmids covalently anchored full length IgG display system cultured at 25 °C in TB showed

surprisingly improved signal intensity and CV providing a selective display system for real affinity maturation of full length IgG (Fig. A2-6 and Fig. A2-7).

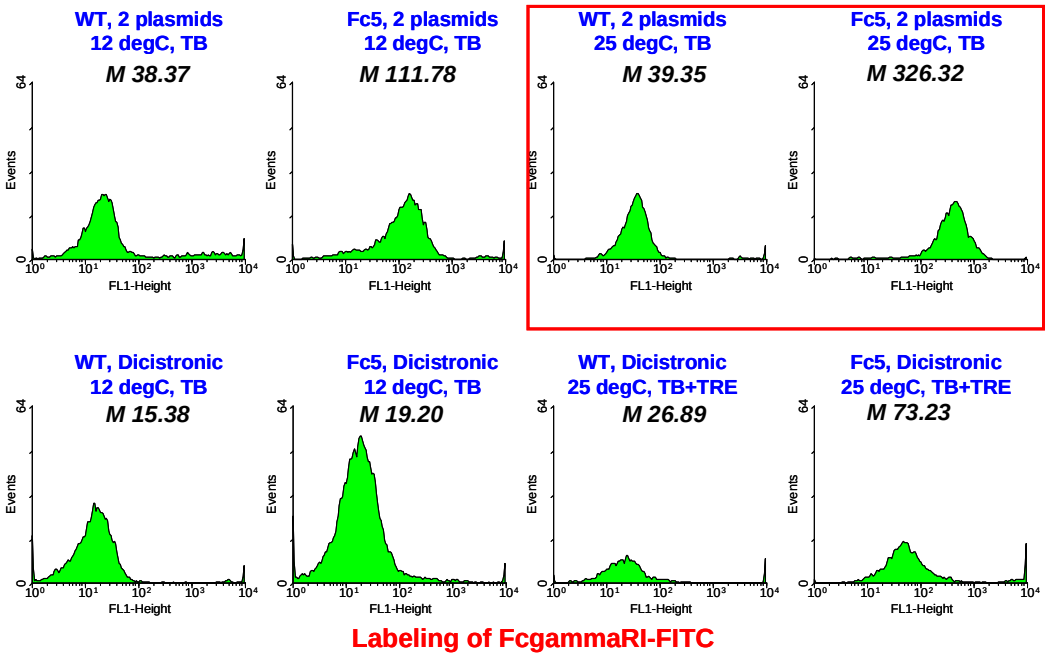

Figure A2-4. Fluorescence histograms showing the binding of FcγRI using either the 2-plasmid system or the dicistronic system. Trastuzumab full length IgG was expressed using either the 2 plasmid anchored full length IgG display system or the dicistronic full length IgG display system. Spheroplasts were incubated with 30 nM FcγRI-FITC probe for detection. M: Mean fluorescence intensity.

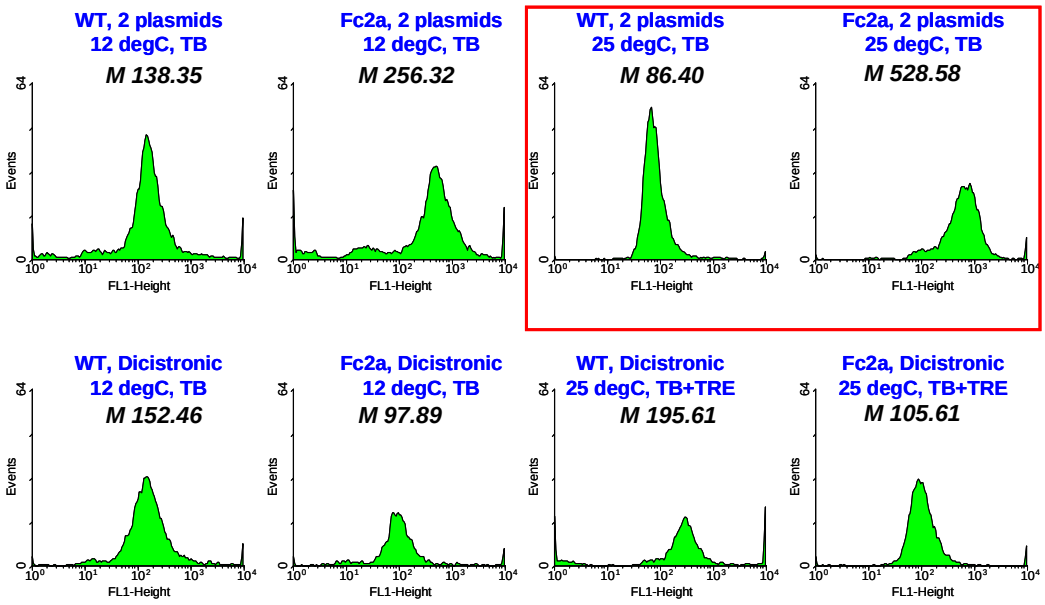

Figure A2-5. Fluorescence histograms showing the binding of FcγRIIa using either the 2-plasmid system or the dicistronic system. Trastuzumab full length IgG was expressed using either the 2 plasmid anchored full length IgG display system or dicistronic full length IgG display system. Spheroplasts were incubated with 30 nM FcγRIIa-GST and labeled with polyclonal anti-GST-FITC (1:200) probe for detection. M: Mean fluorescence intensity.

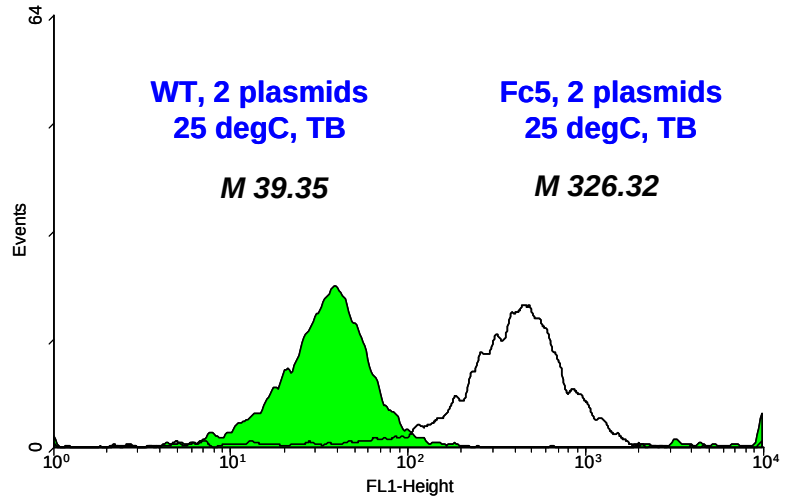

Figure A2-6. FACS analysis of cells displaying covalently anchored full length IgG expressed by 2 plasmids and bound by FcγRI. Spheroplasts expressing trastuzumab full length IgGs were incubated with 30 nM FcγRI-FITC probe for detection. M: Mean fluorescence intensity.

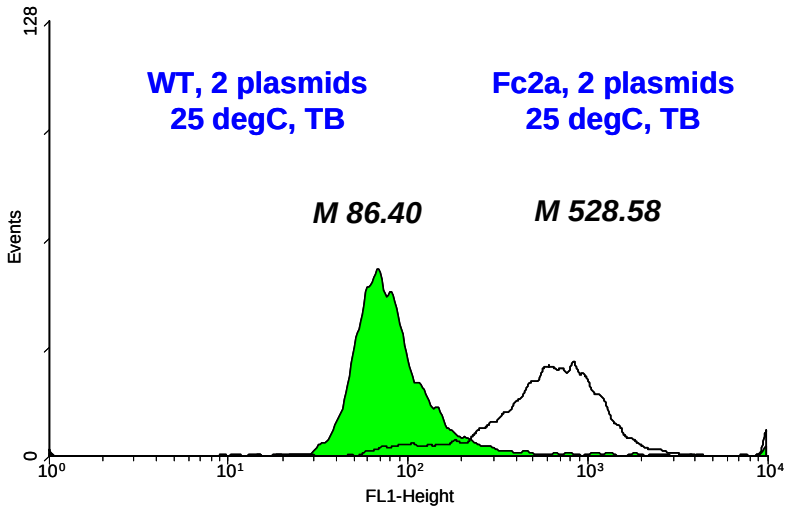

Figure A2-7. FACS analysis of cells displaying covalently anchored full length IgG expressed by 2 plasmids and bound by FcγRIIa. Spheroplasts expressing trastuzumab full length IgGs were incubated with incubated with 30 nM FcγRIIa-GST and labeled with polyclonal anti-GST-FITC (1:200) probe for detection. M: Mean fluorescence intensity.

A2.4 DISCUSSION

Spheroplasts displaying homodimeric Fc fragments were unable to bind to FcγRIIa and therefore not sutible for library screening purposes. While antibodies engineered to bind to FcRIIa in the absence glycosylation behaved as reported, the respective Fc domains did not display any binding. Consequently it was determined that a system for the display of full length IgG needs to be developed in order to isolate mutants that bind the low affinity receptors with biologically relevant affinities. For the display of full length IgG, a 2-plasmid system was employed. In the low copy number dicistonic expression system, antibody light chains (VL-Ck) were expressed with PelB leader peptide for soluble expression and NlpA leader petide for inner membrane anchoring by the lipidation of cystein followed by the NlpA signal sequence. Antibody heavy chains were fused to N-terminal PelB leader peptide and were expressed from the high copy number plasmids pMopac12 also containing the gene for the Skp chaperone which can assist the folding of many antibodies. Tetrameric full length IgG is formed by the covalent disulfide bonds between two heavy chains and between heavy chain and light chain in oxidized *E. coli* periplasmic space. Under optimized culture conditions, spheroplasts displaying aglycosylated full length trastuzumab-Fc5 (which binds to FcγRI) or trastuzumab-Fc2a (which binds to FcγRIIa) generated excellent FACS signal relative to spheroplasts displaying wild type trastuzumab upon labeling with FcγRI-FITC or FcγRIIa-GST followed by GST specific fluorescent secondary antibodies.

It has been known that FcγRs bind to lower hinge region and upper CH2 region (Jefferis et al., 1998). Thus, homodimeric Fc fragments should be capable of binding to FcγRs. However, we found that, in the case of aglycosylated antibodies, the presence of

the antigen binding fragments (Fab) also contributes significantly to binding to FcγRs. One possibility is that the Fab arms might affect the flexibility of Fc hinge region or the conformation of hinge-CH2 region leading to a change the affinity towards FcγRs.

The *E. coli* anchored full-length IgG display system described in this Appendix allows the interaction between full length IgG and IgG binding ligands including FcγRs. This system could be exploited for the screening of aglycosylated full length IgG exhibiting altered binding affinity to Fc receptors (FcγRI, FcγRIIa, FcγRIIb, FcγRIIIa, and FcRn) with novel or improved effector functions.

Appendix 3

E. coli 2 Hybrid Systems for Engineering of Aglycosylated Antibody Fc

A3.1 INTRODUCTION

To identify mutations that allow aglycosylated Fc to bind to the extracellular domain of Fcγ receptors, C1q, or FcRn, it was necessary to develop an *E. coli* display system suitable for the screening of Fc combinatorial libraries. For the bacterial display of dimeric antibody Fc domains three factors should be considered: Firstly, the Fc domain of antibody should be encoded by single gene to prevent the formation of heterodimers. Secondly, the Fc proteins should be expressed in a cellular compartment that enables correct folding and assembly. In *E. coli* the periplasmic space provides an oxidative environment for the formation of disulfide bonds and is suitable for the production of correctly folded and dimerized heterologous protein (Georgiou and Segatori, 2005). Finally, for the efficient isolation of cells displaying high affinity variants, the Fc proteins should stably be anchored to the cells. Proteins that are weakly bound onto spheroplasts are not suitable for screening purposes because they can contaminate other cells displaying different varainrs and reduce the efficiency of enrichment of positive clones. Here we attempted to develop a 2 hybrid display system for aglycosylated homodimeric Fc domains.

A3.2. MATERIALS AND METHODS

A3.2.1 Reagents

Oligonucleotides primers and restriction endonucleases were obtained from Integrated DNA Technologies (Coralville, IA) and New England Biolabs (Ipswich, MA), respectively. *Taq* Polymerase and FITC protein labeling kit were from Invitrogen (Carlsbad, CA). Recombinant human FcγRI/CD64 was purchased from R&D Systems (Minneapolis, MN). Trehalose was obtained from Fisher Scientific (Fair Lawn, NJ). Human IgG-Fc and Rabbit anti-ECS antibody peroxidase conjugated were from Bethyl Laboratories (Montgomery, TX). Digoxigenin-BODIPY (Digoxigenin-4,4-difluoro-5,7-dimethyl-4-bora-3a,4a-diaza-s-indacene-3-propionyl ethtylenediamine) was synthesized as described previously (1). PA-FITC was obtained from List Biological Laboratories (Campbell, CA). Protein A-FITC and analytical grades of all other chemical reagents were purchased from Sigma-Aldrich (St. Louis, MO) unless stated otherwise.

A3.2.2 Construction of plasmids for the display of homodimeric IgG-Fc

All plasmids and primers used in this study are described in Table A3-1 and TableA3-2. Plasmid pPelBHis was generated by ligating *Bam*HI-*Hin*dIII digested *skp* gene from pMopac12 into pMopac1 digested with the same restriction endonucleases. pPelBFLAG was derived from pPelBHis in which polyhistidine tag and c-myc tag were replaced by FLAG tag (DYKDDDDK). Subcloning of PCR amplified and *Sfi*I digested Fc gene encoding human IgG1-Fc fragment, hinge, CH2 and CH3 region of human IgG1 heavy chain (GeneBank Accession No. AF237583) into *Sfi*I digested pPelBHis and

pPelBFLAG generated pPelBHis-Fc and pPelBFLAG-Fc, respectively. pPelBHis-beta 2 microglobulin was constructed by subcloning soluble mature human beta 2 microglobulin gene synthesized from overlap PCR amplification using 10 primers including 2 external primers (STJ#78 and STJ#84) and 8 internal primers (STJ#86-93) into pPelBHis using *Sfi*I restriction endonuclease site. pPelBHis-FcγRIIa was generated by introducing *Sfi*I digested soluble mature human FcγRIIa gene (GeneBank Accession No. P12318) (2) amplified from pDNR-LIB-FcrRIIa (ATCC: MGC-23887) using primers STJ#74 and STJ#80 into pPelBHis. SfiI digested genes from pMoPac1-FLAG-M18 and pMoPac1-FLAG-2610 for M18 scFv (3) and 26-10 scFv (4) specific for the PA antigen of *Bacillus anthracis* and cardiac glycoside digoxin, respectively, were introduced to pPelBFLAG to generate pPelBFLAG-M18 scFv and pPelB-2610 scFv.

pNlpAFLAG-M18 was constructed by ligating *Xba*I–*Hin*dIII digested fragments for NlpA and 6 amino acid residues (CDQSSS) fused M18 scFv gene from pMopac1-FLAG-M18 into pPelBFLAG-M18. pNlpAHis-Fc was generated by subcloning *Sfi*I digested Fc gene into pNlpAFLAG-M18 and by replacing FLAG with polyhistidine tag and c-myc tag. pBADNlpAFLAG-M18 and pBADNlpAHis-Fc were generated by ligating *Xba*I–*Hin*dIII digested M18 scFv gene and Fc gene from pNlpAFLAG-M18 and pNlpAHis-Fc, respectively, into pBAD30 digested with same restriction endonucleases.

To display Fc domain using the leucine zipper pair of cJun-cFos, *Not*I–*Sal*I digested cFos fragments amplified using two primers (STJ#68 and STJ#69) and the cFos(Cys) fragments encoding additional three amino acids including internal two Gly residues and external Cys residue at both ends of C-terminus and N-terminus amplified using two primers (STJ#96 and STJ#97) were cloned into pPelBHis-Fc to make

pPelBHis-Fc-cFos for non-covalent bonding of cJun-cFos interaction pair and pPelBHis-Fc-cFos(Cys) for covalent disulfide bonding of both N terminal and C terminal ends of cJun-cFos pair in *E. coli* periplasmic space. For anchoring periplasmic expressed Fc domain fused to cFos or cFos(Cys), pBADNlpAFLAG-cJun and pBADNlpAFLAG-cJun(Cys) were generated by subcloning *Sfi*I digested cJun fragments amplified with primers (STJ#58 and STJ#59) and cJun(Cys) fragments amplified with primers (STJ#94 and STJ#95) into *Sfi*I digested pBADNlpAFLAG-M18.

For the display of Fc using tight ColE2–Im2 interaction, Im2 gene that is PCR amplified using two primers (ST#116 and STJ#117) and template *E. coli* WTZ1011 ColE2 harboring plasmid ColE2-P9 (The Coli Genetic Stock Center, Yale Univ. CGSC No. 8203) (5) was *Not*I-*Sal*I digested and ligated into pPelBFLAG-Fc, pPelBFLAG-M18, and pPelBFLAG-2610 to generate pPelBFLAG-Fc-Im2, pPelBFLAG-M18-Im2, and pPelbFLAG-2610-Im2. To construct plasmids encoding NlpA-fused ColE2 mutants binding to Im2 with strong protein protein interaction, the catalytic domains of three ColE2 mutants were amplified by overlap PCR with the template plasmid used for Im2 gene amplification and with four primers including two common external primers (STJ#114 and STJ#115) and two internal reverse primers (STJ#120 and STJ#121) for ColE2(H574A), internal primers (STJ#118 and STJ#119) for ColE2(H578A), and internal primers (STJ#122 and STJ#123) for ColE2(H574A/H578A), respectively. The amplified PCR products were SfiI digested and introduced into pBADNlpAHis to generate pBADNlpAHis-ColE2(H574A), pBADNlpAHis-ColE2(H578A), and pBADNlpAHis-ColE2(H574A/H578A).

Subcloning of *Sfi*I digested M18.1 hum scFv (1) and 26-10 scFv gene into pMopac12 generated pMopac12-M18.1 hum scFv and pMopac12-2610 scFv. Also, subcloning of the *Sfi*I digested M18.1 hum scFv and 26-10 scFv into pMopac16 generated pMopac16-M18 scAb and pMopac16-2610 scAb. For pTrcdsabAHis-Fc and pTrcdsbAHis-FcγRIIa, Fc and FcγRIIa gene fragments were PCR amplified using primers (STJ#144 and STJ#139) with the templates pPelBHis-Fc for Fc gene and primers (STJ# 136 and STJ#139) with the template pPelB-FcγRIIa for FcγRIIa gene, respectively, *Sal*I-*Hin*dIII digested, and ligated into dsbA signal sequence (6) inserted into pTrc99A. All plasmids were transformed into *E. coli* Jude-1(F' [Tn*10(*Tet^{r}*)* proAB^{+} *lacI*^{q} Δ(*lacZ*)M15] *mcrA* Δ(*mrr-hsdRMS-mcrBC*) ϕ80d*lac*ZΔM15 Δ*lacX74 deoR recA1 araD139* Δ(*ara leu*)7697 *galU galK rpsL endA1 nupG*) (Kawarasaki et al., 2003).

A2.2.3 Culture conditions for two plasmids system

For the periplasmic display using leucine zippers, cJun-cFos, pPelBHis-Fc-cFos and pPelBHis-Fc-cFos(Cys) were co-transformed with pBADNlpAFLAG-cJun or pBADNlpAFLAG-cJun(Cys) into *E. coli* Jude-1. To display Fc using the interaction of ColE2-Im2, plasmids pPelBFLAG-Fc-Im2, pPelB-M18 scFv-Im2, or pPelBFLAG-2610 scFv-Im2 were co-transformed with either pBADNlpAHis-ColE2(H574A), pBADNlpAHis-ColE2(H578A), or pBADNlpAHis-ColE2(H574/578) respectively containing single or double mutations at C-terminal ColE2 DNase catalytic domain. The transformants harboring two plasmids were grown overnight at 37°C with 250 rpm shaking in Terrific Broth (TB) (Becton Dickinson Diagnostic Systems DIFCO™, Sparks, MD) supplemented with 2% (wt/vol) glucose, chloramphenicol (40 μg/ml) and ampicillin

(50 μg/ml). After overnight culture, the cells were diluted 1:100 in fresh TB medium without glucose, incubated at 37 °C for 2 h and then cooled at 25°C for 20 min. Firstly, PelB signal sequence fused proteins were induced with 1 mM of isopropyl-1-thio-β-D-galactopyranoside (IPTG) to allow time for correct folding in periplasmic space prior to binding to inner membrane anchored ColE2 mutants. And 2 h after IPTG induction, 0.2% (wt/vol) arabinose was added to induce expression of inner membrane anchored cJun, cJun(Cys), ColE2(H574A), ColE2(H578A), or ColE2(H574A/H578A).

Table A3-1. Plasmids used in this study.

Plasmids	Relevant characteristics	Reference or source
pMoPac1	Cm^r, *lac* promoter, *tetA* gene, C-terminal polyhistidine tag and c-myc tag	(Hayhurst et al., 2003)
pMoPac12	Ap^r, *lac* promoter, *tetA* gene, *skp* gene, C-terminal polyhistidine tag and c-myc tag	(Hayhurst et al., 2003)
pMoPac16	Ap^r, *lac* promoter, *tetA* gene, *HuCκ* gene, *skp* gene, C-terminal polyhistidine tag and c-myc tag	(Hayhurst et al., 2003)
pMoPac1-FLAG-M18	NlpA fused *M18 scFv gene*, C-terminal FLAG tag in pMoPac1	(Jung et al., 2007)
pMoPac1-FLAG-2610	NlpA fused *26-10 scFv* gene, C-terminal FLAG in pMoPac1	(Jung et al., 2007)
pPelBHis	Cm^r, *lac* promoter, *tetA* gene, *skp* gene, C-terminal polyhistidine tag and c-myc tag	This study
pPelBHis-Fc	*IgG1-Fc* gene in pPelBHis	This study
pPelBHis-beta 2 microglobulin	*Human beta 2 microglobulin* gene in pPelBHis	This study
pPelBHis-FcγRIIa	*FcγRIIa* gene in pPelBHis	This study
pPelBHis-Fc-cFos	*IgG1-Fc* gene fused to C-terminal *cFos* gene in pPelBHis	This study
pPelBHis-Fc-cFos(Cys)	*IgG1-Fc* gene fused to C-terminal *cFos(Cys)* gene in pPelBHis	This study
pPelBFLAG	Cm^r, *lac* promoter, *tetA* gene, *skp* gene, C-terminal FLAG tag	This study
pPelBFLAG-Fc	*IgG1-Fc* gene in pPelBFLAG	This study
pPelBFLAG-M18 scFv	*M18 scFv* gene in pPelBFLAG	This study
pPelBFLAG-2610 scFv	*26-10 scFv* gene in pPelBFLAG	This study
pPelBFLAG-Fc-Im2	*IgG1-Fc* gene fused to C-terminal *Im2* gene in pPelBFLAG	This study
pPelBFLAG-M18 scFv-Im2	*M18 scFv* gene fused to C-terminal *Im2* gene in pPelBFLAG	This study
pPelBFLAG-2610 scFv-Im2	*26-10 scFv* gene fused to C-terminal *Im2* gene in pPelBFLAG	This study
pMopac12-M18.1 hum scFv	*M18.1 humanized scFv* gene in pMoPac12	This study
pMopac12-2610 scFv	*26-10 scFv* gene in pMoPac12	This study
pMopac16-M18.1 hum scab	*M18.1 humanized scAb* gene in pMoPac16	This study
pMopac16-2610 scAb	*26-10 scAb* gene in pMoPac16	This study
pMAZ360-M18.1-Hum-IgG	*M18.1 humanized IgG1* gene in pMAZ360	(Mazor et al., 2007)
pMAZ360-26.10 IgG	*26-10 IgG1* gene in pMAZ360	(Mazor et al., 2007)
pNlpAFLAG-M18	NlpA fused *M18 scFv* gene in pPelBFLAG	This study
pNlpAHis-Fc	NlpA fused *IgG-Fc* gene in pPelBHis	This study
pBAD30	Ap^r, BAD promoter	(Guzman et al., 1995)
pBADNlpAFLAG-M18	NlpA fused *M18 scFv* gene, C-terminal FLAG tag in pBAD30	This study
pBADNlpAFLAG-cJun	NlpA fused *cJun* gene, C-terminal FLAG tag in pBAD30	This study
pBADNlpAFLAG-cJun(Cys)	NlpA fused *cJun(Cys)* gene, C-terminal FLAG in pBAD30	This study
pBADNlpAHis-Fc	NlpA fused *IgG-Fc* gene, C-terminal polyhistidine tag in pBAD30	This study
pBADNlpAHis-ColE2(H574A)	NlpA fused *ColE2(H574A)* gene, C-terminal polyhistidine tag in pBAD30	This study
pBADNlpAHis-ColE2(H578A)	NlpA fused *ColE2(H578A)* gene, C-terminal polyhistidine tag in pBAD30	This study
pBADNlpAHis-ColE2(H574A/H578A)	NlpA fused *ColE2(H574A/H578A)* gene, C-terminal polyhistidine tag in pBAD30	This study
pTrc99A	Ap^r, trc promoter, $lacI^q$	Amersham Biosci., (Piscataway, NJ)
pTrcdsbAHis-Fc	dsbA fused *IgG-Fc* gene, C-terminal FLAG tag in pTrc99A	This study
pTrcdsbAHis-FcγRIIa	dsbA fused *FcγRIIa* gene, C-terminal polyhistidine tag in pTrc99A	This study

Table A3-2. Primers used in this study. (Underlining indicates the restriction enzyme sites)

Primer Name	Primer nucleotide sequence (5' → 3')
STJ#16	TTGTGAGCGGATAACAATTTC
STJ#58	CGAACTGGCCCAGCCGGCCATCGCCCGGCTAGAGGAAAAAG
STJ#59	CGAACTGGCCCCCGAGGCCCGGTGGTTCATGACTTTCTGTTTAAG
STJ#68	GATATCGCGGCCGCACTGACCGACACCCTGCAGG
STJ#69	TTTTAGGGGTCGACTGCGGCGTGTGCCGCCAGGATGAAC
STJ#74	CGCAGCGAGGCCCAGCCGGCCATGGCGCAAGCTGCTCCCCCAAAGGC
STJ#78	CGCAGCGAGGCCCAGCCGGCCATGGCGATCCAGCGTACTCCAAAGATTC
STJ#80	CGCAATTCGGCCCCCGAGGCCCCAATGACCCCCATTGGTGAAGAG
STJ#84	CGCAATTCGGCCCCCGAGGCCCCCATGTCTCGATCCCACTTAAC
STJ#86	CAGCGTACTCCAAAGATTCAGGTTTACTCACGTCATCCAGCAGAGAATGGAAAG
STJ#87	CAGCAGAGAATGGAAAGTCAAATTTCCTGAATTGCTATGTGTCTGGGTTTCATC
STJ#88	CTATGTGTCTGGGTTTCATCCATCCGACATTGAAGTTGACTTACTGAAGAATGG
STJ#89	GTTGACTTACTGAAGAATGGAGAGAGAATTGAAAAAGTGGAGCATTCAGACTTG
STJ#90	GTACAAGAGATAGAAAGACCAGTCCTTGCTGAAAGACAAGTCTGAATGCTCCAC
STJ#91	ACTCATCTTTTTCAGTGGGGGTGAATTCAGTGTAGTACAAGAGATAGAAAGACC
STJ#92	CTGTGACAAAGTCACATGGTTCACACGGCAGGCATACTCATCTTTTTCAGTGGG
STJ#93	CATGTCTCGATCCCACTTAACTATCTTGGGCTGTGACAAAGTCACATGG
STJ#94	CGAACTGGCCCAGCCGGCCATGGCGTGCGGCGGCATCGCCCGGCTAGAGGAAAA
STJ#95	CGAACTGGCCCCCGAGGCCCGGCAGCCGCCGTGGTTCATGACTTTCTGTTTAAG
STJ#96	GATATCGCGGCCGCATGCGGCGGCCTGACCGACACCCTGCAGG
STJ#97	TTTTAGGGGTCGACTGCGGCGCAGCGCCGTGTGCCGCCAGGATGAAC
STJ#114	GACGAACTGGCCCAGCCGGCCATGGCGGAGAGTAAACGGAATAAGCCAGGGAAG
STJ#115	GCGAACTGGCCCCCGAGGCCCCCTTACCCCGATGAATATCAATATGTCGCTTAG
STJ#116	CGAGATATCGCGGCCGCAATGGAACTGAAACATAGTATTAGTGATTATACCGAG
STJ#117	GTTTTAGGGGTCGACTGCGGCGCCCTGTTTAAATCCTGACTTACCGTTAGC
STJ#118	CTTACCCCGATGAATATCAATCGCTCGCTTAGGTGTGGTCACTCTGATATTATT
STJ#119	GCGAACTGGCCCCCGAGGCCCCCTTACCCCGATGAATATCAATCGCTCGCTTAG
STJ#120	CTTACCCCGCGCAATATCAATATGTCGCTTAGGTGTGGTCACTC
STJ#121	GCGAACTGGCCCCCGAGGCCCCCTTACCCCGCGCAATATCAATATGTCGCTTAG
STJ#122	CTTACCCCGCGCAATATCAATCGCTCGCTTAGGTGTGGTCACTCTGATATTATT
STJ#123	GCGAACTGGCCCCCGAGGCCCCCTTACCCCGCGCAATATCAATCGCTCGCTTAG
STJ#136	TTTTAGGGGTCGACCAAGCTGCTCCCCCAAAGGCTG
STJ#139	TTTAAGGGAAGCTTCTATCAATGGTGGTGGTGGTGGTGATG
STJ#144	TTTTAGGGGTCGACGACAAAACTCACACATGCCCACCGTG
STJ#194	CTAGGGAGCCGCGGGAGGAGCAGTACAACNNSNNSNNSNNSNNSNNSNNSNNSNNS AGCACGTACCGTGTGGTCAGCG
STJ#195	CTAGAGGAATTCGGCCCCCGAGGCCCCTTTAC
STJ#196	CGCAGCGAGGCCCAGCCGGCCATGGCG
STJ#197	CGCAATTCGAATTCGGCCCCCGAGGCCCC
STJ#220	CAATTTTGTCAGCCGCCTGAGCAGAAG

A3.3 RESULTS

Initially, display of Fc was attempted using the leucine zipper interaction between cJun and cFos interaction for tethering onto the inner membrane. The repetitive leucine residues at every seven amino acid of cJun and cFos allow for a strong non-covalent interaction between the two proteins (Kouzarides and Ziff, 1988; Landschulz et al., 1988). Expression of cFos-fused Fc from pPelBHis-Fc-cFos was induced first and followed by induction of protein synthesis from the pBADNlpAFLAG-cJun encoding a fusion between the cJun domain and the NlpA leader sequence and six amino acid residues (CDQSSS) (Fig. A3-1). In separate studies, to ensure covalent attachment between cJun and cFos three amino acid residues including one external Cys and two internal Gly were introduced to the N and C terminal ends of both cJun and cFos. The resulting cJun(Cys)–cFos(Cys) allows the formation of a disulfide bond between the two leucine zippers in the periplasmic space (de Kruif and Logtenberg, 1996). With the APEx displayed pNlpAHis-Fc as a positive control and the pNlpAFLAG-cJun(Cys) not anchoring Fc domains as a negative control, the two Fc display systems were analyzed by flow cytometry after spheroplasting and incubation with Protein A-FITC (Fig. A3-2A). As expected, the periplasmic Fc display system employing engineered cJun(Cys)–cFos(Cys) showed higher fluorescence signal compared with native cJun–cFos suggesting improved anchoring of the Fc domain to inner membrane. However, when the system was compared with other negative controls that express only periplasmic Fc domains without co-expression of anchoring partner cJun or cJun(Cys), it did not show a high signal selectively. Additionally, the spheroplasts harboring pPelBFLAG-Fc for expression of soluble periplasmic Fc secreted via the PelB leader peptide without an

additional inner membrane anchoring motif showed very high fluorescence signal suggesting that periplasmically expressed Fc proteins remain bound to the cells without an inner membrane anchoring motif even after spheroplasting (Fig. A3-2B).

To achieve a stronger tethering of Fc onto spheroplasts, display using stronger protein-protein interaction pairs compared to leucine zippers was also considered. The ColE2–Im2 protein interaction pair, represents one of the tightest protein-protein interactionw in nature (K_D= 10^{-15}) (Li et al., 2004). To display homodimeric Fc using the ColE2-Im2 interaction, Im2 fused-Fc was firstly induced for periplasmic Fc assembly and then the expression of ColE2 mutants fused to the NlpA leader sequence and six amino acids (CDQSSS) was induced for inner membrane anchoring (Fig. A3-3). To prevent autodegradation of host DNA, the zinc binding histidines (H574, H578) were substituted to Ala by site directed mutagenesis (Garinot-Schneider et al., 1996). The resulting three mutants (H574A, H578A, or H574A/H578A) could inhibit host DNase activity while retaining Im2 binding (data not shown). Of the three ColE2 mutants, the single mutant, ColE2 (H578A) showed the best result for the display of Im2 fused 26-10 scFv on the FACS analysis detected by digoxin BODIPY (data not shown). The utility of the display system using the ColE2 (H578A)–Im2 interaction was further investigated with M18 scFv, 26-10 scFv, and also with homodimeric Fc. Im2 fused antibodies, M18 scFv-Im2 and 26-10 scFv-Im2 showed selectively higher fluorescence signal compared with negative controls, M18 scFv and 26-10 scFv not fused to Im2, respectively. However, the higher signals appeared to be due to differences in expression levels. When ColE2 was not expressed, M18 scFv, 26.10 scFv, and Fc were well expressed. However, the

expression of ColE2 with Im2 or without Im2 inhibited the expression of M18 scFv, 26-10 scFv and of Fc partially or completely, respectively (Fig. A3-4).

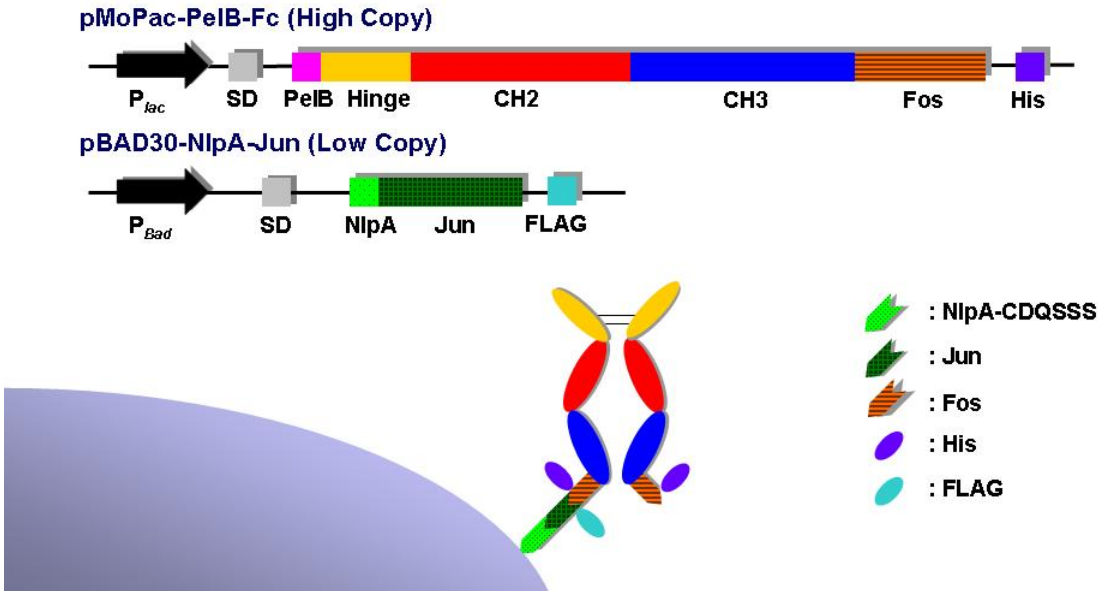

Figure A3-1. Two plasmids system for the periplasmic display of Fc using cJun-cFos or cJun(Cys)-cFos(Cys) interaction.

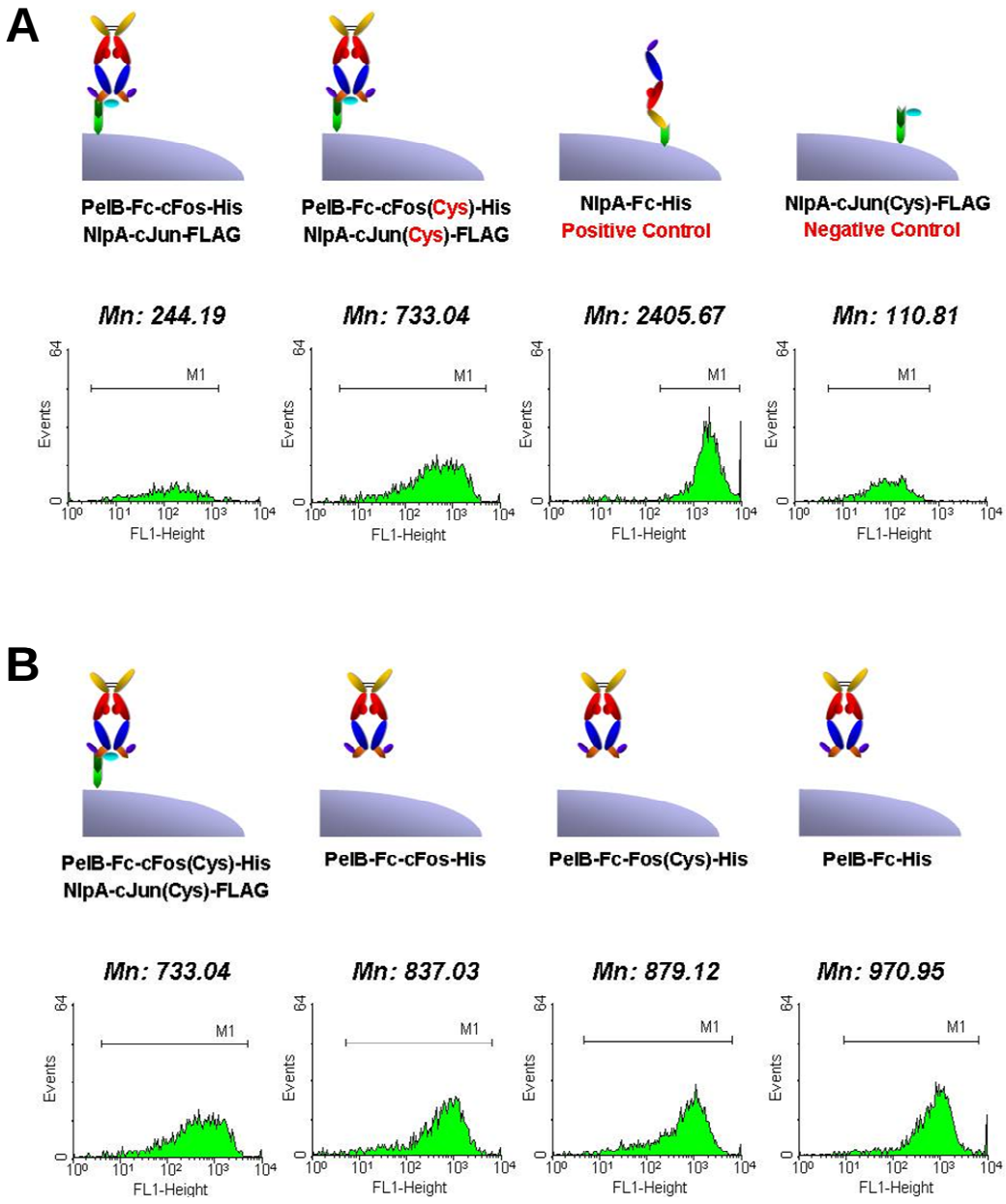

Figure A3-2. FACS analysis results of periplasmic displayed Fc homodimer using cJun-cFos and cJun(Cys)-cFos(Cys) interaction pairs. (A) FACS signals of periplasmic displayed Fc using cJun-cFos and cJun(Cys)-cFos(Cys) were compared with a positive and a negative controls. (B) FACS signals of periplasmic displayed Fc using cJun-cFos and cJun(Cys)-cFos(Cys) were compared with one plasmid systems not co-expressing NlpA and 6 amino acid residues (CDQSSS) fused cJun or cJun(Cys). Spheroplasts were incubated with Protein A-FITC probe for detection. Mn: Mean fluorescence intensity.

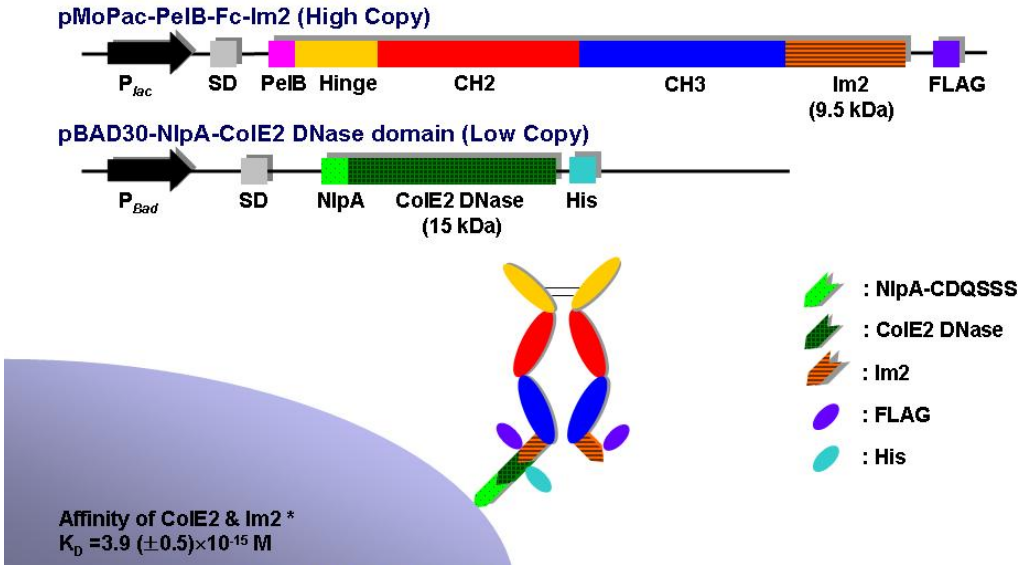

Figure A3-3. Two plasmids system for the periplasmic display of Fc using ColE2-Im2 interaction.

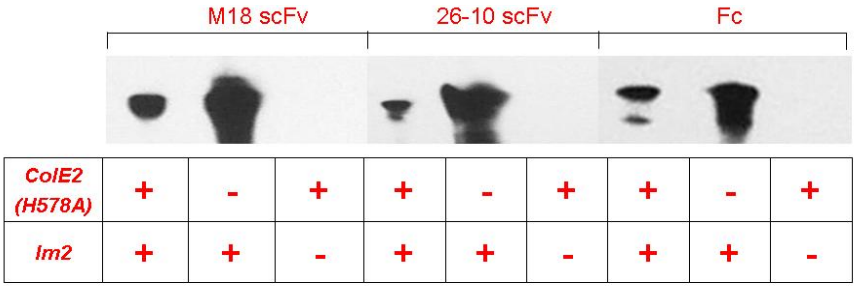

Figure A3-4. Effect of ColE2 on the expression of target proteins, M18 scFv (Lane 1-3), 26-10 scFv (Lane 4-6), and Fc (Lane 7-9). In lane 1, 4 and 7, Im2 fused proteins were co-expressed with APEx displayed ColE2(H578A). In lane 2, 5 and 7, Im2 fused proteins were expressed without APEx displayed ColE2(H578A). In lane 3, 6 and 9, proteins without Im2 fusions were co-expressed APEx displayed ColE2(H578A). Anti-FLAG antibody peroxidase conjugated was used as a detection antibody for Western blot.

A3.4 DISCUSSION

In this study, two different 2 hybrid systems were constructed and employed for the display system of homodimeric IgG Fc domains onto spheroplasted *E.coli*. Secreted Fc domains were fused to heterodimerization domains (cFos or Im2) and co-expressed with heterodimerziation partners (cJun (Kouzarides and Ziff, 1988; Landschulz et al., 1988) or ColE2 (Garinot-Schneider et al., 1996; Li et al., 2004), respectively), N-terminally fused to the inner membrane anchor NlpA(1-6) (Harvey et al., 2004). The fluorescence signal to noise ratio obtained following labeling with Protein A-FITC was not suitable for library screening purposes. However, in the course of these studies, we found that the retention of soluble, secreted Fc domain proteins onto spheroplasted cells was highly dependent on the growth conditions. Optimal specific labeling with Protein A-FITC was obtained in cells expressing Fc secreted with a PelB leader peptide and grown at 25 ºC in the presence of 0.5 M treaholose, as discussed in chapter 2. Under these conditions spheroplasts expressing the Fc protein exhibited 10 fold higher fluorescence than the control. Under the optimized conditions, a library encoding Fc mutant domains followed by a FLAG tag and preceded by a PelB signal peptide for secretion into the periplasm was constructed. *E. coli* cells expressing high affinity Fc domain to Fc binding ligands could be sorted by flow cytometry after spheroplasting and labeling with fluorophore-conjugated Fc domain binding ligands.

Bibliography

Andersen, J.T., Qian, J.D., and Sandlie, I. (2006) The conserved histidine 166 residue of the human neonatal Fc receptor heavy chain is critical for the pH-dependent binding to albumin. *Eur J Immunol*, **36**, 3044-3051.

Anthony, R.M., Nimmerjahn, F., Ashline, D.J., Reinhold, V.N., Paulson, J.C. and Ravetch, J.V. (2008) Recapitulation of IVIG Anti-Inflammatory Activity with a Recombinant IgG Fc. *Science*, **320**, 373-376.

Armour, K.L., van de Winkel, J.G.J, Williamson, L.M. and Clark, M.R. (2003) Differential binding to human FcgammaRIIa and FcgammaRIIb receptors by human IgG wildtype and mutant antibodies. *Mol Immunol*, **40**, 585-593.

Barbas Cf, III, Kang, A.S., Lerner, R.A. and Benkovic, S.J. (1991) Assembly of Combinatorial Antibody Libraries on Phage Surfaces: The Gene III Site. *Proc Natl Acad Sci USA*, **88**, 7978-7982.

Barry, M.A., Dower, W.J. and Johnston, S.A. (1996) Toward cell-targeting gene therapy vectors: Selection of cell-binding peptides from random peptide-presenting phage libraries. *Nat Med*, **2**, 299-305.

Berken, A. and Benacerraf, B. (1966) Properties of antibodies cytophilic for macriphages. *J Exp Med*, **123**, 119-144.

Berntzen, G., Lunde, E., Flobakk, M., Andersen, J.T., Lauvrak, V. and Sandlie, I. (2005) Prolonged and increased expression of soluble Fc receptors, IgG and a TCR-Ig fusion protein by transiently transfected adherent 293E cells. *J Immunol Methods*, **298**, 93-104.

Bevaart, L., Goldstein, J., Vitale, L., Russoniello, C., Treml, J., Zhang, J., Graziano, R.F., Leusen, J.H.W., van de Winkel, J.G.J. and Keler, T. (2006) Direct targeting of genetically modified tumour cells to FcγRI triggers potent tumour cytotoxicity. *Brit J Haematol*, **132**, 317-325.

Binyamin, L., Borghaei, H. and Weiner, L.M. (2006) Cancer therapy with engineered monoclonal antibodies. *Update on Cancer Ther*, **1**, 147-157.

Boder, E.T., Midelfort, K.S. and Wittrup, K.D. (2000) Directed evolution of antibody fragments with monovalent femtomolar antigen-binding affinity. *Proc Natl Acad Sci USA*, **97**, 10701-10705.

Boder, E.T. and Wittrup, K.D. (1997) Yeast surface display for screening combinatorial polypeptide libraries. *Nat Biotechnol*, **15**, 553-557.

Bonmort, M., Dalod, M., Mignot, G., Ullrich, E., Chaput, N. and Zitvogel, L. (2008) Killer dendritic cells: IKDC and the others. *Curr Opin Immunol*, **20**, 558-565.

Bradbury, A.R.M. and Marks, J.D. (2004) Antibodies from phage antibody libraries. *J Immunol Methods*, **290**, 29-49.

Brambell, F.W., Halliday, R. and Morris, I.G. (1958) Interference by human and bovine serum and serum protein fractions with the absorption of antibodies by suckling rats and mice. *Proc R Soc B*, **149**, 1-11.

Brown, K.C. (2000) New approaches for cell-specific targeting: identification of cell-selective peptides from combinatorial libraries. *Curr Opin Chem Biol*, **4**, 16-21.

Burmeister, W.P., Gastinel, L.N., Simister, N.E., Blum, M.L. and Bjorkman, P.J. (1994a) Crystal structure at 2.2 Å resolution of the MHC-related neonatal Fc receptor. *Nature*, **372**, 336-343.

Burmeister, W.P., Huber, A.H. and Bjorkman, P.J. (1994b) Crystal structure of the complex of rat neonatal Fc receptor with Fc. *Nature*, **372**, 379-383.

Burton, D.R. and Dwek, R.A. (2006) Immunology: Sugar Determines Antibody Activity. *Science*, **313**, 627-628.

Carlsson, F., Stalhammar-Carlemalm, M., Flardh, K., Sandin, C., Carlemalm, E. and Lindahl, G. (2006) Signal sequence directs localized secretion of bacterial surface proteins. *Nature*, **442**, 943-946.

Cha, T., Guo, A. and Zhu, X.Y. (2005) Enzymatic activity on a chip: the critical role of protein orientation. *Proteomics*, **5**, 416-419.

Chames, Patrick, Regenmortel, M.V., Weiss, E., Baty, D. (2009) Therapeutic antibodies: successes, limitations and hopes for the future. *Brit J Pharmacol*, **157**, 220-233.

Chen, G., Dubrawsky, I., Mendez, P., Georgiou, G. and Iverson, B.L. (1999) *In vitro* scanning saturation mutagenesis of all the specificity determining residues in an antibody binding site. *Protein Eng*, **12**, 349-356.

Chen, G., Hayhurst, A., Thomas, J.G., Harvey, B.R., Iverson, B.L. and Georgiou, G. (2001) Isolation of high-affinity ligand-binding proteins by periplasmic expression with cytometric screening (PECS). *Nat Biotechnol.*, **19**, 537-542.

Cohen-Solal, J.F., Cassard, L., Fridman, W.H. and Sautes-Fridman, C. (2004) Fc gamma receptors. *Immunol Lett*, **92**, 199-205.

Cormack, B.P., Valdivia, R.H. and Falkow, S. (1996) FACS-optimized mutants of the green fluorescent protein (GFP). *Gene*, **173**, 33-38.

Cox, M.M. (2004) Commercial Production in Insect Cells. *BioProcess International*, **2**, 34-38.

Dall'Acqua, W.F., Kiener, P.A. and Wu, H. (2006) Properties of Human IgG1s Engineered for Enhanced Binding to the Neonatal Fc Receptor (FcRn). *J Biol Chem*, **281**, 23514-23524.

Dall'Acqua, W.F., Woods, R.M., Ward, E.S., Palaszynski, S.R., Patel, N.K., Brewah, Y.A., Wu, H., Kiener, P.A. and Langermann, S. (2002) Increasing the Affinity of a Human IgG1 for the Neonatal Fc Receptor: Biological Consequences. *J Immunol*, **169**, 5171-5180.

Dane, K.Y., Chan, L.A., Rice, J.J. and Daugherty, P.S. (2006) Isolation of cell specific peptide ligands using fluorescent bacterial display libraries. *J Immunol Methods*, **309**, 120-129.

Daugherty, P.S., Chen, G., Iverson, B.L. and Georgiou, G. (2000a) Quantitative analysis of the effect of the mutation frequency on the affinity maturation of single chain Fv antibodies. *Proc Natl Acad Sci USA*, **97**, 2029-2034.

Daugherty, P.S., Iverson, B.L. and Georgiou, G. (2000b) Flow cytometric screening of cell-based libraries. *J Immunol Methods*, **243**, 211-227.

de Kruif, J. and Logtenberg, T. (1996) Leucine zipper dimerized bivalent and bispecific scFv antibodies from a semi-synthetic antibody phage display library. *J Biol Chem*, **271**, 7630-7634.

De Smit, M.H., Duin, J.V. (1990) Control of Prokaryotic Translational Initiation by mRNA Secondary Structure. *Prog in Nucleic Acid Res and Mol Biol*. Academic Press, Vol. Volume 38, pp. 1-35.

Desjarlais, J.R., Lazar, G.A., Zhukovsky, E.A. and Chu, S.Y. (2007) Optimizing engagement of the immune system by anti-tumor antibodies: an engineer's perspective. *Drug Discov Today*, **12**, 898-910.

Dimitrov, D.S. and Marks, J.D. (2009) Therapeutic antibodies: current state and future trends--is a paradigm change coming soon? *Methods Mol Biol*, **525**, 1-27, xiii.

Du, B., Qian, M., Zhou, Z., Wang, P., Wang, L., Zhang, X., Wu, M., Zhang, P. and Mei, B. (2006) *In vitro* panning of a targeting peptide to hepatocarcinoma from a phage display peptide library. *Biochem Biophys Res Commun*, **342**, 956-962.

Duncan, A.R. and Winter, G. (1988) The binding site for C1q on IgG. *Nature*, **332**, 738-740.

Duncan, A.R., Woof, J.M., Partridge, L.J., Burton, D.R. and Winter, G. (1988) Localization of the binding site for the human high-affinity Fc receptor on IgG. *Nature*, **332**, 563-564.

Fanger, N.A., Wardwell, K., Shen, L., Tedder, T.F. and Guyre, P.M. (1996) Type I (CD64) and type II (CD32) Fc gamma receptor-mediated phagocytosis by human blood dendritic cells. *J Immunol*, **157**, 541-548.

Feldhaus, M.J., Siegel, R.W., Opresko, L.K., Coleman, J.R., Feldhaus, J.M., Yeung, Y.A., Cochran, J.R., Heinzelman, P., Colby, D., Swers, J., Graff, C., Wiley, H.S. and Wittrup, K.D. (2003) Flow-cytometric isolation of human antibodies from a nonimmune *Saccharomyces cerevisiae* surface display library. *Nat Biotechnol*, **21**, 163-170.

Francisco, J.A., Campbell, R., Iverson, B.L. and Georgiou, G. (1993) Production and fluorescence-activated cell sorting of *Escherichia coli* expressing a functional antibody fragment on the external surface. *Proc Natl Acad Sci USA*, **90**, 10444-10448.

Fromant, M., Blanquet, S. and Plateau, P. (1995) Direct Random Mutagenesis of Gene-Sized DNA Fragments Using Polymerase Chain Reaction. *Anal Biochem*, **224**, 347-353.

Galon, J., Robertson, M.W., Galinha, A., Mazieres, N., Spagnoli, R., Fridman, W.H. and Sautes, C. (1997) Affinity of the interaction between Fc gamma receptor type III (Fc gammaRIII) and monomeric human IgG subclasses. Role of Fc gammaRIII glycosylation. *Eur J Immunol*, **27**, 1928-1932.

Garinot-Schneider, C., Pommer, A.J., Moore, G.R., Kleanthous, C. and James, R. (1996) Identification of putative active-site residues in the DNase domain of colicin E9 by random mutagenesis. *J Mol Biol*, **260**, 731-742.

Georgiou, G. and Segatori, L. (2005) Preparative expression of secreted proteins in bacteria: status report and future prospects. *Curr Opin Biotechnol*, **16**, 538-545.

Georgiou, G., Stathopoulos, C., Daugherty, P.S., Nayak, A.R., Iverson, B.L. and Curtiss, R., 3rd. (1997) Display of heterologous proteins on the surface of microorganisms: from the screening of combinatorial libraries to live recombinant vaccines. *Nat Biotechnol.*, **15,** 29-34.

Ghetie, V., Popov, S., Borvak, J., Radu, C., Matesoi, D., Medesan, C., Ober, R.J. and Ward, E.S. (1997) Increasing the serum persistence of an IgG fragment by random mutagenesis. *Nat Biotechnol*, **15**, 637-640.

Ghetie, V. and Ward, E.S. (2000) Multiple Roles for the Major Histocompatibility Complex Class I- Related Receptor FcRn. *Annu Rev Immunol*, **18**, 739-766.

Guzman, L.M., Belin, D., Carson, M.J. and Beckwith, J. (1995) Tight regulation, modulation, and high-level expression by vectors containing the arabinose PBAD promoter. *J Bacteriol*, **177**, 4121-4130.

Harvey, B.R., Georgiou, G., Hayhurst, A., Jeong, K.J., Iverson, B.L. and Rogers, G.K. (2004) Anchored periplasmic expression, a versatile technology for the isolation of high-affinity antibodies from Escherichia coli-expressed libraries. *Proc. Natl. Acad. Sci. USA*, **101**, 9193-9198.

Harvey, B.R., Shanafelt, A.B., Baburina, I., Hui, R., Vitone, S., Iverson, B.L. and Georgiou, G. (2006) Engineering of recombinant antibody fragments to methamphetamine by anchored periplasmic expression. *J Immunol Methods*, **308**, 43-52.

Hayhurst, A., Happe, S., Mabry, R., Koch, Z., Iverson, B.L. and Georgiou, G. (2003) Isolation and expression of recombinant antibody fragments to the biological warfare pathogen Brucella melitensis. *J Immunol Methods*, **276**, 185-196.

Hinton, P.R., Johlfs, M.G., Xiong, J.M., Hanestad, K., Ong, K.C., Bullock, C., Keller, S., Tang, M.T., Tso, J.Y., Vasquez, M. and Tsurushita, N. (2004) Engineered human IgG antibodies with longer serum half-lives in primates. *J Biol Chem*, **279**, 6213-6216.

Hinton, P.R., Xiong, J.M., Johlfs, M.G., Tang, M.T., Keller, S. and Tsurushita, N. (2006) An Engineered Human IgG1 Antibody with Longer Serum Half-Life. *J Immunol*, **176**, 346-356.

Hoogenboom, H.R. (2005) Selecting and screening recombinant antibody libraries. *Nat Biotechnol*, **23**, 1105-1116.

Hoover, D.M. and Lubkowski, J. (2002) DNAWorks: an automated method for designing oligonucleotides for PCR-based gene synthesis. *Nucleic Acids Res*, **30**, e43-.

Hulett, M.D., Osman, N., McKenzie, I.F. and Hogarth, P.M. (1991) Chimeric Fc receptors identify functional domains of the murine high affinity receptor for IgG. *J Immunol*, **147**, 1863-1868.

Ivan, E. and Colovai, A.I. (2006) Human Fc Receptors: Critical Targets in the Treatment of Autoimmune Diseases and Transplant Rejections. *Human Immunol*, **67**, 479-491.

Jefferis, R. (2005) Glycosylation of recombinant antibody therapeutics. *Biotechnol Prog*, **21**, 11-16.

Jefferis, R., Lund, J. and Pound, J.D. (1998) IgG-Fc-mediated effector functions: molecular definition of interaction sites for effector ligands and the role of glycosylation. *Immunol Rev*, **163**, 59-76.

Jeong, K.J., Kawarasaki, Y., Gam, J., Harvey, B.R., Iverson, B.L. and Georgiou, G. (2004) A periplasmic fluorescent reporter protein and its application in high-throughput membrane protein topology analysis. *J Mol Biol*, **341**, 901-909.

Jeong, K.J. and Lee, S.Y. (2003) Enhanced production of recombinant proteins in *Escherichia coli* by filamentation suppression. *Appl Environ Microbiol*, **69**, 1295-1298.

Jones, E.A. and Waldmann, T.A. (1972) The mechanism of intestinal uptake and transcellular transport of IgG in the neonatal rat. *J Clin Invest*, **51**, 2916-2927.

Jung, S.T., Jeong, K.J., Iverson, B.L. and Georgiou, G. (2007) Binding and enrichment of *Escherichia coli* spheroplasts expressing inner membrane tethered scFv antibodies on surface immobilized antigens. *Biotechnol Bioeng*, **98**, 39-47.

Jung, S.T., Kim, M.S., Seo, J.Y., Kim, H.C. and Kim, Y. (2003) Purification of enzymatically active human lysyl oxidase and lysyl oxidase-like protein from Escherichia coli inclusion bodies. *Protein Expr Purif*, **31**, 240-246.

Kabat, E.A., Wu, T.T., Perry, H.M., Gottesman, K.S. and Foeller, C. (1991) *Sequences of Proteins of Immunological Interest (U.S. Dept. of Health and Hum. Serv., Bethesda).*

Kacskovics, I. (2004) Fc receptors in livestock species. *Vet Immunol Immunopathol*, **102**, 351-362.

Kalergis, A.M. and Ravetch, J.V. (2002) Inducing Tumor Immunity through the Selective Engagement of Activating Fc{gamma} Receptors on Dendritic Cells. *J. Exp. Med.*, **195**, 1653-1659.

Kaneko, Y., Nimmerjahn, F. and Ravetch, J.V. (2006) Anti-Inflammatory Activity of Immunoglobulin G Resulting from Fc Sialylation. *Science*, **313**, 670-673.

Kawarasaki, Y., Griswold, K.E., Stevenson, J.D., Selzer, T., Benkovic, S.J., Iverson, B.L. and Georgiou, G. (2003) Enhanced crossover SCRATCHY: construction and high-throughput screening of a combinatorial library containing multiple non-homologous crossovers. *Nucleic Acids Res*, **31**, e126.

Kim, J.K., Tsen, M.F., Ghetie, V. and Ward, E.S. (1994) Localization of the site of the murine IgG1 molecule that is involved in binding to the murine intestinal Fc receptor. *Eur J Immunol*, **24**, 2429-2434.

Kouzarides, T. and Ziff, E. (1988) The role of the leucine zipper in the fos-jun interaction. *Nature*, **336**, 646-651.

Krapp, S., Mimura, Y., Jefferis, R., Huber, R. and Sondermann, P. (2003) Structural analysis of human IgG-Fc glycoforms reveals a correlation between glycosylation and structural integrity. *J Mol Biol*, **325**, 979-989.

Krebber, A., Bornhauser, S., Burmester, J., Honegger, A., Willuda, J., Bosshard, H.R. and Pluckthun, A. (1997) Reliable cloning of functional antibody variable domains from hybridomas and spleen cell repertoires employing a reengineered phage display system. *J Immunol Methods*, **201**, 35-55.

Landschulz, W.H., Johnson, P.F. and McKnight, S.L. (1988) The leucine zipper: a hypothetical structure common to a new class of DNA binding proteins. *Science*, **240**, 1759-1764.

Lazar, G.A., Chirino, A.J., Dang, W., Desjarlais, J.R., Doberstein, S.K., Hayes, R.J., Karki, S.B. and Vafa, O. (2009) Optimized Fc variants and methods for their generation. *US Patent 2009/0092599 A1*.

Lazar, G.A., Dang, W., Karki, S., Vafa, O., Peng, J.S., Hyun, L., Chan, C., Chung, H.S., Eivazi, A., Yoder, S.C., Vielmetter, J., Carmichael, D.F., Hayes, R.J. and Dahiyat, B.I. (2006) Engineered antibody Fc variants with enhanced effector function. *Proc Natl Acad Sci USA*, **103**, 4005-4010.

Lefranc, M.-P., Pommié, C., Kaas, Q., Duprat, E., Bosc, N., Guiraudou, D., Jean, C., Ruiz, M., Da Piédade, I., Rouard, M., Foulquier, E., Thouvenin, V. and Lefranc, G. (2005) IMGT unique numbering for immunoglobulin and T cell receptor constant domains and Ig superfamily C-like domains. *Dev Comp Immunol*, **29**, 185-203.

Li, W., Keeble, A.H., Giffard, C., James, R., Moore, G.R. and Kleanthous, C. (2004) Highly discriminating protein-protein interaction specificities in the context of a conserved binding energy hotspot. *J Mol Biol*, **337**, 743-759.

Linenberger, M.L., Maloney, D.G. and Bernstein, I.D. (2002) Antibody-directed therapies for hematological malignancies. *Trends Mol Med*, **8**, 69-76.

Liu, X.-y., Pop, L.M. and Vitetta, E.S. (2008) Engineering therapeutic monoclonal antibodies. *Immunol Rev*, **222**, 9-27.

Lofblom, J., Wernerus, H. and Stahl, S. (2005) Fine affinity discrimination by normalized fluorescence activated cell sorting in staphylococcal surface display. *FEMS Microbiol. Lett.*, **248**, 189-198.

Lund, J., Takahashi, N., Pound, J.D., Goodall, M. and Jefferis, R. (1996) Multiple interactions of IgG with its core oligosaccharide can modulate recognition by complement and human Fc gamma receptor I and influence the synthesis of its oligosaccharide chains. *J Immunol*, **157**, 4963-4969.

Lund, J., Winter, G., Jones, P.T., Pound, J.D., Tanaka, T., Walker, M.R., Artymiuk, P.J., Arata, Y., Burton, D.R., Jefferis, R. and et al. (1991) Human Fc gamma RI and Fc gamma RII interact with distinct but overlapping sites on human IgG. *J Immunol*, **147**, 2657-2662.

Maenaka, K., van der Merwe, P.A., Stuart, D.I., Jones, E.Y. and Sondermann, P. (2001) The Human Low Affinity Fcgamma Receptors IIa, IIb, and III Bind IgG with Fast Kinetics and Distinct Thermodynamic Properties. *J. Biol. Chem.*, **276**, 44898-44904.

Martin, W.L., West, A.P., Gan, L. and Bjorkman, P.J. (2001) Crystal Structure at 2.8 A of an FcRn/Heterodimeric Fc Complex: Mechanism of pH-Dependent Binding. *Molecular Cell*, **7**, 867-877.

Mattanovich, D. and Borth, N. (2006) Applications of cell sorting in biotechnology. *Microbial Cell Factories*, **5**, 12. [Online.] http://www.microbialcellfactories.com/content/15/11/12.

Maxwell, K.F., Powell, M.S., Hulett, M.D., Barton, P.A., McKenzie, I.F., Garrett, T.P. and Hogarth, P.M. (1999) Crystal structure of the human leukocyte Fc receptor, Fc gammaRIIa. *Nat Struct Biol*, **6**, 437-442.

Mazor, Y., Blarcom, T.V., Mabry, R., Iverson, B.L. and Georgiou, G. (2007) Isolation of engineered, full-length antibodies from libraries expressed in *Escherichia coli*. *Nat Biotechnol*, **25**, 563-565.

McGuire, M.J., Sykes, K.F., Samli, K.N., Timares, L., Barry, M.A., Stemke-Hale, K., Tagliaferri, F., Logan, M., Jansa, K., Takashima, A., Brown, K.C. and Johnston, S.A. (2004) A library-selected, langerhans cell-targeting peptide enhances an immune response. *DNA Cell Biol*, **23**, 742-752.

McKelvey, E.M. and Fahey, J.L. (1965) Immunoglobulin changes in disease: quantitation on the basis of heavy polypeptide chains, IgG (gammaG), IgA (gammaA), and IgM (gammaM), and of light polypeptide chains, type K (I) and type L (II). *J Clin Invest*, **44**, 1778-1787.

McLean, G.R., Nakouzi, A., Casadevall, A. and Green, N.S. (2000) Human and murine immunoglobulin expression vector cassettes. *Mol Immunol*, **37**, 837-845.

Medesan, C., Cianga, P., Mummert, M., Stanescu, D., Ghetie, V. and Ward, E.S. (1998) Comparative studies of rat IgG to further delineate the Fc: FcRn interaction site. *Eur J Immunol*, **28**, 2092-2100.

Medesan, C., Matesoi, D., Radu, C., Ghetie, V. and Ward, E.S. (1997) Delineation of the amino acid residues involved in transcytosis and catabolism of mouse IgG1. *J Immunol*, **158**, 2211-2217.

Medesan, C., Radu, C., Kim, J.K., Ghetie, V. and Ward, E.S. (1996) Localization of the site of the IgG molecule that regulates maternofetal transmission in mice. *Eur J Immunol*, **26**, 2533-2536.

Mimura, Y., Sondermann, P., Ghirlando, R., Lund, J., Young, S.P., Goodall, M. and Jefferis, R. (2001) Role of Oligosaccharide Residues of IgG1-Fc in Fcgamma RIIb Binding. *J. Biol. Chem.*, **276**, 45539-45547.

Moretta, A. (2002) Natural killer cells and dendritic cells: rendezvous in abused tissues. *Nat Rev Immunol*, **2**, 957-965.

Nimmerjahn, F. and Ravetch, J.V. (2008) Fc[gamma] receptors as regulators of immune responses. *Nat Rev Immunol*, **8**, 34.

Ober, R.J., Martinez, C., Lai, X., Zhou, J. and Ward, E.S. (2004a) Exocytosis of IgG as mediated by the receptor, FcRn: An analysis at the single-molecule level. *Proc Natl Acad Sci USA*, **101**, 11076-11081.

Ober, R.J., Martinez, C., Vaccaro, C., Zhou, J. and Ward, E.S. (2004b) Visualizing the Site and Dynamics of IgG Salvage by the MHC Class I-Related Receptor, FcRn. *J Immunol*, **172**, 2021-2029.

Oganesyan, V., Damschroder, M.M., Woods, R.M., Cook, K.E., Wu, H. and Dall'Acqua, W.F. (2009) Structural characterization of a human Fc fragment engineered for extended serum half-life. *Mol Immunol*, **46**, 1750-1755.

Paetz, A., Sack, M., Thepen, T., Tur, M.K., Bruell, D., Finnern, R., Fischer, R. and Barth, S. (2005) Recombinant soluble human Fcgamma receptor I with picomolar affinity for immunoglobulin G. *Biochem Biophys Res Commun*, **338**, 1811-1817.

Pfefferkorn, L.C. and Fanger, M.W. (1989) Cross-linking of the high affinity Fc receptor for human immunoglobulin G1 triggers transient activation of NADPH oxidase activity. Continuous oxidase activation requires continuous *de novo* receptor cross-linking. *J Biol Chem*, **264**, 14112-14120.

Presta, L.G. (2006) Engineering of therapeutic antibodies to minimize immunogenicity and optimize function. *Advanced Drug Delivery Reviews*, **58**, 640-656.

Pugsley, A.P. (1993) The complete general secretory pathway in gram-negative bacteria. *Microbiol Rev*, **57**, 50-108.

Radaev, S., Motyka, S., Fridman, W.H., Sautes-Fridman, C. and Sun, P.D. (2001) The structure of a human type III Fcgamma receptor in complex with Fc. *J Biol Chem*, **276**, 16469-16477.

Radaev, S. and Sun, P.D. (2001) Recognition of IgG by Fcgamma receptor. The role of Fc glycosylation and the binding of peptide inhibitors. *J Biol Chem*, **276**, 16478-16483.

Raghavan, M. and Bjorkman, P.J. (1996) Fc receptors and their interactions with immunoglobulins. *Annu Rev Cell Dev Biol*, **12**, 181-220.

Ravetch, J.V. and Bolland, S. (2001) IgG Fc receptors. *Annu Rev Immunol*, **19**, 275-290.

Ravetch, J.V. and Lanier, L.L. (2000) Immune inhibitory receptors. *Science*, **290**, 84-89.

Reichert, J.M., Rosensweig, C.J., Faden, L.B. and Dewitz, M.C. (2005) Monoclonal antibody successes in the clinic. *Nat Biotechnol*, **23**, 1073-1078.

Richards, J.O., Karki, S., Lazar, G.A., Chen, H., Dang, W. and Desjarlais, J.R. (2008) Optimization of antibody binding to Fc{gamma}RIIa enhances macrophage phagocytosis of tumor cells. *Mol Cancer Ther*, **7**, 2517-2527.

Richman, S.A., Healan, S.J., Weber, K.S., Donermeyer, D.L., Dossett, M.L., Greenberg, P.D., Allen, P.M. and Kranz, D.M. (2006) Development of a novel strategy for engineering high-affinity proteins by yeast display. *Protein Eng, Des Sel*, **19**, 255-264.

Rodewald, R. (1976) pH-dependent binding of immunoglobulins to intestinal cells of the neonatal rat. *J Cell Biol.*, **71**, 666-669.

Roopenian, D.C. and Akilesh, S. (2007) FcRn: the neonatal Fc receptor comes of age. *Nat Rev Immunol*, **7**, 715-725.

Sankaran, K. and Wu, H.C. (1994) Lipid modification of bacterial prolipoprotein. Transfer of diacylglyceryl moiety from phosphatidylglycerol. *J Biol Chem*, **269**, 19701-19706.

Sazinsky, S.L., Ott, R.G., Silver, N.W., Tidor, B., Ravetch, J.V. and Wittrup, K.D. (2008) Aglycosylated immunoglobulin G1 variants productively engage activating Fc receptors. *Proc Natl Acad Sci U S A*, **105**, 20167-20172.

Schäkel, K., Mayer, E., Federle, C., Schmitz, M., Riethmüller, G., Rieber, E.P., (1998) A novel dendritic cell population in human blood: one-step immunomagnetic isolation by a specific mAb (M-DC8) and *in vitro* priming of cytotoxic T lymphocytes. *European Journal of Immunology*, **28**, 4084-4093.

Schierle, C.F., Berkmen, M., Huber, D., Kumamoto, C., Boyd, D. and Beckwith, J. (2003) The DsbA signal sequence directs efficient, cotranslational export of passenger proteins to the Escherichia coli periplasm via the signal recognition particle pathway. *J Bacteriol*, **185**, 5706-5713.

Schmidt, R.E. and Gessner, J.E. (2005) Fc receptors and their interaction with complement in autoimmunity. *Immunol Lett*, **100**, 56-67.

Schmitz, M., Zhao, S., Deuse, Y., Schakel, K., Wehner, R., Wohner, H., Holig, K., Wienforth, F., Kiessling, A., Bornhauser, M., Temme, A., Rieger, M.A., Weigle, B., Bachmann, M. and Rieber, E.P. (2005) Tumoricidal potential of native blood dendritic cells: direct tumor cell killing and activation of NK cell-mediated cytotoxicity. *J Immunol*, **174**, 4127-4134.

Schmitz, M., Zhao, S., Schakel, K., Bornhauser, M., Ockert, D. and Rieber, E.P. (2002) Native human blood dendritic cells as potent effectors in antibody-dependent cellular cytotoxicity. *Blood*, **100**, 1502-1504.

Schrama, D., Reisfeld, R.A. and Becker, J.C. (2006) Antibody targeted drugs as cancer therapeutics. *Nat Rev Drug Discov*, **5**, 147-159.

Seong, S.Y. and Choi, C.Y. (2003) Current status of protein chip development in terms of fabrication and application. *Proteomics*, **3**, 2176-2189.

Sergina, N.V. and Moasser, M.M. (2007) The HER family and cancer: emerging molecular mechanisms and therapeutic targets. *Trends Mol Med*, **13**, 527-534.

Shields, R.L., Namenuk, A.K., Hong, K., Meng, Y.G., Rae, J., Briggs, J., Xie, D., Lai, J., Stadlen, A., Li, B., Fox, J.A. and Presta, L.G. (2001) High resolution mapping of the binding site on human IgG1 for Fc gamma RI, Fc gamma RII, Fc gamma RIII, and FcRn and design of IgG1 variants with improved binding to the Fc gamma R. *J Biol Chem*, **276**, 6591-6604.

Siberil, S., Dutertre, C.-A., Boix, C., Bonnin, E., Menez, R., Stura, E., Jorieux, S., Fridman, W.H. and Teillaud, J.L. (2006) Molecular aspects of human Fc[gamma]R interactions with IgG: Functional and therapeutic consequences. *Immunol Lett*, **106**, 111-118.

Simmons, L.C., Reilly, D., Klimowski, L., Raju, T.S., Meng, G., Sims, P., Hong, K., Shields, R.L., Damico, L.A., Rancatore, P. and Yansura, D.G. (2002) Expression of full-length immunoglobulins in *Escherichia coli*: rapid and efficient production of aglycosylated antibodies. *J Immunol Methods*, **263**, 133-147.

Smith, G.P. (1985) Filamentous fusion phage: novel expression vectors that display cloned antigens on the virion surface. *Science*, **228**, 1315-1317.

Sondermann, P., Huber, R. and Jacob, U. (1999) Crystal structure of the soluble form of the human fcgamma-receptor IIb: a new member of the immunoglobulin superfamily at 1.7 A resolution. *Embo J*, **18**, 1095-1103.

Sondermann, P., Huber, R., Oosthuizen, V. and Jacob, U. (2000) The 3.2-[angst] crystal structure of the human IgG1 Fc fragment-FcγRIII complex. *Nature*, **406**, 267-273.

Sondermann, P. and Jacob, U. (1999) Human Fcgamma receptor IIb expressed in Escherichia coli reveals IgG binding capability. *Biol Chem*, **380**, 717-721.

Sondermann, P., Kaiser, J. and Jacob, U. (2001) Molecular Basis for Immune Complex Recognition: A Comparison of Fc-Receptor Structures. *J Mol Biol*, **309**, 737-749.

Spiegelberg, H.L. (1974) Biological activities of immunoglobulins of different classes and subclasses. *Adv Immunol*, **19**, 259-294.

Stavenhagen, J.B., Gorlatov, S., Tuaillon, N., Rankin, C.T., Li, H., Burke, S., Huang, L., Johnson, S., Bonvini, E. and Koenig, S. (2007) Fc optimization of therapeutic antibodies enhances their ability to kill Tumor cells *In vitro* and controls tumor Expansion *in vivo* via Low-Affinity Activating Fcγ Receptors. *Cancer Res*, **67**, 8882-8890.

Suzuki, E., Niwa, R., Saji, S., Muta, M., Hirose, M., Iida, S., Shiotsu, Y., Satoh, M., Shitara, K., Kondo, M. and Toi, M. (2007) A Nonfucosylated Anti-HER2 Antibody Augments Antibody-Dependent Cellular Cytotoxicity in Breast Cancer Patients. *Clin Cancer Res*, **13**, 1875-1882.

Tapia, M.I., Mourez, M., Hofnung, M. and Dassa, E. (1999) Structure-function study of MalF protein by random mutagenesis. *J Bacteriol*, **181**, 2267-2272.

Tillinger, W., Jilch, R., Jilma, B., Brunner, H., Koeller, U., Lichtenberger, C., Waldhor, T. and Reinisch, W. (2009) Expression of the high-affinity IgG receptor FcRI

(CD64) in patients with inflammatory bowel disease: a new biomarker for gastroenterologic diagnostics. *Am J Gastroenterol*, **104**, 102-109.

Vaara, M. and Nurminen, M. (1999) Outer Membrane permeability barrier in Escherichia coli mutants that are defective in the Late Acyltransferases of Lipid A Biosynthesis. *Antimicrob Agents Chemother*, **43**, 1459-1462.

Van de Winkel, J.G.J. and Capel, P.J.A. (1993) Human IgG Fc receptor heterogeneity: molecular aspects and clinical implications. *Immunol Today*, **14**, 215-221.

Vaughn, D.E., Milburn, C.M., Penny, D.M., Martin, W.L., Johnson, J.L. and Bjorkman, P.J. (1997) Identification of critical IgG binding epitopes on the neonatal Fc receptor. *J Mol Biol*, **274**, 597-607.

Wang, W., Singh, S., Zeng, D.L., King, K. and Nema, S. (2007) Antibody structure, instability, and formulation. *J Pharm Sci*, **96**, 1-26.

Wang, X.X. and Shusta, E.V. (2005) The use of scFv-displaying yeast in mammalian cell surface selections. *J Immunol Methods*, **304**, 30-42.

Weng, Z., Gulukota, K., Vaughn, D.E., Bjorkman, P.J. and DeLisi, C. (1998) Computational determination of the structure of rat Fc bound to the neonatal Fc receptor. *J Mol Biol*, **282**, 217-225.

Wesa, A.K. and Storkus, W.J. (2007) Killer dendritic cells: mechanisms of action and therapeutic implications for cancer. *Cell Death Differ*, **15**, 51-57.

West, A.P. and Bjorkman, P.J. (2000) Crystal Structure and Immunoglobulin G Binding Properties of the Human Major Histocompatibility Complex-Related Fc Receptor. *Biochem*, **39**, 9698-9708.

Wright, A. and Morrison, S.L. (1997) Effect of glycosylation on antibody function: implications for genetic engineering. *Trends Biotechnol*, **15**, 26-32.

Yang, R., Xu, D., Zhang, A., Gruber, A., (2001) Immature dendritic cells kill ovarian carcinoma cells by a FAS/FASL pathway, enabling them to sensitize tumor-specific CTLs. *Int J Cancer*, **94**, 407-413.

Yeung, Y.A., Leabman, M.K., Marvin, J.S., Qiu, J., Adams, C.W., Lien, S., Starovasnik, M.A. and Lowman, H.B. (2009) Engineering Human IgG1 Affinity to Human Neonatal Fc Receptor: Impact of Affinity Improvement on Pharmacokinetics in Primates. *J Immunol*, **182**, 7663-7671.

Vita

Sang Taek Jung was born in Daegu, Korea on June 17, 1974, the son of In Hwa Jeong and Song Ja Kim. After graduation from Myungshin High School in Jinju, Korea in 1993, he enrolled in the Department of Chemical Technology (Renamed as school of chemical and biological engineering) of Seoul National University in Seoul, Korea. Upon receiving his Bachelor of Science in Chemical Techonogy in 1997 with Magna Cum Laude honors, he entered the graduate school program in Seoul National University and received the degree of Master of Science in Chemical Technology after completion of his thesis titled "Production and Purification of Recombinant Human Erythropoietin in *Escherichia coli* and Chemical Modification with Monomethoxy Polyethylene Glycol (pegylation)" in 1999. He worked for Green Cross Croporation in Yongin, Korea as a researcher from 1998 to 2001 and for Samyang Genex Biotechnology Institute in Daejun, Korea as a researcher from 2001 until he entered the Graduate School of the University of Texas at Austin in the fall of 2004 to pursue a doctoral degree in the Department of Chemical Engineering.

Permanent address: A-201, Hanshin Greeen APT A-201, 65-8, Jamwon-Dong, Seocho-Gu, Seoul, Korea 137-907

This dissertation was typed by Sang Taek Jung